

METABOLOMIC INVESTIGATIONS INTO HUMAN APOCRINE SWEAT SECRETIONS

Graham Mullard, BSc (Hons), MSc

**Thesis submitted to the University of Nottingham for the Degree of Doctor of
Philosophy**

September 2011

Abstract

Human axillary odour is formed by the action of *Corynebacteria* or *Stephylococci* bacteria on odourless axilla sections. Several groups have identified axillary odorants, including 3-methyl-2-hexanoic acid (3M2H) and 3-hydroxy-3-methyl-hexenoic acid (HMHA), and how they are pre-formed and bound to amino acid conjugates. However, there is currently a lack of LC-MS methodologies and no reported NMR methods, that are required to further identify the non-volatile constituents, which would provide further information to allow understanding of the underlying physiological biochemistry of malodour.

This work has incorporated a three-pronged approach. Firstly, a global strategy, through the use of NMR and LC-MS, provided a complementary unbiased overview of the metabolite composition. Metabolites were identified based on acquired standards, accurate mass and through the use of in-house or online databases. Furthermore, spectra of biological samples are inherently complex, thus, requiring a multivariate data analysis (MVDA) approach to extract the latent chemical information in the data. Secondly, semi-targeted LC-MS/MS methodologies has been used to identify metabolites with a common structural core (i.e. odour precursors) and provide structural information for the reliable identification of known and unknown metabolites. Finally, a targeted LC-MS/MS method provided an increase in specificity and sensitivity to accurately quantify known metabolites of interest (odour precursors).

Initially, all methodologies were developed through the use of either an artificial sweat matrix (global strategy) or through the use of synthetic standards (semi-targeted or targeted strategy). The sample complexity was then increased by applying the methodologies to an ASG5 apocrine cell line, in order to provide further knowledge into apocrine cell metabolism and to identify whether there could be any potential male or female differences due to differences in circulating hormones. Changes in the cell metabolism were identified, and both the NMR and LC-MS data could differentiate between control, tamoxifen- and β -estradiol-treated. However, it is

difficult to attribute these changes to specific pathways, as these hormones or the vehicle used (ethanol) are likely to produce a ripple effect across the cell's metabolism. Nonetheless, NMR spectroscopy quantified 25 metabolites with lactate being the most abundant at 19.1 mM, while HILIC-MS could detect a range of lipids, nucleotides, amino acids, fatty acids and vitamins.

The methodologies were then applied to human apocrine sweat collected from six volunteers across five days. NMR spectroscopy was able to identify 25 and quantify 19 metabolites, with lactate being the most abundant at 13.2 mM. LC-MS/MS readily identified 12 amino acid conjugates with HMHA being the most abundant. Furthermore, a possible 20 unidentified conjugates were detected (LC-MS/MS semi-targeted methodologies) as well as putatively identifying 473 metabolites (LC-MS global methodologies). MVDA techniques such as principal component analysis (PCA) illustrated that intra-individual variation was greater than inter-individual variation, as well as secretions from both the left and right arm being consistent with one another. Moreover, MVDA illustrated the complementary nature of both NMR and MS, as the data acquired with the two types of instrumentation showed the same trends, even though these trends were based on different subsets of metabolites.

The work presented herein, has successfully used a number of analytical technologies to investigate metabolite content of human apocrine sweat. It has been shown that a number of complementary techniques and multivariate analysis can provide a valuable insight into the underlying physiology of malodour.

This work was funded by BBSRC and Unilever (Port Sunlight, UK).

Acknowledgements

I am deeply thankful to my supervisors Dr Clare Daykin and Prof. David Barrett for their encouragement and guidance throughout my time within their lab group. I am also grateful to them for giving me the opportunity to produce this PhD thesis and for always believing in me.

I also wish to thank all those who contributed to the project, including Dr Mark Harker and his team at Unilever, for their help during the project and their role in the sample collection. Your help was both inspiring and invaluable during our collaboration. I would also like to thank Dr Catherine Otori and Paul Cooling for their help and technical support.

Finally, thanks go to everybody else who has helped me through this project, especially Asa Bluck and Gavin Hackett – just for being there and making me laugh. As well as Amy Wong, Gemma Gaw and Philippine Geißler for the good atmosphere, friendship, encouragement and many MS and NMR discussions. I would particularly like to thank Rebecca Cooper for her patience and understanding during my time at the University of Nottingham and whilst writing this thesis. Also, I am indebted to my Mum and Dad who have always encouraged and supported me in everything I have done and for that, I am truly grateful.

“It is very obvious that we have many different kinds of smells, all the way from the odour of violets and roses up to asafoetida. But until you can measure their likeness and differences you can have no science of odour.”

— ALEXANDER GRAHAM BELL, 1914

Table of contents

ABSTRACT I

ACKNOWLEDGEMENTS III

TABLE OF CONTENTS V

ABBREVIATIONS IX

1 INTRODUCTION 1

1.1 METABOLOMICS 1

1.2 APPLICATION OF TECHNIQUES 3

1.3 NMR BACKGROUND AND THEORY 7

1.3.1 1D ¹H NMR Spectroscopy 9

1.3.2 2D NMR Spectroscopy 10

1.4 MASS SPECTROMETRY 12

1.4.1 Electrospray Ionisation 12

1.4.2 Mass Analysers 15

1.4.3 Quadrupole 17

1.4.4 Ion Trap 17

1.4.5 Time-of-Flight 17

1.4.6 Orbital Trap 18

1.4.7 Hybrid Instruments 18

1.5 MULTIVARIATE DATA ANALYSIS 20

1.5.1 Pre-processing of Data 22

1.5.2 Data Pre-treatment Methods 24

1.5.3 Principal Component Analysis 24

1.5.4 Partial Least Squares Regression 25

1.5.5 Principal Component Discriminant Analysis 25

1.6 IDENTIFICATION OF COMPONENTS 26

1.7 SWEAT GLAND BIOLOGY 28

1.7.1 Sweat Glands 29

1.7.2 Chemical Composition of Eccrine Sweat 32

1.7.3 Axillary Malodour Formation 36

1.7.4 Chemical Nature of Body Malodour 38

1.7.5 Natural Precursors/Apocrine Sweat Composition 43

1.8 AIMS OF THE THESIS 50

2 DEVELOPMENT OF ¹H NMR SPECTROSCOPY METHODOLOGY FOR THE METABOLOMIC ANALYSIS OF APOCRINE SWEAT 51

2.1 INTRODUCTION 51

2.2 AIMS 54

2.3	MATERIALS AND METHODS	54
2.3.1	Chemicals.....	54
2.3.2	Sample Preparation	55
2.3.3	¹ H NMR Spectroscopy	57
2.3.4	Spectral analysis and metabolite quantification	58
2.3.5	Data Pre-Processing	58
2.3.6	Partial Least Squares Regression (PLS).....	59
2.4	RESULTS AND DISCUSSION	59
2.4.1	Signal-to-Noise-Ratio	60
2.4.2	Application with Mass Limited Samples	66
2.4.3	The Application of PLS Regression to Determine the Stability of Artificial Sweat Mixture during Storage	70
2.5	CONCLUSION	73
3	DEVELOPMENT OF MASS SPECTROMETRY METHODS FOR THE ANALYSIS OF KEY METABOLITES IN APOCRINE SWEAT	74
3.1	INTRODUCTION	74
3.1.1	Direct Injection Mass Spectrometry (DIMS)	75
3.1.2	Reverse Phase High Performance Liquid Chromatography Mass Spectrometry (RP- HPLC-MS).....	75
3.1.3	Hydrophilic Interaction Liquid Chromatography (HILIC)	76
3.1.4	Analytical Strategies for Profiling Apocrine Sweat Metabolites	84
3.1.5	Aims	86
3.2	MATERIAL AND METHODS.....	86
3.2.1	Chemicals.....	86
3.2.2	LC-MS Columns	87
3.2.3	Sample Preparation	87
3.2.4	Global Profiling by LC-QTOF-MS.....	88
3.2.4.1	Preliminary Development Work for LC-QTOF-MS.....	89
3.2.5	Global Profiling by Direct Injection Mass Spectrometry	90
3.2.6	Targeted Profiling by LC-MS/MS	91
3.2.6.1	Optimisation of compound dependent parameters for MRM Analysis	91
3.2.6.2	Conjugate Profiling using Precursor Ion Scanning	92
3.2.6.3	Chromatographic conditions	93
3.2.7	MS ⁿ for Fragmentation Confirmation	93
3.2.8	Data Analysis	93
3.3	RESULTS AND DISCUSSION	94
3.3.1	Direct Injection Mass Spectrometry.....	94
3.3.2	Global Profiling: HILIC-QTOF	97
3.3.2.1	Column Selection.....	98
3.3.2.2	Solvent and Buffer Selection	100

3.3.3	Targeted LC-MS/MS	107
3.3.3.1	Optimization of the Declustering Potential and Collision Energy	108
3.3.3.2	LC-MS/MS Analysis of Odour Precursor Standard Compounds	108
3.3.3.3	LC-MS/MS profiling of Odour Precursors using Precursor Ion Survey Scan	113
3.4	CONCLUSIONS	115
4	APPLICATION OF ¹H NMR SPECTROSCOPY AND LC-MS TO AN <i>IN-VITRO</i> MODEL OF APOCRINE SWEAT PRODUCED FROM ASG5 CELL LINES	117
4.1	INTRODUCTION	117
4.1.1	Metabolite Extraction from ASG5 cells	119
4.1.2	Aims	121
4.2	MATERIAL AND METHODS	121
4.2.1	Sample Preparation	121
4.2.1.1	Cell Culture	121
4.2.1.2	Cell Extraction	122
4.2.2	¹ H NMR Spectroscopy	122
4.2.3	2D NMR Spectroscopy	123
4.2.4	HILIC-QTOF-MS	123
4.2.5	Targeted LC-MS/MS	123
4.2.6	Quantification of Artificial Apocrine Sweat Metabolites by ¹ NMR Spectroscopy	123
4.2.7	NMR Spectral Data Reduction	123
4.2.8	HILIC-QTOF-MS Data Pre-Processing	124
4.2.9	Multivariate Data Analysis	124
4.2.10	Compound Identification	125
4.3	RESULTS AND DISCUSSION	126
4.3.1	¹ H NMR Spectra of <i>In-Vitro</i> Model of Apocrine Sweat	126
4.3.2	LC-Mass Spectrometry Analysis of <i>In-Vitro</i> Model of Apocrine Sweat	131
4.3.3	Multivariate Data Analysis	134
4.4	CONCLUSIONS	144
5	METABOLOMIC INVESTIGATIONS OF HUMAN AXILLARY SECRETIONS	146
5.1	INTRODUCTION	146
5.2	AIMS	148
5.3	MATERIALS AND METHODS	149
5.3.1	Chemicals	149
5.3.2	LC-MS Column	149
5.3.3	Collection of Odourless Axillary Secretions	149
5.3.4	Sample Preparation	150
5.3.5	¹ H NMR Spectroscopy for the Global Profiling of Axillary Secretions	150
5.3.6	2D NMR Spectroscopy	150
5.3.7	HILIC-QTOF-MS for the Global Profiling of Axillary Secretions	151
5.3.8	UPLC-Orbitrap-MS for the Global Profiling of Axillary Secretions	151

5.3.9	Conjugate Profiling using RP-HPLC-MS/MS	152
5.3.10	Targeted Profiling using RP-HPLC-MS/MS	152
5.3.11	Data Analysis	153
5.3.12	Compound Identification by LC-MS	153
5.4	RESULTS AND DISCUSSION	156
5.4.1	Identification of Small Molecule Components of Human Apocrine Sweat	156
5.4.1.1	Global Analysis using ¹ H NMR Spectroscopy.....	156
5.4.1.2	Global Analysis using High Mass Accuracy LC-MS (HILIC and C ₁₈)	160
5.4.1.3	Semi-Targeted analysis using LC-MS Survey Scanning	166
5.4.1.4	RP-LC-MS/MS Multiple Reaction Monitoring for Targeted Analysis of Odour Precursors in Human Apocrine Sweat Secretions	174
5.4.2	Study of Temporal, Inter- and Intra-Individual Differences in Human Axillary Secretions	178
5.4.2.1	Inter- and Intra-Individual Differences	178
5.4.2.2	Inter-Day Differences	183
5.4.2.3	Left and Right Arm Differences	186
5.4.3	Overall Discussion and Conclusions	198
6	GENERAL DISCUSSION	201
7	REFERENCES	206
	APPENDIX A	236
	APPENDIX B.....	252
	APPENDIX C	255

Abbreviations

2M3H-Cys	S-[1-(2-hydroxy-1-methylethyl)-ethyl]-L-cysteine
3M2H-Gln	N- α -3-methylhex-2-enoyl-L-glutamine
3M2H-Cys-Gly	S-[1-(2-hydroxyethyl)-1-methylbutyl]-L-cysteinylglycine
A. A	Amino acid
apoD	Apolipoprotein D
B_0	Magnetic field
CE	Collision energy
CID	Collision induced dissociation
COSY	Correlation spectroscopy
Ctr	Mean Centered
d	Doublet
dd	Doublet of doublets
DIMS	Direct injection mass spectrometry
DP	Declustering potential
E2	β -Estradiol
EIC	Extracted ion chromatogram
EPI	Enhanced product ion
ESI	Electrospray ionization
Eth	Ethanol
FA	Fatty acid
FFA	Free fatty acid
FT	Fourier transform
FWHM	Full width at half maximum
γ	Magnetogyric ratio
GC-MS	Gas chromatography mass spectrometry
h	Planck's constant (6.62×10^{-34} m ² kg/s)
HILIC	Hydrophilic interaction liquid chromatography
HMBC	Heteronuclear multiple bond coherence
HMDB	Human metabolite database
HMHA-Gln	N- α -3-hydroxy-3-methylhexanoyl-L-glutamine
HMQC	Heteronuclear multiple quantum coherence
HPLC	High performance liquid chromatography
I	Nuclear spin quantum number
Im	Immonium ion $[R-CH=NH_2]^+$
IDA	Information dependent acquisition
J-res	J-resolved spectroscopy
k	Boltzman constant (1.38×10^{-23} J K ⁻¹)

LC	Liquid chromatography
LCFA	Long chain fatty acid
LOD	Limit of detection
LOQ	Limit of quantification
LV	Latent variable
m	Multiplet
μ	Nuclear magnetic moment
MeCN	Acetonitrile
MHC	Major histocompatibility complex
MRM	Multiple reaction monitoring
MS	Mass spectrometry
MVA	Multivariate analysis
NMR	Nuclear magnetic resonance
ns	Number of transients
OD	Optical density
PC	Principle component
PCA	Principal component analysis
PC-DA	Principal component discriminant analysis
PI	Precursor ion
PLS-DA	Partial least squares discriminant analysis
PPM	Parts per million
PR	Pattern recognition
QC	Quality control
QNP	Quattro nucleus probe
QqQLit	Hybrid triple quadrupole linear ion trap
QTOF	Quadrupole time of flight
QTRAP	See QqQLit
R	Correlation coefficient
RD	Relaxation delay
RF	Radio frequency
RP	Reversed phase
s	Singlet
S/N	Signal to noise
SRM	Single reaction monitoring
t	Triplet
TAM	Tamoxifen
TIC	Total ion chromatogram
TOCSY	Total correlation spectroscopy
TSP	Trimethylsilyl [2,2,3,3- ² H ₄] propionate
TXI	Triple resonance inverse probe

Unt	Untreated
UPLC	Ultra performance liquid chromatography
UV	Unit variance
VFA	Volatile fatty acid
VIP	Variable importance in projection
v_0	Larmor frequency

Chapter 1

1 Introduction

1.1 Metabolomics

Metabolomics is the global study of all the naturally occurring low molecular weight molecules, called metabolites, in biological samples such as cells, biofluids (e.g. urine and blood) or tissues. These low molecular weight molecules, which make up the ‘metabolome’, are derived from the interaction of the genome with its environment and are not merely the end products of gene expression, but also form part of the metabolic status of a biological system.

When ‘metabonomics’ was first introduced it was defined as “*the quantitative measurement of the time related multi-parametric metabolic response of living systems to pathophysiological stimuli or genetic modification*” (Nicholson *et al.*, 1999). Whereas metabolomics has been described as “*a comprehensive and quantitative analysis of all metabolites*” (Fiehn, 2001). These terms are often used interchangeably, although groups adhering to these definitions tend to adopt the use of ‘metabolomics’ to discuss work on simple cell systems and intracellular metabolite concentrations and ‘metabonomics’ for the analysis of products of non-enzymatic reactions which interact with and influence metabolite formation (Daykin and Wulfert, 2006). However, it will be up to the reader to distinguish between those definitions. Both terms claim superiority, though ultimately it will be left for the user community to decide. The term metabolomics will be employed here with the realization that either term may be used interchangeably.

As the definition of the metabolome above suggest, in a metabolomics experiment the ultimate goal would be to capture and quantify all the metabolites in a cellular system

simultaneously without pre-selecting a specific pathway. However, metabolites consist of a diverse set of chemical (molecular weight, polarity, solubility) and physical (volatility) properties. Moreover, the metabolome extends over a wide concentration range, which is estimated to be between 7-9 magnitudes of concentration (pM-mM) (Dunn and Ellis, 2005). This diversity means that no one analytical technique is capable for all investigations. Thus, a number of strategies are employed, as listed below, with nuclear magnetic resonance (NMR) and mass spectrometry (MS) coupled to chromatography, being the most prevalent analytical techniques (Dunn *et al.*, 2011b): -

- **Metabolomics**, initially defined as the comprehensive analysis of the entire metabolome. The term is now used to describe one or more of the strategies defined below.
- **Metabolite profiling**, the holistic study of the metabolite complement of a biological system, often employing multiple analytical platforms, to encompass a wide coverage of the metabolome.
- **Metabolic footprinting**, analysis of the extra-cellular metabolome which is composed of metabolites consumed/not consumed from the environment or metabolites secreted from the intra-cellular volume.
- **Metabolite target analysis**, quantitative analysis of a small number of metabolites related to a specific metabolic reaction or pathway, for example; a particular enzyme system that would be affected by abiotic or biotic perturbation.

Whilst these strategies are not universally accepted, they are continuously evolving. Hence, there can be overlap in their definitions; however, the above classification illustrates the options available for monitoring the metabolome (Dunn and Ellis, 2005; Hollywood *et al.*, 2006).

Although metabolomics is complementary with transcriptomics and proteomics, it also has certain advantages. In particular, the metabolome is further downstream from gene to function, thus, any change in cell physiology (resulting from gene deletion or over expression) are amplified through the hierarchy of the transcriptome and

proteome (Goodacre *et al.*, 2004). It is also important to highlight those factors other than gene expression or single nucleotide polymorphisms, which can affect the system biology view of an organism; environmental factors such as diet, age, sex, ethnicity, lifestyle, and microfloral populations all have large influences and these factors need to be deconvolved (Lindon *et al.*, 2004). Hence, metabolic fluxes are not just regulated by gene expression but by both post-transcriptional and post-translational modifications and as such, the metabolome can be considered closer to the phenotype (Hollywood *et al.*, 2006).

Metabolomics has already been widely employed in the study of toxic insult (Lindon *et al.*, 2003b; Nicholson *et al.*, 2002), the study of disease and disease models (Brindle *et al.*, 2002), as a means of discovering novel biomarkers for early disease detection or providing new drug targets as well as providing insights into the disease process itself. Furthermore, metabolomics is increasingly being applied to the study of healthy individuals (e.g. HUSERMET project¹), which aims to provide a metabolic ‘reference map’ of the normal population against which data from other studies can be drawn against. Currently, the samples most commonly analysed are plasma (Daykin *et al.*, 2002; Lenz *et al.*, 2003; Nicholson *et al.*, 1983; Zelena *et al.*, 2009) and urine (Connor *et al.*, 2004; Daykin *et al.*, 2005; Gika *et al.*, 2007), which are considered to be readily accessible and minimally invasive. However, analysis has been performed on other biofluids such as cerebrospinal fluid (Holmes *et al.*, 2006; Sweatman *et al.*, 1993), seminal fluid (Lynch *et al.*, 1994; Spraul *et al.*, 1994b), saliva (Takeda *et al.*, 2009), and eccrine sweat (Harker *et al.*, 2006) as well as tissues and tissue extracts (Dunn *et al.*, 2011a; Xu *et al.*, 2009).

1.2 Application of Techniques

The first requirement for metabolomics analysis is to have techniques available that are as comprehensive as possible. This is especially important, as metabolites are heterogeneous in nature, thus, isolating and measuring them all together (‘true metabolomics’) is extremely difficult. For practical reasons this is never achieved, hence, most metabolomic studies are really ‘metabolic profiling’ of a subset of

¹ <http://www.husermet.org/>

chemical classes (Kell, 2004). Indeed, specific platforms are not a prerequisite for metabolomic studies, so in theory, any technique capable of generating comprehensive data in a relatively short time frame can be used as a powerful means of generating multivariate metabolic data (Robertson, 2005). Thus, the choice of analytical tool is based on the level of chemical information required and the appropriate time frame in which the data must be obtained. However, one must remember that there will be introductions of chemical bias with respect to the method, which are highlighted in Table 1.1.

Table 1.1 Consideration for metabolomics analysis. Reproduced with modifications (Hollywood *et al.*, 2006).

Consideration	Approach	Comments
Chemical information	MS	MS ⁿ will provide some structural information. FT-ICR-MS can generate empirical formulae for $m/z < 500$.
	NMR	Gives detailed structural information, particularly using 2-D NMR of isolated metabolites.
	Chromatography (GC, HPLC, CE)	On its own will not generally lead to metabolite identification. However, coupled with MS and NMR is very powerful for analyte identification.
	FT-IR, Raman	Provides limited structural information, but useful for identification of functional groups.
Chemical bias	GC-MS	Solvent extraction bias: non-polar versus polar analytes. Need for chemical derivatization.
	LC-MS	Solvent bias means it is usually more applicable to polar compounds (HILIC) or non-polar compounds (reverse phase C ₁₈ or C ₈ columns).
	NMR, FT-IR, Raman	Biased by concentration, available functional groups and where they resonate in the spectrum.
Speed	Chromatography (GC, HPLC, CE)	Very useful for separation but typically takes 30 min.
	NMR	Few minutes to hours. Depends on the strength of the magnet, sensitivity can be improved with cryo-probes.
	ESI-MS	1-3 min flow-injection (direct infusion) mode.
	FT-IR	10-60 s.

The two most information-rich techniques that offer atom-specific molecular structural information are MS and NMR. The resolution, sensitivity and selectivity of MS based techniques can be enhanced through coupling to gas chromatography (GC) or liquid chromatography (LC). Furthermore, hyphenating individual systems, LC-NMR-MS, can maximise the information obtained, since the NMR will yield structural information and the MS can determine the mass of each component.

NMR spectroscopy has some specific advantages in the area of metabolomics over other analytical methods discussed in Table 1.1 and these are highlighted in Table 1.2. This is typically the case in regards to analysing biofluids, as it is rapid, non-destructive, requires little or no sample preparation and uses small sample sizes. NMR is based on the fact that nuclei such as ^1H , ^{13}C and ^{31}P can exist at different energy levels due to the differences in nuclear spin, which can be measured by applying an external magnetic field. This means a comprehensive profile of metabolite signals can be produced without the need for pre-selection of measurement parameters or the use of separation or derivatisation procedures (Lindon *et al.*, 2004). Thus, the sample is left unperturbed, allowing rapid analysis of many biochemical molecules simultaneously. Moreover, the non-destructive nature of NMR is particularly useful when further analysis is required for identification of unknown metabolites or when using hyphenated techniques such as LC-NMR-MS (Corcoran and Spraul, 2003); unlike LC-MS where the sample is destroyed after analysis and derivatisation and optimisation procedures can often be expensive and time consuming. More recently, the technique of magic-angle spinning, where the samples are spun rapidly at 54.7° relative to the applied magnetic field has opened up the possibility of applying metabolomics to tissue samples (Lindon *et al.*, 2009; Sitter *et al.*, 2009). This would serve as a tool for linking biofluid changes to the mechanism of action in target tissues, particularly when products of metabolism dominate changes in the biofluids (Robertson, 2005). Further technological advances that have improved the resolution and sensitivity of NMR includes the introduction of cryogenically cooled probes whereby the magnet is super-cooled with cryogenic liquid. This enables the thermal noise of the system to be reduced, thereby, improving the signal-to-noise ratio by approximately four fold (Robosky *et al.*, 2007). This also enables smaller sample volumes to be measured or allows measurements of fixed sample concentrations with a weaker magnetic field strength, which will be more commercially affordable (Kovacs *et al.*, 2005). In comparison, MS also offers a number of advantages as highlighted in Table 1.3. These include an increase in sensitivity and when hyphenated with LC, can detect hundreds or thousands of metabolite features in a given sample as well as providing metabolite identification. Nonetheless, one thing is clear, these two complementary approaches (MS and NMR) will provide information

on different sets of metabolites, and integration of both techniques will provide a more comprehensive characterisation.

Table 1.2 Summary of the main features of ^1H NMR Spectroscopy. Reproduced with modifications (Daykin and Wulfert, 2006).

Feature	Comments
Selectivity	No need for pre-selection of analytical conditions based on the chemical properties of the analyte, or postulation of the metabolites affected by a disease toxicological process.
Non-invasive	NMR spectroscopy is non-invasive, non-destructive and non-equilibrium perturbing, thus, allowing subsequent analysis of a sample with other techniques.
Speed	A typical single ^1H NMR biofluid spectrum is obtainable in <10 minutes, thus, can allow >100 samples/day.
Sample volumes	With standard NMR tubes, a total volume of 600 μl is required for routine spectroscopy, or 5 μl for micro-volume NMR probe.
Sample preparation	Minimal sample preparation for 'global' metabolite profiling. Only the addition of deuterium oxide is required for analysis. However, with complex components (biofluids) physical separation maybe used to simplify spectra.
Dynamic information	Information can be obtained on dynamic biochemical processes in complex matrices and molecular interactions such as protein-ligand binding.
Structural information	Data provides qualitative structural information that can also be quantitative with addition of internal standards at known concentrations.
Reproducibility	NMR spectroscopy is an inherently reproducible analytical method.
Sensitivity	Inherently insensitive technique, realistically detection limits remain in the μM levels for complex samples such as biofluids, though this is improving with cryoprobes and increased field strength magnets.

Table 1.3 Summary of the main features of LC-MS.

Feature	Comments
Selectivity	Dependent on the column, polar compounds (HILIC) and non-polar compound (C_{18} or C_8).
Invasive	Biological fluids (minimally invasive) or tissue samples need to be collected prior to analysis. The sample is destroyed upon analysis.
Speed	LC-MS typically around 30 min per sample, though, DIMS ~1-3 min per sample.
Sample volumes	Typically 5 μl per injection.
Sample preparation	Derivatisation generally not needed. Requires sample extraction, followed by evaporation (overnight) before reconstitution. Also, pooled samples are required to generate QC samples for quality assurance. Targeted methodologies generally require the addition of internal standards.
Dynamic information	Post-translational modifications and single nucleotide polymorphisms in proteome analysis, structure elucidation, metal complex and disulphide bond interactions.
Dynamic range	Depending on mass analyser, can be between 10^4 - 10^6 orders of magnitude.
Structural information	Depending on the mass analyser, can provide fragmentation profiles as well as empirical formula. Data can be both qualitative and quantitative.
Identification	LC-MS libraries are not as robust as GC libraries, thus, can be complex.
Reproducibility	Dependent on sample matrix, typically 120 injections per new column.
Sensitivity	Typically sub picomole concentrations when using targeted methodologies.
Size and cost	Relatively small and cheaper to maintain (ca. NMR).

1.3 NMR Background and Theory

Since the introduction of NMR spectroscopy by Rabi and Breit (Breit and Rabi, 1931; Rabi, 1937) and its further development by Bloch and Purcell (Bloch *et al.*, 1946), NMR spectroscopy has become an invaluable tool for chemists and structural biologists and has increasingly been used in metabolic profiling over the last two decades.

NMR spectroscopy is based on the magnetic properties of the atomic nuclei. Many nuclei (most commonly ^1H , ^{13}C , ^{19}F and ^{31}P) possess a property described as spin, which makes the nuclei behave like magnets, i.e. possesses a nuclear magnetic moment (μ) described by the magnetogyric ratio (γ) for each particular nucleus. The nuclear spin is quantised and is described by the nuclear spin quantum number I , which has values of 0, $\frac{1}{2}$, 1, $1\frac{1}{2}$, etc. in units of $\hbar/2\pi$, where h is the Planck's constant. The actual value of the spin depends on the atomic number and mass number of the nucleus. However, only atoms with odd mass numbers, for example; ^1H , will be considered.

A nucleus of spin I has $2I + 1$ possible energy levels, which are defined by the magnetic quantum number m_I , which has values of $-I, -I + 1, \dots, I - 1, I$, i.e. for a nucleus of spin $\frac{1}{2}$, $m_I = +\frac{1}{2}$ or $-\frac{1}{2}$. There is no difference in energy between nuclei spinning in different directions. However, in the presence of an external magnetic field (B_0), the magnetic dipoles align with or against the external magnetic field resulting in an energy difference between $m_I = +\frac{1}{2}$ and $-\frac{1}{2}$ spin states (see Figure 1.1).

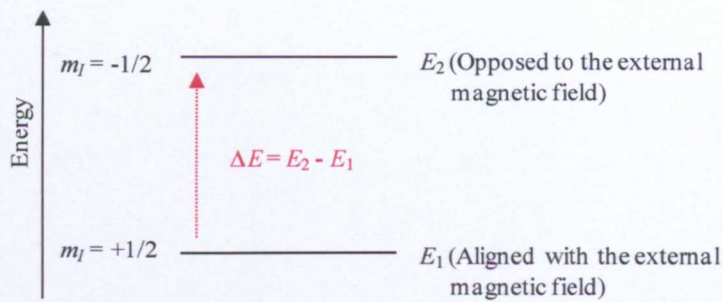


Figure 1.1 Schematic representing the splitting of nuclear spin states in the presence of an external magnetic field.

The energy of this interaction is proportional to μ and B_0 and is explained in Equation 1.1.

$$\Delta E = \frac{\hbar B_0}{2\pi}$$

Equation 1.1

The difference between these energy levels increase with an increase in B_0 . The relative distribution of these populations is described by Boltzmann distribution (Equation 1.2)

$$\frac{N_{-1/2}}{N_{+1/2}} = e^{\left(-\frac{\Delta E}{kT}\right)}$$

Equation 1.2

where N is the fraction of the population of nuclei in each energy state, T is the temperature, and k = Boltzmann constant ($1.38 \times 10^{-23} \text{ J K}^{-1}$). The majority of the spins occupy the lower level, resulting in a weak net magnetisation aligned along the axis of B_0 . It is this weak net magnetisation that is measured in NMR spectroscopy. The net magnetisation will start to precess around the direction of the B_0 (also termed as the z-axis) at the Larmor frequency (ν_0) as depicted in Figure 1.2.

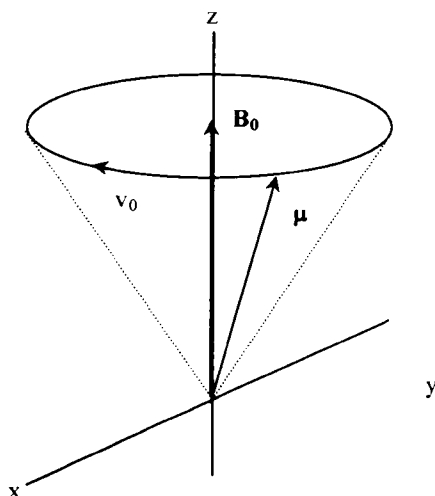


Figure 1.2 Schematic to illustrate precessional orbit . The vector μ of the magnetic moment precesses in a static field with the Larmor frequency ν_0 about the direction of the magnetic vector B_0 .

A particular nucleus (^1H , ^{13}C etc.) resonates at a characteristic frequency, i.e. absorbs radio frequencies (RF) within a certain range, for example: ^1H resonance frequency is 100 MHz. By applying RF pulses (also termed B_1) 90° to the z-axis at exactly the frequency of the nucleus, the net magnetisation can be flipped from the z-axis into the x-y plane, thereby creating an observable signal. Once the RF pulse is removed, the perturbed spin system will begin to relax back towards its equilibrium condition in the z-axis. The emissions from the net magnetisation decay are recorded by the spectrometer as a function of time in the form of free induction decay (FID). The signal is then Fourier transformed to obtain the spectrum in the frequency domain. For a more detailed description of NMR spectroscopy, a number of books are available (Abraham *et al.*, 1988; Claridge, 2008; Keeler, 2010).

1.3.1 1D ^1H NMR Spectroscopy

1D ^1H NMR spectrum contains chemical shift and J-coupling information for each proton in a molecule, which are indicative of the chemical environment (i.e. number of spin active neighbours, connecting bonds and geometrical relationships) and is independent of the applied field strength. Interpretation of this information is used for structural identification of compounds.

The chemical shift is a combination of the B_0 and the magnetic field at the nucleus; with the difference between these two termed nuclear shielding. Each chemical environment will precess at a slightly different frequency, giving rise to different signals in the spectrum, with an increase in chemical shift values resulting from more electronegative groups. Typically, chemical shift is always measured against a suitable reference, often trimethylsilyl [2,2,3,3- $^2\text{H}_4$] propionate (TSP, $\delta = 0$), and is defined as: -

$$\delta = \frac{\nu_{\text{sample}} - \nu_{\text{reference}}}{\text{oscillator frequency (Hz)}} \times 10^6 (\text{ppm})$$

Equation 1.3

Where $\nu_{\text{reference}}$ and ν_{sample} are the resonant frequency of their respective nuclei. This definition allows the resonance frequency of a signal to be expressed independently of the field strength. The chemical shift is expressed in parts per million (ppm) with the range being dependent on the nucleus being monitored, for example: ^1H NMR range ~ 10 ppm.

J-coupling is the peak splitting pattern between adjacent nuclear spins due to the influence of bonding electrons or two nuclei in close proximity in which they interact with the spin-state of its neighbour. This is governed by the n number of equivalent coupled nuclei, each of spin $I = \frac{1}{2}$, where the multiplicity of the signal will be split $n + 1$ times. The relative intensities of split peaks will be governed by Pascal's triangle, for example: a triplet has intensities of $1 : (1 + 1) : 1$, and a quartet has intensities of $1 : (1 + 2) : (2 + 1) : 1$. The distance between each of the signals is measured in Hertz.

1.3.2 2D NMR Spectroscopy

Biological samples produce complex ^1H NMR spectra, often with heavily overlapping peaks in 3-4.5 ppm region. Thus, 2D NMR experiments (Table 1.4) can be used to increase spectral dispersion in the second dimension, allowing separation of overlapping peaks. Furthermore, 2D NMR experiments can be used to provide

unequivocal identification by obtaining information from correlations between homonuclear (^1H - ^1H) and heteronuclear (^1H - ^{13}C) coupling.

In comparison to 1D ^1H NMR spectra, where the signal is obtained as a function of time, 2D NMR spectra, the signal is recorded as a function of two time variables, denoted as F1 and F2, with the resulting data Fourier transformed twice to yield a spectrum which is a function of two frequency variables. 2D data acquisition can be considered as an extension of a 1D NMR experiment. Initially, the sample is excited by an external magnetic field, which is allowed to evolve for a specific duration, F1. Further pulses then excite the nuclei, which is known as the mixing time, transferring the excitation to another nucleus, where the FID is recorded as function of F2 for each value of F1. The data is presented as a contour plot, where the interactions of the nuclei during the mixing time will result in diagonal cross- peaks arising from through bond (scalar) or through space (dipolar) interactions.

Table 1.4 Summary of NMR experiments, which can be useful for assigning peaks in the ^1H NMR spectra of complex mixtures (Aue *et al.*, 1976; Bax and Davis, 1985; Braunschweiler and Ernst, 1983; Cloarec *et al.*, 2005; Lindon *et al.*, 1996; Nagayama *et al.*, 1980; Pullen *et al.*, 1995).

Correlation Spectroscopy (COSY)	The simplest type of 2D NMR experiment. It is used to establish connectivity between protons in a molecule or help simplify a spectrum of a complex mixture.
Total Correlation Spectroscopy (TOCSY)	Similar to COSY, but in theory gives a total correlation of all protons in an unbroken spin system.
Statistical Total Correlation Spectroscopy (STOCSY)	Takes advantage of the multicollinearity of the intensity variables in a set ^1H NMR spectra to generate a pseudo-2D NMR spectrum that displays the correlation among the intensities of various peaks across the whole sample.
J-Resolved Spectroscopy (J-Res)	Used to establish the multiplicity of peaks in regions of heavy spectral overlap (particularly useful for sugars).
^1H-^{13}C Heteronuclear Single Quantum Coherence Spectroscopy (HSQC)	Used to establish correlation between ^{13}C chemical shifts and ^1H chemical shifts of compounds and hence lead to identification of compounds.
HPLC-NMR-MS	Used to simplify NMR spectra by physical separation and provide simultaneous mass spectra in the same chromatographic run. In theory it can be less labour intensive than off-line separation followed by NMR.

1.4 Mass Spectrometry

Mass spectrometry was developed over a century ago by Thompson and Aston, which has been recently reviewed (Griffiths, 1997). In the period since, many advances have been observed into what it is today, a highly sensitive tool that is capable of analysing small and large molecules. The basis of a mass spectrometer is the measurement of an ion's mass-to-charge ratio (m/z). A mass spectrometer is made up of three main separate systems: the ion source, the mass analyser and the detector. Ions are generated by inducing either the loss or the gain of a charge from a neutral species. Once formed, the ions are electrostatically directed into the spectrometer where they can be separated according to their m/z and finally detected. The result of ionisation, ion separation and detection is a mass spectrum that can provide molecular weight and structural information. For a more detailed description of MS, a number of books are available (Hoffmann and Stroobant, 2001; McMaster, 2005; Siuzdak, 1996).

1.4.1 Electrospray Ionisation

Electrospray ionisation (ESI) is the most common ionisation method used in LC-MS analysis for the production of gaseous ions from a liquid solution and has been described in several reviews (Gabelica and De Pauw, 2005; Gaskell, 1997; Kebarle and Verkerk, 2009). However, a number of other ionisation modes can be employed, such as electron impact (GC-MS), chemical ionisation (GC-MS) and APCI (LC-MS), with the latter two being less frequently used.

ESI is considered as a soft ionisation technique that results in little fragmentation and is generally suited to metabolites of high polarity. The Electrospray can be considered as a fine spray of highly charged droplets, which is generated by applying a strong electric field (typically +4 kV in positive ion mode and -4 kV in negative ion mode) under atmospheric conditions to the capillary tip, in which the eluent passes through. Assuming a positive potential is applied to the capillary tip, positive ions will accumulate at the tip to form a 'Taylor cone' which continuously produces positively charged droplets that are directed towards a counter electrode of lower potential, as depicted in Figure 1.3. Heated dry gas (typically nitrogen) is also injected coaxially in

order to promote solvent evaporation. As the solvent evaporates, the droplets reduce in size, resulting in an increase in charge density on the droplets surface. This continues until the so called 'Rayleigh limit', where 'Coulomb fission' occurs, resulting from the mutual repulsion between like charges exceeding the surface tension of the droplet. As the evaporation proceeds, the progeny droplets also undergo fission, which is repeated until a singly or multiply charged ion is produced, which is then directed into the MS. Two models have been suggested for the generation of gas-phased ions: the ion evaporation mechanism proposed by Iribarne and Thomson (Thomson and Iribarne, 1979) and the charged residue mechanism proposed by Dole (Dole *et al.*, 1968). Though the ESI mechanism is still in debate, it is generally accepted that small ions are produced from the ion evaporation mechanism and larger molecules such as globular proteins are produced *via* the charged residue mechanism (Gabelica and De Pauw, 2005).

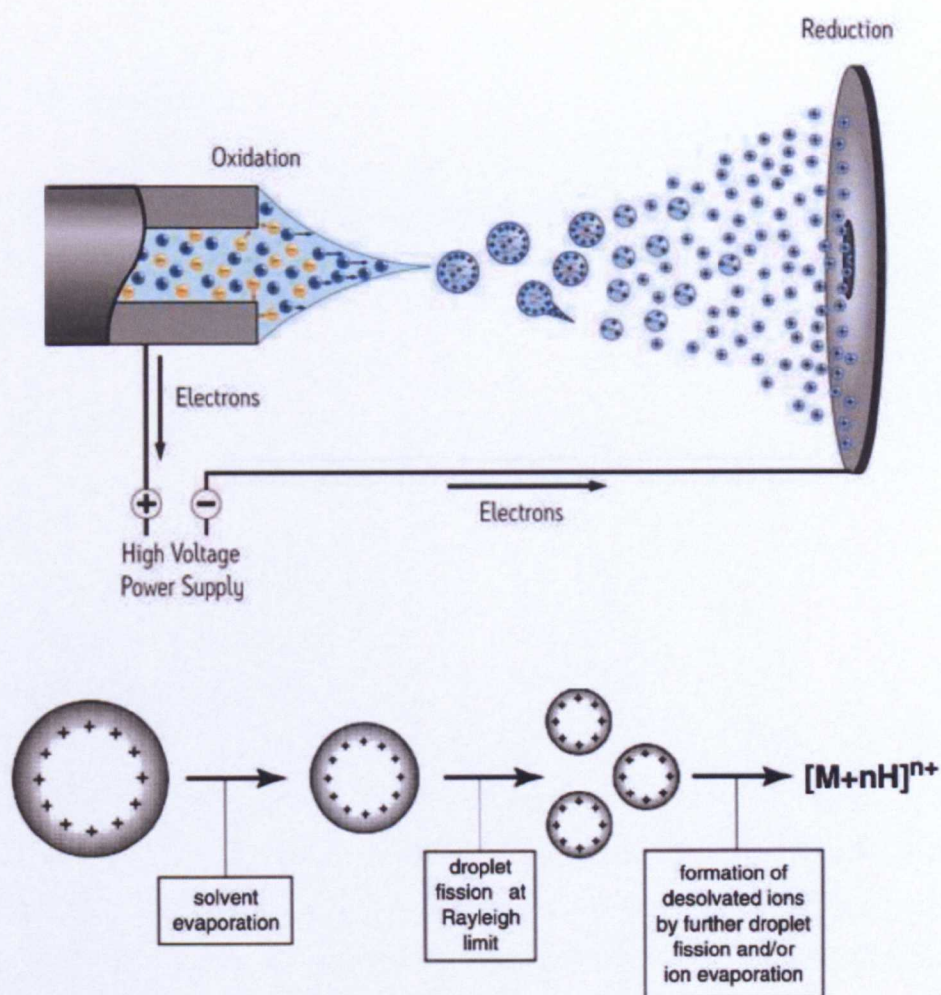


Figure 1.3 Schematic representation of the generation of an electrospray and droplet formation in positive mode (modified from www.waters.com).

1.4.2 Mass Analysers

Mass analysers scan or select ions over a particular mass range. The key feature of all mass analysers is their measurement of m/z , which for a protonated molecule can be described as: -

$$m/z = [M + nH] / nH$$

Where

m/z – mass to charge ratio

M – molecular mass

nH – number of protons

However, other species such as sodium, ammonium or potassium adducts can also form. Furthermore, if the ion is multiply charged then the m/z will be significantly less than the actual mass. Multiple charging and the formation of adducts can yield many peaks that correspond to the same metabolite, which can make data analysis complex. Mass analysers have variations in their capabilities, such as accuracy, dynamic range and resolution, as summarised in Table 1.5. The resolution of a mass analyser is defined as the ability to distinguish between ions of different m/z ratios. Thus, greater resolution corresponds directly to the increased ability to differentiate ions (Siuzdak, 1996). The most common definition for resolution is given by: -

$$\text{Resolution} = M / \Delta M$$

where M and ΔM correspond to m/z and full width half maximum (FWHM) respectively. For example, an m/z of 500 and FWHM of one will have a resolution equal to 500. High resolution mass analysers allow separation of an ion's individual isotopes rather than a weighted average of all isotopes of each constituent element of the molecule, thereby, producing narrow peaks allowing more accurate determination of its position. Thus, the resolving power of the mass analyser to a certain extent determines the accuracy of the instrument.

Table 1.5 General comparison of mass analysers (Hu *et al.*, 2005; Makarov *et al.*, 2006; McLuckey and Wells, 2001; Siuzdak, 1996).

Mass Analyser	Quantity Measured	Mass Range (<i>m/z</i>)	Resolution	Dynamic Range	Mass Accuracy (ppm)	Advantages	Disadvantages
Quadrupole	Filters of <i>m/z</i>	50-4000	4000	10^3 - 10^6	100-1000	Tolerant of high pressures, Suited for electrospray, Ease of polarity switching, Small size, and Cost	Mass range limited to <i>m/z</i> 3000, Low resolution
Ion trap	Frequency	50 -2000; 200-4000	10 000	10^4	100-1000	Small Size, Medium resolution, Suited for tandem MS, Ease of polarity switching, and low cost	Limited mass range, Space charging effects, Precursor ion scanning and neutral loss scanning not available
Time-of-flight (TOF)	Flight time	No upper limit	10 000 – 40 000	10^4	5-10	High mass range, fast scan speed, adaptation for MALDI, and low cost	Low resolution, Less accurate than an orbitrap
Orbitrap	Frequency	50-2000; 200-4000	100 000 at mass 400	10^5	<5	High resolution, More accurate than a TOF	High vacuum ($<10^{-7}$ Torr), Space charging effects, Instrument is large

1.4.3 Quadrupole

Quadrupole mass analysers comprise four parallel rods with a fixed direct current (which can be positive or negative) and a superimposed radio-frequency (RF) potential being applied on opposing rods. The field on the quadrupoles functions as a mass filter by determining which ions are allowed to reach the detector. Ions entering this region will oscillate depending on their m/z ratio and depending on the applied radio frequency, only ions of a particular m/z will pass through. All other ions will have an unstable flight, causing the ions to be lost *via* contact with the rods.

1.4.4 Ion Trap

An ion trap analyser can conceptually be considered as a quadrupole bent on itself in order to form a closed loop, consisting of a ring electrode and two ellipsoid end caps that form a chamber. Ions with different masses entering the chamber are trapped together by an electric field and selectively expelled according to their mass by increasing the voltage on the ring electrode. There is a finite volume and capacity for the ions which limits the dynamic range, especially when analysing complex matrices. Furthermore, MS/MS fragmentation experiments are limited; for example, neutral loss scanning or precursor ion scanning cannot be conducted due to the ion trap being time-dependent rather than space-dependent, like quadrupoles. However, due to the structural similarities to quadrupoles, they are often hybridised (often called linear ion traps) to incorporate the functionalities of both, allowing on-the-fly experiments which would not be possible with either alone.

1.4.5 Time-of-Flight

Time-of-flight (TOF) is based on accelerating a set of ions to the detector (predetermined distance) with the same amount of kinetic energy, whereby the resulting velocity is characteristic of their m/z ratio. The smaller ions reach the detector first because of their greater velocity. More recent TOF instruments are combined with reflectors and ion pushers to further improve mass accuracy and resolution.

1.4.6 Orbital Trap

The orbitrap is a mass analyser that dynamically traps ions in an electric field formed between a central spindle electrode and two bell-shaped outer barrel electrodes (Hu *et al.*, 2005; Makarov, 2000). Electrostatic and centrifugal forces cause the ions to oscillate in both the axial and radial directions. The axial frequency is used to derive the m/z ratio because it is independent of the initial properties of the ions. The time domain transients are detected by the outer electrodes and converted to mass spectra through Fourier transformation. The orbitrap provides a higher mass resolution than most time-of-flight instruments ($\sim 10\,000$) and approaches that of FTICR ($\sim 100\,000$), to ensure higher mass accuracy and to enable confident discrimination between co-eluting, isobaric compounds in complex mixtures. The orbitrap analyser has also been coupled to a linear ion trap, allowing high resolution spectra while simultaneously conducting data-dependent MS/MS in the ion trap to aid identification of unknown metabolites (Hogenboom *et al.*, 2009) as MS^n alone is not adequate for metabolite identification. A limited number of studies have reported the use of linear ion orbitrap in metabolomic analysis of microbes (Herebian *et al.*, 2009b), plants (Herebian *et al.*, 2009a), and animals (Dunn *et al.*, 2008; Zhang *et al.*, 2009).

1.4.7 Hybrid Instruments

The power of a given mass analyser can be increased by coupling to it another of the same or different type to obtain desirable performance characteristics. For example, QTOF or a hybrid quadrupole linear ion trap (QqQLit) (also referred to as QTRAP) mass spectrometer systems have special advantages in MS/MS studies, such as providing structural elucidation of metabolites. In the case of the QTOF, accurate mass measurements in the TOF can be performed on precursor or product ions. The QTRAP has the standard configuration of a QQQ mass spectrometer; however, Q3 can be operated as a linear ion trap on demand. This enables a number of scan functions; product ion scanning, precursor ion scanning (PI), natural loss scanning, and multiple reaction monitoring (MRM) as depicted in Figure 1.4. In addition to these scan functions common to a QQQ; the linear ion trap also includes Enhanced

MS (EMS), Enhanced Product Ion (EPI), MS³, Enhanced Resolution (ER), Enhanced Multiply Charged (EMC), and Time Delay Fragmentation.

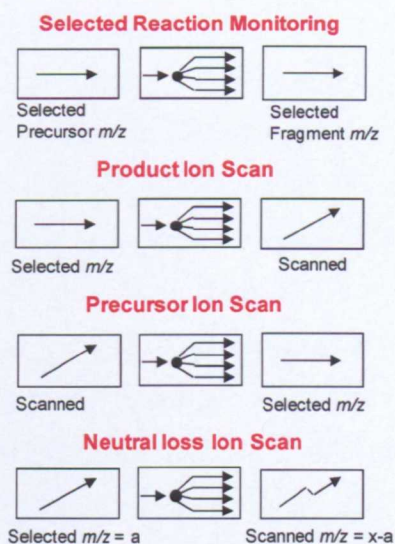


Figure 1.4 Main MS/MS scan functions offered in tandem mass spectrometry.

The definitions of these scans are as follows: MRM (also referred to as single reaction monitoring (SRM)) consists of monitoring a fragmentation reaction, in which Q1 and Q3 are focused on selected masses. PI scanning consists of selecting a common fragment to monitor in order to determine the precursor ions. All the precursor ions that produce ions with the selected fragment mass in Q3 will be detected. EPI is generally coupled to an information dependent acquisition (IDA) function, whereby if the detected analyte signal meets a certain criteria (i.e. signal intensity), ions transmitted to Q3 are accumulated and scanned out to produce full ion spectra.

1.5 Multivariate Data Analysis

Multivariate analysis (MVA) can be broadly thought of as the application of mathematical and statistical methods for the aid of pattern recognition (PR) in chemical numerical data (Lindon *et al.*, 2004; Robertson, 2005). Metabolomics data, by definition, is multivariate since there are multiple measurements per sample, which typically exhibit correlated traits. Thus, MVA or PR is necessary for the investigation of such data (for example, spectra obtained from ^1H NMR spectroscopy or mass spectrometry), due to the fact that visual interpretation is impractical and the user will often miss the correlations between measurements, which will greatly reduce the amount of information that can be extracted from the dataset. Currently, the PR strategies typically pursued in metabolomics fall under the heading of ‘unsupervised’ and ‘supervised’, in order to generate the models depicted in Figure 1.5. Indeed, the general aim of PR is to classify an object or predict the origin of an object, based on the inherent patterns in a set of experimental measurements or descriptors in a way that will allow biological interpretation (Lindon *et al.*, 2004; Lindon *et al.*, 2003a). Like other ‘omic’ data, patterns provide one level of information, but the spectra can be drilled down to obtain the identification of individual components within the sample mixture (Robertson, 2005). Thus, MVA is an essential tool for investigating such data. However, there are obvious cost implications in terms of instrument time and ‘man-hours’ for the analysis of the data obtained. Though, through computational advancement in both hardware and software, these methods can now be achieved in a reasonable time frame.

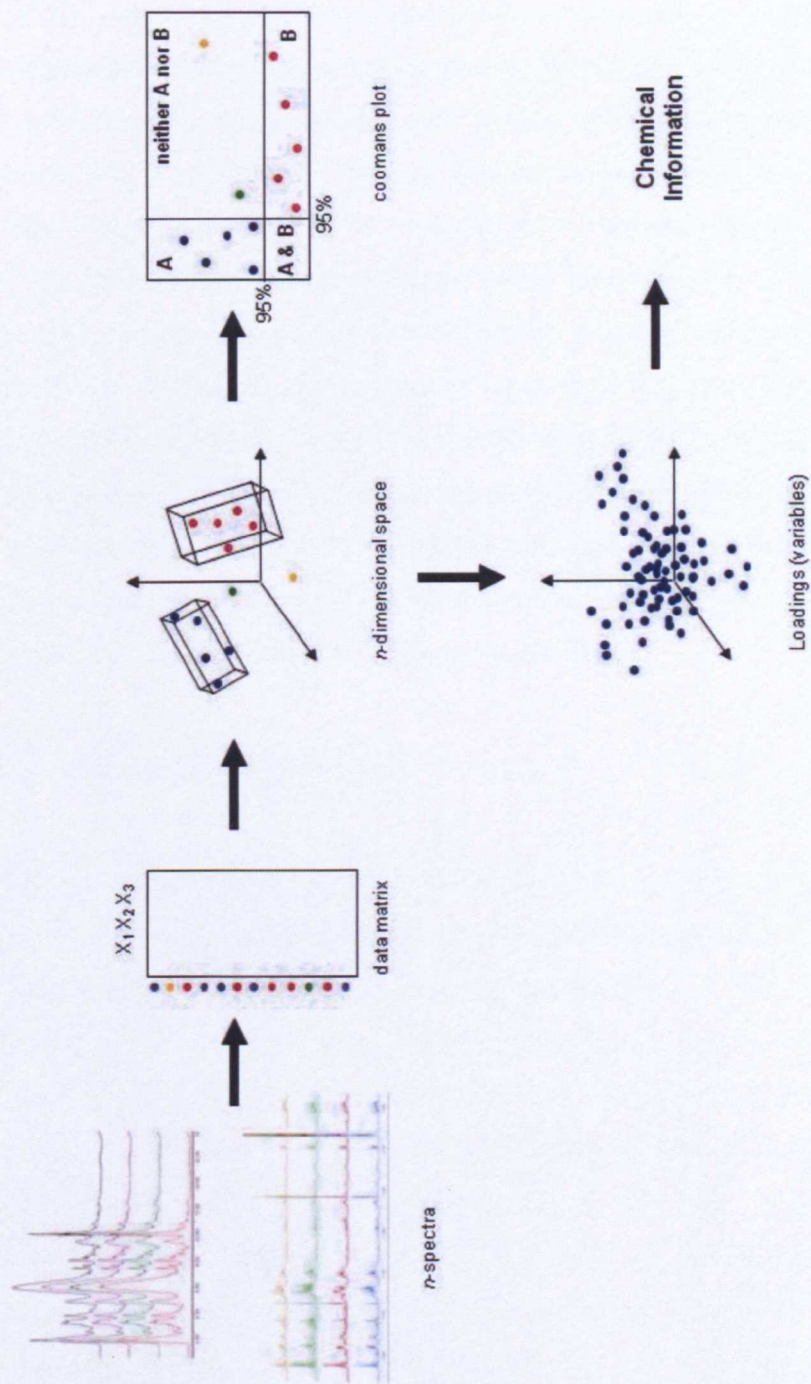


Figure 1.5 Schematic diagram representing the process of assessing sample class from raw data obtained from either NMR or LC-MS. Reproduced with modifications (Holmes and Antti, 2002).

As mentioned previously, metabolomics data are essentially multivariate. Thus, the starting point for data analysis is a single matrix $N \times D$, where N is the number of samples (either biological or technical replicates) and D is the number of metabolites or variables. In the case of NMR data, the variables are often the chemical shift values, while for MS data this is most commonly represented as m/z . Each independent variable may be regarded as constituting a different dimension, thus, for n variables, the object resides at a unique position in n -dimensional hyperspace (Goodacre *et al.*, 2007). Thus, the underlying theme of MVA is simplification or dimensionality reduction, for example, from several hundreds of peaks to a few coefficients, thereby facilitating in the aid of visualization of inherent patterns within the data. This may be achieved by unsupervised dimensionality reduction (through the use of projections), clustering (identifying groups of points which are similar to each), and supervised pattern recognition or machine learning (where knowledge about class membership is used to help discriminate between groups). It is beyond the scope of this thesis to describe in detail all the available methods on multivariate analysis; however, the following resources will provide a good overview (Beebe *et al.*, 1998; Duda *et al.*, 2001; Everitt, 1993; Hastie *et al.*, 2001).

1.5.1 Pre-processing of Data

Data pre-processing is arguably the most important stage of data analysis as the quality of any model produced will solely depend on the quality of the data presented (Daykin and Wulfert, 2006), i.e. garbage in, garbage out. The data initially collected by the analytical instrumentation is classed as raw data, which then can be exported in multiple different computer readable formats (generally for compatibility) before the pre-processing can be performed. The first stage of pre-processing is to reduce the file size, through reduction in data complexity, in order to make analysis less computationally extensive as well as presenting the data in a format suitable for a range of software packages such as SIMCA P (Umetrics, Umeå). The second stage is to remove or reduce any inaccuracies so that a single metabolite is reported as one feature. In terms of NMR data, one method would be to use integrals of a specific spectral peak. However, this is not only computational intensive, it can also be detrimental to the production of useful multivariate models because of any slight

variation of peak chemical shifts which can be brought about *via* changes in pH or ionic strength between samples. For example, citrate is particularly sensitive to these changes and whilst these shifts pose little problem by eye, from a data analysis perspective, if a certain peak is not consistently being expressed in the same position, the model will interpret the change as a different metabolite, making the model redundant. However, calculating the peak areas within specified segments, commonly referred to as ‘bucketing’ or ‘binning’ (Holmes *et al.*, 1997; Spraul *et al.*, 1994a), into bin widths of 0.04 ppm is a common tactic to solve this problem, as illustrated in Figure 1.6. This approach is adequate in most cases, though, it can be rather crude, as subtle metabolic differences between groups of data may be lost. For this reason, several authors prefer to align peaks with genetic algorithms, especially for high-resolution NMR data. Thus, a number of approaches have been proposed for this (Forshed *et al.*, 2003; Kassidas *et al.*, 1998; Lee and Woodruff, 2004; Stoyanova *et al.*, 2004; Vogels *et al.*, 1993). However, these are generally not feasible in metabolomic studies since the spectra can show either the complete loss of some peaks or appearance of new peaks. MS based data are generally converted from a 3D matrix of time vs mass vs intensity, to a matrix of chromatographic peaks (with associated retention time and accurate mass) and peak area. This deconvolution can be achieved either by using the manufacture’s proprietary software (e.g. MarkerLynx supplied by Waters and SIEVE supplied by Thermo Scientific), or converting the raw data to produce a text-based file known as NetCDF (network common data format) (Rew and Davis, 1990), in order to use open-source software such as XCMS, Metalign, MZmine, MathDAMP (Baran *et al.*, 2006; Katajamaa and Oresic, 2005; Lommen, 2009; Nordstrom *et al.*, 2006).

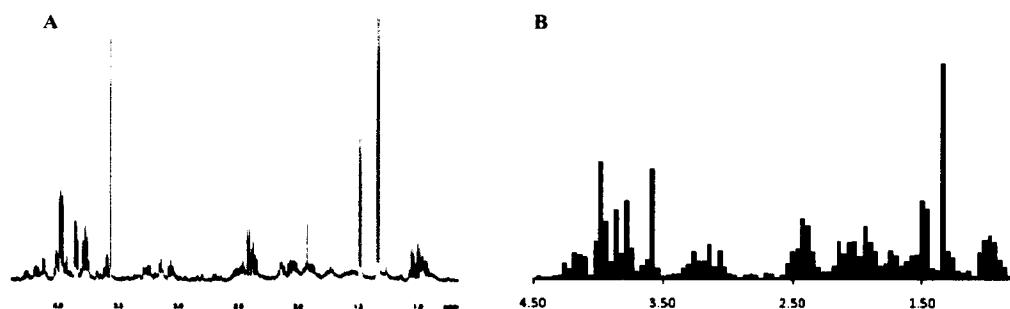


Figure 1.6 An example of **A** NMR spectrum **B** segmented spectrum after bucketing to a width of 0.04 ppm. Own data obtained from the analysis of human apocrine sweat.

1.5.2 Data Pre-treatment Methods

Different pre-treatment methods can be used for generate MVA models, which can affect the level of biological information obtained. The two main methods currently used in metabolomics studies are mean centring and unit variance scaling (also known as auto scaling) (Eriksson *et al.*, 2001). Mean centring focuses on the differences in the data and not the similarities by removing the offset from the data to zero, instead of around the mean of each metabolite concentration. However, this can bias the model to the metabolites that are higher in concentration. Unit variance compares metabolites based on correlations, as all metabolites have a standard deviation of one (i.e. become equally important). Thus, large peaks that dominate the spectra are treated as equally as small peaks. However, this can have undesirable effects as the baseline noise is inflated. These data pre-treatment methods, as well as other less common scaling and transformation methods are described further by van den Berg (van den Berg *et al.*, 2006).

1.5.3 Principal Component Analysis

Probably one of the oldest and most used techniques of multivariate analysis is PCA, which allows the expression of most of the variance within the data set in a small number of factors or principal components (PCs). This is achieved by transforming the original set of variables into a new set of uncorrelated variables called PCs. These new variables are created from linear combinations of the initial descriptors with appropriate weighted coefficients. Indeed, this reduces the dimensionality of the data set while accounting for as much variation as possible. The properties of the PCs are such that each PC is orthogonal (uncorrelated) to each other and that each successive PC explains the largest variation of the data set not accounted for by the previous PCs. Thus, this will remove any 'noise' since after the first few PC, the axes will be due to random noise in the data set. Hence, the first few PCs will describe most of the variation, but the number is dependent upon the application e.g. for clinical applications you may use many more. Plotting two PCs summarises the observations in K-space by projecting each variable along each PC. The co-ordinate values on this plane are called scores, hence, plotting the projected configuration is known as a score

plot. Observations which are close to one another are similar in composition, whereas observations which are at opposite sides are significantly different. In order to determine which variables are influential or how the variables are correlated, a loading plot is used. The loadings define the orientation of the PC plane with respect to the original variables. Thus, variables which are inversely correlated are positioned in opposite sides of the plot and the distance from the origin represents how influential each variable is on the model.

1.5.4 Partial Least Squares Regression

There are a large number of supervised methods (i.e. class membership of the samples are included in the calculation). One of the most popular is PLS (Partial Least Squares), which is commonly used to determine whether a relationship exists between two matrices, **X** and **Y**. The **X** matrix usually comprises of spectral or chromatographic data, while, the **Y** matrix contains quantitative values for those samples (*a priori* knowledge), for example, concentration, drug dosage or storage time (Lindon *et al.*, 2006; Trygg *et al.*, 2007). These relationships are derived through the use of latent variables of the original matrix **X** (known as the predictor variable) and the observed vector **Y** (known as the response variable), which are acquired by an iterative procedure. These latent variables are used to create linear combinations of columns (**X** and **Y**) so that their covariance is maximised. When the first latent vector is found, it is subtracted from both **X** and **Y** and repeated until **X**'s components tend to a zero value (Wold *et al.*, 1999). The resulting model can then be used to predict the analyte concentrations or examine the influence of time on a data set from the spectra of a new sample.

1.5.5 Principal Component Discriminant Analysis

PC-DA can be considered when more than two **Y** variables are being compared at any one time. It has the ability to summarise metabolite differentiation between-group variability, while overlooking within-group variation. Initially, the mean spectra for each class are calculated as per PCA, in order to construct significant limits for each specified class. Then the individual spectra, from each class, are projected onto the

PCA model, illustrating how close individual samples are to their respective means. However, unlike PLS, classification and prediction performance can only be qualitatively measured.

1.6 Identification of Components

Identification of individual metabolites from the obtained data is not always mandatory, while in other studies it is a critical part for the biological interpretation. For commonly analyzed biosamples, such as blood and urine, this can be achieved by comparison with spectral databases (see Table 5.2 on page 155), literature, and two-dimensional NMR spectroscopy. Moreover, for MS based approaches, a workflow summarised in Figure 1.7, can be followed in order to reduce the number of initial hits from databases in order to putatively identify unknown endogenous metabolites which can then be later confirmed by spiking the sample with internal standards. Nonetheless, for other samples, which are less well reported, these avenues of investigation will not result in positive metabolite identification. In this case, separation techniques such as LC-NMR-MS are required to gain full structural information. LC-NMR-MS can allow unequivocal identification of metabolites where neither LC-NMR nor LC-MS alone could generate all the necessary information. Once identified, the information can be stored in a database for future reference.

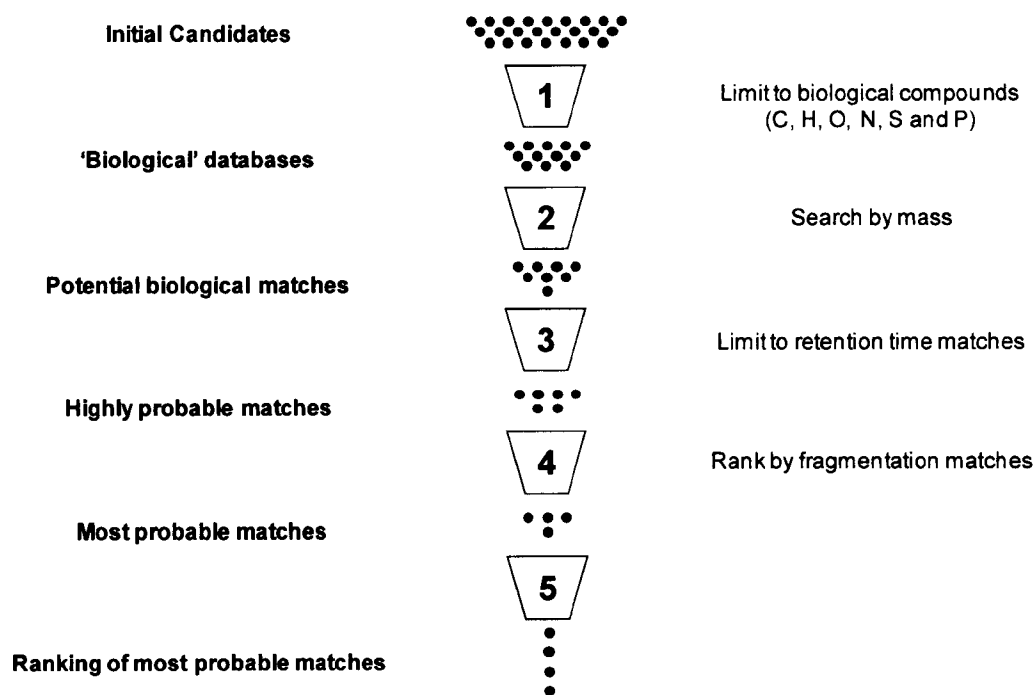


Figure 1.7 Summary of the proposed workflow for reducing potential matches from databases searches.

1.7 Sweat Gland Biology

Skin is regarded as the most versatile organ of the human body (Wilke *et al.*, 2007) and accounts for 12-15% of body weight (Gallagher *et al.*, 2008). A vast amount of research has been published on the different roles, either from a barrier function or as a first-line immune response system (Menon and Kligman, 2009). However, relatively few studies have focussed on sweat glands or their biology even though regulation of core body temperature by sweating is a fundamental process for survival. Constant core body temperatures above 40°C result in protein denaturation and cell death, resulting in multiple organ failure. Hence, the most useful purpose of the sweating mechanism is to down-regulate the body core temperature by releasing thermal energy through the evaporation of water from the skin surface.

The nervous system ultimately governs the rate of perspiration to meet the requirement of the body and therefore production increases in proportion to the level of environmental stress and metabolic rate. This process is regarded as thermoregulatory sweating and involves eccrine glands, which are distributed over the whole body surface. Since thermoregulatory sweating serves as a system for temperature reduction, failure in this system will therefore lead to hyperthermia and death (Wilke *et al.*, 2007). The onset of thermal sweating is caused when the sum of the internal body temperature has a 10-fold increase over the mean skin temperature, i.e. the internal temperature increases by a significant amount to what is experienced on the surface. It is also important to note that sweating can be affected by many internal factors such as gender, physical fitness, menstrual cycle and circadian rhythm as well as external factors like humidity. Thus, the sweating rate can vary from each individual. The onset of sweating can also arise from emotional stress (emotional sweating) or through the consumption of highly spicy food (gustatory sweating). The former is caused by a physical reaction to emotive stimuli, for example; anxiety, fear or pain, and can occur over the whole body but are mainly confined to the palms, soles, and axillary region (Allen *et al.*, 1973; Eisenach *et al.*, 2005). Thus, in this instance, sweating occurs independently of ambient temperature and decreases during relaxation (Wilke *et al.*, 2007). However, emotional sweating does not occur until the

onset of puberty, which leads to the assumption that apocrine and apoeccrine sweat glands are involved, as these glands become functional during this development stage (Lonsdale-Eccles *et al.*, 2003). Gustatory sweating on the other hand is the direct or indirect thermal effect of ingestion of certain foods (e.g. hot and spicy substances) and is confined to the face, scalp, and neck. Its onset is usually triggered within a few seconds of food entering the mouth, rarely by smelling of food and is not triggered through food reaching the stomach, chewing inert substances, or thought of food (Bloor, 1969; Bronshvag, 1978). Ingestion of food also causes an increase in metabolism, which leads to an increase in body temperature and the onset of thermal sweating.

1.7.1 Sweat Glands

Sweat glands are cutaneous appendages like hair follicles or sebaceous glands, forming tiny coiled tubes embedded in the dermis or subcutaneous fat. They contain myoepithelial cells, which, when contracted, squeeze the gland to discharge the accumulated secretions *via* the duct to the outer skin surface. Glands are characterised through their morphology or by their mode of secretion. For example: sweat glands secrete eccrine (secretion is released from the cell as a liquid without disintegration) or apocrine (secretion occurs via pinch off of outer cell parts) (Lonsdale-Eccles *et al.*, 2003; Wilke *et al.*, 2007). Through this distinction there are said to be two types of sweat glands: eccrine (also known as merocrine sweat glands) and apocrine glands. The morphology of the eccrine and apocrine sweat glands is depicted in Figure 1.8, whereby, the green (DiI stained) and red (Nileblue stained) outlines the coil cellular boundaries and nuclei respectively. While immunolabelling with MFG, a marker for eccrine glands, or CD15, a marker for apocrine glands, is also shown. Wilke and co-workers have reported a number of other antibodies that can also be used to differentiate between eccrine and apocrine glands in order to describe their structural diversity (Wilke *et al.*, 2006). The apocrine gland coil is ~800 µm in diameter (ca. to eccrine gland coil ~500-700 µm), with an outer and internal tubule diameter of ~200 µm and ~100 µm respectively. The duct and secretory coil is a very short straight tube (ca. to eccrine duct which is generally a corkscrew channel ~2000 µm in length) and is located near to the hair follicle. The secretory cells consist of a single layer of

columnar shaped cells situated near to the basal membrane. In comparison, the eccrine outer and internal tubule diameter is $\sim 120\ \mu\text{m}$ and $\sim 40\ \mu\text{m}$ respectively.

Sato and co-workers reported the existence of a third type of sweat gland which could not be classified as either eccrine or apocrine gland and showed characteristics of both, hence, it was termed the 'apoeccrine' gland (also known as mixed-type gland) (Sato *et al.*, 1987). It is questionable however, as to whether this third type of sweat gland exists. Recently, Bovell and co-workers (Bovell *et al.*, 2007) investigated the axillary skin of ten volunteers, and tried to identify apoeccrine glands by a means of serial sectioning histology and immunofluorescence using CD15, CD44, S100 and HMFG-1 antibodies. They concluded that no evidence of apoeccrine glands was found either by histology or by immunofluorescence. Thus, the lack of distinct features does not comply with the definition proposed by Sato (Sato *et al.*, 1987). To the author's knowledge, this work has not been repeated, thus, to overcome this controversy further investigations are needed on normhydrotic and hyperhidrotic patients, in addition to the effects of dissection on glandular appearance, to reveal if there really is a 'third' type of sweat gland.

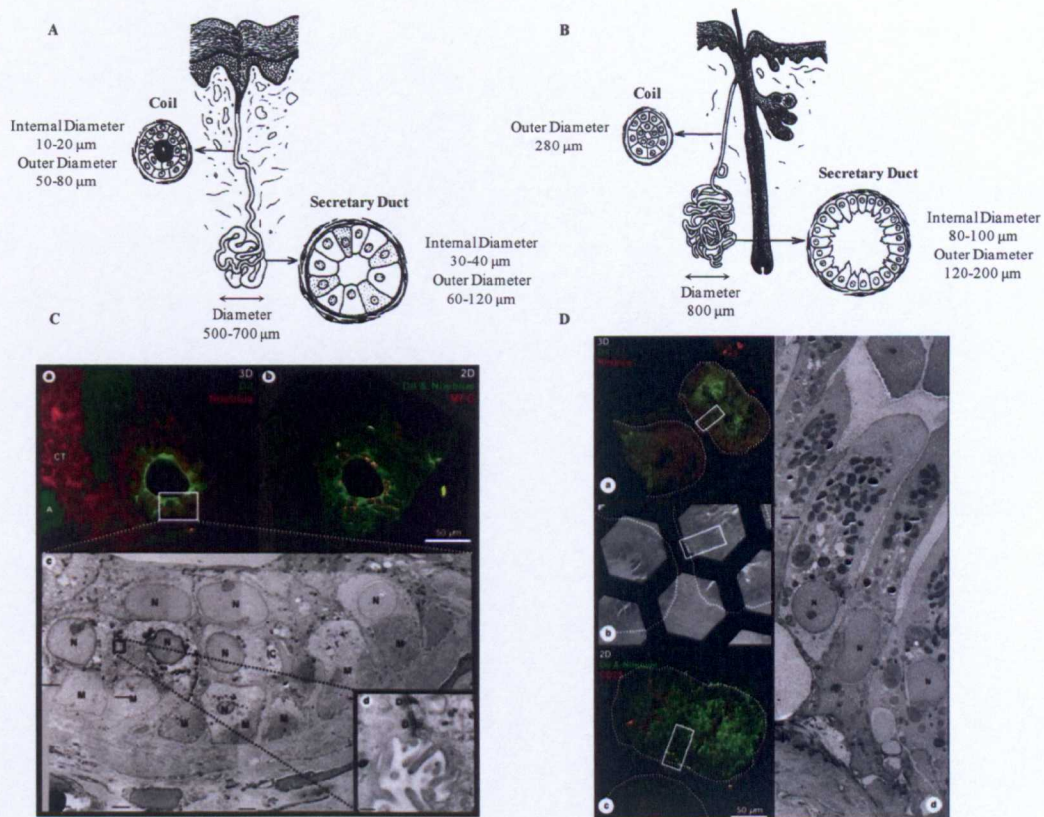


Figure 1.8 Upper: Schematic diagram of **A** eccrine gland **B** apocrine gland showing both a cross-section of the coil and duct. Lower: Correlative microscopy of **C** eccrine coil **D** apocrine coil. Myoepithelial cells (M), Intracellular canaliculi (IC), Nuclei (N), and desmosomal contacts (D). Reproduced with modifications (Weiner and Hellmann, 1960; Wilke *et al.*, 2008).

1.7.2 Chemical Composition of Eccrine Sweat

Excreted sweat can vary in composition and electrolyte concentration depending on the secretory and reabsorptive properties at the coil and duct, respectively. When sweat is initially formed in the secretory coil it is near iso-osmotic (Sato *et al.*, 1987), and following excretion the sweat is relatively hypo-osmotic and acidic (Patterson *et al.*, 2000). This change in sweat osmolality and acidity can vary between skin regions (Sato and Dobson, 1970), as it is reliant on the functional capacity of the sweat gland, which is ultimately governed by the ductal transport processes. From an analytical perspective this adds further complexity to the study of human sweat as variation in sweat composition can vary significantly within an individual.

Sweat is primarily composed of water (99%), and is therefore well suited for evaporative cooling. A diverse array of organic and inorganic compounds can be found in sweat, many of which are found in plasma but at much lower concentrations (Harker *et al.*, 2006), thus, sweat glands appear to selectively secrete some substances and retain others (Robinson and Robinson, 1954). There are approximately 61 compounds reported in eccrine sweat with varying concentrations reported in the literature (see Table 1.6). To the author's knowledge, there is no reported literature on electrolytes and ionic constituents, or their respective concentrations in apocrine sweat. However, it is likely they would be of similar magnitude. Furthermore, it is important to establish chemical composition of eccrine sweat as this could provide useful information in identifying components present in apocrine sweat, which will be discussed in further detail later (see Section 1.7.5).

Table 1.6 Median values of eccrine sweat constituents. Reproduced with modifications (Harvey *et al.*, 2010; Stefaniak and Harvey, 2006).

Components	Molecular Formula	Median (min and max) concentration (M)
<i>Electrolytes</i>		
Sodium	Na ⁺	3.1x10 ⁻² (1.1x10 ⁻⁴ - 3.9x10 ⁻¹)
Chloride	Cl ⁻	2.3x10 ⁻² (1.7x10 ⁻⁵ - 2.8x10 ⁻¹)
Calcium	Ca ²⁺	5.2x10 ⁻³ (4.7x10 ⁻⁶ - 1.5x10 ⁻²)
Potassium	K ⁺	6.1x10 ⁻³ (6.7x10 ⁻⁶ - 3.8x10 ⁻²)
Magnesium	Mg ²⁺	8.2x10 ⁻⁵ (7.4x10 ⁻⁸ - 3.8x10 ⁻³)
Phosphate	PO ₄ ³⁻	3.1x10 ⁻⁴ (2.3x10 ⁻⁵ - 1.1x10 ⁻³)
<i>Inorganic Ions</i>		
Ammonium	NH ₄ ⁺	5.2x10 ⁻³ (4.7x10 ⁻⁴ - 2.5x10 ⁻²)
Bicarbonate	HCO ₃ ⁻	3.0x10 ⁻³ (2.6x10 ⁻⁴ - 2.0x10 ⁻²)
<i>Ionic Species</i>		
Sulfate	SO ₄ ²⁻	4.2x10 ⁻⁴ (7.0x10 ⁻⁵ - 2.0x10 ⁻³)
Sulfur	S	2.3x10 ⁻³ (2.2x10 ⁻⁴ - 2.3x10 ⁻³)
Fluoride	F	1.1x10 ⁻⁵ (5.8x10 ⁻⁸ - 9.5x10 ⁻⁵)
Phosphorous	P	1.3x10 ⁻⁵ (2.2x10 ⁻⁸ - 1.5x10 ⁻³)
Bromine	Br	2.3x10 ⁻⁶ (4.4x10 ⁻⁹ - 6.3x10 ⁻⁶)
Cadmium	Cd	1.8x10 ⁻⁸ (1.2x10 ⁻⁸ - 2.3x10 ⁻⁸)
Copper	Cu	9.4x10 ⁻⁷ (1.3x10 ⁻⁸ - 1.2x10 ⁻³)
Iodide	I	7.1x10 ⁻⁸ (7.9x10 ⁻¹¹ - 7.5x10 ⁻⁵)
Iron	Fe	9.8x10 ⁻⁶ (1.5x10 ⁻⁸ - 1.1x10 ⁻³)
Lead	Pb	1.2x10 ⁻⁷ (3.5x10 ⁻⁹ - 2.0x10 ⁻⁷)
Manganese	Mn	1.1x10 ⁻⁶ (1.1x10 ⁻⁹ - 1.3x10 ⁻³)
Nickel	Ni	4.2x10 ⁻⁷ (1.7x10 ⁻⁹ - 8.3x10 ⁻⁷)
Zinc	Zn	1.3x10 ⁻⁵ (1.4x10 ⁻⁸ - 2.3x10 ⁻⁵)
<i>Amino acids</i>		
Alanine	C ₃ H ₇ NO ₂	3.6x10 ⁻⁴ (NA)
Valine	C ₅ H ₁₁ NO ₂	2.5x10 ⁻⁴ (1.3x10 ⁻⁴ - 3.8x10 ⁻⁴)
Leucine	C ₆ H ₁₃ NO ₂	2.1x10 ⁻⁴ (9.1x10 ⁻⁵ - 3.2x10 ⁻⁴)
Isoleucine	C ₆ H ₁₃ NO ₂	1.7x10 ⁻⁴ (7.6x10 ⁻⁵ - 2.8x10 ⁻⁴)
Phenylalanine	C ₉ H ₁₁ NO ₂	1.3x10 ⁻⁴ (6.1x10 ⁻⁵ - 2.1x10 ⁻⁴)
Glycine	C ₂ H ₅ NO ₂	3.9x10 ⁻⁴ (NA)
Threonine	C ₄ H ₉ NO ₃	4.5x10 ⁻⁴ (1.4x10 ⁻⁴ - 7.6x10 ⁻⁴)
Tyrosine	C ₉ H ₁₁ NO ₃	1.7x10 ⁻⁴ (6.6x10 ⁻⁵ - 3.0x10 ⁻⁴)
Aspartic acid	C ₄ H ₇ NO ₄	3.4x10 ⁻⁴ (NA)
Glutamic acid	C ₅ H ₉ NO ₄	3.7x10 ⁻⁴ (NA)
Histidine	C ₆ H ₉ N ₃ O ₂	5.2x10 ⁻⁴ (2.7x10 ⁻⁴ - 1.3x10 ⁻²)
Lysine	C ₆ H ₁₄ N ₂ O ₂	1.5x10 ⁻⁴ (9.6x10 ⁻⁵ - 2.2x10 ⁻³)

Table 1.6 continued

Components	Molecular Formula	Median (min and max) concentration (M)
Arginine	$C_6H_{14}N_4O_2$	7.8×10^{-4} (3.3×10^{-4} - 4.4×10^{-3})
Tryptophan	$C_{11}H_{12}N_2O_2$	5.5×10^{-5} (2.0×10^{-5} - 9.1×10^{-5})
Creatine	$C_4H_9N_3O_2$	1.5×10^{-5} (NA)
Ornithine	$C_5H_{12}N_2O_2$	1.5×10^{-4} (NA)
Citrulline	$C_6H_{13}N_3O_3$	4.0×10^{-4} (NA)
<i>p</i> -Aminobenzoic acid	$C_7H_7NO_2$	7.1×10^{-8} (5.8×10^{-9} - 1.8×10^{-2})
Hydroxy/Keto Acids		
Pyruvic acid	$C_3H_4O_3$	1.8×10^{-4} (1.0×10^{-7} - 1.0×10^{-3})
Lactic acid	$C_3H_6O_3$	1.4×10^{-2} (3.7×10^{-3} - 5.0×10^{-2})
Fatty Acids		
Acetic acid	$C_2H_4O_2$	1.3×10^{-4} (5.9×10^{-5} - 4.2×10^{-4})
Propionic acid	$C_3H_6O_2$	3.5×10^{-6} (1.2×10^{-6} - 7.4×10^{-6})
Butyric acid	$C_4H_8O_2$	2.4×10^{-6} (5.0×10^{-7} - 6.0×10^{-6})
Isobutyric acid	$C_4H_8O_2$	8.0×10^{-7} (NA)
Isovaleric acid	$C_5H_{10}O_2$	1.1×10^{-6} (2.0×10^{-7} - 4.5×10^{-6})
Hexanoic acid	$C_6H_{12}O_2$	9.0×10^{-7} (2.0×10^{-7} - 3.5×10^{-6})
Carbohydrates		
Dehydroascorbic acid	$C_6H_6O_6$	1.1×10^{-5} (7.6×10^{-9} - 8.6×10^{-4})
Glucose	$C_6H_{12}O_6$	1.7×10^{-4} (5.6×10^{-6} - 2.2×10^{-3})
Amino Ketones		
Urea	CH_4N_2O	1.0×10^{-2} (1.8×10^{-3} - 4.6×10^{-2})
Creatinine	$C_4H_7N_3O$	8.4×10^{-5} (8.8×10^{-6} - 2.0×10^{-3})
Purines and Purine Derivatives		
Uric acid	$C_5H_4N_4O_3$	5.9×10^{-5} (4.2×10^{-6} - 4.8×10^{-3})
Vitamins		
Choline	$C_5H_{14}NO$	2.6×10^{-5} (6.8×10^{-7} - 1.5×10^{-4})
Ascorbic acid	$C_6H_8O_6$	1.0×10^{-5} (1.1×10^{-7} - 3.6×10^{-5})
Inositol	$C_6H_{12}O_6$	1.6×10^{-6} (8.3×10^{-7} - 1.2)
Nicotinic acid	$C_6H_5NO_2$	4.1×10^{-1} (1.4×10^{-7} - 3.7)
Pantothenic acid	$C_9H_{17}NO_5$	1.3×10^{-1} (6.8×10^{-8} - 3.6)
Pyridoxine	$C_8H_{11}NO_3$	1.0×10^{-8} (2.4×10^{-9} - 5.0×10^{-3})
Riboflavin	$C_{17}H_{20}N_4O_6$	2.0×10^{-2} (1.3×10^{-8} - 8.0×10^{-1})
Folic acid	$C_{19}H_{19}N_7O_6$	1.6×10^{-8} (1.2×10^{-8} - 2.0×10^{-8})
Thiamine	$C_{12}H_{17}ClN_4OS$	5.0×10^{-3} (4.5×10^{-9} - 5)

The major cations (Na^+ , K^+ , Ca^{2+} , Mg^{2+}) and anions (Cl^- , PO_4^{3-} , HCO_3^-) located in sweat are similar to that found in plasma. The most concentrated solute in sweat is NaCl, which ranges from 5 mM to as high as 148 mM (Robinson and Robinson, 1954). Any salt depletion produced by sweating can cause heat cramps and fatigue resulting from the reduction in extracellular fluid volumes due to the reduction in tonicity. Furthermore, a relationship between sweat Na^+ concentration and pH has been reported, whereby, the greater the concentration of Na^+ the greater the pH (Kaiser *et al.*, 1974). Hence there is considerable variation in the observed pH of sweat. In the literature, the observed pH ranges from 2.1-8.2 (median 5.3) for eccrine sweat (Stefaniak and Harvey, 2006), which has been found to be more acidic than that of apocrine sweat (Robinson and Robinson, 1954).

Potassium concentration tends to be lower than that of sodium or chloride averaging approximately 4.5 mM. It has been reported by Locke (Locke *et al.*, 1951), that potassium concentration varies inversely with sodium concentration and that the ratio of Na/K varies directly with sodium concentration. While Patterson and co-workers reported a positive relationship between lactate and K^+ concentration (Patterson *et al.*, 2000).

Lactic acid and pyruvate have both been measured in sweat secretion, values of which range from 4-40 mM and 0.1-0.8 mM, respectively (Robinson and Robinson, 1954), of which, both substances are more concentrated than that of blood or urine. Despite lactate being present in high concentrations, little attention has been made to its functioning role within the sweat gland. It has been suggested that lactic acid may come from the blood for a regulatory purpose in preventing an excess accumulation of blood and tissue lactate (Robinson and Robinson, 1954). However, it is debatable as to whether lactate present in sweat is derived from blood lactate. Others have suggested that lactate is produced from the gland's metabolism (Gordon *et al.*, 1971; Sato and Dobson, 1971; Weiner and Vanheyningen, 1952). In the literature, it is currently unclear as to why there is such a varied concentration range in both lactate and pyruvate with respect to changes in temperature, sweating rate, sweating duration and acclimatisation, although these factors have been studied in regards to sodium and chloride concentration of sweat. Nonetheless, there have been a few studies highlighting an inverse relationship between lactate concentration and exercise

intensity (Lamont, 1987; Meyer *et al.*, 2007). Although, this relationship is likely be due to a dilution effect resulting from the increase in sweat secretion (Buono *et al.*; Green *et al.*, 2004).

Nitrogenous constituents of sweat vary in concentration when compared to blood plasma. For example: ammonia is typically 100 times more concentrated in sweat; urea is about twice as concentrated in sweat; amino acid concentrations are similar or slightly lower than in plasma, although the concentrations of individual amino acids may differ; and both uric acid and creatinine are more dilute in sweat. Typical nitrogen concentrations of sweat reported in the literature vary from 0.5-8 mM (Sato *et al.*, 1989). Other amino acids, including cysteine, methionine, proline, and serine have also been detected in eccrine sweat, however, their quantitative concentration have not been reported (Coltman *et al.*, 1966; Liappis and Hungerla, 1972; Stefaniak and Harvey, 2006).

1.7.3 Axillary Malodour Formation

The human body generates a variety of different odours, for example; scalp, hair mouth, axilla, foot, and general skin surface all possess characteristic odours. Of all the human scents, axillary odour is probably the most powerful and easily recognisable (Hasegawa *et al.*, 2004).

Axillary odours possess a distinctive malodorous scent communally called “body odour” which originates from the axilla regions. These regions contain a dense arrangement of apocrine, eccrine, sebaceous, and apoeccrine glands (see Table 1.7 for an overview between the differences of the glands), and volatile substances evaporating from these areas make a key contribution to human body odour (Zeng *et al.*, 1996a). This has been examined and discussed from an analytical, biological and a behavioural-physiology point of view (Hasegawa *et al.*, 2004). Although, in today’s society, body odour is deemed unpleasant, several studies have illustrated that axilla odour may contain chemical signals that affect the menstrual cycle (Natsch *et al.*, 2004), or that it may be involved in mate selection depending on the major histocompatibility complex (MHC)-allele (Natsch *et al.*, 2004). Axillary secretions

are an ideal source of pheromones, thus, are generally secreted into areas that often contain hair that can greatly increase the surface area for dispersion and aid in volatilization. Hence, axilla is a focal point for a multi-billion-dollar consumer product industry since the general consensus in today’s society is to eliminate or mask these body odours (Gautschi *et al.*, 2007; Wysocki and Preti, 2004).

Table 1.7 Difference between eccrine, apocrine and apo-eccrine sweat glands. Reproduced with modifications (Lonsdale-Eccles *et al.*, 2003; Sato *et al.*, 1989).

	Eccrine	Apocrine	Apo-eccrine
Age of onset of gland activity	Birth	Adolescence	Adolescence
Distribution of sweat glands	Whole body – excluding auditory canal, clitoris and labia minora	Axilla, breast and labia	Hair-bearing area of axilla
Stimulation	Cholinergic >> Adrenergic	Cholinergic = Adrenergic	Cholinergic > Adrenergic
Gland size	Small	Large	Variable
Location of secretory coil	Mid-dermis	Deep-dermis/fat	Deep-dermis
Duct	Long – connecting directly to skin surface	Short – connecting to hair follicle	Long – connecting directly to skin surface
Cell type	Secretory (clear), dark and myoepithelial	Columnar secretory cell, myoepithelial	Dilated segments resemble apocrine gland and non-dilated resemble eccrine glands
Sweat secretion rate	Continuous – high output	Transient and intermittent – low volume	Continuous – very high output
Gland product	Water fluid	Turbid fluid – protein rich	Water fluid

The ultimate source of axillary odour is apocrine sweat, which, when initially secreted is both sterile and odourless (Leyden *et al.*, 1981), and since the pioneering work of Shelly *et al.* (Shelley *et al.*, 1953), it is known that the action of skin bacteria is needed to generate the odoriferous components from the non-smelling molecules present within these secretions. Indeed, the axilla is a skin region supporting a dense bacterial population (~10⁶ cells cm⁻²), which are dominated by two genera *Staphylococcus* and *Corynebacteria* (Austin and Ellis, 2003; Natsch *et al.*, 2003), both of which are best adapted for the conversion of fresh apocrine sweat to the ‘classic male locker room smell’ (Troccaz *et al.*, 2004).

Most individuals carry a flora that is dominated by either one of these two genera; however, strong correlations between high populations of *Corynebacteria* and strong axillary odour formation have been found. For example, certain strains of *Corynebacteria* have been associated with the clinical condition of plantar bromidrosis (acute offensive body odour) (Troccaz *et al.*, 2004). Thus, *Corynebacteria* and certain *Staphylococci* possess all the enzymatic machinery required to carry out biochemical conversions of proteins, lipids and steroids into odorous components (Natsch *et al.*, 2004; Troccaz *et al.*, 2004). As practical consequence of these findings, the cosmetic industry introduced halogenated antibacterials and aluminium preparations for reducing bacterial populations as their main active ingredient in deodorants over the last 40 years (Gautschi *et al.*, 2007; Natsch *et al.*, 2003). Considerable progress has been made since these initial observations, in terms of identifying odorous compounds, however, there has been less attention to the biochemistry of axillary odour formation. Hence there is only a limited amount of literature available regarding the structures of precursors isolated from axilla secretions, and no specific bacterial enzymes capable of generating these precursors have been isolated.

1.7.4 Chemical Nature of Body Malodour

The composition of sweat odour comprises of four principle components. First, a steroidal fraction comprising of four pungent steroids, 5 α -androst-16-en-3-one, androsta-4,16-dien-3-one, and their respective alcohols, 5 α -androst-16-en-3 α -ol and androsta-4,16-dien-3 α -ol. It has only been recently that the identities of these volatile steroids precursors present in apocrine sweat have been identified (Austin and Ellis, 2003). From their discoveries, Austin and Ellis proposed a new metabolic map (Scheme 1.1) of the biotransformations needed to generate odorous components from non-odorous precursors. They also illustrated that no single bacterium isolated was capable of carrying out the full complement of enzymatic transformations, thereby, generating a blend of 16-androstenes. Furthermore, the overall ability of *Corynebacteria* to biotransform odorous steroids from androsta -5,16-dien-3 α -ol is low (Austin and Ellis, 2003).

acids such as isostearic acid (heterogeneous C₁₆₋₁₈ branched and unbranched fatty acids) are metabolised into a range of highly odorous 2-methyl-C₆₋₁₄ fatty acids (Troccaz *et al.*, 2004).

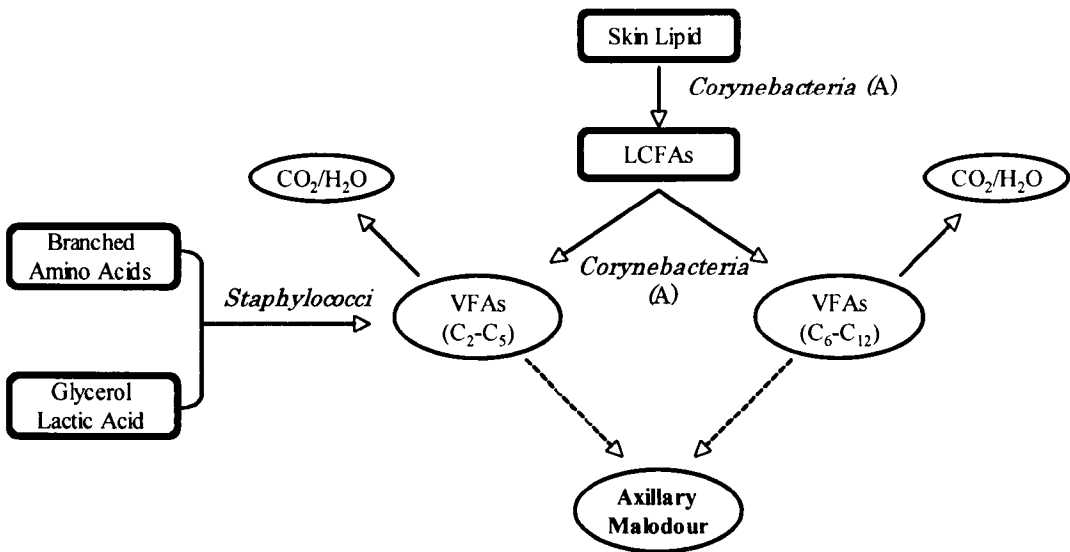
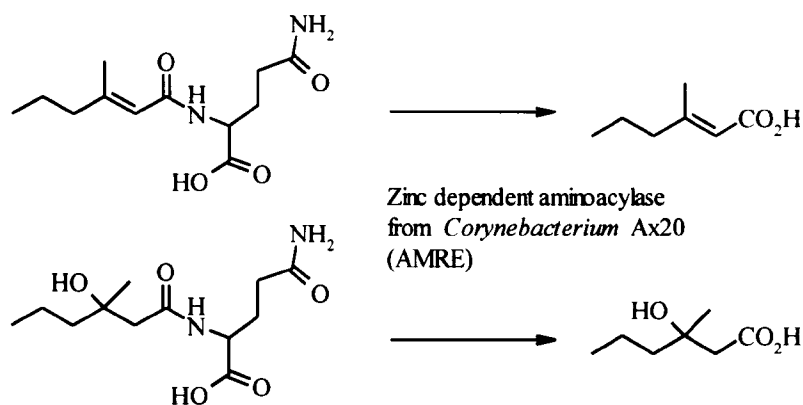


Figure 1.9 Formation of VFA by *Corynebacteria* and *Staphylococci*. Reproduced with modifications from (James *et al.*, 2004).

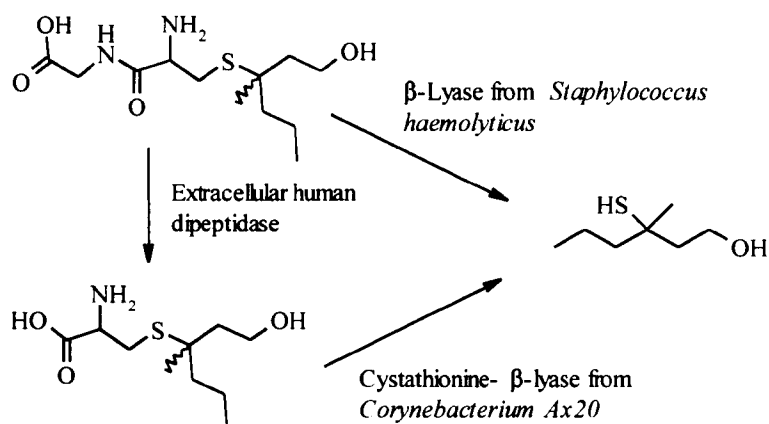
Thirdly, the predominant olfactory contributor in axillary sweat, (E)-3-methylhex-2-enoic acid (3M2H), is described as being the key odour component and was first presented by Zeng and co-workers (Zeng *et al.*, 1992; Zeng *et al.*, 1991). This compound had initially been found in the sweat of schizophrenic patients (Smith *et al.*, 1969) until Gordon and co-workers (Gordon *et al.*, 1973) showed that 3M2H was detectable in both normal population and schizophrenics, indicating there was no special relationship between 3M2H and schizophrenia (Akutsu *et al.*, 2006). In a later study, Spielmen and co-workers (Spielman *et al.*, 1995) illustrated that 3M2H was non-covalently associated with two proteins, which have been designated as apocrine secretion odour-binding proteins 1 and 2 (ASOB1, 45 kDa, and ASOB2, 26 kDa). The ASOB2 protein was identified as apolipoprotein D (apoD), a member of the lipocalin family of carrier proteins (James *et al.*, 2004; Zeng *et al.*, 1996a). However, Natsch and co-workers (Natsch *et al.*, 2003) produced a contradictory study, whereby, 3M2H and the chemically related 3-hydroxy-3-methylhexanoic acid (HMHA), are instead non-covalently bound to the carrier protein in the form of glutamine conjugates and

are released by the action of corynebacterial *N*-acylglutamine aminoacylase (Scheme 1.2). It was then postulated that once cleaved from the glutamine conjugate, the acids might be able to associate non-covalently with apoD (James *et al.*, 2004). More recently, Martin and co-workers described the relationship between axillary odorants and the *ABCC11* gene (Martin *et al.*, 2010). They reported that individuals who were AA homozygotic for single nucleotide polymorphism (SNP), 538G→A, leading to a G180R substitution, were found to have a significantly smaller amount of axillary odorants to those from AG and GG phenotypes. *ABCC11* gene has also been previously shown to function in the auditory canal, where, 538G→A SNP is associated with dry white ear wax phenotype that is predominant in Asians (80-95%) and rare in Africans or Europeans (0-3%) (Yoshiura *et al.*, 2006). This same SNP predominates in the Asian population, which nearly leads to a complete loss of typical body odour. The *ABCC11* protein is expressed and localised in the apocrine sweat gland and appears to have an essential role in the secretion or formation of glutamine precursors. Furthermore, the work presented by Martin *et al* (2010) is similar to the work present by Jacoby *et al*, where they reported the concentration of ASOB2 to be low or undetectable in Asians, compared to non-Asian subjects, where it was readily detected (Jacoby *et al.*, 2004). Thus, the relationship between ASOB2 and *ABCC11* protein and their regulation of odour production still needs to be assessed.



Scheme 1.2 Release of sweat acids from glutamine. Reproduced from (Gautschi *et al.*, 2007).

Finally, sulfanylalkanols, sulfur containing thiols; have also been shown to have a key role in the perception of sweat malodour, possessing a sweat/onion-like character. This is derived from the action of pyridoxal phosphate-dependent β -lyase activity (probably related to cystathionine β -lyase) upon secreted sulfur-containing amino acids (Scheme 1.3) (Natsch *et al.*, 2003; Troccaz *et al.*, 2004). However, this has been proposed without data on the structure of the secreted precursor or isolation of the bacterial enzyme, as structure elucidation has proven to be more complex. Furthermore, certain bacteria have been associated with β -elimination activity for cysteine S-conjugates, primarily through the action of lipase, β -cystathionase (an enzyme involved in methionine biosynthesis), γ -cystathionase, tryptophanase (a transaminase) and β -lyases (again involved in methionine biosynthesis, whereby they cleave the intermediate (S)-cystathionine) (Natsch *et al.*, 2004; Troccaz *et al.*, 2004). In addition, sulfanylalkanols were recently found to be bound to the Cys-Gly dipeptide in axilla secretions (Natsch *et al.*, 2006).



Scheme 1.3 Release of sulfanylalkanols from the Cys-Gly precursors Reproduced from (Gautschi *et al.*, 2007).

1.7.5 Natural Precursors/Apocrine Sweat Composition

Many years after the work of Shelley and co-workers (Shelley *et al.*, 1953), only speculations with respect to the chemical nature of apocrine sweat precursors were available. However, over the last decade a few authors have started to tackle this gap within the literature, mainly due to the analytical and computational advances, which enable the correct identification of these metabolites. Appendix A illustrates the full spectrum of compounds currently extracted from apocrine sweat (Natsch *et al.*, 2006; Natsch *et al.*, 2004; Troccaz *et al.*, 2004), while known odour precursors are summarised in Table 1.8.

Table 1.8 Summary of reported odour precursors present in human apocrine sweat. See Appendix A for full complement of metabolites reported in apocrine sweat.

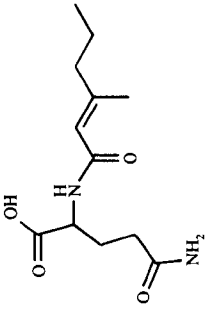
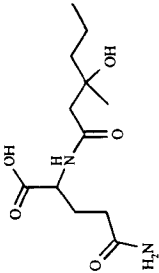
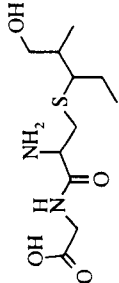
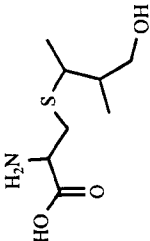
Components	Structure	Molecule	Mass	M+H	Other Names
N- α -3-methylhex-2-enoyl-L-glutamine		$C_{12}H_{20}N_2O_4$	256.1423	257.1501	Gln-conjugate + 3-Methylhex-2-enoic acid
N- α -3-hydroxy-3-methylhexanoyl-L-glutamine		$C_{12}H_{22}N_2O_5$	274.1529	275.1607	Gln-conjugate + 3-Hydroxy-3-methylhexanoic acid
S-[1-(2-hydroxy-1-methylethyl)-2-methylethyl]-L-cysteine/lycine		$C_{11}H_{22}N_2O_4S$	278.1300	279.1379	Cys-Gly-S-conjugate + 2-Methyl-3-sulfanylbutan-1-ol
S-[1-(2-hydroxy-1-methylethyl)-ethyl]-L-cysteine		$C_8H_{17}NO_3S$	207.0929	208.1007	Cys-conjugate + 2-Methyl-3-sulfanylbutan-1-ol

Table 1.8 continued

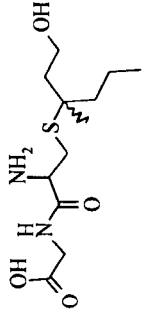
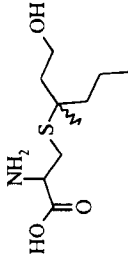
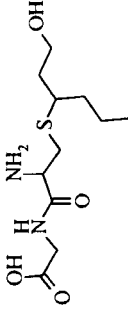
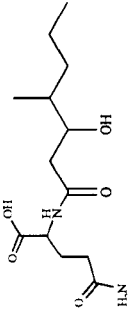
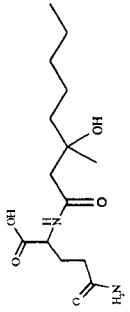
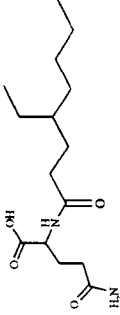
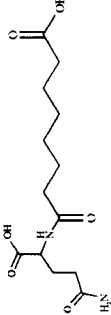
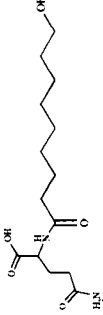
Components	Structure	Molecule	Mass	M+H	Other Names
S-[1-(2-hydroxyethyl)-1-methylbutyl]-L-cysteinylglycine		$C_{12}H_{24}N_2O_4S$	292.1457	293.1535	Cys-Gly-S-conjugate + 3-Methyl-3-sulfanylhexas-1-ol
S-[1-(2-hydroxyethyl)-1-methylbutyl]-L-cystein		$C_{10}H_{21}NO_3S$	235.1242	236.1320	Cys-S-conjugate + 3-Methyl-3-sulfanylhexas-1-ol
S-[1-(2-hydroxyethyl)-butyl]-L-cysteinylglycine		$C_{11}H_{22}N_2O_4S$	278.1300	279.1379	Cys-Gly-S-conjugate + 3-Sulfanylhexas-1-ol
N-α-3-hydroxy-4-methylhept anoyl- L-glutamine		$C_{13}H_{24}N_2O_5$	288.1685	289.1763	Gln-conjugate + 3-Hydroxy-4-methylheptanoic acid
N-α-3-hydroxy-3-methyloct anoyl- L-glutamine		$C_{14}H_{26}N_2O_5$	302.1842	303.1920	Gln-conjugate + 3-Hydroxy-3-methyloctanoic acid conjugate

Table 1.8 continued

Components	Structure	Molecule	Mass	M+H	Other Names
N- α -4-methyl-1-3-oct-enoyl- L-glutamine		$C_{14}H_{24}N_2O_4$	284.1736	285.1814	Gln-conjugate + (E)-4-Methyloct-3-enoic acid
N- α -3-methyl-2-oxopent-anoyl- L-glutamine		$C_{11}H_{18}N_2O_5$	258.1216	259.1294	Gln-conjugate + 3-Methyl-2-oxopentanoic acid
N- α -4-methyl-2-oxopent-anoyl- L-glutamine		$C_{11}H_{18}N_2O_5$	258.1216	259.1294	Gln-conjugate + 4-Methyl-2-oxopentanoic acid
N- α -4-ethyl-1-hept-anoyl- L-glutamine		$C_{14}H_{26}N_2O_4$	286.1893	287.1971	Gln-conjugate + 4-Ethylheptanoic acid
N- α -4-hydroxyphenyl-acetyl- L-glutamine		$C_{13}H_{16}N_2O_5$	280.1059	281.1137	Gln-conjugate + Phenylacetic acid

Table 1.8 continued

Components	Structure	Molecule	Mass	M+H	Other Names
N- α -4-ethyl-oct-anoyl- L-glutamine		$C_{15}H_{28}N_2O_4$	300.2049	301.2127	Gln-conjugate + 4-Ethyl octanoic acid
N- α -7-carboxy-hept-anoyl- L-glutamine		$C_{13}H_{22}N_2O_6$	302.1478	303.1556	Gln-conjugate + Octanedioic acid
N- α -9-hydroxy- non-anoyl- L-glutamine		$C_{14}H_{26}N_2O_5$	302.1842	303.1920	Gln-conjugate + 9-Hydroxynonanoic acid

It has been speculated that body odour formation arises from common metabolic pathways of skin microflora and therefore is a by-product of bacterial metabolism that utilises these sweat secretions, which are essentially the by-products of the body's metabolism. Examples of bacterial metabolism include the catabolism of L-leucine into isovaleric acid (3-methylbutanoic acid) and the formation of short acids by the incomplete degradation of skin lipids (Natsch *et al.*, 2003). However, the recently identified glutamine conjugate (3M2H-Gln) is somewhat contradictory. Thus, it is more likely that these compounds are synthesised specifically to exert their action once secreted in the axilla region rather than just being a by-product of metabolism. The actual benefit of being secreted in precursor form instead of direct secretion of the acids could be many fold. For instance, the use of a precursor would lead to a controlled release and make the chemical signal longer lasting. More of a physiological approach would suggest that transporting low molecular weight acids is more achievable when they are in a water-soluble precursor form (Natsch *et al.*, 2003). This would indicate co-evolution between skin micro flora and humans, since the bacteria have adapted their enzymes to recognise the precursor structure of axilla secretions.

The work produced by Natsch (Natsch *et al.*, 2003) has illustrated that the aminoacylase is unique, whereby, it is very selective for the Gln residue but has a very broad substrate specificity regarding the acyl part. This would readily lend itself to being more malleable to other Gln-containing precursor structures. Furthermore, they confirmed the findings of Zeng's group (Zeng *et al.*, 1991), that other branched amino acids are also present in axilla secretions. Although, it was highlighted that further investigations would be needed to identify if these too are linked to Gln-conjugates.

Thiols and methylsulfanyl metabolites, in which sulfur is derived from the glutathione, have been identified in secretion products of xenobiotics. Typically, glutathione-(S)-conjugates undergo enzymatic hydrolysis to yield Cys-(S)-conjugates, firstly, by the cleavage of the γ -glutamyl moiety *via* γ -glutamyl *trans*-peptidase and then followed by the action of a carboxypeptidase (Starkenmann *et al.*, 2005). The formation of volatile sulfur compounds from Cys-(S)-conjugates have

been described in wine, passion fruit, *Allium* species and have been described as the substrates for β -lyase. Starkenmann group also postulated that the production of the Cys-(S)-conjugate takes place before excretion of the sweat onto the skin surface. Furthermore, this group speculated that the formation of 3-methyl-3-sulfanylhexan-1-ol, 3-sulfanylhexan-1-ol, and 2-methyl-3-sulfanylbutan-1-ol are produced through their Cys-Gly-(S)-conjugates precursors.

Currently, there is lack of comprehensive analytical approaches to measuring the complex biochemicals excreted in apocrine sweat. Thus, this study exploits a range of LC-MS platforms and NMR techniques, coupled with a modern metabolomics approach, to provide further information in understanding the underlying physiological biochemistry of malodour. Global profiling *via* LC-MS, using high mass accuracy instrumentation such as QTOF or an orbitrap, and NMR will provide complementary metabolite information (Lanza *et al.*, 2010; Lenz *et al.*, 2004; Williams *et al.*, 2005a). This approach is typically used when biological knowledge is limited. A large number of metabolites are detected without *a priori* information, thereby, increasing the complexity of the data and as a result does not provide automatic chemical identification. Metabolite identification is currently one area that requires significant development, typically with LC-MS data. In comparison to NMR data, metabolite identification is less complex due to NMR databases being relatively well defined. The information obtained, coupled to MVA techniques, aims to identify inter- and intra-individual differences as well as providing further knowledge into the chemical composition of apocrine sweat. Targeted or semi-targeted LC-MS will provide information about metabolites of interest (either monitoring for specific metabolites using unique MRMs or a survey analysis for the same class of metabolites such as odour precursors). These strategies require the use of QQQ mass spectrometers which provide greater specificity compared to that of a QTOF or orbitrap spectrometers. The data obtained is often less complex than data obtained from global methodologies. Furthermore, targeted methodologies provide an increase in sensitivity (readily detecting sub picomolar concentrations) and provide quantitative information when using internal standards. Thus, the targeted methodologies will be able to screen for known odour precursors, while the semi-

targeted methodology using PI scanning provides the ability to screen for known and unknown odour precursors present in human apocrine sweat.

1.8 Aims of the Thesis

The overall aim of this project is to develop analytical methods that will ultimately allow the composition of axillary malodour to be identified, with particular reference to identifying new odour precursors. The project aims to achieve this by: -

- Developing and optimising, both NMR and LC-MS methodologies for the global analysis of human apocrine sweat secretions
- Developing and optimising mass spectrometry methodology for the analysis of conjugated fatty acids and thiols present in human apocrine sweat secretions
- Assessing inter-subject variability
- Assessing intra-individual differences between secretion obtained from the left and right arm
- Providing further knowledge to the chemical composition of human apocrine sweat

Chapter 2

2 Development of ^1H NMR Spectroscopy Methodology for the Metabolomic Analysis of Apocrine Sweat

2.1 Introduction

NMR spectroscopy is one of the major technologies for metabolic profiling (Griffin, 2006; Lindon and Nicholson, 2008) due to its ability in providing comprehensive chemical information about unknown metabolites as well as providing information on a variety of dynamic processes, such as protein ligand binding (Liu *et al.*, 1997; Luo *et al.*, 1999; Medek *et al.*, 2000; Pellecchia *et al.*, 2002). Moreover, NMR spectroscopy benefits from being a specific and yet a non-selective technique (i.e. independent of the chemical properties of the metabolites being analysed). This means each observable resonance is specific to a particular metabolite, thereby, aiding identification of individual constituents. Moreover, the same observable nuclei (i.e. all ^1H) have the same sensitivity, thus, in theory absolute concentration of metabolites can be determined when measured with an internal standard (e.g. TSP). The majority of biological samples analysed by NMR spectroscopy are measured in solution state, however, intact tissue samples using high resolution magic angle spinning (HR-MAS) can also be analysed (Sitter *et al.*, 2009). In addition, NMR requires minimal sample preparation, with only the addition of deuterated solvents such as D_2O or CDCl_3 to provide a frequency lock of the magnetic field as well as being non-destructive allowing several analyses to be conducted on the same sample. Currently, no NMR-based study to date has attempted to qualitatively and quantitatively profile endogenous metabolites present in human apocrine sweat. Thus, NMR spectroscopy could provide a powerful tool for the analysis of human apocrine sweat. However, apocrine sweat is secreted in low volumes, typically 5 μl , with the majority of the metabolites present being lower concentrations than those found in plasma. Thus,

NMR methodologies need to be developed in order to compensate for the restricted sample volumes.

Over the last 50 years, the field of NMR has developed a sophisticated array of experimental capabilities (Braun and Berger, 2004). For example, 1D NOESYPR1D pulse sequence provides good solvent suppression while a 1D ^1H Carr-Purcell-Meiboom-Gill (CPMG) pulse sequence (Meiboom and Gill, 1958) can be used to reduce signals from large macromolecules such as phospholipids triglycerides and lipoproteins which give rise to broad signals while retaining those from smaller molecules such as amino acids and carbohydrates (Foxall *et al.*, 1993; Harker *et al.*, 2006; Nicholson *et al.*, 1995). However, compared to other common spectroscopic methods of molecular characterisation, NMR is by far the least sensitive as shown in Table 2.1 (Lacey *et al.*, 1999).

Table 2.1 Limit of detection for common analytical techniques (Lacey *et al.*, 1999).

Method	LOD (mol)
Fluorescence	10^{-18} - 10^{-23}
Mass Spectrometry	10^{-13} - 10^{-21}
Electrochemical	10^{-15} - 10^{-19}
Radiochemical	10^{-14} - 10^{-19}
UV-Vis absorbance	10^{-13} - 10^{-16}
NMR	10^{-9} - 10^{-11}

NMR insensitivity stems from the fact that the energy levels of transitions are narrowly separated. Maxwell-Boltzmann statistics dictates that the population differences between the upper and lower energy states represents only a tiny fraction (<0.01%) of the nuclear spins from the total number of molecules (Lacey *et al.*, 1999). Thus, NMR spectroscopy can only detect and quantify metabolites present in relatively high concentrations, whereby, 20-40 metabolites are typically detected in tissues (Griffin *et al.*, 2001), 20-30 and 30-100 metabolites detected in blood plasma (Brindle *et al.*, 2002) and urine samples respectively (Connor *et al.*, 2004).

Historically, the need for relatively large sample volumes was dictated by the low sensitivity of the NMR instrument. However, modern advances in technology have brought about higher field strength magnets and a steady improvement of NMR probes, which have increased the overall sensitivity of the method (Eisenreich and Bacher, 2007; Schlotterbeck *et al.*, 2006). For instance, ultra high field NMR spectrometers (up to 900 MHz) and cryogenically cooled detector coils are available (Wishart, 2008). Nevertheless, analysis of micro volume samples, e.g. natural section of body fluid (apocrine sweat), still remains challenging (Schlotterbeck *et al.*, 2002).

The introduction of cryogenically cooled probes offers an increase in sensitivity by a factor of three to four compared to conventional probes by super cooling the receiver coil and preamplifiers to 25 K or below, resulting in a reduction of the thermal noise (Schroeder and Gronquist, 2006; Spraul *et al.*, 2003). However, the spectral dispersion of each signal remains the same (Schroeder and Gronquist, 2006). Nonetheless, in terms of cost implication, the cryoprobe offers considerable advantage over installing higher-field spectrometers, for example; 900 MHz only offers an increase in sensitivity by a factor of two as compared to at 600 MHz, therefore the increase in sensitivity is only modest in comparison (Rinaldi, 2004).

The simplest and cheapest approach to increasing the signal-to-noise without acquiring more expensive higher-field strength magnets or changing the RF coil is to use small sample tubes to decrease the volume required for acquisition. Typically, a total volume of 600 μ l is required for sample acquisition when using 5 mm OD NMR tubes, as this volume is enough to 'fill' the coil of the probe so the field homogeneity will not be disturbed. Specially designed tubes such as capillary tubes or spherical inserts can be used to limit the sample volume to just the volume of the receiver coil, while a Shigemi tube compensates for less volume by using D₂O matched glass. Thus, the aim of this chapter was to evaluate different NMR field strengths (400 and 500 MHz), probes (5 mm quattro nucleus probe (QNP), 1 mm micro-volume triple resonance inverse probe (TXI), and 5 mm TXI cryoprobe) and NMR tubes (e.g. standard tubes, Shigemi tubes, capillary tubes) in order to find the optimum analytical set-up which will ultimately be applied to the analyse of apocrine sweat which typically have 5 μ l sample size volume.

2.2 Aims

- To create an artificial sweat matrix suitable for method development.
- Establish suitable NMR methodology to provide the optimum sensitivity for the analysis of low sample volumes, which, will be later used for the analysis of apocrine sweat.
- Use multivariate analysis to determine whether any correlation exists between the storage lengths of the artificial sweat matrix.

2.3 Materials and Methods

2.3.1 Chemicals

Creatine, D₂O, pyruvate, and trimethylsilyl [2,2,3,3,-²H₄] propionate (TSP), was purchased from Fisher Scientific (Loughborough, UK). Citric acid, lactic acid, ornithine, and potassium phosphate were purchased from Sigma Aldrich (Poole, UK). Creatinine was purchased from Alfa Aesar (Heysham, UK). Neocate was purchased from SHS International Ltd (Liverpool, UK). Neocate is composed of dried glucose syrup, non-hydrogenated coconut oil, high oleic sunflower oil, refined vegetable oils (canola, sunflower), arginine, aspartate, leucine, lysine acetate, glutamine, calcium phosphate dibasic, proline, valine, emulsifier (E472c), tripotassium citrate, isoleucine, glycine, threonine, tyrosine, phenylalanine, serine, histidine, alanine, cystine, tryptophan, sodium chloride, methionine, magnesium aspartate, high arachidonic single cell vegetable oil, choline bitartrate, magnesium chloride, tricalcium citrate, ascorbic acid, potassium chloride, myo-inositol, high docosahexaenoic acid single cell vegetable oil, taurine, ferrous sulphate, zinc sulphate, carnitine, nicotinamide, DL-alpha tocopheryl acetate, calcium D-pantothenate, antioxidants (E304, E307 and E306), manganese sulphate, copper sulphate, vitamin A acetate, pyridoxine hydrochloride, thiamine hydrochloride, riboflavin, potassium iodide, folic acid, chromium chloride, sodium molybdate, vitamin K₁, D-biotin, sodium selenite, vitamin D₃ and cyanocobalamin.

2.3.2 Sample Preparation

Apocrine sweat is a complex mixture with a wide range of metabolite concentration with different chemical properties. This diversity together with limited sample availability creates an analytical challenge when developing analytical methodologies. Thus, an artificial sweat matrix was developed for the purpose of developing analytical methodologies and was not intended to replicate apocrine secretions *per se*. An artificial sweat model (see Table 2.2) was proposed through personal communication with Dr Mark Harker (Unilever). However, due to the complex nature of blood plasma, the premise of the artificial sweat matrix was based on an amino acid hypoallergenic infant formula from Neocate (www.neocate.co.uk). The use of the Neocate as a biological matrix meant that the full quantitative composition of all the components were known (see www.neocate.co.uk/aaa_neocate/15999-ingredients.html) compared to a biological matrix from blood plasma, which is considerably more complex. Thus, Neocate provided a suitable matrix that was well-defined (in comparison with blood plasma), protein free (allowing comparative evaluation of the metabolites without complication from protein binding) and contains both low molecular weight metabolites and lipids. Additional metabolites that have been reported in eccrine sweat were also added. Each metabolite (see Table 2.3) was individually weighed out and spiked into the Neocate to create the desired concentration and made up to 1 ml with phosphate buffer (pH 6, 0.1 M). For storage purposes, the stock solution was then aliquoted into smaller sample volumes of 40 µl and stored at either -20°C or 4°C until required.

Table 2.2 Artificial apocrine secretion model initially proposed for method development through collaboration with Unilever.

Ingredient	Level in µg/ml
Cholesterol	18.75
Cholesterol esters	0.25
Wax esters (lanolin)	0.9
Squalene	0.005
Glycerides (tristearin)	2.5
Fatty acids (stearic acid)	2.5
Lysozyme	40,000
ApoD	5,000
Zn -α-glycoprotein	5,000
Amino acids/conjugates	10,000
Glutamine conjugate	Estimate 5
Cysteine conjugate	Estimate 5
Carbohydrate (glucose)	1000
Androsterone sulphate	5
Dehydroepiandrosterone sulphate	5
Synthetic plasma with phosphate buffer (pH 6)	To 1 ml

Table 2.3 Artificial sweat matrix composition used for NMR method development. The amount of Neocate used was based on the amino acid content to reflect that of the apocrine secretion model above.

Metabolite	Level in mg/ml	Reference
Ornithine	0.017	(Coltman <i>et al.</i> , 1966; Liappis and Hungerla.H, 1972)
Creatinine	0.061	(Fukumoto <i>et al.</i> , 1988; Mosher, 1933; Stjohnlyburn, 1956)
Creatine	0.0079	(Stjohnlyburn, 1956)
Pyruvate	0.086	(Jin <i>et al.</i> , 2001)
Citric acid	0.068	(Leake, 1922)
Lactic acid	3.90	(Mosher, 1933; Patterson <i>et al.</i> , 2000; Stjohnlyburn, 1956; Weiner and Vanheyningen, 1952)
Neocate powder	61.48	
<i>Nutritional summary of Neocate</i>		
Protein equivalent	7.92	
Total amino acids	9.53	
Carbohydrates	33.12	
Sugars	3.01	
Fat	14.14	
As saturates	5.16	
Monounsaturates	5.53	
Polyunsaturates	2.77	

2.3.3 ^1H NMR Spectroscopy

The preparation of the artificial sweat mixture for ^1H NMR analyses varied depending on the type of NMR tubes being utilised. 5 μl of the actual amount of artificial sweat used remained constant, while the amount of D_2O containing a primary reference standard, trimethylsilyl [2,2,3,3,- $^2\text{H}_4$] propionate (TSP, ~ 7.6 mM) varied as follows: -

- Standard 5 mm OD NMR tubes, 650 μl D_2O .
- Shigemi tube, 300 μl D_2O
- Capillary NMR tubes, 180 μl D_2O
- Spherical insert, 10 μl D_2O
- 1 mm Micro-volume probe, 3 μl D_2O

^1H NMR spectra were acquired on a Bruker Avance 400 spectrometer, operating at 400.13 MHz ^1H observation frequency and equipped with a quadruple resonance (^1H , ^{13}C , ^{31}P , ^{19}F) QNP probe with an internal probe temperature of 298 K, a TXI 1 mm micro-volume probe equipped with Z-gradient with a internal probe temperature of 298 K and a Bruker DRX-500 spectrometer, operating at 500.18 MHz ^1H observation frequency, equipped with a triple resonance (^1H , ^{13}C , ^{15}N) cryogenically cooled TXI probe with an internal probe temperature of 303 K.

Spectra were acquired using a conventional solvent presaturation pulse sequence for solvent suppression based on the start of the NOSEY pulse sequence [RD- 90° - t_1 - 90° - t_m - 90° -acquire free induction decay], where 90° represents a non-selective 90° RF pulse, RD is a relaxation delay of 1.5 s during which the water peak was selectively irradiated, and t_1 corresponds to a fixed interval of 3 μs . Typically, 256 transients were collected into 32 K data points with a spectral width of 8000 Hz. Prior to Fourier Transform, exponential line broadening of 0.3 Hz was applied to FIDs which were zero-filled by a factor of 2. All spectra were manually corrected for phase and baseline distortions within TopSpinTM 2.1 (Bruker Analytische GmbH, Germany) and chemical shifts referenced to TSP standard at $\delta 0.00$ ppm.

2.3.4 Spectral analysis and metabolite quantification

Relative quantification of each identified metabolite peak was achieved by integration of ^1H NMR peaks using Bruker AMIX program. ^1H NMR can be used to analyse the relative concentrations of different metabolites because the area under each resonance is directly proportional to the number of nuclei giving rise to that resonance. Resonances from these metabolites were integrated along with those from the internal standard, TSP. The amount of each metabolite was then calculated in mmol/L using Equation 2.1 and then converted from molar concentration to mg/L afterwards.

$$C_m = \frac{I_m}{I_s} \times \frac{N_s}{N_m} \times C_s$$

Equation 2.1

where

- m = Metabolite
- s = Standard
- I = Peak area integral
- N = Number of protons
- C = Concentration

2.3.5 Data Pre-Processing

The ^1H NMR spectra were reduced into consecutive integrated spectral regions of widths 0.04 ppm using AMIX software (Analysis of MIXtures, Bruker), also referred to as “bucketing”. The region δ 4.50-5.18, surrounding the water resonance was excluded from the analysis in order to remove the effects of variations in the suppression of the water resonance. The resulting data matrix was exported into Microsoft Excel 2007 and block-normalised by calculating the intensity of each bucketed spectral region as a percentage of the total spectral area, in order to minimise the effects of any concentration differences between samples.

2.3.6 Partial Least Squares Regression (PLS)

PLS regression was carried out using SIMCA-P version 11 (Umetrics, Umeå, Sweden) in order to determine the covariance between the NMR profiles and the observed storage time. PLS regression is a well established technique for modeling biochemical data and has been thoroughly described and explained by Geladi and Kowalski (Geladi and Kowalski, 1986). PLS builds a regressive model by maximizing the covariance between a set of variables **X** and a dependent variable **y** and it thus called a supervised method. The model is then used to predict values of **y** for a given set of **X** variables. The number of latent variables (LV) used to predict **y** is determined using cross-validation where the sample set is divided into a number of segments which in turn are excluded before re-entering into the model in order to estimate the prediction error. The optimal number of LV's used in the prediction model is chosen when the least error in prediction is observed. To evaluate the models performance, a random sub-set cross-validation was used where two thirds of the samples were used to create a training set and a third used as a test set.

2.4 Results and Discussion

The basic premise underlying the development was to obtain the highest possible S/N ratio from a limited sample volume (5 µl). This enhancement was also coupled with the desire to be cost effective and user-friendly. It has been well documented that decreasing the sample concentration by half requires quadrupling the number of transients to maintain a given S/N (Martin and Hadden, 1999). It was on this basis that the comparison between 5mm OD NMR tubes, 1.7 mm capillary NMR tube, Shigemi tube as well as the use of the 1 mm NMR micro-volume probe on a 400 MHz spectrometer and 500 MHz with a cryo-probe was conducted. This study compared the results obtained from ¹H NMR spectra of artificial sweat matrix.

A typical 400 MHz ¹H NMR spectrum of the artificial sweat mixture is given in Figure 2.1. At this stage, all peak assignments are tentative, based on comparison against spectra of authentic reference standards contained in a spectral database. Verification of these peak assignments will require the acquisition of 2D NMR

spectra such as correlation spectra (COSY), total correlation spectra (TOCSY) and J-Resolved spectra (J-Res). However, due the composition of the artificial sweat matrix being well defined this was not necessary.

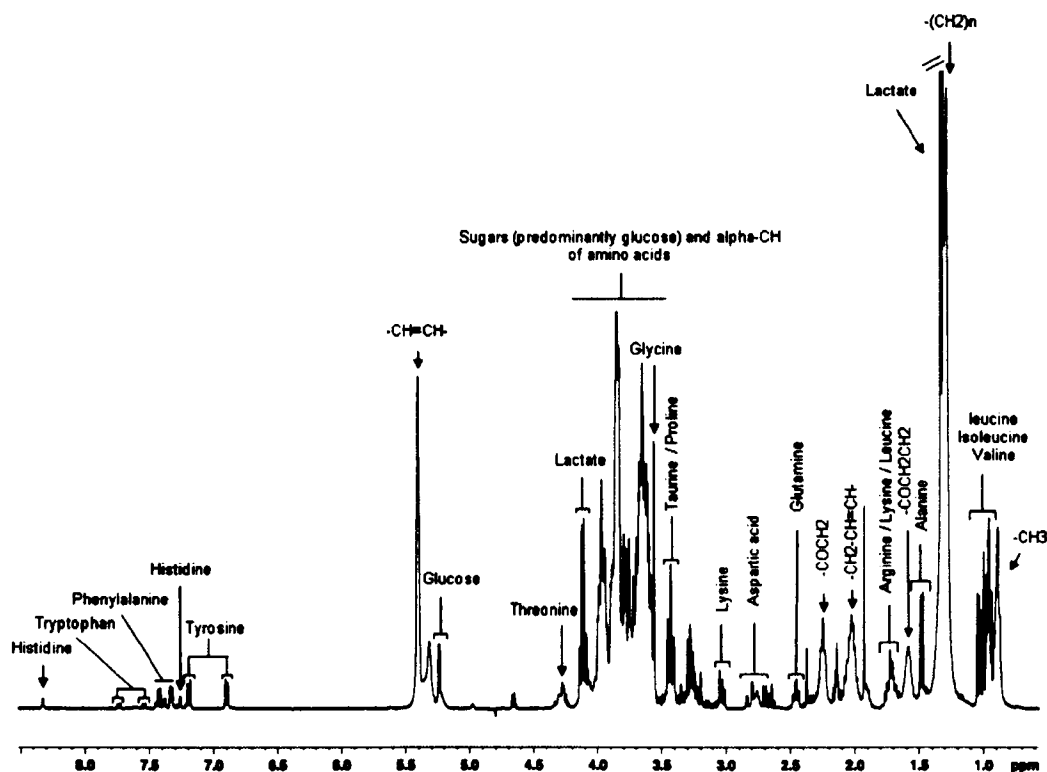


Figure 2.1 Typical 400 MHz ^1H NMR spectrum of artificial sweat mixture obtained using 1 mm micro-volume probe. The metabolites are tentatively assigned. Spectra were acquired using a standard 1D NOESYPRESAT sequence where $ns = 256$ scans.

2.4.1 Signal-to-Noise-Ratio

In NMR, the S/N is typically defined as the ratio of the height of any given peak in an NMR spectrum divided by two times the root mean-square of the noise floor (Lacey *et al.*, 1999). The sensitivity of an NMR experiment is governed by the properties of the probe for a given field strength and sample concentration. Other parameters such as the number of transients (ns) and total acquisition time (t_{acq}) can affect spectral results since the S/N ratio is proportional to the square root of the number of spectra

accumulated. Thus, the S/N ratio of a single scan can be increased by a factor of two by acquiring four scans, resulting in a four-fold increase in acquisition time. Similarly, the same S/N ratio may be obtained in one fourth of the time by doubling the sample concentration (Abraham *et al.*, 1988).

Table 2.4 highlights the mass sensitivity of the 5 mm QNP probe with the use of either capillary, Shigemi, and conventional 5 mm OD NMR tubes compared to that of a conventional 5 mm TXI cryo-probe and 1 mm micro-volume TXI probe.

Table 2.4 Comparing the signal-to-noise of detectable metabolites obtained from 5 mm OD standard NMR tube (600 μ l total volume), 2.5 mm OD capillary NMR tube (180 μ l total volume), 5 mm Shigemi tube (300 μ l total volume) and 1 mm micro-volume probe (8 μ l total volume) at 400 MHz and 500 MHz.

Chemical Shift (PPM)	Tentative Assignment	400 MHz		500 MHz Cryo-Probe			
		5mm Tube ^a	Capillary Tube ^b	Shigemi Tube ^c	1mm Tube ^d	5mm Tube ^e Capillary Tube ^f	
0.9	Lipid CH ₃	22.0 ± 1.3	35.5 ± 3.8	69.9 ± 5.9	163.1 ± 4.0	193.5 ± 14.1	131.9
0.96	Leucine/Isoleucine	23.7 ± 0.7	26.6 ± 3.2	48.3 ± 5.2	173.4 ± 10.9	221.2 ± 6.8	124.4
1.04	Valine	15.3 ± 1.7	13.3 ± 1.9	17.7 ± 3.8	99.3 ± 6.3	110.6 ± 4.3	57.4
1.29	Lipid CH ₂	71.4 ± 3.6	122.4 ± 15	261.4 ± 17.5	560.6 ± 20.1	610.0 ± 46.7	433.7
1.33	Lactate/Threonine	189.8 ± 25.4	185.8 ± 23	338.0 ± 47.7	1178.9 ± 54.6	1335.3 ± 68.5	758.4
1.48	Alanine	15.9 ± 2	13.4 ± 1.6	20.4 ± 3.1	99.5 ± 6.1	105.4 ± 5.3	55.5
1.59	Lipid COCH ₂ CH ₃	6.9 ± 0.6	11.7 ± 1.4	26.4 ± 1.8	57 ± 1.9	67.8 ± 5.6	49.0
1.72	Arg/Lys/Leu	6.9 ± 0.4	8.5 ± 0.8	16.5 ± 1.4	55.9 ± 4.3	49.1 ± 2.2	29.1
1.92	unknown/Arginine/Lysine	28.2 ± 7.7	17.2 ± 0.4	24.2 ± 6.1	166.2 ± 14	170.2 ± 11.0	81.9
2.03	Lipid CH ₂ -CH=CH	9.5 ± 0.5	15.4 ± 1.8	33.1 ± 1.7	85.3 ± 0.6	83.8 ± 6.0	58.8
2.14	Glutamine/Methionine	13.7 ± 0.7	8.7 ± 0.6	16.0 ± 2.4	55.3 ± 4.3	113.4 ± 8.3	44.9
2.26	Lipid COCH ₂	9.6 ± 0.5	17.1 ± 2	33.0 ± 2.7	82.3 ± 1.8	100.7 ± 7.8	69.4
2.37	Proline	4.5 ± 0.9	4.3 ± 0.9	7.8 ± 1.3	49.0 ± 4.8	46.0 ± 2.2	23.7
2.45	Glutamine	4.9 ± 0.9	4.4 ± 1	7.6 ± 0.8	28.0 ± 1.3	36.0 ± 2.3	17.1
2.64	Methionine	0 ± 0	0 ± 0	0 ± 0	21.8 ± 1.0	17.8 ± 0.3	10.9
2.81	Aspartic acid	3.7 ± 0.5	3.6 ± 0.3	7.1 ± 0.4	24.5 ± 1.3	26.3 ± 0.9	14.8
3.02	Lysine	4.8 ± 0.5	5.2 ± 0.3	9.1 ± 1.4	34.3 ± 2.6	35.4 ± 2.1	20.8
3.42	Proline/Taurine	18.1 ± 0.3	19.1 ± 1.9	34.1 ± 5.1	131.0 ± 9.5	149.5 ± 5.2	84.2
3.55	Glycine	29.6 ± 5.4	23.9 ± 2.0	35.5 ± 5.7	219.4 ± 18.0	200.9 ± 7.5	107.3
4.11	Lactate	24.2 ± 5.0	18.8 ± 0.4	32.1 ± 6.6	164.6 ± 10.8	169.6 ± 9.9	94.4
4.28	Threonine	0 ± 0	4.4 ± 1.2	8.3 ± 0.7	24.4 ± 0.5	28.2 ± 3.2	19.3
5.23	Glucose	8.8 ± 0.5	10.2 ± 0.5	20.5 ± 0.9	58.3 ± 3.4	83.6 ± 2.4	50.9
5.4	Lipid CH=CH	43.4 ± 2.2	53.3 ± 6.0	106.4 ± 7.8	303.8 ± 21	399.3 ± 13.9	231.8
6.9	Tyrosine	3.0 ± 0.7	2.7 ± 0.2	3.5 ± 0.3	23.9 ± 2.8	20.5 ± 1.2	10.0
7.55	Tryptophan	3.9 ± 0.6	4.0 ± 0.6	5.1 ± 0.7	23.2 ± 2.2	25.8 ± 1.1	20.2
7.36	Phenylalanine	3 ± 0.2	3.1 ± 0.3	4.5 ± 0.2	20.0 ± 1.6	20.7 ± 0.5	12.5
8.01	Histidine	0 ± 0	0.8 ± 1.3	2.9 ± 0.4	10.7 ± 1.6	11.5 ± 1.7	9.4

Number of analytical replicates: a, n=3; b, n=3; c, n=2; d, n=3; e, n=3; f, n=1

From a practical point of view, the conventional NMR tubes (OD 5 mm) which are filled to a total volume of 600 μl , are user-friendly and with the use of the cryo-probe offer considerable advantage over the same tubes used on the 400 MHz spectrometer.

The simplest approach to potentially increasing the S/N without having to upgrade the field strength or probe design is to use smaller sample tubes (which may feature deuterium matched glass) or tube inserts to decrease the total volume required for an experiment. In theory, if the sample volume is decreased by a factor of four then the concentration can be increased by a factor of four, however, the number of spins (^1H of each atom) detected remains constant (Lacey *et al.*, 1999).

The Shigemi tubes (which have a total volume of 300 μl) are expensive and difficult to handle, and unlike the options available above, automation is not possible and therefore labour intensive and for this reason these were only acquired on the 400 MHz spectrometer. The results obtained are illustrated in Table 2.4. The use of solvent susceptibility matched shigemi tube should improve solvent suppression, RF homogeneity and overall performance resulting in a two-three fold increase in sensitivity (Schroeder and Gronquist, 2006). As illustrated in Table 2.4, the general increase observed was two to three-fold when compared to standard 5 mm OD NMR tubes. However, due to the expense and labour intensive nature of preparing the samples for acquisition this method was not considered as a viable option.

The capillary NMR tubes (OD 2.5 mm, L 178 mm) reduced the total volume required to 180 μl . However, as illustrated in Table 2.4, only offered a marginal increase in sensitivity over the conventional NMR tubes and proved to be less sensitive when acquired on the 500 MHz equipped with a cryo-probe. The lack of increase in sensitivity could be related to the fill factor as the RF field can be inhomogeneous with space, which is determined by the probe design (Jahnke, 1996). Since the capillary tube is further away from the B_1 field, compared to the standard tubes, the accuracy of the NMR measurements therefore diminishes causing line-broadening effects and reducing the overall sensitivity.

Alternatively, the sample can be contained in a spherical microcell bulb as depicted in Figure 2.2, reducing the volume to 18 μl (www.wilmad-labglass.com/group/2015).

The PTFE holder holds the microcell within the standard 5 mm OD NMR tube, and the positioning rod allows one to insert and remove the assembly from the tube. Both the PTFE holder and positioning rod are reusable while the inserts are intended for one time use. It must be stressed that locating the active region of the RF coil is not a trivial task. Moreover, shimming the sample is also difficult due to the air/glass interface within the NMR coil, resulting, in inhomogeneity of the sample, which again contributes to further line broadening effects. As a result, no useful data could be attained from using this method.

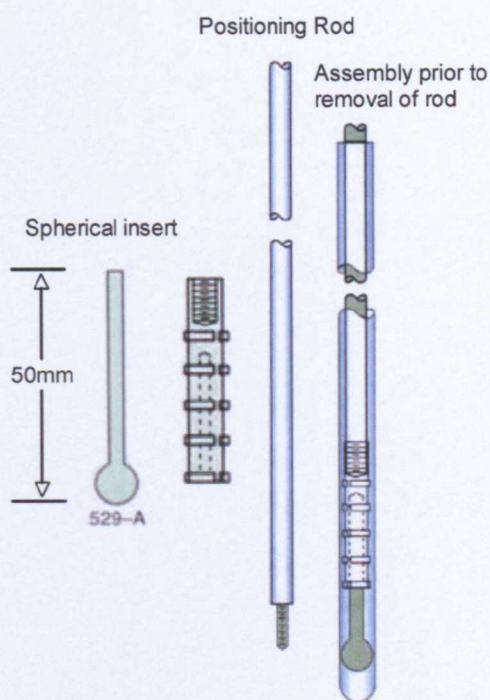


Figure 2.2 Schematic diagram of the 5 mm micro-cell assembly.

Micro-volume probes allow samples as small as 5 μl to be handled successfully; however, quantitative transfer of a sample this small from the container to the NMR tube is still problematic. This is especially true when dealing with rare samples (e.g. sweat) rather than a diluted stock solution, although this problem could be minimised *via* the use of robotics. Another consideration, which would not be problematic for larger volume sizes, is the rate of moisture sorption. With the sample handling problems aside, there are additional advantages to using a micro-volume probes. For

example, signals from solvent impurities are much less prominent and ‘solvent noise’ from electrically conductive solvents (salt containing solutions) is reduced (Martin and Hadden, 1999). Another advantage of using small volumes is the reduction in the amount of expensive deuterated solvents (Schlotterbeck *et al.*, 2002) as well as the reduction in data acquisition time.

The results obtained are illustrated in Table 2.4. The comparative performance in the study demonstrates that the 1 mm micro-volume probe offered at least a 5-8 fold performance advantage over data acquired with a 5 mm OD NMR tube and offered a similar S/N ratio of the standard NMR tubes acquired with 500 MHz equipped with a cryo-probe. Thereby, using small sample volumes without the need for diluting the sample, offered a considerable advantage in sensitivity over the other techniques examined. Compared to the 5 mm tubes, the mean enhancement of 7.8 represents a decrease in data acquisition time of 60.84 (7.8^2) or the ability to perform an experiment in the same amount of time with 12.8% ($1/7.8$) of the sample mass.

The S/N value is directly proportional to the active volume of the probe (V_{obs}) for a concentration-limited samples. Thus, if an NMR tube is placed in the probe which has a two-fold decrease in its inner diameter; V_{obs} is decreased four-fold, as well as the concentration sensitivity. Thus, to maximise the S/N, the tubes with the largest V_{obs} (up to the maximum allowed by the probe) should be used, but at the expense of using additional sample. While a reduction in the diameter of the receiver coil increases the S/N ratio (Schroeder and Gronquist, 2006), a reduction in coil diameter inevitably results in a decrease in the sample volume, thus, micro-volume probes will only provide a sensitivity advantage where the mass-limited sample is fully soluble in the smaller volume. However, for concentration-limited samples, micro-volume probes will offer no competitive advantage as the small probe will accommodate less of the sample compared to that of conventional probes.

Cryogenic probes substantially increase the S/N ratio as shown in Table 2.4. In general these probes offer an advantage when the sample concentration is low, 2D or 3D experiments are required due to the low intrinsic sensitivity, and when the experiment time needs to be reduced.

2.4.2 Application with Mass Limited Samples

The spectra depicted in Figure 2.3 clearly show the power of reducing the sample volume size for metabolite identification. Using the 1 mm micro-volume probe we have been able to acquire ^1H NMR spectra from a limited sample volume of 5 μl which has comparable sensitivity to that of the 500 MHz equipped with a cryo-probe.

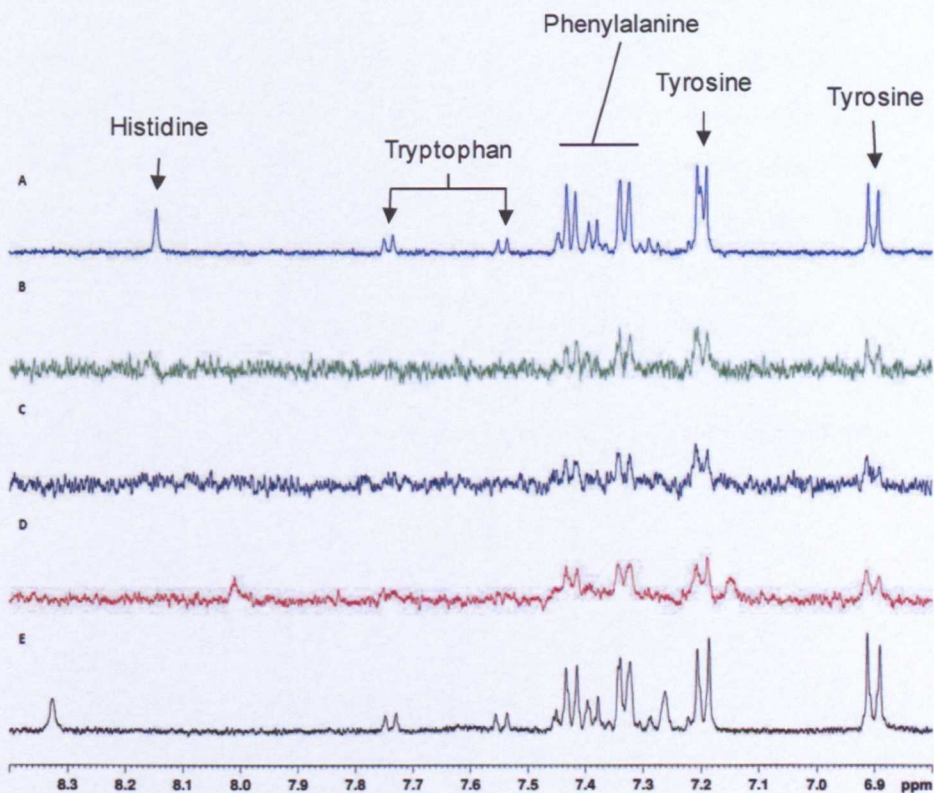


Figure 2.3 Spectra comparison of the artificial sweat matrix obtained from **A** 5 mm OD NMR tube acquired on a 500 MHz equipped with a cryo-probe. **B-E** acquired on a 400 MHz spectrometer with **B** 5 mm OD NMR tube **C** Shigemitsu tube **D** capillary tube **E** micro-volume probe.

The limit of detection (LOD) and limit of quantification (LOQ) are defined as being 3 or 10 times the intensity of the noise respectively (Olson *et al.*, 1998). This is shown in Table 2.5 and was calculated by using Equation 2.1, substituting I_m for the average noise intensity as previously reported (Savage *et al.*, 2011). The concentration LODs are in the low mg/ml range which may seem high, they correspond to nanomole amounts of sample, which is consistent with previous reports (Olson *et al.*, 1998). The ability to acquire high resolution spectra with 5 μ l samples with improved mass sensitivity can further increase NMR popularity to biological applications in cases where only a limited volume of biofluid is available. The reduced volume also has the added advantage of reducing the background noise, as there is a smaller signal from the residual protonated solvent which is less detrimental to the quality of the spectrum obtained. Furthermore, there is a reduction of the “solvent noise” arising from electrically conductive solvents such as salt containing solutions. This has been shown by Olson and co-workers, where they reported a reduction in the S/N of <10% from a 30 mM sucrose concentration in the presence of 500 mM KCl (Olson *et al.*, 2004). An additional advantage of small-volume NMR probes is the reduction in the amount of expensive deuterated solvents (often by two orders of magnitudes).

Table 2.5 Calculated limit of detection and limit of quantification of artificial sweat mixture. No adjustments have been made for differences in T_1 relaxation.

400 MHz																
Compound	5 mm Tube				Capillary Tube				Shigemi Tube				Micro-Vol Probe			
	LOD	LOQ	LOD	LOQ	LOD	LOQ	LOD	LOQ	LOD	LOQ	LOD	LOQ	LOD	LOQ	LOD	LOQ
	nmol	mg/L	nmol	mg/L	nmol	mg/L	nmol	mg/L	nmol	mg/L	nmol	mg/L	nmol	mg/L	nmol	mg/L
Ornithine	4.08	0.83	13.62	2.77	2.45	1.80	8.17	6.00	3.53	1.56	11.78	5.19	0.83	13.72	2.77	45.72
Creatinine	2.72	0.47	9.08	1.58	1.63	1.03	5.44	3.42	2.36	0.89	7.85	2.96	0.55	7.83	1.85	26.09
Creatine	2.72	0.55	9.08	1.83	1.63	1.19	5.44	3.97	2.36	1.03	7.85	3.43	0.55	9.07	1.85	30.24
Pyruvate	2.72	0.37	9.08	1.23	1.63	0.80	5.44	2.66	2.36	0.69	7.85	2.30	0.55	6.09	1.85	20.31
Citric acid	4.08	1.19	13.62	3.96	2.45	2.57	8.17	8.58	3.53	2.23	11.78	7.42	0.83	19.62	2.77	65.39
Lactic acid	8.17	1.13	27.23	3.77	4.90	2.45	16.33	8.17	7.07	2.12	23.55	7.07	1.66	18.70	5.54	62.33
Alanine	2.72	0.37	9.08	1.24	1.63	0.81	5.44	2.69	2.36	0.70	7.85	2.33	0.55	6.16	1.85	20.55
Valine	2.72	0.49	9.08	1.64	1.63	1.06	5.44	3.54	2.36	0.92	7.85	3.07	0.55	8.11	1.85	27.02
Leucine	2.72	0.55	9.08	1.83	1.63	1.19	5.44	3.97	2.36	1.03	7.85	3.43	0.55	9.08	1.85	30.25
Isoleucine	2.72	0.55	9.08	1.83	1.63	1.19	5.44	3.97	2.36	1.03	7.85	3.43	0.55	9.08	1.85	30.25
Proline	4.08	0.72	13.62	2.41	2.45	1.57	8.17	5.22	3.53	1.36	11.78	4.52	0.83	11.95	2.77	39.83
Methionine	4.08	0.94	13.62	3.13	2.45	2.03	8.17	6.77	3.53	1.76	11.78	5.86	0.83	15.49	2.77	51.62
Phenylalanine	4.08	1.04	13.62	3.46	2.45	2.25	8.17	7.50	3.53	1.95	11.78	6.48	0.83	17.15	2.77	57.15
Tryptophan	8.17	2.58	27.23	8.59	4.90	5.58	16.33	18.61	7.07	4.83	23.55	16.10	1.66	42.57	5.54	141.91
Glycine	4.08	0.47	13.62	1.57	2.45	1.02	8.17	3.41	3.53	0.88	11.78	2.95	0.83	7.79	2.77	25.97
Serine	4.08	0.66	13.62	2.20	2.45	1.43	8.17	4.77	3.53	1.24	11.78	4.13	0.83	10.91	2.77	36.36
Threonine	8.17	1.50	27.23	4.99	4.90	3.24	16.33	10.81	7.07	2.81	23.55	9.35	1.66	24.73	5.54	82.42
Cysteine	4.08	0.76	13.62	2.54	2.45	1.65	8.17	5.50	3.53	1.43	11.78	4.76	0.83	12.58	2.77	41.92
Tyrosine	4.08	1.14	13.62	3.80	2.45	2.47	8.17	8.22	3.53	2.13	11.78	7.11	0.83	18.81	2.77	62.69
Asparagine	4.08	0.83	13.62	2.77	2.45	1.80	8.17	5.99	3.53	1.56	11.78	5.19	0.83	13.71	2.77	45.71
Glutamine	4.08	0.92	13.62	3.06	2.45	1.99	8.17	6.63	3.53	1.72	11.78	5.74	0.83	15.17	2.77	50.56
Histidine	8.17	1.95	27.23	6.50	4.90	4.22	16.33	14.08	7.07	3.65	23.55	12.18	1.66	32.21	5.54	107.36
Lysine	4.08	0.92	13.62	3.06	2.45	1.99	8.17	6.63	3.53	1.72	11.78	5.74	0.83	15.17	2.77	50.58
Arginine	4.08	1.09	13.62	3.65	2.45	2.37	8.17	7.90	3.53	2.05	11.78	6.84	0.83	18.08	2.77	60.27
Glucose	8.17	2.26	27.23	7.55	4.90	4.90	16.33	16.35	7.07	4.24	23.55	14.14	1.66	37.40	5.54	124.66

Table 2.5 continued

Compound	500 MHz				5 mm Tube				Capillary Tube			
	LOD		LOQ		LOD		LOQ		LOD		LOQ	
	nmol	mg/L	nmol	mg/L	nmol	mg/L	nmol	mg/L	nmol	mg/L	nmol	mg/L
Ornithine	0.61	0.12	2.03	0.41	0.38	0.28	1.28	0.94				
Creatinine	0.41	0.07	1.35	0.24	0.26	0.16	0.85	0.54				
Creatine	0.41	0.08	1.35	0.27	0.26	0.19	0.85	0.62				
Pyruvate	0.41	0.05	1.35	0.18	0.26	0.13	0.85	0.42				
Citric acid	0.61	0.18	2.03	0.59	0.38	0.40	1.28	1.35				
Lactic acid	1.22	0.17	4.06	0.56	0.77	0.39	2.56	1.28				
Alanine	0.41	0.06	1.35	0.19	0.26	0.13	0.85	0.42				
Valine	0.41	0.07	1.35	0.24	0.26	0.17	0.85	0.56				
Leucine	0.41	0.08	1.35	0.27	0.26	0.19	0.85	0.62				
Isoleucine	0.41	0.08	1.35	0.27	0.26	0.19	0.85	0.62				
Proline	0.61	0.11	2.03	0.36	0.38	0.25	1.28	0.82				
Methionine	0.61	0.14	2.03	0.47	0.38	0.32	1.28	1.06				
Phenylalanine	0.61	0.15	2.03	0.52	0.38	0.35	1.28	1.18				
Tryptophan	1.22	0.38	4.06	1.28	0.77	0.88	2.56	2.92				
Glycine	0.61	0.07	2.03	0.23	0.38	0.16	1.28	0.53				
Serine	0.61	0.10	2.03	0.33	0.38	0.22	1.28	0.75				
Threonine	1.22	0.22	4.06	0.74	0.77	0.51	2.56	1.70				
Cysteine	0.61	0.11	2.03	0.38	0.38	0.26	1.28	0.86				
Tyrosine	0.61	0.17	2.03	0.57	0.38	0.39	1.28	1.29				
Asparagine	0.61	0.12	2.03	0.41	0.38	0.28	1.28	0.94				
Glutamine	0.61	0.14	2.03	0.46	0.38	0.31	1.28	1.04				
Histidine	1.22	0.29	4.06	0.97	0.77	0.66	2.56	2.21				
Lysine	0.61	0.14	2.03	0.46	0.38	0.31	1.28	1.04				
Arginine	0.61	0.16	2.03	0.54	0.38	0.37	1.28	1.24				
Glucose	1.22	0.34	4.06	1.13	0.77	0.77	2.56	2.57				

2.4.3 The Application of PLS Regression to Determine the Stability of Artificial Sweat Mixture during Storage

There were no obvious differences between the NMR spectra of the artificial sweat mixture acquired at varying storage time points when analysed by visual inspection. Thus, applying multivariate techniques through the use of projections will provide useful analysis to determine the relationship between multitudes of signals detected in the NMR spectrum over the storage period of one month. PCA is purely used as a visualisation method to highlight any major trends in the data (i.e. any variation in the NMR profiles) but gives no information how this is related to the amount of time being stored either at 4°C or -20°C. In comparison, PLS allows correlation with external variables to be evaluated in order to determine whether any correlation exists between the NMR profiles (**X**) and the storage period (**y**). To test the predictive power of the model, the data set was split into a training set containing the majority of the samples and a test set containing approximately one third of data. This equated to randomly removing whole days, because data included from replicate measurements in the training set will bias the model towards a better fit. To validate the predictions, five iterations were produced for both storage conditions to gain an accurate representation of the models in order to obtain stable prediction errors. In order to evaluate the performance of the predicative models the Root Mean Square Error (RMSE) in combination with the correlation coefficient (*r*) are used as a measure. RMSE is defined as follows:

$$RMSE = \frac{\sqrt{\sum (y_{pred} - y_{ref})^2}}{N}$$

Equation 2.2

where y_{pred} is the predicted value, y_{ref} is the measured value, and *N* is the number of samples. RMSEE is the root mean square error of the observations/training set and RMSECV is the root mean square error of cross validation which evaluates the stability of the current data set. If the model is good the RMSEE and RMSECV should be quite similar.

Three samples were omitted from both storage models due to poor NMR spectral quality. Leave one out internal cross validation of the training sets indicated two latent variables (LV) was optimal for the 4°C storage and one latent variable was optimal for the -20°C storage. The results from using five random subset cross validation procedures for both storage conditions are summarized in Table 2.6, while a representative model from both storage conditions are depicted in Figure 2.4, where the predicted versus observed values (days) are plotted for both the training set and test set.

Table 2.6 Performance of PLS regression models from the artificial sweat matrix stored at 4°C and -20°C. ¹H NMR spectra as X variable and storage day as y variable. Mean values are calculated from five iterations.

Condition	LV ^a	R ² X(cum) ^b	R ² Y(cum) ^b	Q ² (cum) ^c	RMSEE ^d	RMSECV ^e	R _{Predictive} ^f	R _{Training} ^f
4°C	2	0.27 ± 0.02	0.87 ± 0.02	0.49 ± 0.15	2.94 ± 0.4	55.52 ± 73.22	0.44 ± 0.17	0.93 ± 0.01
-20°C	1	0.18 ± 0.02	0.74 ± 0.09	0.54 ± 0.16	3.77 ± 1.04	8.35 ± 3.31	0.61 ± 0.2	0.86 ± 0.05
-20°C (no day 0)	1	0.18 ± 0.03	0.71 ± 0.1	0.4 ± 0.26	3.85 ± 0.85	10.94 ± 5.06	0.37 ± 0.27	0.84 ± 0.06

^a LV = Number of latent variables

^b R² (X or Y)cum = Cumulative fraction of Sum of Squares (SS) of all the X's or Y's explained after each extracted component

^c Q²cum = The cumulative Q² for the extracted components

^d RMSEE = Root mean square error of the fit for observations in the work set

^e RMSECV = Root mean square error of cross validation of the prediction set

^f R = Correlation coefficient

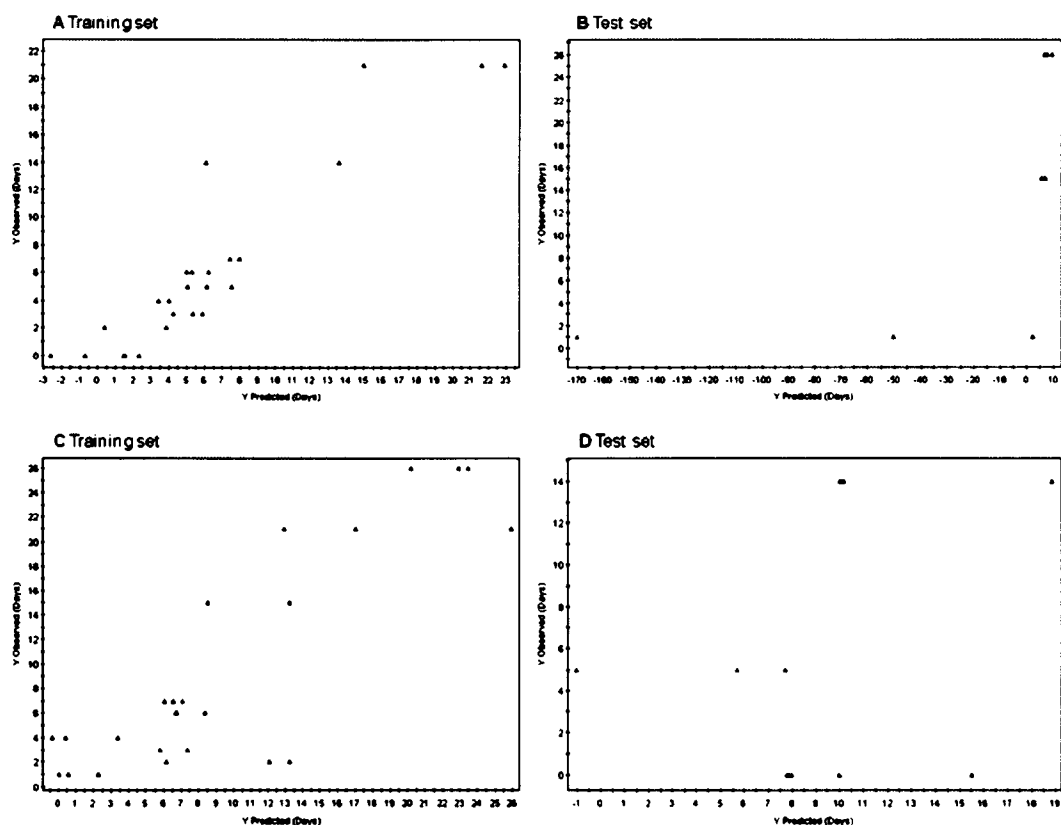


Figure 2.4 PLS derived relationship between observed and predicted storage day using ^1H NMR spectra of the artificial sweat matrix. **A** and **B** PLS models from the artificial sweat stored at 4°C, **C** and **D** are the PLS models from the artificial sweat stored at -20°C. The predicted values of the test set are plotted against the observed storage day to visualise the predictive power of each model.

The results of the PLS models produced average $R^2X(\text{cum})$ and $R^2Y(\text{cum})$ values of 0.27 and 0.87 respectively and $Q^2(\text{cum})$ was 0.49 for the 4°C storage condition and $R^2X(\text{cum})$ and $R^2Y(\text{cum})$ values of 0.18 and 0.74 respectively and $Q^2(\text{cum})$ was 0.54 for the -20°C storage condition. Generally, $R^2X(\text{cum})$, $R^2Y(\text{cum})$ and Q^2 values should be well balanced as any differences larger than 0.2 indicate the presence of irrelevant model terms or a few outlying data points (Eriksson *et al.*, 2001). Together with a correlation coefficient (r) of 0.44 and RMSECV 55 days for the 4°C storage and r 0.54 and RMSECV 8 days for -20°C storage shows there is weak linear correlation between NMR profile and the number of days in storage and poor prediction ability for both models. A large standard deviation error of RMSECV indicates that the models are not stable. Furthermore, the r value of 0.9 and 0.44 for the 4°C storage condition and r 0.86 and 0.61 for the -20°C storage condition for the training set and predictive set respectively, indicate the model could be over fitted as these values are unbalanced. From this, it can be concluded that both storage

conditions don't significantly change over a course of a month and that any alterations in sample composition are likely to be random. Moreover, models with day 0 being omitted from the training set for the -20°C storage condition were produced to see if freezing the samples had an effect. As illustrated in Table 2.6, these models are similar and therefore can be concluded that freezing had minimal effect.

2.5 Conclusion

The aim of this chapter was to create an artificial sweat matrix, designed to broadly replicate apocrine gland secretions, in order to develop NMR methodology which will be suitable for the analysis of low sample volumes. The comparative performance assessment described in this study demonstrate that the 1 mm micro-volume probe offers an ~ 5.3 fold performance advantage over data acquired for the same mass limited sample using specialist tubes with a 5 mm sample probe. Furthermore, the micro-volume probe offers a similar enhancement to that offered from a 500 MHz instrument equipped with a cryoprobe. However, in terms of maintenance and cost, it is more viable to use the micro-volume probe. NMR spectroscopy-based studies on the whole are typically robust and reproducible and differences in solvent suppression are generally minor when compared to the effects caused by biological change. The stability study showed that there was minimal change over the storage of one month in both the samples stored at 4°C and -20°C. Thus, when comparing the reproducibility and sensitivity of different methods, storage conditions can be removed as an interfering factor. The high sensitivity offered by the 1 mm micro-volume probe opens many new potential avenues of investigation of limited volumes, weights, and low cell counts in biological sample, e.g. rodent CSF (Griffin *et al.*, 2002), urine and serum (Grimes and O'Connell, 2011) or apocrine sweat.

Chapter 3

3 Development of Mass Spectrometry Methods for the Analysis of Key Metabolites in Apocrine Sweat

3.1 Introduction

Mass spectrometry is a mature and well established analytical technique which can be applied with or without chromatographic separation before detection. MS can offer a number of advantages over other analytical techniques, including increase in sensitivity, chemical identification capabilities *via* accurate mass measurements or mass spectrum interpretation, as well as the ability to quantitatively detect hundreds of metabolites in a given sample when combined with chromatography. In comparison to NMR spectroscopy, samples physically interact with the instrument which can change the response over short to medium periods of time, highlighting the importance of QC samples, as well as being destructive to the sample.

The analysis of apocrine sweat in the literature is predominantly focused on odour content, thus, the analytical strategies commonly used are GC-MS or variations of this (e.g. headspace analysis), which will be able to describe the volatile organic compounds that are present in apocrine sweat (Gower *et al.*, 1997; Natsch *et al.*, 2006; Penn *et al.*, 2007). However, these studies are mostly intended to characterise malodour rather than individual odour *per se*. Although the components of sweat have been studied, there is comparatively little attention to the biochemistry of axillary odour formation. Consequently there is limited literature available regarding the chemical structures of odour precursors isolated from axilla secretions, and no specific bacterial enzymes capable of recognising these precursors have been isolated. Furthermore, estimates for inter-individual variability or intra-individual consistency as well as the identities of individual odour need to be addressed.

A range of MS-based methods have been developed over recent years to undertake metabolic profiling of biological tissues, and the major approaches are summarised here.

3.1.1 Direct Injection Mass Spectrometry (DIMS)

The analysis of metabolite profiles from crude samples or sample extracts by DIMS can be performed in 1-3 min, providing a rapid, high throughput method, capable of screening up to 1000 samples per day (Rashed *et al.*, 1997). The samples can be introduced into the MS either through the use of the HPLC system (Kaderbhai *et al.*, 2003) or infused with syringe pumps (Goodacre *et al.*, 2002), resulting in one mass spectrum per sample, which is used for sample classification. Direct injection can avoid the disadvantages of LC system; noise levels, retention time shifts and high variability in signal intensities (Boernsen *et al.*, 2005). However, it is not without its pitfalls, as analysis is susceptible to ion suppression effects that arise from the competitive ionization with other compounds within the matrix. For example, the types of interference that can occur during acquisition are typically from ionic compounds such as salts, charged organic compounds, organic acids/bases, and hydrophobic compounds. However, through the use of a nano electrospray setup, these effects can be reduced due to the increase in ionization efficiency (Bedair and Sumner, 2008). Definitive metabolite identification is also a limitation with this technique due to the inability to distinguish between isomeric compounds.

3.1.2 Reverse Phase High Performance Liquid Chromatography Mass Spectrometry (RP-HPLC-MS)

MS based metabolomics are predominantly linked with GC (Fiehn *et al.*, 2000; Welthagen *et al.*, 2005), HPLC (Idborg-Bjorkman *et al.*, 2003; Jander *et al.*, 2004; Plumb *et al.*, 2002), or CE (Baidoo *et al.*, 2008; Sato *et al.*, 2004; Soga *et al.*, 2003), which can overcome many of the drawbacks of DIMS such as; increasing sensitivity due to reduction in background noise, reducing ion suppression caused by co-eluting compounds, and reducing isobaric interferences. For metabolomic purposes, HPLC-MS separations have primarily relied on using reversed-phase (RP) chromatography

coupled to electrospray ionization (ESI) in both positive and negative mode to obtain a comprehensive metabolic profile (Lenz and Wilson, 2007). RP-HPLC columns are composed of a non-polar stationary phase, typically silica, which has been modified with dimethylchlorosilane, containing a bulky alkyl group such as C₁₈H₃₇ or C₈H₁₇ to form the hydrophobic surface and an aqueous polar mobile phase. Thus, RP-HPLC separations are suitable for compounds of medium and low polarity, while more polar compounds (e.g. amino acids and sugars), are not well retained and non-polar compounds (e.g. lipids) are difficult to elute. These limitations can be partially overcome through the use of graphitized carbon columns (Tornkvist *et al.*, 2004), pre-column derivatization or through the use of ion-pairing agents (e.g. perfluorinated carboxylic acids). Such approaches have not found widespread use because of practical difficulties in applying to biological extracts. Thus, these polar and ionic metabolites have traditionally been under represented in metabolomic studies.

HPLC-MS is capable of moderate to high throughput analysis with a reasonable dynamic range. However, unlike ¹H NMR spectroscopy, HPLC-MS is chemically biased, as compounds need to be ionized in order to be detected as well as the column chemistry being selective to certain chemical species (typically non-polar metabolites, including lipids for RP-HPLC). Moreover, HPLC methods involve several parameters that need to be checked and validated such as sample handling, mobile phase composition, column chemistry, and gradient, which can be a time consuming process.

3.1.3 Hydrophilic Interaction Liquid Chromatography (HILIC)

An alternative technique for the separation of polar compounds is hydrophilic interaction liquid chromatography (HILIC), which was first introduced by Alpert for the separation of peptides, nucleic acids and other polar compounds (Alpert, 1990) and later used by Strege for drug research (Strege, 1998). HILIC is analogous to normal phase chromatography in that it utilizes a hydrophilic stationary phase, allowing the retention of polar analytes (Cubbon *et al.*, 2007). However, unlike normal phase, HILIC allows the use of aqueous/polar organic solvents, which are more compatible with ESI-MS system. In contrast to RP-HPLC, gradient elution

begins with low-polarity organic solvent and elutes polar analytes by increasing the polar aqueous content. However, the exact retention mechanism for HILIC is still open to debate within the scientific community. Alpert (Alpert, 1990) suggests that compounds are partitioned between a polar organic mobile phase and the water-enriched layer of the mobile phase that is partially immobilized on the polar stationary phase. Others have reported that separation is mainly governed by polar-polar interactions i.e., hydrogen bonding which depend on the acidity or basicity of the solutes, electrostatic interactions, dipole-dipole interactions, which rely on the dipole moments and polarizabilities of molecules (Wang *et al.*, 2008; Yoshida, 2004). In a recent review, Hemstrom and Irgum (Hemstrom and Irgum, 2006) considered the contribution from both the partitioning and adsorption processes and found that they fit better with the Snyder-Soczewinski adsorption model (Snyder and Poppe, 1980) than the partitioning model (Wang *et al.*, 2008). The advantages of HILIC have been summarised (McCalley, 2007) as:

- Good retention of polar and ionic compounds compared to RP-HPLC.
- The order of elution of solutes is generally the opposite of that found in RP-HPLC, thereby, providing an alternative selectivity.
- Higher flow rates are possible due to the high organic content of typical mobile phases.
- ESI-MS sensitivity is enhanced in comparison to normal phase due to the high organic content in the mobile phase and the high efficiency of spraying and desolvation techniques.
- Good peak shape can be obtained for bases.

In HILIC mode, the mobile phase generally consists of between 5 and 50% water (Alpert, 1990), however, the composition is dependent on the polarity of both the stationary phases and the analytes to be separated. The water content must be low enough to achieve separation, but high enough for the mobile phase to dissolve the analytes and elute them in a reasonable timeframe. Typically, the more polar the stationary phase and the analyte, the higher the water content is needed for separation. The polar organic solvent of choice is generally acetonitrile (Churms, 1996) but other mixtures such as water-methanol (Valette *et al.*, 2004), dichloromethane-methanol

(Herbreteau *et al.*, 1992), isopropanol (Li and Huang, 2004), and ethanol have been used (Nguyen and Schug, 2008). Various hydrophilic columns have been employed in the HILIC mode, depending on the specific applications. Typically, nonbonded silica columns, polar-bonded silica phases have been employed in the literature. These include aminopropylamide-, poly(succinimide)-, diol-, cyanopropyl-, and sulfoalkylbetaine silica phases. The properties of these stationary phases have been discussed in a recent review by Hemstrom and Irgum (Hemstrom and Irgum, 2006). HILIC has shown promise in bioanalytical applications for a wide variety of polar and hydrophilic compounds which are summarised in Table 3.1. Generally, in HILIC mode, acetonitrile is used as the organic component with the addition of ammonium acetate, typically 5-20 mM, in addition to having long analysis times, typically 30 min.

To date no study has attempted to qualitatively and quantitatively determine the profile of human apocrine sweat. Thus, two additional MS analytical approaches will be developed to provide complementary information to the NMR data. Firstly, a global fingerprint of metabolites of medium to high polarity and secondly, identify specific odour precursors in a qualitative and quantitative manner. Moreover, the targeted based method will allow more definitive identification of unknown odour precursors, as although accurate mass can be obtained in the global methodology, this information does not provide any hits in biological databases such as HMDB or Lipid Maps. The former method will be optimised with an artificial sweat matrix and the complexity will then be increased using more representative biological sample (see chapter 4). The latter method will be developed with available standards.

Table 3.1 Representative applications of HILIC reported in the literature

Sample	Column	Mobile phase	Total run time (min)	Detector	Author
Pharmaceutical drugs					
Small polar compounds e.g. cytosine/aspirin	4 columns (Zic-HILIC)	85% MeCN, 20 mM ammonium acetate	20	UV 228 nm	(Guo and Gaiki, 2005)
Mildronate and related substances	6 columns tested (Zic-HILIC)	90% MeCN + 0.1% formic acid or ammonium formate	-	ESI MS (+ve mode)	(Hmelnickis <i>et al.</i> , 2008)
Isoniazid in plasma	Hypersil silica	[A] 0.1% HOAC, 2.5 mM ammonium acetate [B] MeCN, 0.1% HOAC	10	ESI MS (+ve mode)	(Huang <i>et al.</i> , 2009)
Cyanobacterial toxins	TSK-gel amide	[A] 2 mM ammonium formate, 3.6 mM formic acid, pH 3.5 [B] 95% MeCN, 2 mM ammonium formate, 3.6 mM formic acid, pH 3.5	-	API MS (+ve mode)	(Dell'Aversano <i>et al.</i> , 2004)
3 Pharmaceuticals in human plasma	YMC Silica	82% MeCN and 18% 10 mM ammonium acetate pH 5	2	ESI MS (+ve mode)	(Apostolou <i>et al.</i> , 2008)
Aromatic, NH ₂ , OH	YMC-Pack Diol-120-NP	95% MeCN + 10 mM NH ₄ Cl	20	UV 215 nm	(Wang <i>et al.</i> , 2005)
Oseltamivir in plasma and urine	ZIC-HILIC (SeQuant)	[A] 10 mM ammonium acetate, 1% formic acid [B] MeCN		ESI MS (+ve mode)	(Lindegardh <i>et al.</i> , 2007)
Opioids and glucuronides	ZIC-HILIC (SeQuant)	[A] 90% MeCN, ammonium formate [B] 50/50 MeCN	30	UV (220 nm) and ESI MS (+ve mode)	(Vikingsson <i>et al.</i> , 2008)
Plasma					
Polar metabolites in plasma	Acquity silica UPLC BEH	[A] Water [B] 95% MeCN + 10 mM ammonium acetate	15	ESI MS (+ve/-ve mode)	(Cai <i>et al.</i> , 2009)

Table 3.1 continued

Sample	Column	Mobile phase	Total run time (min)	Detector	Author
Dasatinib, imatinib and nilotinib in mouse plasma	Silica/diol/pyridine/imidazole HILIC (Sepax)	[A] water + 0.1% formic acid/4 mM ammonium acetate [B] MeCN + 0.1% formic acid/4 mM ammonium acetate	1	ESI/APCI MS (+ve mode)	(Hsieh <i>et al.</i> , 2009)
Propofol in plasma	Atlantis HILIC	MeCN, water, 100 mM ammonium acetate, pH 5 (87:1:12)	12	ESI MS (-ve mode)	Cohen, 2007
Miglustat in human plasma and CSF	Atlantis HILIC	MeCN/water/100 mM ammonium acetate pH 5 (75/10/15 v/v)		ESI MS (+ve mode)	(Guitton <i>et al.</i> , 2009)
Doxazosin in human plasma	Atlantis silica	MeCN + 100 mM ammonium formate, pH 4.5 (93:7 v/v)	3	ESI MS (+ve mode)	(Ji <i>et al.</i> , 2008)
Carvedilol in human plasma	Atlantis silica	MeCN + ammonium formate (50 mM, pH 4.5) (90:10 v/v)	2.5	ESI MS (+ve mode)	(Jeong <i>et al.</i> , 2007)
Acetyl and carnitines	Atlantis silica	[A] 5% MeCN, 5 mM ammonium acetate [B] 95% MeCN, 5 mM ammonium acetate	5	ESI MS (+ve mode)	(Liu <i>et al.</i> , 2008b)
Arginine, plasma ADMA & SDMA	Luna silica	[A] MeCN, trifluoroacetic acid, acetic acid (1000:25:10) [B] water, trifluoroacetic acid, acetic acid (1000:25:10)	5	ESI MS (+ve mode)	(D'Apolito <i>et al.</i> , 2008)
Polar metabolites e.g. creatinine, uracil and hippuric acid	Supersphere Si	[A] 100 mM NH ₃ [B] MeCN + 0.2% formic acid	37	ESI MS (+ve mode)	(Godejohann, 2007)

Table 3.1 continued

Sample	Column	Mobile phase	Total run time (min)	Detector	Author
Dacarbazine in plasma	TSK-gel amide	[A] MeCN [B] 0.1% formic acid	6	ESI MS (+ve mode)	(Liu <i>et al.</i> , 2008a)
Methylmalonic acid in human plasma	PEEK Zic-HILIC (SeQuant)	80% MeCN and 20% 100 mM ammonium pH 4.5	10	ESI MS (-ve mode)	(Lakso <i>et al.</i> , 2008)
Urine					
Liver cancer	Acquity silica	[A] 100 mM ammonium formate + 0.1% formic acid [B] MeCN	35	ESI MS (+ve mode)	(Chen <i>et al.</i> , 2009)
Urine	Luna silica	[A] 100% MeCN [B] 13 mM ammonium acetate, pH 9.1	30	ESI MS (+ve/-ve mode)	(Kind <i>et al.</i> , 2007)
Estrogen conjugates in urine	TSK-gel amide	85% MeCN, 5 mM ammonium acetate, pH 6.8	25	ESI MS (-ve mode)	(Qin <i>et al.</i> , 2008)
Urine	ZIC-HILIC (SeQuant)	[A] 5 mM ammonium acetate + 0.1% formic acid [B] MeCN + 0.1% formic acid	30	ESI MS (+ve/-ve mode)	(Cubbon <i>et al.</i> , 2007)
Urine	ZIC-HILIC (SeQuant)	[A] 5 mM ammonium acetate, pH 4 [B] MeCN + 0.025% formic acid	30	ESI MS (+ve mode)	(Idborg <i>et al.</i> , 2005)
Plant					
Organic acids	TSK-gel amide	[A] 90% MeCN, 0.65 mM ammonium acetate, pH 5.5 [B] 60% MeCN, 2.6 mM ammonium acetate, pH 5.5	90	ESI MS (+ve/-ve mode)	(Schlichtherle-Cerny <i>et al.</i> , 2003)
Plant compounds	TSK-gel amide	[A] MeCN [B] 6.5 mM ammonium acetate, pH 5.5	60	ESI MS (+ve/-ve mode)	(Tolstikov and Fiehn, 2002)

Table 3.1 continued

Sample	Column	Mobile phase	Total run time (min)	Detector	Author
Mixture metabolites: amino acids - bases	TSK-gel amide	[A] water, 0.1% v/v formic acid [B] 90% MeCN, 0.1% v/v formic acid	30	ESI MS (+ve mode)	(t'Kindt <i>et al.</i> , 2008)
Carbohydrate-related compounds	ZIC-HILIC (SeQuant)	[A] MeCN + 0.1% formic acid [B] 5 mM ammonium acetate + 0.1% formic acid (pH 4)	30	ESI MS (-ve mode)	(Antonio <i>et al.</i> , 2008)
Melamine and cyanuric acid	ZIC-HILIC (SeQuant)	[A] 95% MeCN, 0.1% formic acid [B] MeCN, 20 mM ammonium formate	14	ESI MS (+ve/-ve mode)	(Heller and Nochetto, 2008)
Ascorbic acid	ZIC-HILIC (SeQuant)	MeCN, 50 mM ammonium acetate, pH 6.8	5	UV 268 nm	(Novakova <i>et al.</i> , 2008)
Phytosiderophores in plants	ZIC-HILIC (SeQuant)	[A] 90% MeCN, 10 mM ammonium acetate, pH 7.3 [B] 20% MeCN, 30 mM ammonium acetate, pH 7.3	60	ESI MS (+ve/-ve mode)	(Xuan <i>et al.</i> , 2006)
DTC fungicide	ZIC-HILIC (SeQuant)	[A] MeCN [B] 10 mM ammonium acetate	23	ESI MS (-ve mode)	(Crnogorac and Schwack, 2007)
Breath Exhaled breath	ZIC-HILIC (SeQuant)	[A] MeCN, 0.025% formic acid [B] 5 mM ammonium acetate, pH 4	30	ESI MS (+ve mode)	(Conventz <i>et al.</i> , 2007)
Cells Bacteria	ZIC-HILIC (SeQuant)	[A] 0.1% formic acid [B] MeCN + 0.1% formic acid	32	ESI MS (+ve/-ve mode)	(Kamleh <i>et al.</i> , 2008)

Table 3.1 continued

Sample	Column	Mobile phase	Total run time (min)	Detector	Author
Cisplatin and its monohydrolyzed metabolite	ZIC-HILIC (SeQuant)	70% DMF/20 mM ammonium acetate or 70% MeCN/30% 20 mM ammonium acetate	30	ESI MS (+ve mode)	(Nguyen and Schug, 2008)
Cell lysate acetylcholine	ZIC-HILIC (SeQuant)	65% MeCN 35% 10 mM ammonium formate, 0.02% formic acid	10	ESI MS (+ve mode)	(Schebb <i>et al.</i> , 2008)
Long chain acylcarnitine	Atlantis silica	200 mM ammonium formate, pH 3, MeCN, and Water (5:86:9)	28	ESI MS (+ve mode)	(Jauregui <i>et al.</i> , 2007)
Human milk					
N-linked glycoproteins in human milk	ZIC-HILIC (SeQuant)	80% MeCN, 1% formic acid	-	MALDI and ESI MS (+ve mode)	(Picariello <i>et al.</i> , 2008)
Others					
Amino acids	TSK-gel amide	[A] 90% MeCN, 0.5 mM ammonium acetate, pH 5.5 [B] 60% MeCN, 2.5 mM ammonium acetate, pH 5.5		ESI MS (+ve mode)	(Langrock <i>et al.</i> , 2006)
Acetylcholine in subcutaneous tissue	ZIC-HILIC (SeQuant)	70% MeCN, 10 mM ammonium formate, pH 4	15	ESI MS (+ve mode)	(Fu <i>et al.</i> , 2008)
Amino acid analysis	ZIC-HILIC (SeQuant)	[A] 10 mM acetic acid [B] MeCN	88	ESI MS (+ve mode)	(Kato <i>et al.</i> , 2009)
Organoarsenicals	ZIC-HILIC (SeQuant)	[A] 70% MeCN [B] 125 mM ammonium acetate, pH 8.3	60	ESI MS (+ve mode)	(Xie <i>et al.</i> , 2008)
N- and O-glycopeptides	Capillary ZIC-HILIC (SeQuant)	[A] 50% MeCN, 10 mM ammonium acetate [B] 80% MeCN, 10 mM ammonium acetate	80	ESI MS (-ve mode)	(Takegawa <i>et al.</i> , 2008)

3.1.4 Analytical Strategies for Profiling Apocrine Sweat Metabolites

The following information was taken into account when developing methods in this chapter.

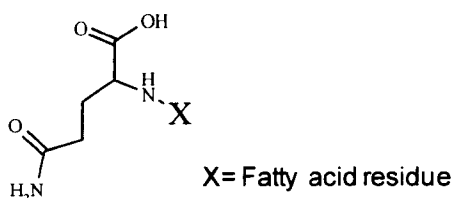
Global approach

In using DIMS or HPLC-MS in a comprehensive global approach, the intention is to measure as many of the small molecule components as possible in the sample. With regards to HPLC-MS, this intention puts large demands on the applied chromatographic separation capability. The stationary phase will also influence, in terms of retention properties of metabolites, the range of different chemical properties of the separated metabolites. Although the fingerprint regions would likely look different on different stationary phases, they are not expected to have a higher information content. Thus, the approach taken herein is to obtain a method that is capable of separating a range of polar compound in under 30 min.

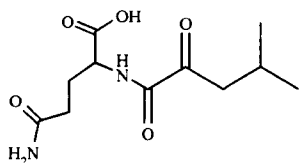
Gln, Cys and Cys-Gly -conjugate profiling

The general structures of the odour precursors all contain one of three common moieties (see Appendix A); Gln, Cys or a Cys-Gly residue, an example of which is depicted in Figure 3.1. Thus, a precursor ion scanning method was developed which would be later used to screen actual apocrine gland secretions in order to help identify all the amino acid conjugates present, including unknowns, in a single run without making prior assumptions of identity.

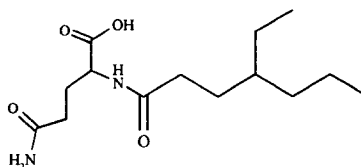
Gln Conjugates: -



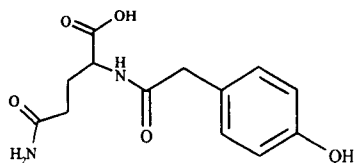
Gln Conjugates Examples: -



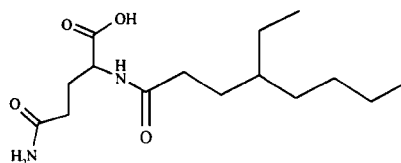
N-α-4-methyl-2-oxopent-anoyl- L-glutamine



N-α-4-ethyl-hept-anoyl- L-glutamine



N-α-4-hydroxyphenyl-acetyl- L-glutamine



N-α-4-ethyl-oct-anoyl- L-glutamine

Figure 3.1 An example of common glutamine conjugates.

Specific targeted analysis of odour precursors

In a targeted approach, the main aim is to identify and quantify specific compounds of interest. As a consequence, the standard route of method development is to find the optimum chromatographic conditions to separate representative standards from one another as well as from matrix interferences. However, compromises will have to be made for the eluent composition to ensure sufficient analysis times, optimum peak capacity, and the stability of the sample profiles, in addition to the MS parameters, as one set of conditions is unlikely to suit all compounds.

3.1.5 Aims

- To establish an analytical method that would be capable of detecting and identifying a broad range of metabolites present in human apocrine sweat, either by DIMS or LC-MS.
- To establish an analytical method capable of identifying odour precursors from a common structure.
- To establish an analytical method to specifically identify odour precursors in human apocrine sweat using MRM analysis coupled with full product ion spectra.

3.2 Material and Methods

3.2.1 Chemicals

HPLC grade acetonitrile (far UV), methanol, ammonium formate, and glucose were purchased from Fisher Scientific UK Ltd (Loughborough, UK). HPLC grade water was obtained from a Millipore Milli-Q Gradient purification system (Bedford, MA). Formic acid, ammonium hydroxide, cholesterol, and stearic acid was obtained from Sigma Aldrich (Poole, UK) and stored at 4°C. Ammonium acetate was of ACS grade and tristearine from Fluka. L-alanine, L-valine, L-leucine, L-isoleucine, L-proline, L-methionine, L-phenylalanine, L-tryptophan, L-glycine, L-serine, L-threonine, L-cysteine, L-tyrosine, L-asparagine, L-glutamine, L-aspartic acid, L-glutamic acid, L-histidine, L-lysine, L-arginine were sourced from Sigma-Aldrich at a purity of 99%. Lanolin was sourced from Alfa Aesar (Heysham, UK). 3-methylhex-2-enoyl-L-glutamine (3M2H-Gln), N- α -3-hydroxy-3-methylhex-2-enoyl-L-glutamine (HMHA-Gln), S-[1-(2-hydroxy-1-methylethyl)-ethyl]-L-cysteine (2M3H-Cys) and S-[1-(2-hydroxyethyl)-1-methylbutyl]-L-cysteine-glycine (3M3SH-Cys-Gly) were supplied by Dr Mark Harker (Unilever R&D, Bebington, UK).

3.2.2 LC-MS Columns

The C₁₈ Synergi Hydro-RP 80Å, (4 µm, 150 x 2 mm) was purchased from Phenomenex (Macclesfield, UK). An Atlantis C₁₈ column (3 µm, 100 x 2.1 mm) was purchased from Waters (Manchester, UK). A ZIC-HILIC (5 µm, 150 x 2.1 mm) column along with a guard column (20 x 2.1 mm) was purchased from SeQuant (Umeå, Sweden). All columns were equilibrated with mobile phase prior to use and washed as per manufacturer recommendations.

3.2.3 Sample Preparation

Apocrine secretion is a turbid fluid that is complex in nature, containing a wide range of compounds such as proteins, lipids and steroids (Labows *et al.*, 1979). The secretion of this fluid from the apocrine gland is transient and intermittent, with only low volume being produced. Obtaining this fluid from human volunteers is very costly, thus, an artificial sweat matrix was developed for the purpose of developing analytical methodologies, as depicted in Table 3.2, and not intended to replicate apocrine sweat secretions but to have chemical characteristics in common. Blood plasma (human venous blood collected from the Nottingham University Hospital and placed into vials containing lithium heparin as an anticoagulant) was used as the underlying matrix for the artificial sweat matrix, due to the plasma containing common metabolites, in particular the non-polar species like cholesterol, glycerides and fatty acids. The proteins present in the blood plasma were removed by precipitation, using a 3:1 acetonitrile before the addition of amino acids standards. Furthermore, the use of blood plasma as the matrix overcomes the difficulties of dissolving polar and non-polar components into a solution, due to many of the components being present in blood plasma. An amino acid standard mixture containing all the amino acids listed in Section 3.2.1 was also separately prepared at a concentration 40 µg/ml.

Table 3.2 Artificial apocrine secretion matrix used for method development.

Ingredient	Level in µg/ml	Ingredient	Level in µg/ml
Plasma	500 µl	Threonine	40
Alanine	40	Cysteine	40
Valine	40	Tyrosine	40
Leucine	40	Asparagine	40
Isoleucine	40	Glutamine	40
Proline	40	Aspartic acid	40
Methionine	40	Glutamic acid	40
Phenylalanine	40	Histidine	40
Tryptophan	40	Lysine	40
Glycine	40	Arginine	40
Serine	40		

3.2.4 Global Profiling by LC-QTOF-MS

All experiments were conducted on a Shimadzu LC system (10AD VP) equipped with two Shimadzu binary pumps (LC-10AD), a vacuum degasser, a cooled autosampler (SIL-HTc) and a column oven (Shimadzu, Columbia, MD, USA). The HPLC system was coupled to a Waters QTOF Premier system (Water MS Technologies, Manchester, UK) equipped with an electrospray source operating in positive ion mode. The source temperature was set to 125°C with a cone gas flow of 56 l/h, a desolvation gas temperature of 350°C and a desolvation gas flow of 400 l/h. A capillary voltage and a cone voltage were set to 3.0 kV and 25 V, respectively. The MCP detector voltage was set to 1850 V. The QTOF acquisition rate was set to 0.3 s with a 0.01 s interscan delay. Tune page was used to regulate the sample cone voltage. Argon was employed as the collision gas at a flow rate of 0.4 ml/min. The mass spectrometer was mass calibrated prior to use with sodium formate (0.05 M sodium hydroxide and 0.5% formic acid in 90:10 2-propanol:water v/v) between m/z 50-1000 with a residual error $<1.79 \times 10^{-4}$ amu.

A 5 µl aliquot of artificial sweat mixture was injected onto a SeQuant ZIC[®]-HILIC column, 150 x 2.1 mm (5 µm particle size) along with a guard column (20 x 2.1 mm) operated at 25°C, with all the eluent from the LC column being directly transferred

into the ion source of the MS without post-column splitting. The final optimised mobile phase contained [A] 10 mM ammonium acetate and 90% acetonitrile at pH 5 and [B] 10 mM ammonium acetate. The gradient duration was 25 min at a flow rate of 250 µl/min. From the start to 2.5 min [A] was kept constant at 100% and linearly decreased to 50% in 7.5 mins and held constant for 3.5 mins. Finally, at the end of a gradient an 11.5 min re-equilibration period was employed. The mass spectrometric data was collected in full scan mode from m/z 50 to 1000 from 0-25 min.

3.2.4.1 Preliminary Development Work for LC-QTOF-MS

A range of different HPLC columns and mobile phase conditions were used during the method development and are listed below. The final optimised LC-QTOF-MS method is noted above (Section 3.2.4).

Initial Column Selection Conditions

C₁₈ Synergi Hydro-RP 80Å, (4 µm, 150 x 2 mm): - Mobile phase [A] consisted of 100% water and 0.1% formic acid [B] acetonitrile and 0.1% formic acid. The gradient duration was 10 min at a flow rate of 250 µl/min as follows: an isocratic stage of 0% [A] for 2 min, followed by a linear raise to 50% [A] in 8 min.

ZIC-HILIC column (5 µm, 150 x 2.1 mm): - Mobile phase [A] consisted of 90% acetonitrile and 5 mM ammonium acetate [B] 5 mM ammonium acetate, pH 6.2. The gradient duration was 10 min at a flow rate of 250 µl/min as follows: an isocratic stage of 0% [B] for 2 min, followed by a linear raise to 60% [B] in 8 min, and at 10 min decreased back to the initial 0% [B] for 5 min to re-equilibrate the column.

Isocratic Elution

Mobile phase consisted of 80% acetonitrile and 10-30 mM ammonium acetate, pH 5 or 70-90% acetonitrile and 20 mM ammonium acetate, pH 5. The elution duration was 50 min at a flow rate of 250 µl/min.

Effect of Ionic Strength

Mobile phase [A] consisted of 100% acetonitrile or 100% acetonitrile and 0.1% formic acid [B] 10-80 mM ammonium acetate, pH 5. The gradient duration was 40 min at a flow rate of 250 µl/min as follows: an isocratic stage of 5% [B] for 6 min, followed by a linear raise to 40% [B] in 14 min, further linear rise to 60% [B] in 10 min and at 30.0 min decreased back to the initial 5% [B] for 10 min to re-equilibrate the column.

Mobile phase [A] consisted of 90% acetonitrile and 0.5 mM ammonium acetate, pH 5 [B] 60% acetonitrile and 1-10 mM ammonium acetate, pH 5. The gradient duration was 45 min at a flow rate of 250 µl/min as follows: 5% [B] and increasing linearly to 60% over a period of 28.5 min, further increase to 95% [B] in 5 min and at 34 min decreased back to the initial 5% [B] for 10 min to re-equilibrate the column.

Effect of pH

Mobile phase [A] consisted of 95% acetonitrile and 10 mM ammonium acetate [B] 10 mM ammonium acetate. The pH was varied in both mobile phases between 4-8. The gradient duration was 40 min at a flow rate of 250 µl/min as follows: an isocratic stage of 0% [B] for 6 min, followed by a linear raise to 35% [B] in 14 min, a further linear rise to 55% [B] in 10 min and at 30.0 min decreased back to the initial 0% [B] for 10 min to re-equilibrate the column.

3.2.5 Global Profiling by Direct Injection Mass Spectrometry

Direct injection mass spectrometry was acquired with the same MS conditions and setting as noted in Section 3.2.4. The HPLC system was used to load 5 µl of the sample into the LC sample loop using LC solvents (50:50 v/v mixture of acetonitrile and water containing 0.1% formic acid) and pumped from 100-500 µl/min for one min. All the eluent directly transferred into the ion source of the MS. Three blanks were run between each sample to reduce any carry over from the HPLC-tubing.

3.2.6 Targeted Profiling by LC-MS/MS

Analysis was conducted on a Shimadzu LC system (10AD VP) equipped with two Shimadzu binary pumps (LC-10AD), a vacuum degasser, a cooled autosampler (SIL-HTc) and a column oven (Shimadzu, Columbia, MD, USA). The HPLC system was coupled to a Applied Biosystems 4000 QTRAP® (QqQLit) hybrid triple quadrupole linear ion trap (Foster City, CA, USA) equipped with a Turbolon electrospray source operating in positive ion mode.

3.2.6.1 Optimisation of compound dependent parameters for MRM Analysis

Analyses were performed using multiple reaction monitoring (MRM) for 3M2H-Gln ($C_{12}H_{20}N_2O_4$, MW: 256.14), HMHA-Gln ($C_{12}H_{22}N_2O_5$, MW: 274.15), 2M3H-Cys ($C_8H_{17}NO_3S$, MW: 207.09) and 3M3SH-Cys-Gly ($C_{12}H_{24}N_2O_4S$, MW: 292.15). The optimisation of the precursor to product ion dissociation was performed by infusion into the MS of separate standard solutions (10 µg/ml) in 50:50 v/v of [A]/[B] mobile phase (see below) for each analyte at a flow rate of 10 µl/min. The probe capillary voltage (IS) was optimised at 5000 V; temperature of the turbo gas (TEM) 350°C; nebulizer gas (GS1), auxiliary gas (GS2), curtain gas (CUR) were set to 20, 10, and 10, respectively (arbitrary values). Nitrogen was used for collisionally induced dissociation (CID). Optimal declustering potential (DP) and collision energy (CE) values were then used for the determination of 14 MRM transitions, each representing an individual odour precursor (see Table 3.4). Each transition was performed with a 25 ms dwell time. DP and CE voltages for those conjugate precursors for which standards were unavailable, were predicted from those obtained from a closely related standard. The mass spectrometer was also set to use the information dependent acquisition (IDA) function, where the instrument utilises an MRM as survey scan to trigger a consecutive enhanced product ion (EPI) scan (MS/MS) for structural confirmation (Figure 3.2). IDA criteria were set to select those MRM transitions above a signal intensity of 5000 counts. Dynamic exclusion was set to 15 sec. Full product ion spectral data as well as retention times of each of the standards were used for structural and peak identification, respectively.

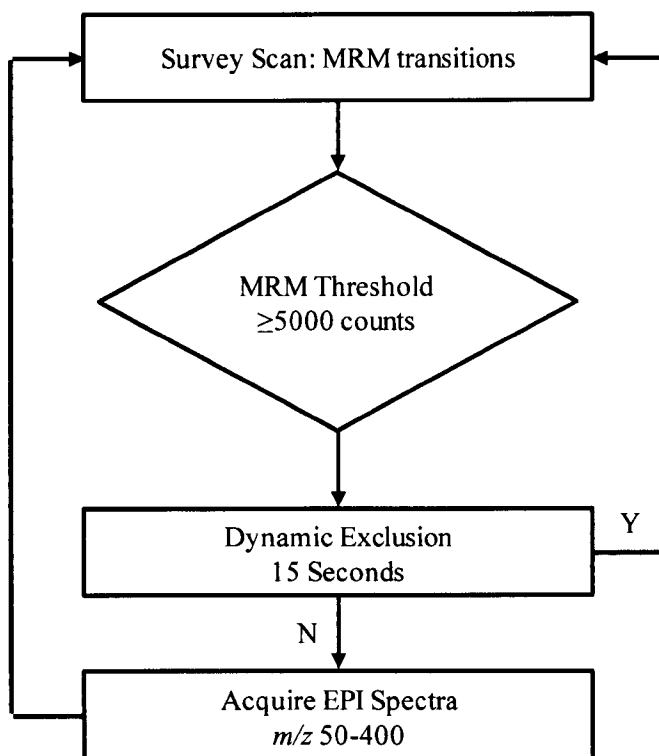


Figure 3.2 Schematic of the IDA driven acquisition procedure.

3.2.6.2 Conjugate Profiling using Precursor Ion Scanning

Based on the evidence in the literature and available standards, Gln, Cys, and Cys-Gly conjugates, all fragmented under CID to produce their respected amino acid residue, m/z 147, 179 and 105 respectively. Thus, these ions were chosen as the signature product ions for the precursor ion scan. Subsequent ion trap scans were triggered when the threshold of the precursor ion scan reached 2×10^4 counts. Each precursor ion scan ranged from m/z 200-400 over a scan time of 1.2 s and EPI MS/MS spectra were obtained over a range m/z 50-400 by ramping DP and CE from 25-35 V and 15-30 eV respectively. The quadrupoles were set to unit resolution with the mass range covering the range of analytes expected. PI scan was used as a filter to select candidates of interest on-the-fly, once the selection criteria are satisfied, mass spectra are obtained by fixing the first quadrupole (Q1) for the m/z of the pseudomolecular ion which is then passed through to a collision cell and scanned through the appropriate mass range in Q3. The mass accuracy of the spectra obtained is based on

the limitations of the quadrupole. However, such error can be corrected for by the use of EPI scan that follows each survey scan. When EPI spectra are collected, Q3 is acting as a linear ion trap rather than being scanned out, thus, ions are stored for a predetermined amount of time before being expelled and recorded.

3.2.6.3 Chromatographic conditions

A 5 μ l aliquot of each standard was injected onto a Atlantis C₁₈ column (3 μ m, 100 x 2.1 mm) operated at 40°C, with all the eluent from the LC column being directly transferred into the ion source of the MS without post column splitting. The elution solvents were [A] water containing 0.1% formic acid and [B] methanol containing 0.1% formic acid. The gradient profile started at 15% [B] (0.5 min), increased to 90% (6 min) and maintained at 90% [B] for 5 min.

3.2.7 MSⁿ for Fragmentation Confirmation

Fragmentation confirmation was performed with a LTQ Velos dual pressure linear ion trap (Thermo, Hemel Hempstead, U.K.). The analyses on the Velos instrument were performed using heated electrospray ionization (h-ESI) in positive mode at sheath, auxiliary and sweep gas flows of 5, 1 and 0.2 respectively (arbitrary units). The capillary and source heater temperatures were set to 240 and 40°C respectively. The ion spray voltage was adjusted to 2.5 kV. Analysis of the 2M3H-Cys, 3M3SH-Cys-Gly, HMHA-Gln, and 3M2H-Gln standards at 10 μ g/ml were carried out by direct infusion at a flow rate 5 μ l/min into the ion source as well as the mobile phase flow rate of 250 μ l/min to produce a stable signal.

3.2.8 Data Analysis

QTOF – Results obtained from LC-MS were analyzed by the Micromass MarkerLynx v4.1 application manager (Waters, UK); the retention time (t_r) and m/z data pair for each peak were detected by the software.

QTRAP – Results obtained from LC-MS/MS analysis were processed by Analyst v1.4 (Applied Biosystems).

3.3 Results and Discussion

The strategy undertaken for method development was three-fold. Firstly, a method was developed that would be capable of identifying metabolites on a global scale (to complement the NMR data) either *via* DIMS or LC-MS. This global approach was initially developed with the use of an artificial sweat matrix with qualitative assessments being made in order to highlight optimum conditions for further investigation. The optimum conditions would then be further tested by increasing the complexity of the sample to that of apocrine sweat produced from cell lines (see chapter four) in addition to being more representative of the actual sample type under investigation. Secondly, a LC-MS/MS method was developed that was capable of specifically screening for known and unknown odour precursors by exploiting their common structural similarities. Finally, a LC-MS/MS method was developed that can qualitatively and quantitatively identify known odour precursors.

3.3.1 Direct Injection Mass Spectrometry

DIMS provided a sensitive high throughput method without chromatographic separation, with the speed of analysis usually less than 5 min. A typical DIMS mass spectrum of the amino acids present in the artificial sweat matrix is depicted in Figure 3.3. It is evident that a broad range of metabolites can be readily detected, including all the amino acids as well as lipophilic metabolites. The higher mass ranges (i.e. lipid content) are the most intense metabolites detected. Furthermore, when analysing amino acid standards in the artificial sweat matrix, ion suppression was observed across all analytes, in particular alanine, glycine, serine, cysteine, tyrosine, asparagine, and glutamic acid. Ion suppression effects (also known as matrix effect (King *et al.*, 2000)) can be viewed as a competition for ionisation between molecules that have simultaneously been introduced into the MS source. The ion suppression effect has a dramatic effect on the reproducibility between samples as depicted in Figure 3.4, in which the average coefficient of variation (CV) for the amino acids

present in the pseudo sweat mixture 43.9%. In contrast to LC-MS, the CV is expected to be less than 15% for an optimised method (FDA, 2001). Furthermore, in-source fragmentation could be observed for leucine/isoleucine and valine, which could be tentatively assigned to the product ions m/z 86 and m/z 72 respectively. This fragmentation is due to the loss of H_2O and CO leading to immonium ions $[Im]^+ = [R-CH=NH_2]^+$, where R is the residue of the amino acids (Petritis *et al.*, 2000; Qu *et al.*, 2002). Conversely, this approach would allow a variety of metabolites (e.g. lipids and organic acids) to be detected in one brief analysis and have been used in microbial (Goodacre *et al.*, 1999; Vaidyanathan *et al.*, 2002) and plant (Goodacre *et al.*, 2003; Mauri and Pietta, 2000) studies.

However, this approach cannot distinguish between isomeric compounds such as leucine/isoleucine. In order to distinguish between isomers and reduce ion suppression effects, separation through chromatographic means will need to be in place. Moreover, analytical separation would result in an increase in sensitivity and MS data quality due to the reduction in background noise.

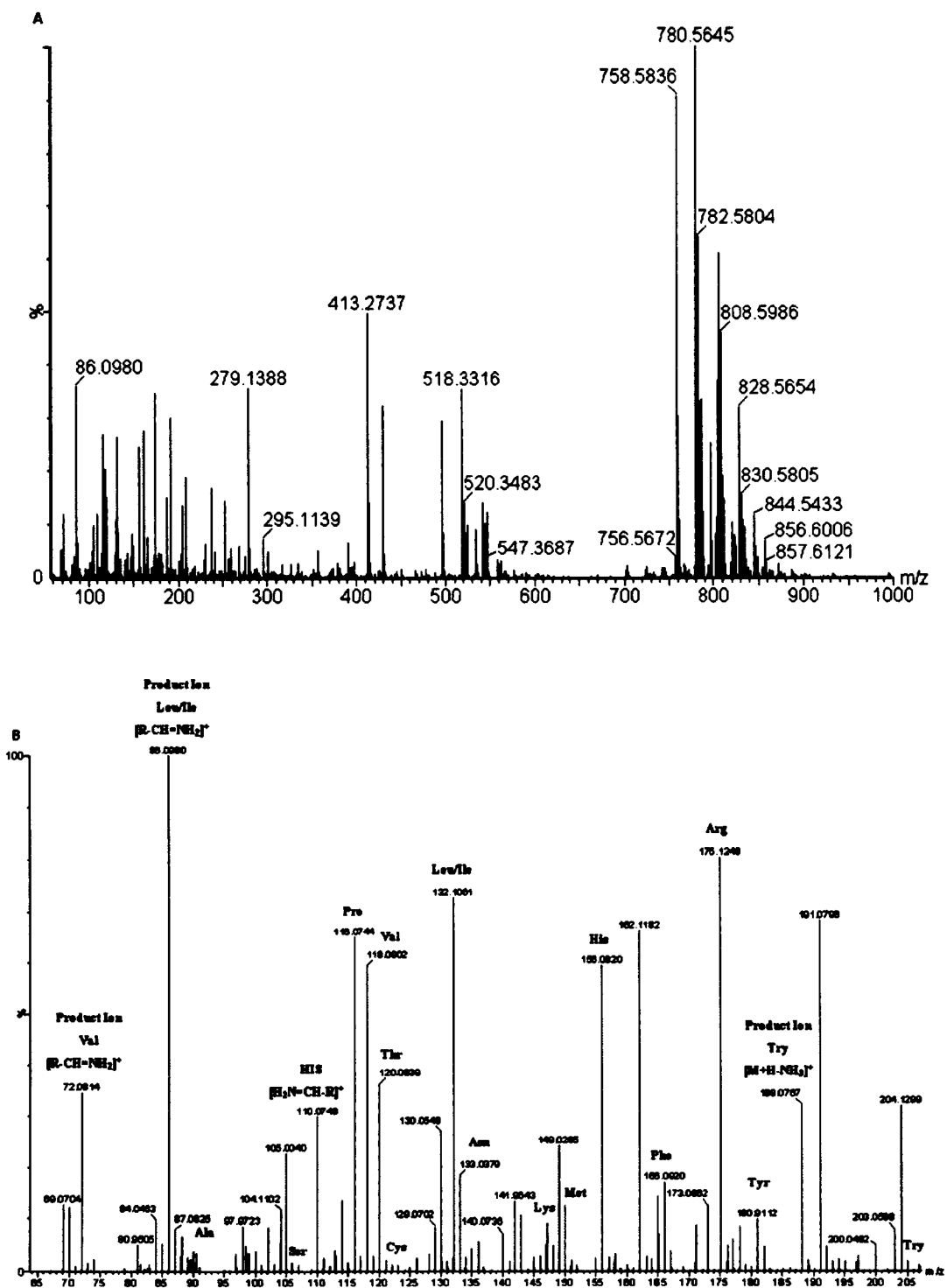


Figure 3.3 DIMS mass spectra in positive mode **A** whole profile **B** range m/z 65-205 of artificial sweat matrix (amino acids content is at 40 $\mu\text{g/ml}$).

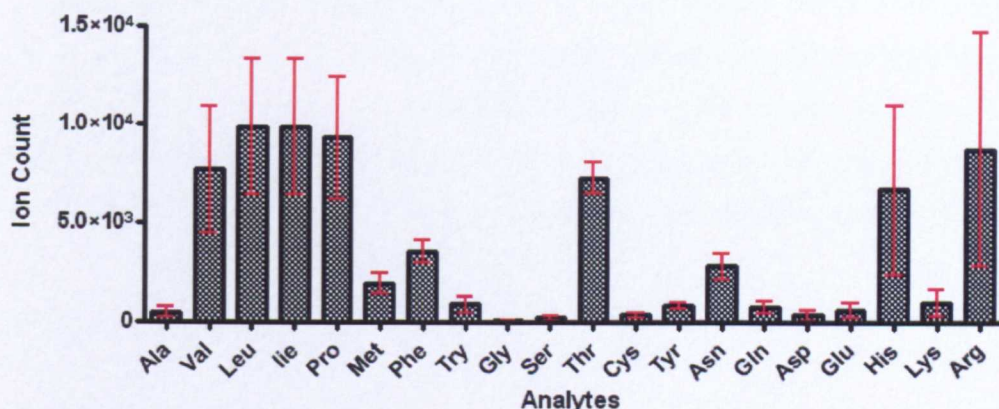


Figure 3.4 DIMS reproducibility of the amino acid content present in artificial sweat matrix. The error bars represent the standard deviation ($n=5$).

In conclusion, this approach would allow information-rich ESI-MS spectra from human apocrine samples to be generated without the need for chromatographic separation. However, the poor precision reported from this methodology suggests this method is suited to more of a screening approach rather than a quantitative method. The absence of chromatographic separation can be detrimental to mass accuracy arising from peak overlap with monoisotopic differences of less than 0.025 Da (Dunn and Ellis, 2005) as well reducing the overall sensitivity arising from competitive ionisation (Mas *et al.*, 2007; Villas-Boas *et al.*, 2005). Furthermore, structural isomers have the same monoisotopic mass and would require LC-MS to be detected separately. In addition, the classification of in-source fragmentation or adduct formation is complicated. In the literature, application of DIMS is mainly focused in the microbial (Castrillo *et al.*, 2003) and plant areas (Overy *et al.*, 2005), and when used in disease diagnostics, a MS/MS approach is taken (Rashed, 2001). Thus, this approach will no longer be pursued as it is not suitable to provide adequate identification of unknowns.

3.3.2 Global Profiling: HILIC-QTOF

As previously mentioned, the majority of the work published on apocrine sweat is predominately GC-MS based, focussing on volatile fatty acids (VFA). The limited LC-work that has been published is based on RP-HPLC systems (Emter and Natsch, 2008; Martin *et al.*, 2010; Natsch *et al.*, 2003; Troccaz *et al.*, 2009) leading to large

knowledge of non-polar metabolites. Thus, this work focuses on the developing a global method for the analysis of the more polar metabolites that are typically not well retained on a C₁₈ column. Systematic changes to the column, mobile phases, gradients, flow rates, and total analysis times were made in order to optimise the separation of the more polar compounds present in the pseudo sweat mixture.

3.3.2.1 Column Selection

Column selection depends largely on prior knowledge on the type of analyte, i.e. range of target compounds of interest. Thus, to evaluate the retention of polar metabolites in order to identify which type of column would be most suited for development, the amino acids content in the artificial sweat matrix were used. Amino acids represent a diverse range of polarities, thus, covering an adequate polarity range suitable for a global method development of polar to medium polar metabolites (Table 3.3). Initially, two columns were evaluated; a ZIC-HILIC column (5 µm, 150 x 2.1 mm) and a C₁₈ Synergi Hydro-RP 80Å, (4 µm, 150 x 2 mm) to identify which would be most suited for this application. The initial results obtained are illustrated in Table 3.3. The amino acids were poorly retained on the C₁₈ column, with the exception of Leu, Ile, Phe Try, and Tyr due to these particular analytes being more hydrophobic in nature. In comparison, the HILIC column was able to retain all the amino acids, which typically eluted around 5-8 min. The elution order from the HILIC column was generally from least polar to polar, which is opposite of traditional RP-LC. However, the basic amino acids, His, Lys, and Arg, were relatively less retained on the HILIC compared to the polar, non-polar or acidic amino acids, which eluted around 2-3 min. Thus, from this preliminary study, the C₁₈ column will be omitted from further development due to poor retention of the amino acids, while the HILIC column will be subjected to further development.

Table 3.3 Retention time of standard compounds at 40 µg/ml on a HILIC and C₁₈ column.

Name	Molecule	pK _a of α-COOH Group	pK _a of α-NH ₃ ⁺ Group	pK _a of Ionizing Side Chain	Log P	MW	m/z (M+H)	HILIC	
								RT/min	C ₁₈ RT/min
Nonpolar									
Alanine	C ₃ H ₇ NO ₂	2.3	9.7	-	-2.77	89.09	90.0555	7.39	-
Valine	C ₃ H ₁₁ NO ₂	2.3	9.6	-	-2.29	117.15	118.0868	5.36	1.40
Leucine	C ₆ H ₁₃ NO ₂	2.4	9.6	-	-1.72	131.17	132.1024	3.84	3.15
Isoleucine	C ₆ H ₁₃ NO ₂	2.4	9.7	-	-1.80	131.17	132.1024	4.96	3.15
Proline	C ₃ H ₉ NO ₂	2.0	10.6	-	-2.62	115.13	116.0711	5.41	1.39
Methionine	C ₃ H ₁₁ NO ₂ S	2.3	9.2	-	-2.10	149.21	150.0589	4.57	1.45
Phenylalanine	C ₉ H ₁₁ NO ₂	1.8	9.1	-	-1.44	165.19	166.0868	3.72	7.35
Tryptophan	C ₁₁ H ₁₂ N ₂ O ₂	2.4	9.4	-	-1.15	205.09	205.0977	4.50	7.85
Uncharged polar									
Glycine	C ₂ H ₅ NO ₂	2.3	9.6	-	-3.00	75.07	76.0398	8.09	1.15
Serine	C ₃ H ₇ NO ₃	2.2	9.2	-	-3.00	105.09	106.0504	8.23	1.19
Threonine	C ₄ H ₉ NO ₃	2.6	10.4	-	-2.83	119.12	120.0660	7.62	1.22
Cysteine	C ₃ H ₇ NO ₂ S	1.8	10.8	8.3	-2.55	121.16	122.0276	9.69	1.29
Tyrosine	C ₉ H ₁₁ NO ₃	2.2	9.6	10.1	-2.11	181.19	182.0817	6.66	4.25
Asparagine	C ₄ H ₈ N ₂ O ₃	2.0	8.8	-	-3.48	132.12	133.0613	8.30	1.19
Glutamine	C ₃ H ₁₀ N ₂ O ₃	2.2	9.1	-	-3.11	146.14	147.0769	7.90	1.26
Acidic									
Aspartic acid	C ₄ H ₇ NO ₄	2.1	9.8	3.9	-3.61	133.10	134.0453	8.60	1.21
Glutamic acid	C ₃ H ₉ NO ₄	2.2	9.7	4.2	-3.51	147.13	148.0610	8.36	1.26
Basic									
Histidine	C ₆ H ₉ N ₃ O ₂	1.8	9.2	6.0	-2.85	155.15	156.0773	3.09	1.11
Lysine	C ₆ H ₁₄ N ₂ O ₂	2.2	9.0	10.0	-3.77	146.19	147.1130	2.17	1.05
Arginine	C ₆ H ₁₄ N ₄ O ₂	2.2	9.0	12.5	-3.79	174.20	175.1195	2.12	1.13

Log P (Partition coefficient) of amino acids taken from Tayar and co-workers(Tayar *et al.*, 1992).

3.3.2.2 Solvent and Buffer Selection

Reviews of the relevant literature (Table 3.1) revealed that acetonitrile was the most effective solvent for the separation of polar/semi-polar compounds using HILIC; hence, mobile phase method development was based on this solvent (Alpert, 1990; Alpert *et al.*, 1993; Olsen, 2001; Schlichtherle-Cerny *et al.*, 2003; Valette *et al.*, 2004).

The buffers typically used for HILIC are either ammonium acetate or formate (5-20 mM) due to their compatibility with MS, solubility in high organic solvent and pH range from 3-8. Initially, binary solvent systems were evaluated as this overcomes some of the difficulties associated with retention time shifts due to column equilibration. The acetonitrile content or ammonium acetate concentration was separately altered between 70-90% and 10-30 mM respectively. As depicted in Figure 3.5 A, the organic content had a profound effect on retention, with increasing organic content resulting in longer retention of all amino acids, which is consistent with the literature (Guo and Gaiki, 2005; McCalley, 2010; Novakova *et al.*, 2008). Separation could be achieved with the use of high organic content, however, this would result in a long analytical run time (>40 min) due to the basic amino acids being well retained, which is considered unfavourable. In comparison, the change in salt concentration slightly increased the retention of all except the basic amino acids (Figure 3.5 B). A binary solvent system is not desirable, thus, a gradient profile was sought after in order to reduce the overall analytical runtime.

The effect of ionic strength and pH were then independently investigated through the use of gradient elution conditions. Initially, the ammonium acetate was varied between 1-80 mM as depicted in Figure 3.6 A-C. High salt concentrations resulted in a marginal increase in retention across all the amino acids, except the basic amino acid residues, His, Lys, and Arg, which decreased in retention. This observed effect is consistent with the HILIC mechanism (Bicker *et al.*, 2008; Lammerhofer *et al.*, 2008; Wu *et al.*, 2008) and the current literature (McCalley, 2010; Novakova *et al.*, 2008). The increase in salt concentration potentially reduces the electrostatic repulsion,

since the sulfonate groups on the sulfobetaine stationary phase are negatively charged and prevent the carboxyl groups from interacting with the positively charged quaternary amine groups located closer to the silica surface (Guo *et al.*, 2007). Thus, as the salt concentration increases, the retention of basic compounds on the negatively charged sites are reduced, while the repulsion of acidic compounds from the same sites is reduced, thereby increasing the retention of the acidic metabolites.

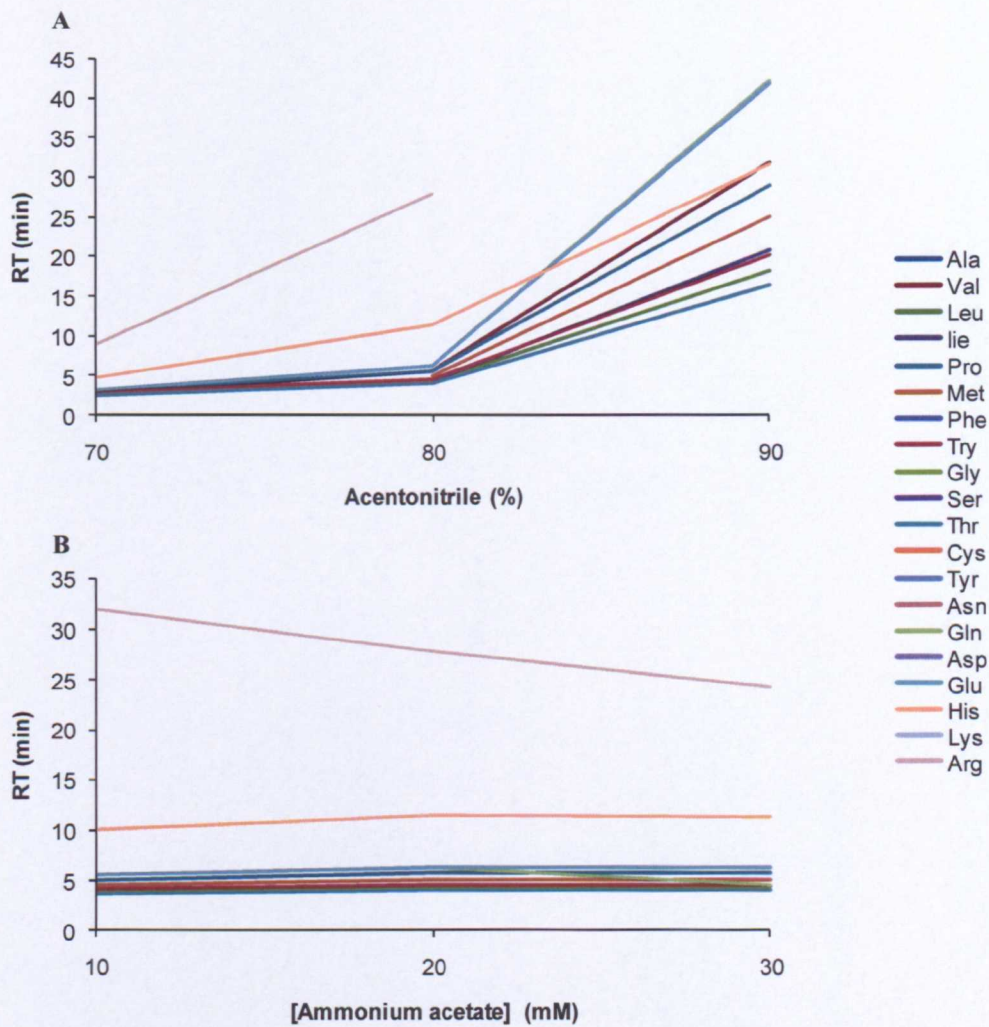


Figure 3.5 Effect of **A** increasing organic content **B** salt concentration on amino acid retention time in a binary solvent system.

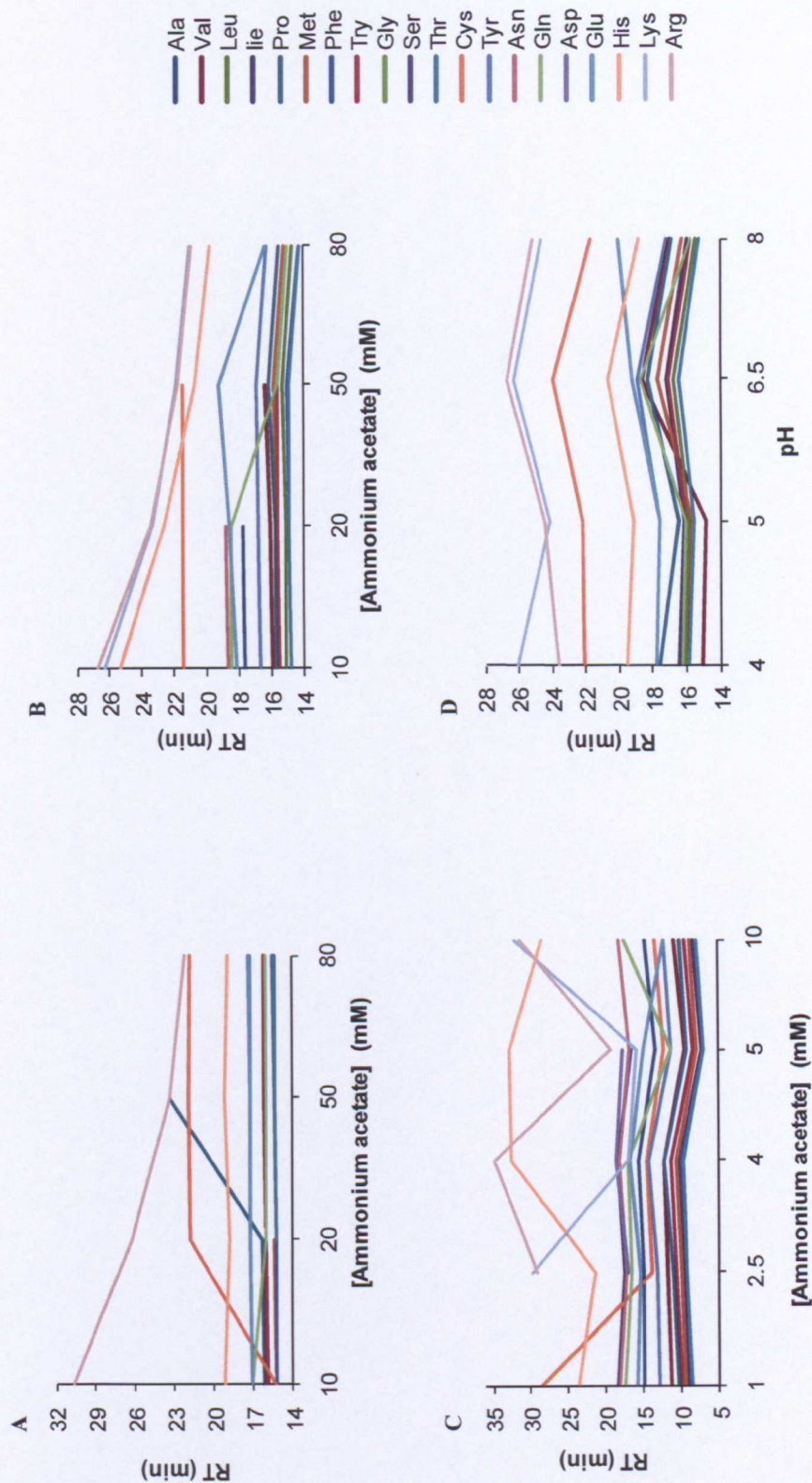


Figure 3.6 Effect of salt concentration or pH on amino acid retention time. **A** and **B** Mobile phase [A] 100% acetonitrile or 100% acetonitrile + 0.1% formic acid respectively [B] 100% water with various concentration of NH_4Ac , **C** Mobile phase [A] 90% acetonitrile + 0.5 mM NH_4Ac [B] 60% acetonitrile with various concentration of NH_4Ac , **D** Mobile phase [A] 95% acetonitrile + 10 mM NH_4Ac [B] 100% water + 10 mM NH_4Ac . pH change was consistent in both [A] and [B].

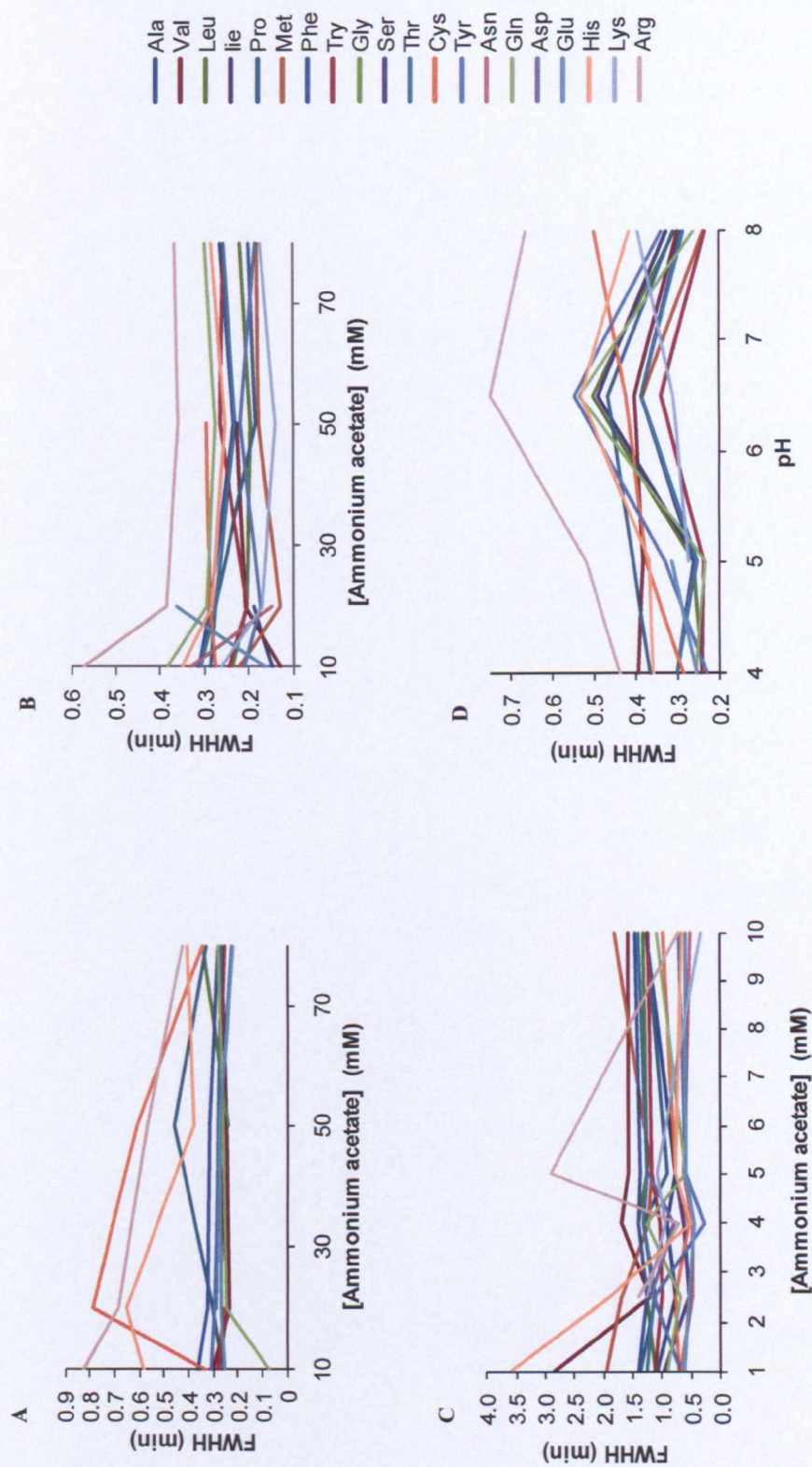


Figure 3.7 Effect of salt concentration or pH on the amino acids peak width at half height. **A** and **B** Mobile phase [A] 100% acetonitrile or 100% acetonitrile + 0.1% formic acid respectively [B] 100% water with various concentration of NH_4Ac , **C** Mobile phase [A] 90% acetonitrile + 0.5 mM NH_4Ac [B] 60% acetonitrile with various concentration of NH_4Ac , **D** Mobile phase [A] 95% acetonitrile + 10 mM NH_4Ac [B] 100% water + 10 mM NH_4Ac . pH change was consistent in both [A] and [B].

The effect of the mobile phase pH on the RP-HPLC is known to have a significant effect on the retention properties due to changes in the ionisation properties of the analyte. For example, a weak acid with a pKa value ~ 3 will be ionised at two pH units above or non-ionised two pH below, which will increase or decrease the retention respectively. Further changes in greater than two pH units either side of the pKa values will have minimal effect on retention because the ionisation of the analyte will remain unchanged (Snyder *et al.*, 1988). The effect of pH on HILIC separation was therefore investigated between pH 4-8, by altering stock salt concentration before mixing with acetonitrile. The absolute pH of the mobile phase was not directly measured and would presumably deviate from that of the stock solution (Barbosa and Sanznebot, 1994). Figure 3.6 D summarise the effect of altering pH on the HILIC retention of amino acids. The pKa values of the amino acids are summarised in Table 3.3. The COOH group and NH₃ group of all the amino acids will be ionised between pH 3-8. Only the ionisation state of the Asp, Glu, and His side chain will change under the experimental pH conditions. As depicted in Figure 3.7 D, the retention time essentially remained unchanged, with all the amino acids behaving in similar way. Thus, it is likely that the ion exchange effect is contributing to the overall retention, thereby, masking any pH effect. This is similar to Guo and co-workers (Guo and Gaiki, 2005) were they illustrated that pH had a minimal effect on retention when analysing salicylic acid, cytosine and cytidine, however, the retention of aspirin gradually decreased when reducing the pH.

The effect of ionic strength and pH on the peak width (FWHH), which is an indication of peak sharpness and, in general, an indication of column efficiency, is depicted in Figure 3.7. A change in pH was shown to have a marginal effect on FWHH. When the pH was increased to 6.5, FWHH tended to get broader across all the amino acids. In contrast to the salt concentration, peak width remained relatively constant, except in Figure 3.7 A, in which an increase in salt concentration reduced FWHH. This is likely due to the pH of the mobile phase under these conditions, which would be more basic as formic acid was not added to mobile phase [A].

It was concluded from these studies that 10 mM ammonium acetate at pH 5 would be the optimum conditions. Lower buffer concentrations are more favourable for MS detection and an acidic pH value resulted in an increase in peak efficiency. Figure 3.8

A and B represents extracted ion chromatograms of the amino acids standards and amino acids from artificial sweat matrix on a ZIC-HILIC column obtained from the optimum conditions, which ultimately will be used for the analysis of apocrine gland secretions. Not all peaks were fully resolved or contain a Gaussian peak shape (i.e. good chromatographic peak shapes). The basic amino acids, typically in the artificial sweat matrix, were more difficult to detect. This is most likely due to the poor peak shapes eluting over a longer periods of time and ion suppression effects from co-eluting metabolites. However, overall a good compromise between the broad ranges of polarities have been achieved within a 25 min runtime.

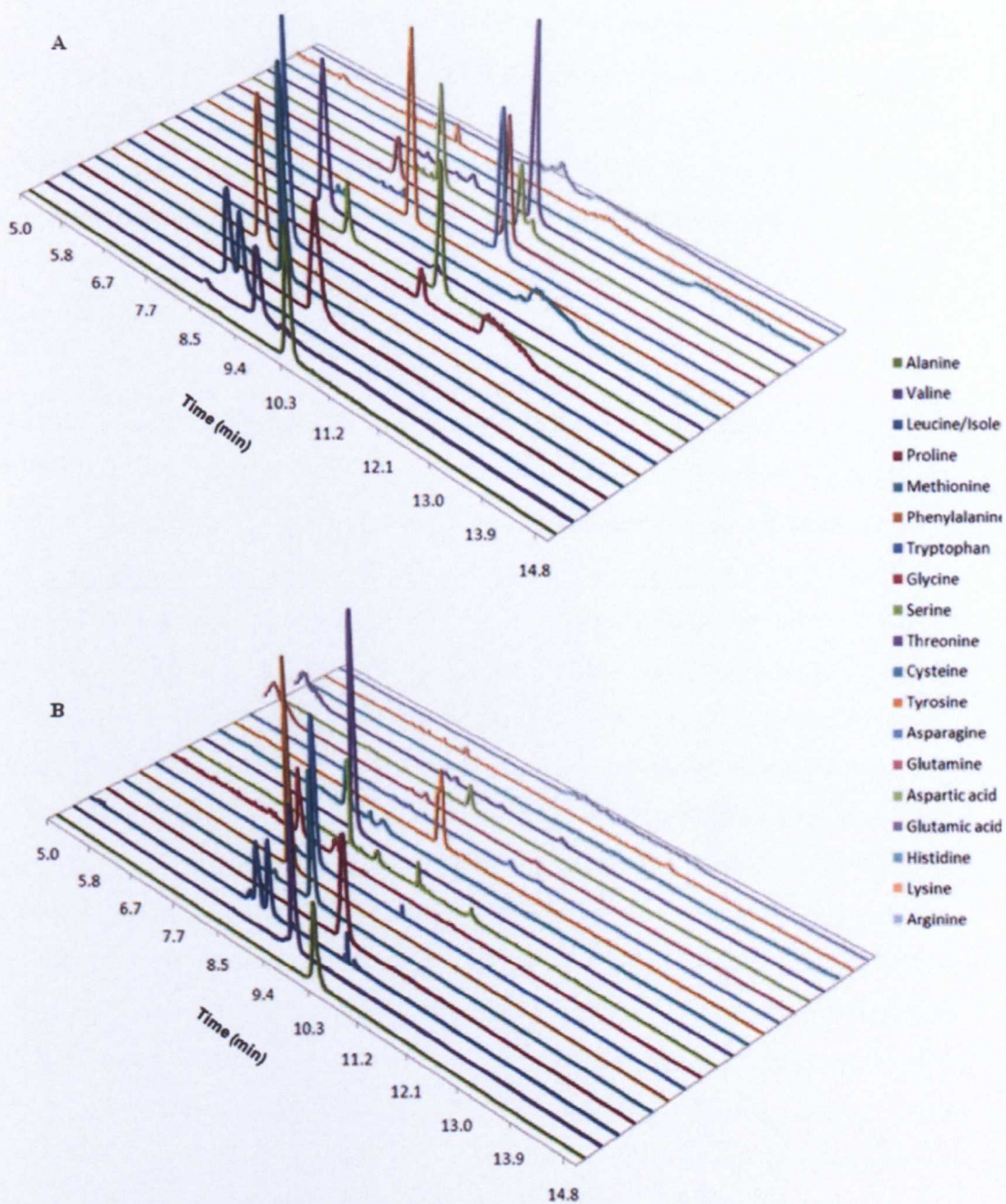


Figure 3.8 3D extracted ion chromatogram of **A** amino standards **B** amino standards present in the pseudo sweat mixture.

In summary, the HILIC method shows a good alternative in providing retention of polar metabolites compared to that of RP-HPLC. In contrast to the nature of and amount of organic modifier, both the investigated ranges of salt concentration and pH were found to have little effect compared to the amount of water present. This indicates considerable stability of the elution conditions for this stationary phase, which is desirable for retention time stability in metabolomics analysis.

3.3.3 Targeted LC-MS/MS

By employing the QTRAP[®] instrument and exploiting its unique scan capabilities (Hager, 2002; Hager and Le Blanc, 2003) it was possible to devise an analytical strategy capable of obtaining quantitative and qualitative data of metabolites in complex matrices as well as specifically tailoring for the survey of common structural moieties. The survey scans are generally based on pre-defined selection criteria of either a common precursor ion or a common natural loss which is processed “on-the-fly” in order to determine the pseudomolecular ion from a single injection. Once the selection criteria are satisfied, an enhanced product ion (EPI) scan is triggered to produce spectra which give full structural information. An enhanced resolution (ER) scan can also be triggered before acquisition of the EPI scan, in order to confirm the m/z value of the unknown pseudomolecular ion. However, when analysing complex mixture, the pseudomolecular ion might not be the most intense peak during that scan cycle resulting in the wrong ion being selected for EPI scan, thus, this function was removed. Nonetheless, three types of scans can be generated in a single cycle time that is very much lower than conventional triple-quadrupole (Q-q-Q) mass spectrometers and when the QTRAP[®] is switched to operate as an ion trap, higher quality spectra are obtained compared to that of a conventional Q-q-Q mass spectrometers.

3.3.3.1 Optimization of the Declustering Potential and Collision Energy

The MRM optimisation procedure involves a sequence of experiments where the voltages of the various ion optics parameters (i.e. DP and CE) are ramped to determine the maximum signal intensity for each ion. The optimum DP for each standard was obtained by direct infusion while systematically increasing the DP from 0 to 120 V. Optimum values for each of the standards were around 30 V. The CE was ramped between 5 and 100 V with the intensity of the amino acid product ion *m/z* 147 (Gln), *m/z* 105 (Cys) and *m/z* 179 (Cys-Gly) being plotted with each of the standards producing a similar maximum of around 20 V as summarised in Table 3.4.

Table 3.4 Retention times and optimised declustering potential and collision energies for the odour precursor standards.

Standard	Retention Time (min)	Precursor Ion (<i>m/z</i>)	Product Ion (<i>m/z</i>)	Declustering Potential (V)	Collision Energy (eV)
2M3H-Cys	3.2	208.1	105.1	40	20
3M3SH-Cys-Gly	4.9	293.1	179.1	30	20
HMHA-Gln	5.2	275.1	147.1	30	25
3M2H-Gln	6.5	257.1	147.1	30	20

3.3.3.2 LC-MS/MS Analysis of Odour Precursor Standard Compounds

MS Production Fragmentation

MS/MS transitions were generated as a result of the selective determination of the pseudomolecular ion and the most abundant product ion for each available amino acid conjugate standard. The literature is currently limited with respect to MRM analysis of odour precursors, and the LC-MS work that has been published is focused on single ion monitoring (SIM) (Troccaz *et al.*, 2009), with the majority of published work being with GC-MS. For the odour precursors for which there are no standards available, theoretical transitions were used based on fragmentation patterns from standards. Any co-eluting compounds were detected by defining a time in which the transition was excluded (dynamic exclusion) after acquiring the EPI scan. Figure 3.9 shows the EPI spectra of the four standards while their respective chromatographic separation is depicted in Figure 3.10. Source-dependent parameters optimised for

MRM remain the same for EPI scans. However, the DP and CE were ramped during the EPI scan cycle from 25-45 V and 15-30 V respectively. This was in order to obtain full fragmentation profiles of each standard to aid identification. It was experimentally observed that the mass accuracy of the EPI scan was usually within either 0.2 or 0.1 amu of the expected value. These EPI spectra are helpful in the confirmation of structural identification of amino acid conjugates in a complex biological sample. To my knowledge, this is the first work that presents full product ion spectra of any of the amino acid conjugates.

The elucidation of fragmentation mechanisms was not the main aim of this project, hence, fragmentation confirmation was only carried out on the available standards with the use of the MSⁿ. Confirmation of the fragmentation behaviour will provide additional information which will be later used when analysing data obtained from the PI survey scanning methodology. The 2M3H-Cys conjugate (m/z 208) contained fragments m/z 191, 105, and 87 (see Figure 3.9 A). The fragment at m/z 191 is consistent with a loss of OH, and m/z 105 is interpreted as cysteine residue $[M+H-NH_3]^+$ which can be further broken down to form m/z 87 $[105-H_2O]$ as well as coming from 2-methyl-3-sulfanylbutan-1-ol with the loss of H₂S (m/z 34). The collisionally activated dissociation of the amino acid $[M+H]^+$ ions have been observed by other ionisation methods and the mechanisms of their formation has been explained (Biemann and McCloskey, 1962; Bouchonnet *et al.*, 1992; Dookeran *et al.*, 1996; Kulik and Heerma, 1988; Petritis *et al.*, 2000).

The 3M2H-Gln conjugate (m/z 257) contained fragments m/z 240, 147, 129 and 111 (see Figure 3.9 B). The fragment at m/z 240 was consistent with the loss of OH and can further fragmented to produce fragments of m/z 130 and 111 which are interpreted as the loss of glutamine $[M+H-NH_3]^+$ and 3-methylhex-2-enoic acid respectively. The peak at m/z 147 is considered as glutamine residue $[M+H]^+$ and can further be fragmented to produce an m/z 130 through a loss of NH₃. The peak at 129 is also interpreted as glutamine residue $[M+H-H_2O]^+$ and in turn can be further fragmented to form m/z 83 $[Im-NH_3]^+$.

The 3M3SH-Cys-Gly conjugate (m/z 293) contained fragments m/z 179, 162, 144, and 116 (see Figure 3.9 C). The fragment at m/z 179 was consistent with the loss of

Cys-Gly residue. The fragment of m/z 162 and 144 was consistent with the loss OH and a combined loss of OH from NH_3 respectively, from the Cys-Gly residue. The peak at m/z 116 is considered as the 3M3SH with the loss of H_2S (m/z 34).

The HMHA-Gln conjugate (m/z 275) contained fragments of m/z 257, 240, 147, 130, and 111 (see Figure 3.9 D). The fragment of m/z 257 and 240 is consistent with a loss of OH and a combined loss of OH and NH_3 from 3M2H and Gln respectively. The peak at m/z 147 and 130 is considered as glutamine residue $[\text{M}+\text{H}]^+$ and $[\text{M}+\text{H}-\text{NH}_3]^+$ respectively.

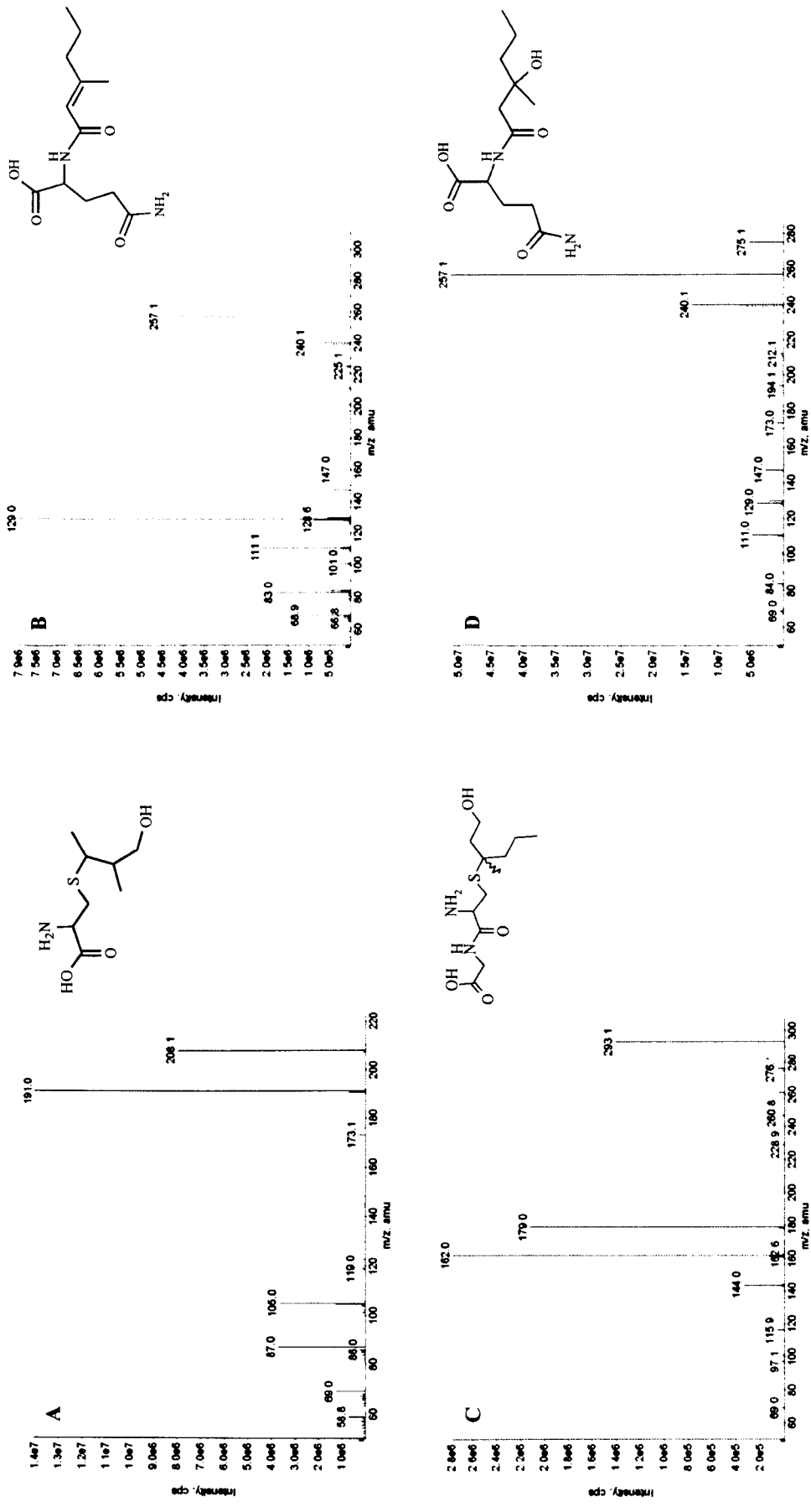


Figure 3.9 EPI spectra of **A** 2M3H-Cys **B** 3M2H-Gln **C** 3M3SH-Cys-Gly **D** HMHA-Gln conjugate obtained using MRM as a trigger.

LC-MS/MS Analysis of the Conjugates

The analytical method was initially optimised with four odour precursors (3M2H-Gln, HMHA-Gln, 2M3H-Cys and 3M3SH-Cys-Gly) which were purchased *via* custom synthesis from Unilever (Bebington, UK). The chromatographic method was initially modified from the work published by Troccaz and co-workers (Troccaz *et al.*, 2009). The racemic odour precursors were prepared at a concentration of 1 µg/ml and injected on to the HPLC column, while the MS was in MRM mode. Figure 3.10 shows a typical extracted ion chromatogram of the optimal chromatographic conditions, with an elution profile of 2M3H-Cys conjugate (3.2 min), 3M3SH-Cys-Gly conjugate (4.9 min), HMHA-Gln conjugate (5.2 min) and 3M2H-Gln conjugate (6.5 min). The diastereoisomers of Cys conjugate at 3.2 min showed peak splitting which previously have been reported to co-elute (Troccaz *et al.*, 2009). This was confirmed by full MS/MS product ion scanning, which produced identical fragmentation patterns. Modifying the pH of the mobile phase affected the intensity of each standard with minimal effect on the peak splitting of the 2M3H-Cys conjugate. Experiments comparing methanol and acetonitrile as the organic mobile phases resulted in methanol providing improved retention of the 2M3H-Cys conjugate.

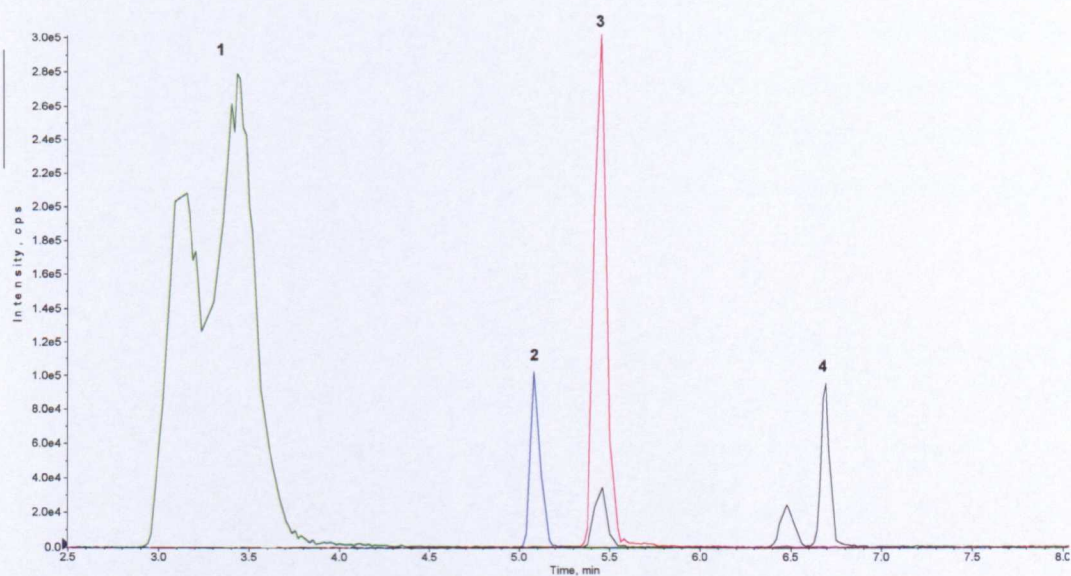


Figure 3.10 Extracted ion chromatogram of 1) 2M3H-Cys 2) 3M3SH-Cys-Gly 3) HMHA-Gln 4) 3M2H-Gln conjugate reference standards containing 1 µg/ml of each precursor.

3.3.3.3 LC-MS/MS profiling of Odour Precursors using Precursor Ion Survey Scan

As depicted in Figure 3.11 - Figure 3.13, the PI scanning approach was able to detect each of the standards at the correct retention time compared with the verified LC-MS/MS targeted analysis and were positively identified using the EPI spectra. As noted previously in Section 3.3.3.2, 2M3H-Cys conjugate has a double peak (see Figure 3.11), where each peak produces similar EPI spectra as previously mentioned. Figure 3.12 also shows a double peak in the extracted ion chromatogram; both peaks produce a similar EPI spectrum suggesting that one peak may arise from an impurity present in the synthetic standard. The EPI spectra obtained from PI scanning were similar to that produced in the targeted MS/MS approach (see Figure 3.9), thereby, allowing identification of odour precursors without making assumptions of their absolute identity. Nonetheless, there were limitations to this scanning method. The EPI threshold was set higher than that of the LC-MS/MS method by an order of magnitude. This was to allow high quality spectra to be obtained at the expense of detecting conjugates at a low concentration range as well as limiting false positives. Furthermore, this method is not as sensitive as MRM analysis by at least one order of magnitude. This is due to compromises in the CE and DP being made in order to cover a range of metabolites, longer scan times (s instead of ms) resulting in fewer data points across any one peak, and an increase in background ions. However, any peaks of interest that have been detected can be added to the MRM methodology in order to increase the sensitivity.

In summary, the precursor ion scan coupled with full product ion spectra has the potential to identify common structural moieties of the odour precursors in order to identify possible new conjugates in biological extracts. Once new compounds have been identified by the precursor ion approach, then precursor and product ion can be used to monitor for these new conjugates in a biological extract.

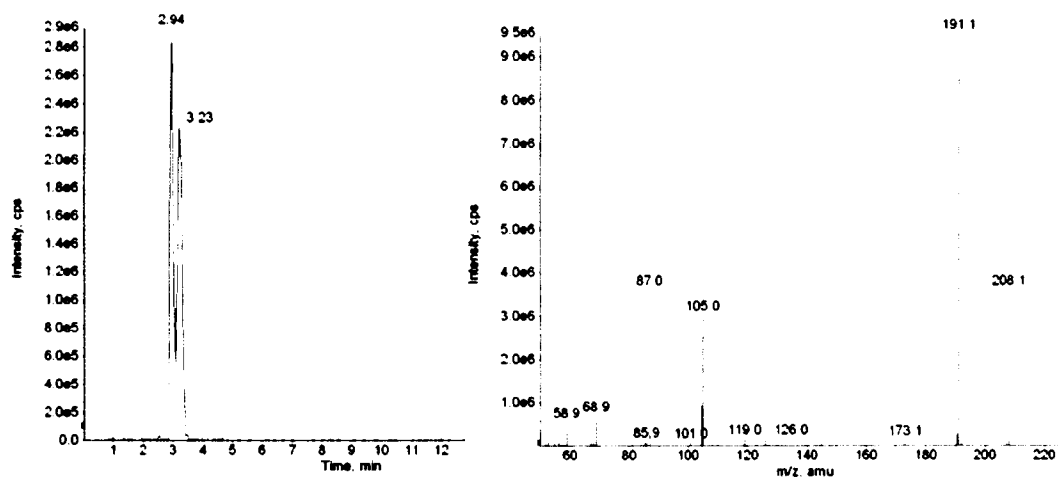


Figure 3.11 Extracted ion chromatogram of 2M3H-Cys (m/z 208) and EPI spectrum of the peak at 3.2 min from an EPI triggered PI scan of m/z 105. Both peaks produce similar EPI spectra.

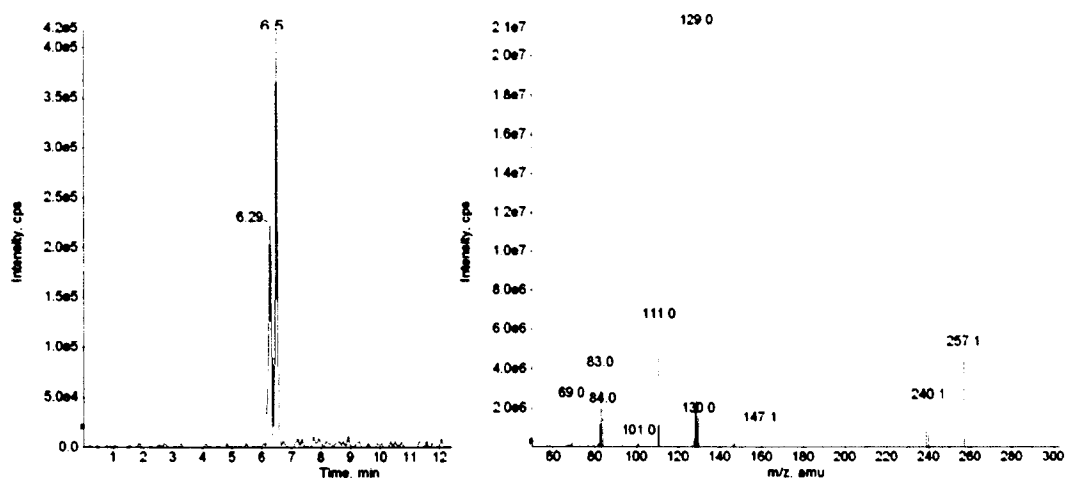


Figure 3.12 Extracted ion chromatogram of 3M2H-Gln (m/z 257) and EPI spectrum of the peak at 6.5 min from an EPI triggered PI scan of m/z 147.

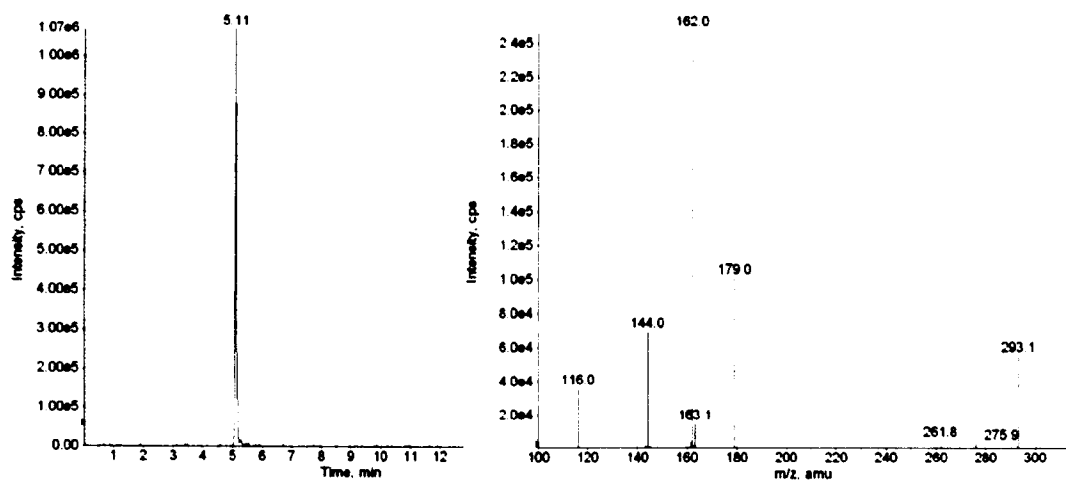


Figure 3.13 Extracted ion chromatogram of 3M3SH-Cys-Gly (m/z 293) and EPI spectrum of the peak at 5.1 min from an EPI triggered PI scan of m/z 179.

3.4 Conclusions

The choice of analytical methodology to pursue is highly dependent on the level of chemical information required about the metabolites of interest as highlighted in Table 3.5. Currently, there is no one analytical technique, i.e. ‘gold standard’, capable of providing all the information required for analysis of apocrine sweat samples. Thus, a range of methods have been developed to provide complementary information on metabolites in apocrine sweat samples.

The LC-MS(MS) methodologies developed herein represent a significant step forward in providing identification for the full range of metabolites present in apocrine sweat samples as a whole, as well as specifically identifying and quantifying odour precursors. Although there is a large body of literature on the analysis of apocrine sweat, these are predominantly GC-MS based methods providing identities of only the volatile components present. To my knowledge there has been no global or MRM LC-MS work published to date, adding to the uniqueness of the present work. The DIMS approach did provide quick analysis times; however, the data obtained would be too complex and insufficient in providing metabolite identification, thus, will no longer be pursued.

The LC-MS(MS) methodologies have been developed using artificial sweat mixture or standard precursors. These methods will be further tested on samples that are more representative of that of apocrine sweat, which will be discussed in the following chapter.

Overall, the global MS method will provide complementary information to that of the NMR data, and with the use of a high mass accuracy instrument, empirical formula and tentative identification can be found. The MRM and precursor ion scanning-IDA-EPI approach carried out in this chapter provides informative product ion spectra which will provide a useful tool for structural confirmation. Furthermore, by monitoring for common structural moieties, the semi-targeted method is no longer restricted to the availability of standards.

Table 3.5 Summary of the analytical conditions that have been developed.

	Global Profiling		Broad-profiling	Semi/Targeted
	NMR	DIMS	HILIC-MS for profiling polar metabolites	LC-MS/MS for amino acid conjugates
Chemical Information	Gives detailed structural information, particularly using 2-D NMR of isolated metabolites	Qualitative and not quantitative. Inability to distinguish between isomeric compounds	High mass accuracy (5-10 ppm) for empirical formulae generation	Characteristic fragment-ion information that is related to chemical structure
Chemical Bias	These methods have little chemical bias (high conc metabolites) and can be used directly on the sample	Solvent bias means it is usually more applicable to polar compounds	Solvent bias means it is usually more applicable to polar compounds	Bias to the analytes of interest i.e. odour precursors
Speed	25 min	3 min	25 min	18 min
Reproducibility	Minimal variation (<5% RSD)	Matrix and Ion suppression effects vary	Reequilibration, temperature and number of injections can all cause chromatographic variation	Reequilibration, temperature and number of injections can all cause chromatographic variation
Sample Size	8 µl	5 µl	5 µl	5 µl
Limit of Detection	Low µM concentrations	< µM concentrations	< µM concentrations	< µM concentrations
Advantages	non-biased detector, non-invasive, highly reproducible, relatively easy to identify metabolites	Rapid screen of metabolites, minimal sample clean up	High sensitivity, average to high chromatographic resolution, empirical formula generation	High sensitivity, structural information
Disadvantages	Lower sensitivity than MS	Matrix effects, identification of metabolites require MS/MS	Identification of unknown is labour intensive, limited structural information, more costly than NMR	Ion suppression effects, more costly than NMR, requires <i>a priori</i> knowledge of analytes

Chapter 4

4 Application of ^1H NMR Spectroscopy and LC-MS to an *In-Vitro* Model of Apocrine Sweat Produced from ASG5 Cell Lines

4.1 Introduction

Apocrine glands secrete a turbid fluid comprised of water, electrolytes, fatty acids, steroids, lipids, proteins and nitrogen metabolites such as ammonium and urea (Gower *et al.*, 1986; Zernecke *et al.*, 2010). When exposed to micro-flora populations present on the skin, the lipidic solutes, including steroids and short chain fatty acids, are transformed to malodorous compounds. Apocrine sweat is produced in low volumes, typically less than 5 μl , and secreted into the hair follicle, after which, there is a lag time of 24-48 h before further apocrine sweat can be produced. Apocrine sweat is both difficult to collect and very costly. Hence, a practical way of investigating apocrine secretions is to use a long-term proliferating ASG5 cell line (Burry *et al.*, 2008), that closely mimic the function of an apocrine gland *in situ*. The development of such an *in vitro* model has potential benefits not only in providing a suitable matrix for future method development, but potentially in assisting in the identification of transport secretory mechanisms, screening of malodorous compounds and determining effective concentrations of metabolites present.

The morphology of the ASG5 apocrine cell line are depicted in Figure 4.1, whereby, microvilli (M) and apical blebs (A) are present at the luminal membrane, as well as secretory granules (S) being present throughout the cytoplasm. The typical pinching off (mode of secretion) is also observed (Figure 4.1 B and C). This data is comparable to apocrine secretory morphology *in vivo* (Montagna *et al.*, 1953).

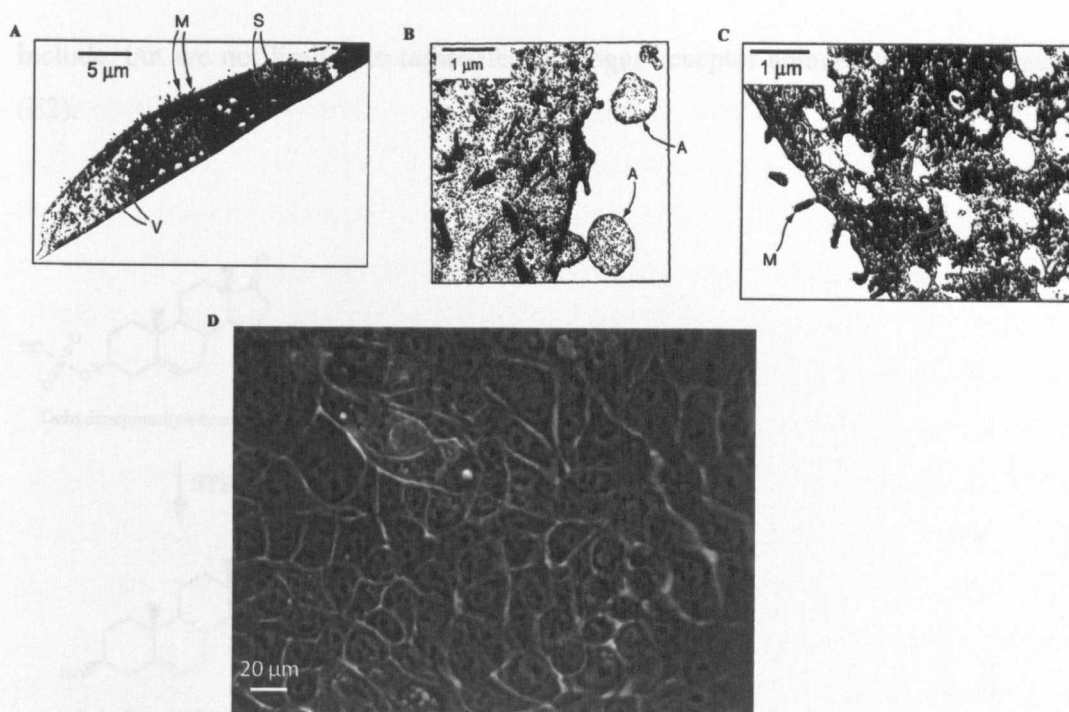


Figure 4.1 Ultrastructure of an ASG5 apocrine cell using 200 hexagonal copper grids for transmission electron microscopy. Microvilli (M), apical blebs (A), secretory granules (S) and empty vesicles (V). Reproduced from (Burry *et al.*, 2008).

Apocrine glands do not begin to function until puberty, thus, it is thought that androgens (sex steroid hormones) play some part in the regulation of apocrine gland activity due to the presence of androgen receptors (Beier *et al.*, 2005; Labrie, 1991). This is further supported by the fact that cholesterol biosynthesis is upregulated in the presence of androgens (Heemers *et al.*, 2003), which could be used as a precursor for the production of volatile steroids (Cowley and Brooksbank, 1991; Grosser *et al.*, 2000). The ASG5 cell line possesses the genes required for androgen and estrogen synthesis, in addition to necessary β receptors required to mediate the response. Furthermore, the ASG5 cell line expresses the *ABCC11* gene, as well as the apoD, which is known to be associated with cellular secretory processes (Martin *et al.*, 2010; Spielman *et al.*, 1998; Spielman *et al.*, 1995; Zeng *et al.*, 1996b). The ASG5 cell line possesses the GG phenotype (538G→A SNP), that is associated with wet ear wax type (Yoshiura *et al.*, 2006) and increased levels of axillary odour. The ASG5 cell line also retains many of the steroidogenic features present *in vivo* secretions as depicted in Figure 4.2 (Burry *et al.*, 2008). Thus, production of malodorous compounds and odour precursors, as well as cell proliferation, would be expected to be compromised by compounds known to interfere with the androgen pathway. Such compounds

include, but are not limited to tamoxifen (estrogen receptor antagonist) or β -estradiol (E2).

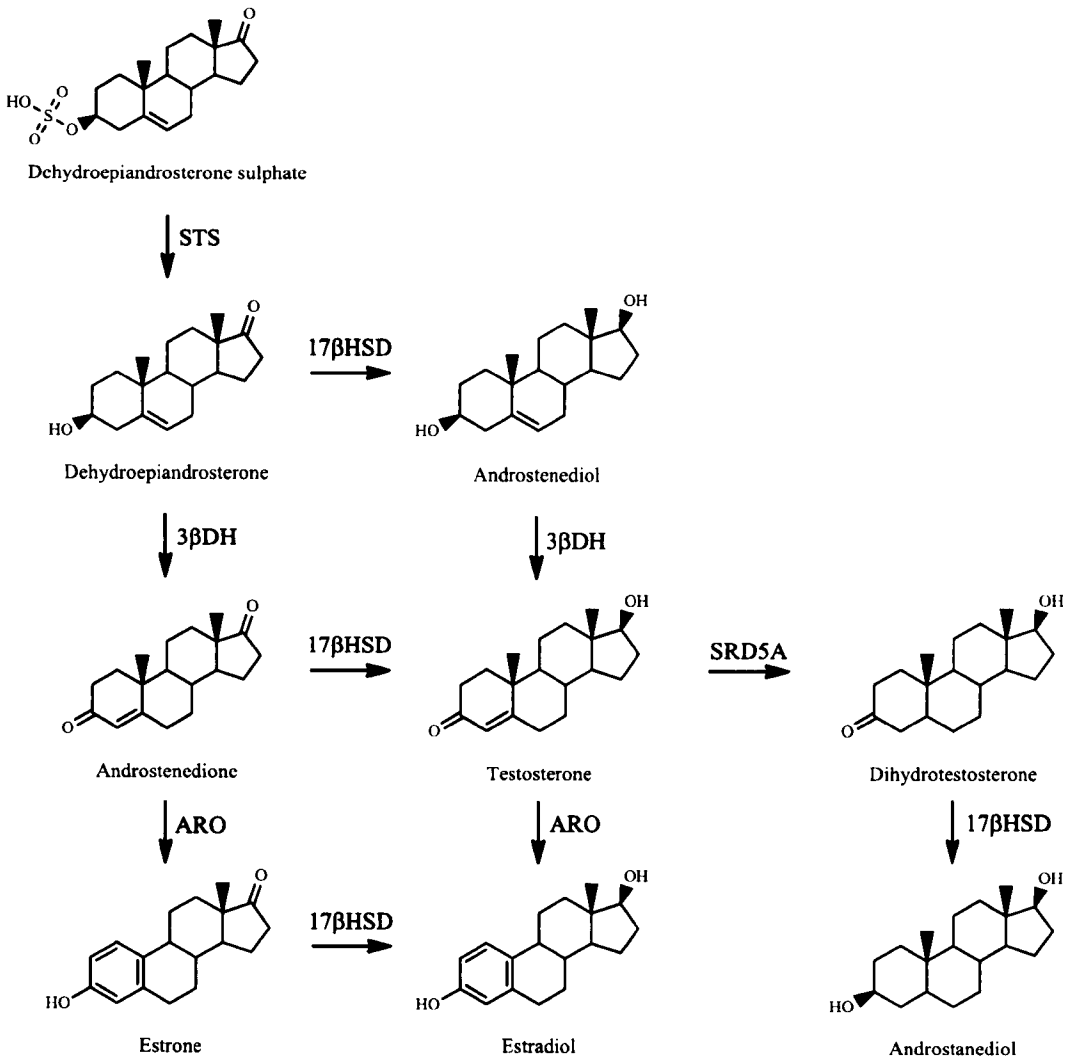


Figure 4.2 Schematic of the steroid synthesis pathway present in ASG5 apocrine cell lines. Key: STS (steroid sulphotase), HSD (hydroxysteroid dehydrogenase), DH (dehydrogenase), ARO (aromatase) and SRD5A (5 α -reductase). Reproduced with modifications (Burry *et al.*, 2008).

4.1.1 Metabolite Extraction from ASG5 cells

Prior to analysis with the methodologies developed in chapters two and three, the cellular metabolites have to be extracted. Ideally, the extraction method should extract

the largest number of metabolites, be nonselective, nondestructive or modify metabolites through chemical or physical means (Maharjan and Ferenci, 2003). However, there is no ideal technique to simultaneously extract all classes of metabolites, due to their high variability in the chemical and physical properties, thus, a variety of extraction methods have been developed. For example, perchloric acid is widely used to precipitate proteins and extract hydrophilic metabolites. Although advantageous for extracting amines, acidic treatment can have detrimental effects on the structural stability of metabolites (Lin *et al.*, 2007) and can directly interfere with analytical methods. Polar organic solvents (methanol, ethanol or acetonitrile) on the other hand, are typically mixed with water to extract hydrophilic metabolites, while chloroform is used to extract hydrophobic metabolites (Lin *et al.*, 2007). Given that the optimal extraction method will be essential in metabolome studies, several protocols have been developed with varying levels of success. The commonly used methods involve hot (90°C) ethanol (Tweeddale *et al.*, 1998), hot (70°C) methanol (Shryock *et al.*, 1986), cold (-40°C) methanol, perchloric acid (Shryock *et al.*, 1986), alkali (KOH) (Gonzalez *et al.*, 1997), and methanol/chloroform (Dekoning and Vandam, 1992). There have been several studies comparing the different types of extraction methods (see (Faijes *et al.*, 2007; Lin *et al.*, 2007)). Maharjan and co-workers (Maharjan and Ferenci, 2003) considered the problems associated with the different extraction protocols and concluded that the cold methanol protocol has distinct advantages over the other methodologies. Since the extraction is carried out at -40°C, stability and enzyme quenching minimise any metabolite transformations. Moreover, this method has all the advantages of hot methanol or ethanol protocols; denaturing and precipitating proteins and polysaccharides, no salts are added, easy to evaporate or concentrate extracts and minimal effect on pH.

At present, there is limited research available with regards to the use of ASG5 cell lines in metabolomic studies. The work that has been presented focuses on GC-MS as the primary analytical tool for the analysis of metabolites present in the ASG5 cell lines (Burry *et al.*, 2008). For the first time, NMR or LC-MS methodologies will be applied to analyse the metabolic composition the ASG5 apocrine cell lines. The developed analytical methodologies in both chapter two and three will have the potential to provide further insight into the apocrine cellular metabolism, as well as

identifying if male and female apocrine glands have the potential to behave differently due to the differences in circulating hormones. The use of applying multiple analytical platforms for metabolomic profiling of biological samples is gaining precedence (Hodson *et al.*, 2007; Lanza *et al.*, 2010; Lenz *et al.*, 2004; Lenz *et al.*, 2007; Williams *et al.*, 2005a), as it provides a better strategy for covering, detecting and identifying metabolites than relying on any single technique alone.

4.1.2 Aims

- Evaluate the analytical methodologies developed in chapters two and three by identifying whether each technique can discriminate between tamoxifen (estrogen receptor antagonist) or β -estradiol treated cell lines.
- Identify metabolites in ^1H NMR spectra which could be used as a reference for identifying metabolites from human axillary secretions.

4.2 Material and Methods

4.2.1 Sample Preparation

4.2.1.1 Cell Culture

Cell culture and preparation of cell pellets was undertaken by Dr Mark Harker and co-workers at Unilever (Port Sunlight, UK). Initially, a long-term proliferating cell line derived from axillary apocrine glands (ASG5) was generated as described previously (Burry *et al.*, 2008). ASG5 cells passage number 47 or 48 were grown in 15 ml Mammary Epithelial Growth Medium (MEGM), supplemented with 10 ng/ml EGF, 10 $\mu\text{g/ml}$ insulin, 0.5 $\mu\text{g/ml}$ hydrocortisone, 30 $\mu\text{g/ml}$ bovine pituitary extract, 50 $\mu\text{g/ml}$ gentamicin and 50 ng/ml amphotericin, under incubation in a 95% air / 5% CO_2 humidified incubator at 37°C, the medium was changed every three days. After four or five days the cultured cells ($n=5$) were treated with tamoxifen (TAM) in ethanol (2.7 nM), β -estradiol (E2) in ethanol (10 nM), vehicle (ethanol) or left untreated for three days prior to harvest. Harvesting was performed using trypsin

0.25% solution (incubation time 8 min, 37°C). The resultant cell suspension was centrifuged (2000 rpm, 7 min) with the supernatant being discarded. The pellet was re-suspended in 1 ml fresh medium and transferred to 1.5 ml eppendorf tubes. The cells were centrifuged in a microfuge at 6000 rpm for 5 min and the supernatant discarded. The pellets were stored at -80°C.

4.2.1.2 Cell Extraction

The cells were extracted with an equal volume of cold (-20°C) absolute methanol. After vortexing (30 s), the tube was transferred into a dry ice bath for 30 min and subsequently thawed in an ice bath for 10 min. Centrifugation (13,000 rpm, 10 min) was carried out and the supernatant was collected. The cell pellet was subjected to a second extraction with 50% v/v cold (-20°C) methanol, and the first and second extracts were combined. The pooled supernatants were evaporated to dryness with a centrifugal concentrator (~4 h) and then re-suspended in 20 µl of water. Each sample was aliquoted as follows: 5 µl aliquots into 1 mm NMR tubes with the addition of 3 µl deuterated potassium phosphate buffer (pH* 6.0, 0.1 M) containing TSP (7.6 mM), 10 µl aliquots into MS vials with the addition of 85% acetonitrile, and the remaining 5 µl was pooled together in order to create QC samples with the addition of 85% acetonitrile.

4.2.2 ¹H NMR Spectroscopy

Development of the methodology for the analysis of human apocrine gland sweat secretions is discussed in chapter two (Section 2.3.3). In summary, spectra were acquired on a Bruker Avance 400 spectrometer, operating at 400.13 MHz ¹H observation frequency equipped with a 1 mm TXI micro-volume with an internal probe temperature of 298 K and with 256 transients being collected. All spectra were manually corrected for phase and baseline distortions using TopSpin™ 2.1 (Bruker GmbH, Germany) and chemical shifts referenced to TSP standard at 80.00 ppm.

4.2.3 2D NMR Spectroscopy

To aid spectral assignment, 2D ^1H - ^1H COSY spectra were measured with solvent presaturation pulse sequence on each sample. Acquisition and processing parameters for the COSY spectra included a relaxation decay of 1.86 s, a spectral width in F1 and F2 of 5995.2 Hz, 2 k time domain points, 128 F1 increments, 64 transients per increment and qsine apodization in F1 and F2.

4.2.4 HILIC-QTOF-MS

HILIC-QTOF-MS was used for a global profiling approach as previously described in chapter three (Section 3.2.4). In summary, data was acquired m/z 80-1000 in positive ion mode over 25 min.

4.2.5 Targeted LC-MS/MS

RP-HPLC-MS/MS was used to specifically target amino acid conjugates as previously described in chapter three (Section 3.2.6). This method was only conducted on the QC samples due to the limitation in sample volumes.

4.2.6 Quantification of Artificial Apocrine Sweat Metabolites by ^1H NMR Spectroscopy

Quantification was carried out as previously described in chapter two (Section 2.3.4).

4.2.7 NMR Spectral Data Reduction

Pre-processing of NMR spectra was carried out as previously described in chapter two (Section 2.3.5).

4.2.8 HILIC-QTOF-MS Data Pre-Processing

LC-MS data were prepared for multivariate data analysis using Micromass MarkerLynx Application Manager (Version 4.0, Waters, UK). MarkerLynx incorporates an ApekTrack-peak detection algorithm which allows detection and retention time alignment of the peaks eluting in each chromatogram. The data were combined into a single data matrix by aligning peaks with the same mass/retention time pair together from each data file in the dataset, along with their associated intensities. Only peaks between 1.5 min to 14 min retention times were included in the final data matrix and the intensity of each ion was normalised to the samples total signal intensity.

4.2.9 Multivariate Data Analysis

Umetrics SIMCA-P version 11 was used for multivariate data analysis. Two types of scaling were used, mean-centring (subtracting the calculated average of a variable from the data so that the mean for each variable is 0) and mean-centring followed by autoscaling (division of each variable by the standard deviation for that variable). The use of mean-centred but not autoscaled data in basic multivariate analyses such as PCA, often results in an emphasis on perturbation of the metabolites that are present in high concentrations, whereas autoscaled data standardise the variance of each variable to one, thus, is more sensitive to changes in the levels of minor metabolites as each variable has an equal weight. For the purpose of illustrating the results of this study, autoscaling of the data is reported.

Principal component analysis was used for initial visualization of both the ^1H NMR spectra and mass spectral data. PCA is a well-established method for the interpretation of chemical data that has been thoroughly described previously (e.g. (Massart and Kaufman, 1983)). PCA reduces the dimensionality of a dataset, which has a large number of variables, while describing as much variation within the data as possible. The results of PCA are discussed in terms of component score vectors (observation coordinate along a PC) and loading vectors (direction coefficient of a PC).

Supervised analysis using principal components discriminant analysis (PC-DA) (Coolen *et al.*, 2008; Harker *et al.*, 2006; Hoogerbrugge *et al.*, 1983) was then used to maximise separation between the sample groups. PC-DA was preferred over other options such as PLS-DA because it is more suitable for multi-class clustering, such as in this study, whereas PLS-DA is more suitable for cases where there are two classes.

4.2.10 Compound Identification

Metabolite identification *via* HILIC-MS is based on accurately measuring pseudomolecular ions to determine their m/z or chemical formula in order to extract potential structures from databases. In order to calculate the most likely and chemically correct formula, rules need to be followed and adhered to in order to constrain thousands of possible candidates. A set of rules for this purpose has been published (Kind and Fiehn, 2007) and these have been used to aid compound identification from MS data in this chapter: -

- Apply heuristic restrictions for number of elements during formula generation (e.g. ^{12}C at 1000 Da follows $1000/12 = 83$ maximum limit for a hypothetical molecule that consists exclusively of carbon)
- Nitrogen rule (odd nominal mass implies odd number of N)
- Perform isotopic pattern filter
- Perform H/C ratio check (hydrogen/carbon ratio >0.125 and <3)
- Perform NOPS ratio check (N (0-1.3), O (0-1.2), P (0-0.3), and S/C (0-0.8) ratios)
- Perform heuristic HNOPS probability check (H, N, O, P, S/C high probability ratios)

A list of freely and commercially accessible online databases are summarised in chapter five (Table 5.2). The main databases used in this chapter were biological databases such as HMDB and Lipid Maps.

4.3 Results and Discussion

4.3.1 ^1H NMR Spectra of *In-Vitro* Model of Apocrine Sweat

Figure 4.3 shows a typical 400 MHz ^1H NMR comparative spectra for each apocrine cell extract, acquired using only 5 μl of extract and increasing the method sensitivity by use of a 1 mm micro-volume probe. The spectrum depicted clearly illustrates the power of the miniaturized probe when there is only a limited volume of the biofluid available. The mass sensitivity per sample quantity is inversely proportional to the diameter, thus, enhancement of the probe can be approximated since $S/N \propto 1/(\text{coil diameter})$ (Olson *et al.*, 1998; Peck *et al.*, 1995). This equated to a ~ 5.3 -fold increase compared to conventional 5 mm NMR probes, thus, providing a similar performance to that seen on a 500 MHz spectrometer equipped with a cryo-probe (data not shown). This increase in sensitivity enabled 29 metabolites to be readily identified, with 25 being quantified. Many of the resonances have been assigned by comparison with existing literature (Harker *et al.*, 2006; Lindon *et al.*, 2000; Nicholson *et al.*, 1995) in combination with an in-house spectral database and confirmed by ^1H - ^1H 2D COSY. These assignments are tabulated (Table 4.1), together with typical concentrations of metabolites found in the control samples. The most abundant metabolites detected were lactic acid and several amino acids including glycine, alanine, and tyrosine, with the former being present at concentrations of 19.1 ± 10.8 mM and the latter ranging from 1.6 – 3.6 mM. Any high variability in the concentration, e.g. lactate; is likely due to overlapping peaks, e.g. CH_2 lipid peaks, during the integration process. In order to minimise the error, multiple resonances of the same metabolite were averaged where possible. The reported concentrations are consistent with observations made previously following the NMR spectroscopic analysis of eccrine sweat (Harker *et al.*, 2006).

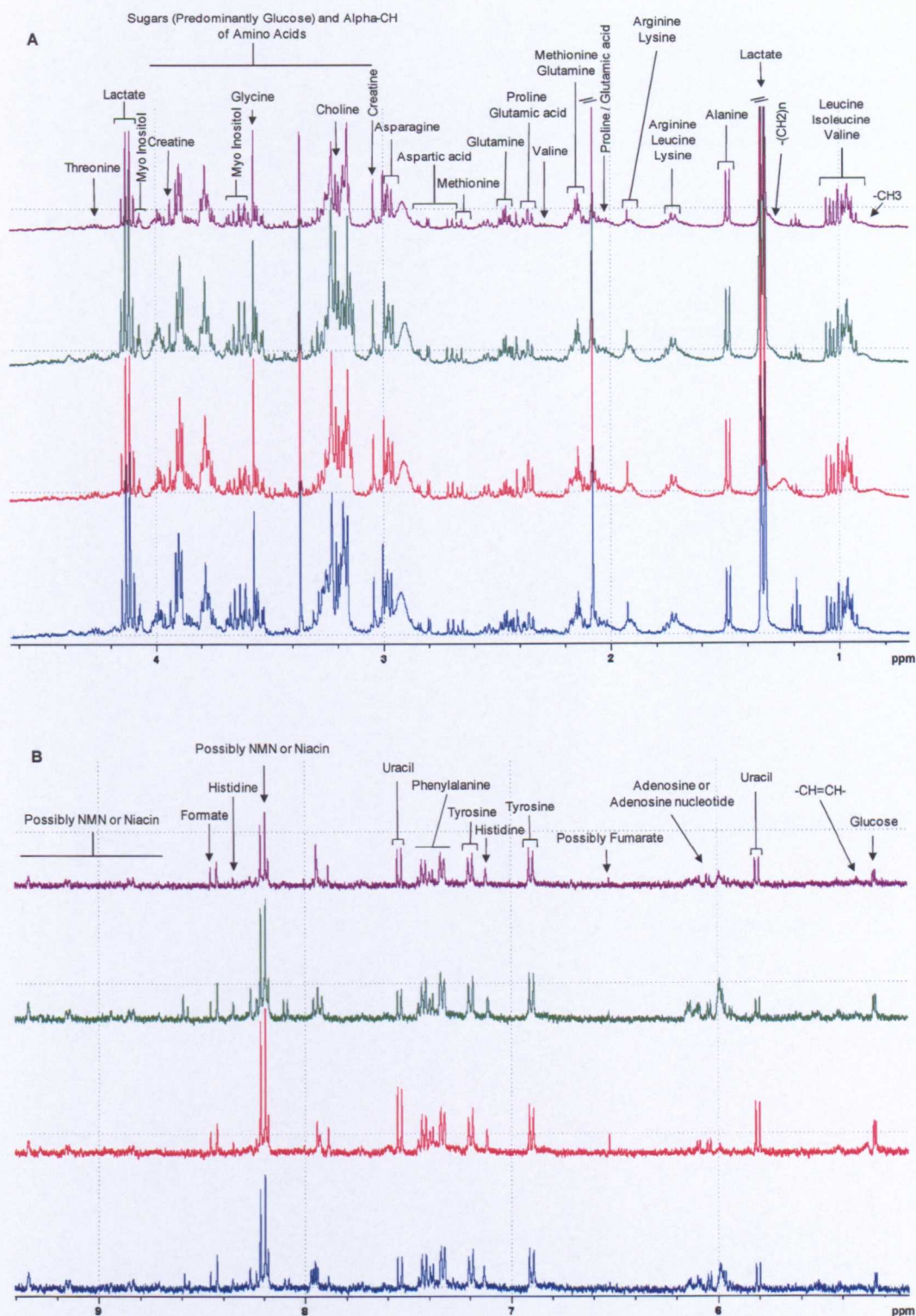


Figure 4.3 400-MHz 1D ^1H NMR comparative spectra of an ASG5 cell extract acquired using a 1 mm TXI NMR probe, A δ 0.5-4.5 region and B δ 5.5-9.2 region. Key, blue (TAM), red (E2), Green (Eth), and purple (Unt).

Table 4.1 Relative concentrations of identified metabolites from AGS5 cell extract determined by NMR spectroscopy equipped with 1 mm micro-volume probe. No correction for differences in T₁ relaxation.

Chemical Shift (PPM)	Assignment	Metabolite	Typical Concentration (mM)
0.89 (m)	CH ₃	Lipid	-
0.92 (t)	δ-CH ₃	Isoleucine	2.4 ± 1.4 (0.9 - 3.8)
0.99 (d)	β-CH ₃		
0.96 (t)	δ-CH ₃	Leucine	3.6 ± 2.1 (1.3 - 5.5)
1.72 (m)	CH ₂		
3.72 (m)	α-CH		
0.98 (d)	CH ₃	Valine	1.6 ± 0.9 (0.5 - 2.4)
1.03 (d)	CH ₃		
2.26 (m)	β-CH		
3.59 (d) ^a	α-CH		
1.18 (d)	CH ₃	3-β-hydroxybutyrate	0.2 ± 0.1 (0.04 - 0.4)
2.28 (ABX) ^a	CH ₂		
1.30 (m)	CH ₂	Lipid	-
1.33 (d)	CH ₃	Lactate	19.1 ± 10.8 (6.6 - 28.6)
4.11 (q)	CH		
1.48 (d)	CH ₃	Alanine	2.6 ± 1.5 (0.9 - 4.1)
1.48 (m) ^a	γ-CH ₂	Lysine	4.2 ± 2.2 (1.7 - 6.2)
1.73 (m)	δ-CH ₂		
1.90 (m)	β-CH ₂		
3.04 (t) ^a	ε-CH ₂		
1.92 (s)	CH ₃	Acetate	0.6 ± 0.4 (0.2 - 0.9)
2.07 (s)	CH ₃	Acetamide ^b	3.6 ± 1.7 (1.8 - 5.1)
2.03 (m)	γ-CH ₂	Proline	1.7 ± 1 (0.5 - 2.5)
2.36 (m) ^a	β-CH ₂		
3.35 (m)	δ-CH ₂		
3.43 (m)	δ-CH ₂		
4.15 (m) ^a	α-CH		

Table 4.1 continued

Chemical Shift (PPM)	Assignment	Metabolite	Typical Concentration (mM)
2.07 (m) ^a	β-CH ₂	Glutamate	3.3 ± 2 (1.1 - 5)
2.35 (m)	γ-CH ₂		
3.77 (m) ^a	α-CH		
2.15 (m) ^a	β-CH ₂	Glutamine	3.4 ± 2 (1.2 - 5.1)
2.46 (m)	γ-CH ₂		
3.77 (d) ^a	α-CH		
2.51 (AB) ^a	½ CH ₂	Citrate	1.1 ± 0.7 (0.3 - 1.8)
2.65 (AB) ^a	½ CH ₂		
2.68 (ABX) ^a	β-CH ₂	Aspartate	0.8 ± 0.5 (0.2 - 1.4)
2.82 (ABX)	β-CH ₂		
3.90 (ABX) ^a	α-CH		
3.04 (s)	CH ₃	Creatine	1.3 ± 0.7 (0.5 - 1.9)
3.93 (s)	CH ₂		
3.20 (s)	N(CH ₃) ₃	Choline	0.8 ± 0.5 (0.3 - 1.2)
3.51 (m)	NCH ₂		
4.05 (m)	OCH ₂		
3.28 (t) ^a	H5	Myo-inositol	-
3.53 (dd) ^a	H1/H3		
3.63 (dd) ^a	H4/H6		
4.06 (t) ^a	H2		
3.36 (s)		Residual methanol from the extraction procedure	
3.31 (ABX)	CH ₂	Tryptophan ^c	-
3.49 (ABX)	CH ₂		
4.06 (ABX)	CH		
7.21 (t)	C5H		
7.29 (t)	C6H		
7.33 (s)	C2H		
7.55 (d)	C7H		
7.74 (d)	C4H		

Table 4.1 continued

Chemical Shift (PPM)	Assignment	Metabolite	Typical Concentration (mM)
3.41 (m)	C-H4	Glucose	0.4 ± 0.2 (0.2 - 0.5)
3.48 (t)	C-H3		
3.53 (dd)	C-H2		
3.73 (dd)	C-H6'		
3.85 (m)	C-H6		
3.90 (dd) ^a	C-H6		
5.24 (d)	C-H1		
3.56 (s)	CH ₂	Glycine	3.7 ± 2.3 (1.2 - 5.9)
3.59	α-CH	Threonine	3.2 ± 1.8 (1.1 - 5)
4.26 (m)	β-CH		
3.85 (dd) ^a	α-CH	Serine	3.7 ± 2.3 (1.1 - 5.8)
3.95 (dd) ^a	β-CH ₂		
4.00 (dd) ^a	β-CH ₂		
5.32 (m)	-HC=CH-	Lipid	0.2 ± 0.2 (0.1 - 0.6)
5.80 (d)	CH	Uracil ^b	0.5 ± 0.4 (0.1 - 0.9)
7.54 (d)	CH		
6.90 (d)	H3/H5	Tyrosine	0.6 ± 0.4 (0.2 - 1)
7.19 (d)	H2/H6		
7.33 (m)	H2/H6	Phenylalanine	0.7 ± 0.5 (0.2 - 1.1)
7.39 (m)	H4		
7.43 (m)	H/H5		
8.46 (s)	CH	Formate	0.2 ± 0.1 (0.1 - 0.3)

^aPartially obscured resonances^bTentatively assigned^cBelow limit of quantification

Multiplicity is indicated as s = singlet, d = doublet, t = triplet, q = quartet, m = multiplet

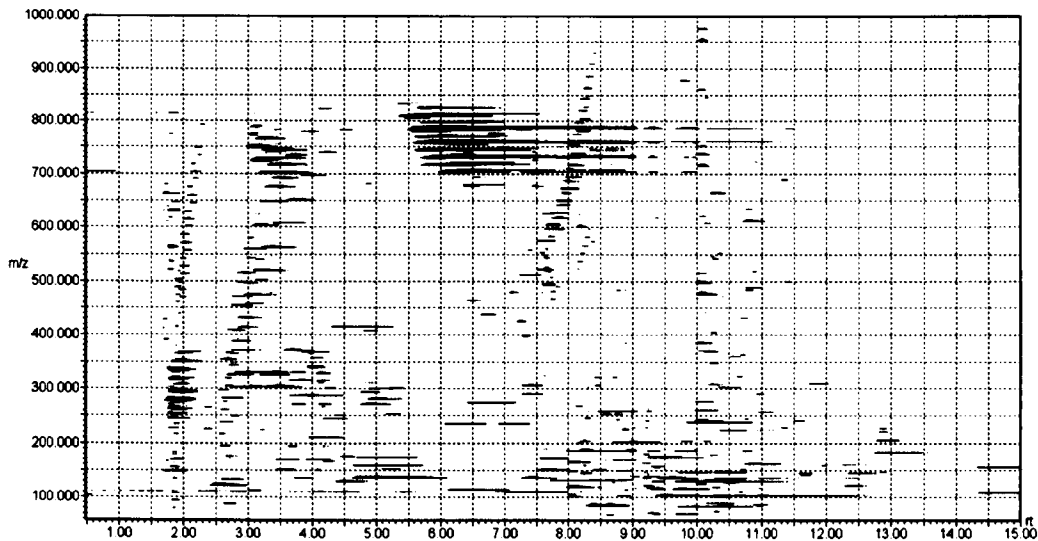
4.3.2 LC-Mass Spectrometry Analysis of *In-Vitro* Model of Apocrine Sweat

Figure 4.4 shows comparative 2-D LC-MS maps (horizontal axis: retention time, vertical axis: m/z) for each of the ASG5 cell extracts using HILIC-TOF-MS. More than 1000 features were detected in this sample during a 25 min acquisition period, highlighting both the sensitivity of the technique and the complexity of the sample. However, it should be noted that not all these features may be represented as individual compounds due to fragmentation or adducts during the ionisation process. As with the NMR data, visual inspection would be tedious, inefficient and prone to subjective error. Thus, examination of the data was carried out through the use of multivariate analysis.

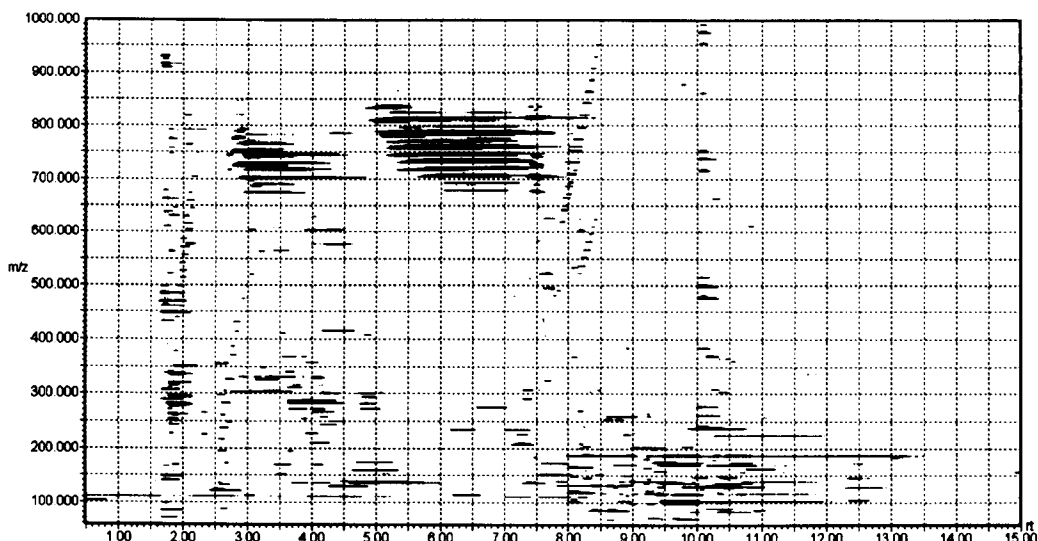
Both the global approach (HILIC-MS) and the targeted (RP-LC-MS/MS) approach proved to be unsuccessful in detecting known odour precursors in apocrine secretions, including 3M2H-Gln. However, a previous report using the ASG5 cell lines have reported the ability to detect 3M2H-Gln using GC-MS and a different extraction procedure (Burry *et al.*, 2008). Thus, it is likely that the cold methanol extraction used herein, did not extract these metabolites or that the presence was not represented in all sample classes, resulting in being diluted down in the QC samples, thereby, being below the limit of detection. Furthermore, none of the androgens in Figure 4.2 were detected. Androstenediol ($C_{19}H_{32}O_2$ m/z 331.2039 [M+K]) produced a possible hit with a potassium adduct, which had a retention time of 3.75 min and an associated mass error of 5.2 ppm. However, this is likely to be a false positive due to the other androgens not being detected as well not detecting the pseudomolecular ion or any other adducts. Cholesterol and squalene, which have been detected previously (Burry *et al.*, 2008), were also not detected. As mentioned previously, it likely that these metabolites were not extracted with the cold methanol procedure or that they eluted off the column in the void volume. However, 275 metabolites were putatively identified such as phospholipids, glycerolipids, fatty acids and amino acids (see Appendix B). This is in line with previous reports (Burry *et al.*, 2008), and further supports that the evidence that the ASG5 cell line mimics the functions of an apocrine gland. However, false positives are always found, though could be significantly

reduced by acquiring fragmentation spectra (MS/MS or MSⁿ) and comparing it to an authentic standard or to an insilico derived fragmentation mass spectra (Wolf *et al.*, 2010).

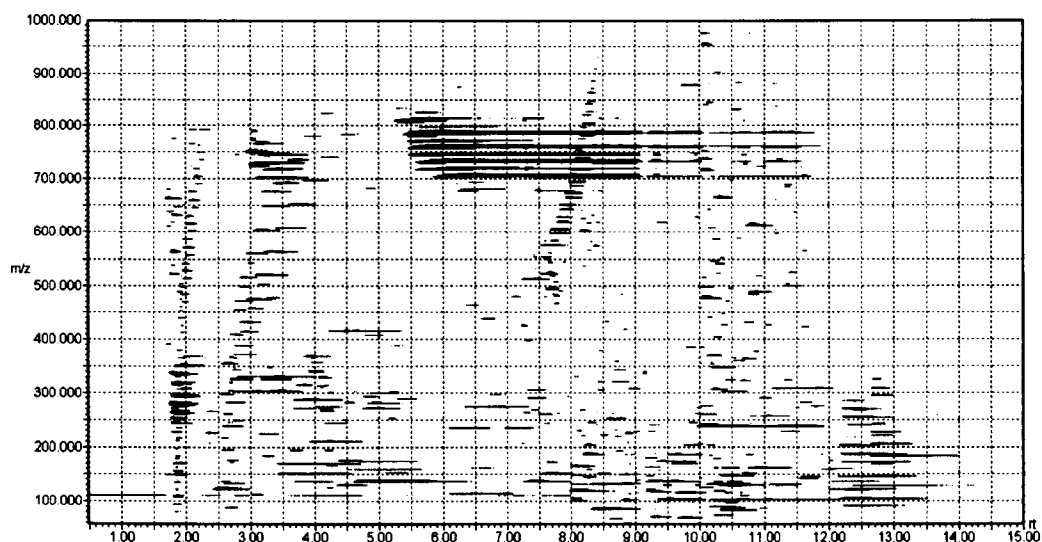
A



B



C



D

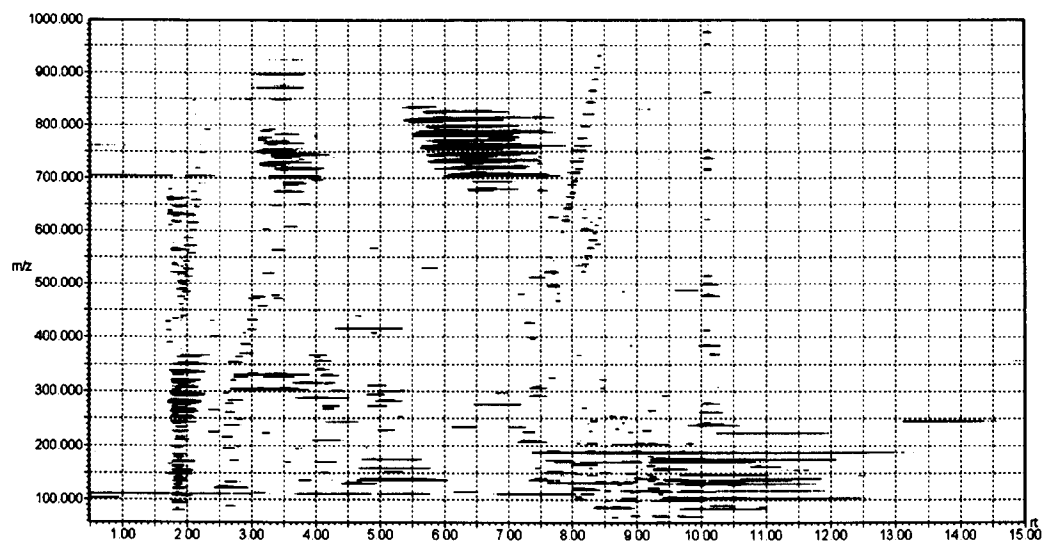


Figure 4.4 Two dimensional mass versus retention ‘map’ obtained from QTOF-HILIC-MS analysis of ASG5 cell extract of **A** TAM, **B** E2, **C** Eth and **D** Unt. Typically, over 1000 features can be detected in 15 min.

4.3.3 Multivariate Data Analysis

Both the NMR and LC-MS data were initially analysed with PCA to obtain a global unbiased view and to find the systemic metabolic changes between each of the treatments. UV scaling was used for all the models presented in this section, as compared to mean centred data, all metabolites become equally important. PCA scores plots of the ^1H NMR spectral data and HILIC-MS spectra are depicted in Figure 4.5 A and B, which explains 54.2% (PC1 vs PC2 vs PC3) and 54.8% (PC1 vs PC2) of the total variation, respectively.

PCA of the NMR data showed separation of the treatment groups split across three PCs, and therefore supervised clustering was performed *via* PC-DA to ease visualisation and interpretation of the data. PC-DA model employs *a priori* knowledge relating to group information in order to construct the model. Due to the limited sample size, PC-DA models were initially constructed on the average response to the different cell treatments. The original data were then projected onto the model in order to determine the predictability of the model. The clustering of samples shown in Figure 4.6 is consistent with that of the LC-MS data, with the samples clustering according to the different treatments; however, ethanol and tamoxifen treated were clustered together across all discriminant axes, regardless of the analytical method. Thus, TAM can be considered as having no additional effect to that of the vehicle or any effect incurred by the TAM is masked by the effect of the vehicle. The first discriminant axis is mainly responsible for explaining the difference between treatments with the E2 inhibitor. In a similar way, the second discriminant axis is important for explaining the difference between untreated and TAM and ethanol treated cells. It can be seen in Figure 4.5 and Figure 4.6 that the E2 treated and control groups can be easily distinguished using both PCA and PC-DA, thus, demonstrating a clear influence that hormones have on the metabolic composition of apocrine sweat *in vitro*, as well as highlighting the complementary nature of both analytical methodologies.

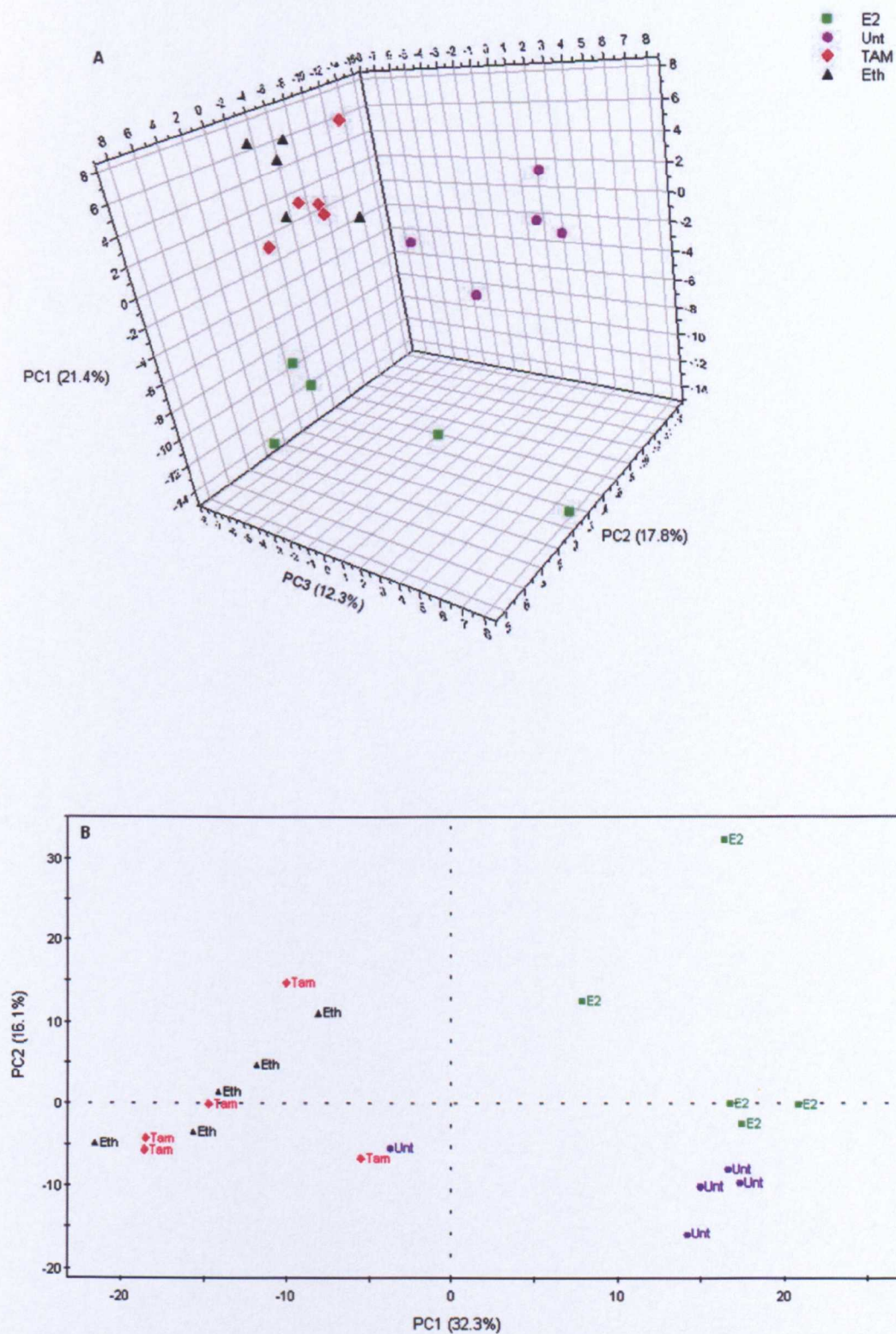


Figure 4.5 PCA scores plot (UV scaled) obtained from **A** ^1H NMR spectra and **B** HILIC MS data from the analysis of ASG5 apocrine cell lines treated with tamoxifen, β -estradiol and ethanol ($n=5$).

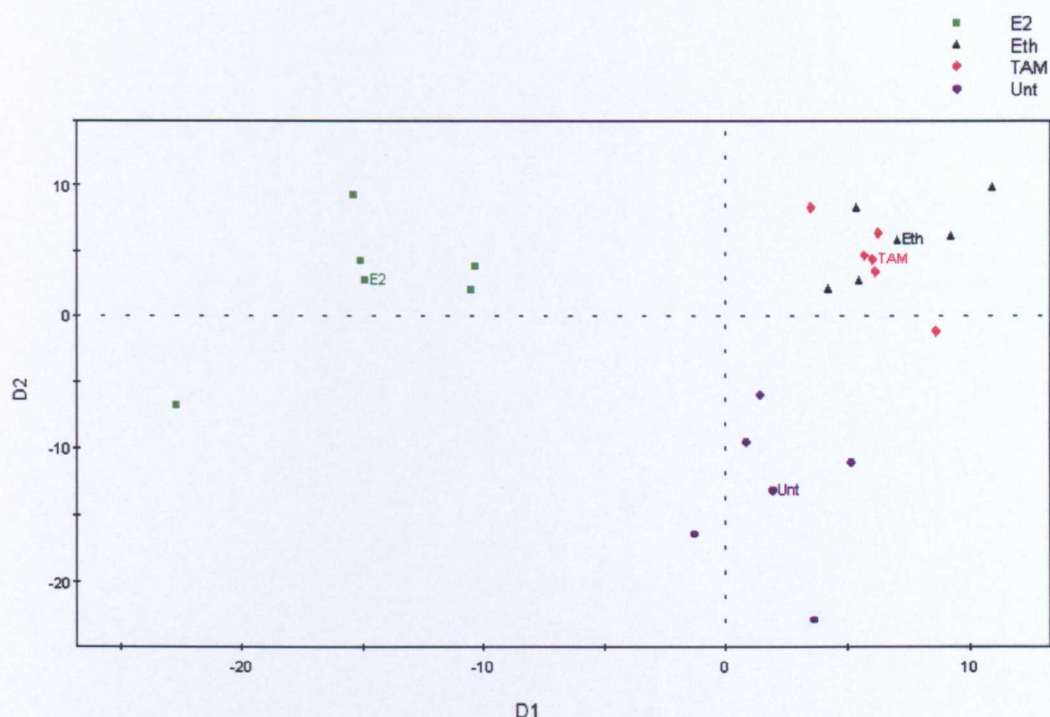


Figure 4.6 PC-DA score plot (UV-scaled) obtained from ^1H NMR spectra from the analysis of ASG5 apocrine cell lines treated with tamoxifen, β -estradiol and ethanol ($n=5$).

Determining the regions of interest between the different treatments is extremely difficult as there is an abundance of information from both methodologies. The NMR data showed a clear distinction between E2 and TAM, ethanol, and untreated groups, while the difference between untreated and TAM and ethanol were more subtle. In the case of ^1H NMR the metabolites responsible for clustering of the E2 group include glucose, acetate, and β -hydroxybutyrate whilst the TAM and ethanol treated samples are characterised by lactate, myo-inositol and unknown metabolites that are putatively identified as nucleotides or nucleotide derivatives. Untreated cells are grouped by other amino acids such as valine, leucine and isoleucine as well as lipids peaks and formate. Table 4.2 summarises the main findings, where changes were supported by the PC-DA generated loading plot of the NMR data. The perturbations in metabolite profiles highlighted here show that the cells react differently to different levels of circulating hormones.

Table 4.2 Key changes in the endogenous metabolites responsible for defining the hormonal treatment observed using PC-DA. The mean normalised bucketed values are reported.

Tentative Assignment	Buckets	$\bar{x} \pm SD$			
		Untreated	β -Estradiol	Ethanol	Tamoxifen
Lactate	4.14, 4.1, 1.38, 1.34, 1.3	4.60 \pm 0.42	3.56 \pm 0.82	5.26 \pm 0.75	4.68 \pm 0.21
Trp/Myo Inositol	4.06	0.70 \pm 0.05	0.61 \pm 0.14	0.97 \pm 0.11	0.92 \pm 0.08
Unkown	4.02	0.69 \pm 0.08	0.65 \pm 0.05	0.88 \pm 0.04	0.8 \pm 0.11
Phe/Ser	3.98	1.05 \pm 0.14	0.97 \pm 0.16	1.51 \pm 0.17	1.39 \pm 0.11
Creatine/A.A possibly Tyr	3.94	1.23 \pm 0.39	1.18 \pm 0.21	1.06 \pm 0.09	1.01 \pm 0.07
A.A possibly Asp	3.9	3.36 \pm 0.33	3.49 \pm 0.32	2.99 \pm 0.23	3.31 \pm 0.25
Sugar possibly Glucose	3.86, 3.82	0.89 \pm 0.11	1.30 \pm 0.49	1.06 \pm 0.19	1.00 \pm 0.09
Unkown possibly A. A	3.78	3.12 \pm 0.14	3.14 \pm 0.19	2.46 \pm 0.21	2.76 \pm 0.15
Glucose	3.74, 3.7, 3.68, 3.5, 3.46, 3.42, 3.38	0.65 \pm 0.13	1.13 \pm 0.38	0.71 \pm 0.07	0.68 \pm 0.07
Myo inositol	3.62, 3.54	1.19 \pm 0.09	1.10 \pm 0.10	1.62 \pm 0.20	1.56 \pm 0.11
Proline	3.34, 2.02	0.90 \pm 0.23	0.83 \pm 0.21	0.66 \pm 0.09	0.69 \pm 0.03
Myo inositol/A. A possibly Pro	3.3	2.01 \pm 1.13	2.01 \pm 0.89	1.37 \pm 0.61	1.22 \pm 0.19
A.A possibly Tyr	3.18	4.13 \pm 1.35	3.67 \pm 0.67	3.78 \pm 0.55	4.6 \pm 0.74
A.A possibly Phe	3.14	1.79 \pm 1.02	1.75 \pm 1.03	2.41 \pm 1.30	2.10 \pm 0.77
Creatine/A.A possibly Lys	3.02	1.93 \pm 0.70	1.85 \pm 0.63	1.27 \pm 0.38	1.37 \pm 0.29
A.A probably Asn	2.98	1.75 \pm 0.21	1.71 \pm 0.14	1.57 \pm 0.23	1.64 \pm 0.15
Lipid	2.94, 2.9	1.93 \pm 0.57	1.89 \pm 0.55	1.81 \pm 0.47	1.96 \pm 0.24
Unknown possibly Methylamine	2.54	0.53 \pm 0.05	0.55 \pm 0.03	0.37 \pm 0.06	0.47 \pm 0.03
Glutamine	2.46, 2.18, 2.14	1.31 \pm 0.06	1.06 \pm 0.07	0.95 \pm 0.06	1.02 \pm 0.05
Glutamic acid	2.38, 2.34	0.70 \pm 0.07	0.83 \pm 0.09	0.55 \pm 0.08	0.65 \pm 0.05
Unknown possibly acetamide	2.06	3.14 \pm 0.71	3.46 \pm 0.58	2.86 \pm 0.10	2.86 \pm 0.31
Lipid (CH ₂) _n	1.26, 1.22	0.33 \pm 0.07	1.00 \pm 0.43	0.33 \pm 0.07	0.32 \pm 0.05
β -hydroxybutyrate	1.18	0.27 \pm 0.13	1.21 \pm 1.11	0.37 \pm 0.11	0.38 \pm 0.18
Leu/Ile/val	1.02, 0.98, 0.94, 0.9	1.29 \pm 0.09	1.13 \pm 0.11	1.13 \pm 0.07	1.13 \pm 0.03
lipid (CH ₃)	0.86, 0.82	0.09 \pm 0.03	0.40 \pm 0.16	0.11 \pm 0.03	0.11 \pm 0.02

TAM has a complex pharmacology as it is a selective estrogen receptor modulator which can prevent estrogen from stimulating growth as well as possessing agonistic effects such as the induction of calcium signalling (Zhang *et al.*, 2000) and influencing bone and lipid metabolism (Love *et al.*, 1992; Riggs and Hartmann, 2003). TAM has been shown to increase intracellular triglycerides (Hozumi *et al.*, 1998) and disrupts fatty acid metabolism (Lelliott *et al.*, 2005). Furthermore, TAM can affect the lipoprotein concentrations by reducing levels LDL-cholesterol due to increasing LDL receptor activity (Bruning *et al.*, 1988; Powles *et al.*, 1989; Walsh *et al.*, 1991). However, with the data presented it is difficult to state whether they agree with the current literature as cholesterol compounds and their derivatives were not detected. Lactate dehydrogenase, which catalyzes the conversion of pyruvate into

lactate, has been shown to increase with E2 (Thomas *et al.*, 1989). However, the data presented contradicts these findings, although, it does agree with the fact that TAM has no effect on lactate production. TAM ($C_{26}H_{29}NO$; m/z 372.2327 [M+H]) is known to be metabolised into *N*-desmethyltamoxifen ($C_{25}H_{27}NO$; m/z 358.2170 [M+H]) and 4-hydroxytamoxifen ($C_{26}H_{29}NO_2$; m/z 388.2276 [M+H]), where oxidation of these primary metabolites results in formation of 4-hydroxy-*N*-desmethyltamoxifen (endoxifen; $C_{25}H_{27}NO_2$; m/z 374.2119 [M+H]) by hepatic cytochrome P450s (Desta *et al.*, 2004; Hoskins *et al.*, 2009). These metabolites along with E2 ($C_{18}H_{24}O_2$; m/z 273.1854 [M+H]) were not identified in the samples prior to MVA. In comparison to the NMR data analysis, TAM and E2 were considered to be below the limit of detection. It is important to remove any drug metabolites to avoid miss-interpretation of the data, as the models produced would predominately describe the variation between the different drugs and their corresponding metabolites.

The principle ions contributing to the PCA grouping from HILIC-MS data were, m/z 447.3474, 289.1790, 461.3638, 312.3637, 368.4240, 312.3637, 284.3296, 256.2993 and 228.2674 which were shown to be only present in the E2 group. The untreated group were grouped due to the lipid content (e.g. glycerophosphocholines) whilst those at m/z 247.0581, 405.0090 152.0561 and 229.1538 were more prevalent in the TAM and ethanol treated samples. Furthermore, the phospholipids content is generally lower in concentration with TAM treatment when compared against the E2 treated cells, while nucleotide metabolites were shown to be elevated in the TAM treated cells. Molecular mass, postulated elemental composition and chromatographic retention time data for the ions relating to the differences are given in Table 4.3. However, as with tentative assignments for the ions responsible for distinguishing between the different treatments, these metabolites are as yet unidentified despite searches of available databases using the accurate masses and atomic compositions. Further investigations, such as metabolite isolation *via* fraction collection which would then be subjected to further NMR and MS analysis, would be required in an attempt to characterise and identify these compounds. Moreover, a continuing problem with the confirmation of the identity of many compounds is the lack of authenticated standards to provide unequivocal structures, thus, calculating the correct empirical formula is essential (Kind and Fiehn, 2007). Many of the changes observed are also unlikely to be directly relevant to apocrine sweat. There will be many

changes caused by the addition of ethanol and other disruptions caused by hormone interactions which will produce a rippling effect across intracellular metabolism. Nonetheless, the analytical methodologies used can reveal many of these global changes. However, it is more difficult to attribute these changes to specific pathways, but not impossible since many of the steroid hormone effects are characterised.

Table 4.3 Key changes in endogenous metabolites after addition of either E2, TAM, ethanol, with respect to the untreated control observed from PCA analysis with HILIC-MS data acquired in positive ion mode.

$\bar{x} \pm SD$ (Peak area)								
Ret. Time (min)	<i>m/z</i>	Tentative Formula	<i>m/z</i> Error (ppm)	Tentative Assignment	Untreated	E2	Ethanol	TAM
Principle ions from E2								
1.72	483.3455 ^b	C ₂₆ H ₄₃ NO ₆	3.31	Glycocholic acid	0 ± 0	2.94 ± 0.99	0 ± 0	0 ± 0
1.72	447.3474 ^b	C ₂₃ H ₄₃ NO ₆	8.05	Hexadecanedioic acid mono-L-carnitine ester	0.02 ± 0.05	204.15 ± 38.58	0 ± 0	0.01 ± 0.01
1.73	433.3304	C ₂₇ H ₄₄ O ₄	4.15	24-Hydroxycalcitriol	0 ± 0	7.66 ± 1.64	0 ± 0	0 ± 0
1.73	167.0338 ^a	C ₆ H ₈ O ₄	10.78	3-Methylglutaconic acid/3-Hexenedioic acid	1.39 ± 0.41	2.60 ± 0.39	0.80 ± 0.16	1.07 ± 0.24
1.73	307.1892 ^f	C ₈ H ₁₄ O ₂	2.28	2-Octenoic acid	0 ± 0	12.37 ± 1.75	0 ± 0	0 ± 0.01
1.73	307.1892 ^b	C ₁₃ H ₂₃ NO ₆	7.49	3-Methylglutaryl/carnitine	0 ± 0	12.37 ± 1.75	0 ± 0	0 ± 0.01
1.73	289.1797	C ₁₈ H ₂₄ O ₃	2.42	16,17-Epiestriol/17-Epiestriol/2-Hydroxyestradiol	0 ± 0.01	27.6 ± 5.45	0 ± 0	0 ± 0
1.73	461.3638 ^d	C ₂₈ H ₄₄ O ₃	1.52	Ercalcitriol	0 ± 0	29.44 ± 6.17	0 ± 0	0 ± 0
1.74	945.6660 ^f	C ₂₄ H ₄₇ NO ₇	6.03	Galactosyl/sphingosine	0 ± 0	0.95 ± 0.94	0 ± 0	0 ± 0
3.29	326.3772	C ₂₂ H ₄₇ N	4.60	-	57.90 ± 34.04	202.32 ± 292.04	154.64 ± 113.55	114.49 ± 155.67
3.41	332.3306	C ₁₈ H ₄₁ N ₃ O ₂	8.73	-	11.50 ± 4.65	32.41 ± 43.72	22.50 ± 15.43	18.62 ± 21.09
3.47	304.2982	C ₁₆ H ₃₇ N ₃ O ₂	5.92	-	40.04 ± 17.63	122.47 ± 167.07	85.80 ± 55.31	68.67 ± 79.31
3.68	368.424	C ₂₅ H ₅₃ N	4.34	-	0.01 ± 0.02	10.36 ± 1.41	0 ± 0.01	0 ± 0
3.7	340.3945	C ₂₃ H ₄₉ N	0.59	-	0 ± 0	4.66 ± 0.68	0 ± 0	0 ± 0
3.76	312.3637	C ₂₁ H ₄₅ N	2.24	-	0.01 ± 0.02	14.96 ± 1.73	0 ± 0	0 ± 0
3.85	284.3293	C ₁₉ H ₄₁ N	8.44	-	0.14 ± 0.30	830.27 ± 115.47	0.22 ± 0.14	0.23 ± 0.22
3.95	256.2993	C ₁₇ H ₃₇ N	4.29	-	0.01 ± 0.01	2.64 ± 2.49	0 ± 0	0.01 ± 0.01
4.04	228.2674	C ₁₅ H ₃₃ N	7.45	-	0.05 ± 0.06	10.82 ± 2.80	0.04 ± 0.07	0.04 ± 0.06
4.25	258.2784 ^b	C ₁₆ H ₃₂ O	5.03	Palmitaldehyde	0 ± 0	3.25 ± 3.11	0.06 ± 0.11	0.05 ± 0.08
4.34	300.3259 ^b	C ₁₉ H ₄₁ NO	2.33	Pristanal	0 ± 0	10.69 ± 1.53	0 ± 0	0 ± 0
5.49	834.6022	C ₄₈ H ₈₄ NO ₈ P	0.12	PC	6.13 ± 5.26	15.89 ± 3.69	1.27 ± 1.49	1.98 ± 0.85
5.56	806.5686	C ₄₆ H ₈₀ NO ₈ P	1.74	PC	11.22 ± 2.69	15.74 ± 1.89	5.93 ± 2.77	7.07 ± 2.22
6.85	776.5832 ^d	C ₄₁ H ₇₈ NO ₈ P	2.70	PE	10.46 ± 3.53	16.17 ± 3.36	1.36 ± 1.53	1.50 ± 2.23

Table 4.3 continued

$\bar{x} \pm SD$ (Peak area)								
Ret. Time (min)	<i>m/z</i>	Tentative Formula	<i>m/z</i> Error (ppm)	Tentative Assignment	Untreated	E2	Ethanol	TAM
Principle ions from Untreated								
1.81	282.2789	C ₁₈ H ₃₅ NO	2.83	Oleamide	145.01 ± 44.74	60.24 ± 11.27	90.1 ± 22.97	85.31 ± 36.36
1.87	280.2621	C ₁₈ H ₃₃ NO	6.78	-	101.54 ± 36.81	44.00 ± 15.02	58.46 ± 13.11	57.41 ± 14.75
3.03	776.5591	C ₄₅ H ₇₈ NO ₇ P	0.39	PE	6.78 ± 2.48	7.30 ± 4.81	1.62 ± 1.33	1.10 ± 1.51
3.3	674.5131	C ₃₇ H ₇₂ NO ₇ P	0.89	PE	17.45 ± 6.29	17.02 ± 8.38	8.46 ± 1.06	9.83 ± 3.92
3.3	742.5393	C ₄₁ H ₇₆ NO ₈ P	0.80	PE or PC	17.79 ± 7.37	5.23 ± 4.18	1.87 ± 2.28	1.17 ± 1.61
3.37	744.5562	C ₄₁ H ₇₈ NO ₈ P	2.55	PE or PC	90.54 ± 50.48	40.30 ± 16.46	28.00 ± 6.02	28.94 ± 4.77
3.4	716.5237	C ₃₉ H ₇₄ NO ₈ P	2.79	PE	57.11 ± 17.18	26.49 ± 10.36	13.73 ± 3.17	14.75 ± 2.44
3.51	690.5083	C ₃₇ H ₇₂ NO ₈ P	1.30	PE	16.19 ± 11.11	5.25 ± 3.90	2.00 ± 2.78	0.26 ± 0.58
4.46	130.1579	C ₈ H ₁₉ N	13.06	-	45.48 ± 15.35	28.96 ± 16.49	28.23 ± 6.01	18.35 ± 7.77
5.79	784.5883	C ₄₄ H ₈₂ NO ₈ P	3.44	PC	143.58 ± 17.01	121.29 ± 19.49	64.04 ± 39.66	78.61 ± 27.46
5.88	786.6024	C ₄₄ H ₈₄ NO ₈ P	1.40	PC	873.87 ± 310.62	793.55 ± 350.45	570.02 ± 67.74	612.78 ± 50.16
5.89	756.5544	C ₄₂ H ₇₈ NO ₈ P	0.13	PC/PE	72.36 ± 10.6	42.21 ± 5.58	41.89 ± 5.83	42.25 ± 7.68
5.97	758.5714	C ₄₂ H ₈₀ NO ₈ P	1.85	PC/PE/PE-NMe	936.35 ± 88.15	768.21 ± 93.32	480.43 ± 154.36	563.43 ± 73.98
6.09	760.5859	C ₄₂ H ₈₂ NO ₈ P	0.39	PC	454.41 ± 492.96	548.11 ± 327.08	565.63 ± 41.83	389.76 ± 266.78
6.18	732.5549	C ₄₀ H ₇₈ NO ₈ P	0.82	PE or PC	752.84 ± 127.35	405.25 ± 207.14	457.57 ± 55.35	415.8 ± 124.28
6.51	706.5389	C ₃₈ H ₇₆ NO ₈ P	0.42	PE or PC	163.77 ± 66.44	47.19 ± 36.98	50.24 ± 46.82	41.95 ± 34.73
8.02	775.4798 ^g	C ₂₁ H ₃₆ O ₅	4.77	Cortol	5.34 ± 1.57	3.82 ± 1.95	1.94 ± 0.32	2.35 ± 0.86
8.09	819.5059 ^c	C ₄₂ H ₇₉ O ₁₀ P	8.42	PG	4.09 ± 1.23	3.23 ± 1.48	1.83 ± 0.20	2.12 ± 0.51
8.82	104.1064 ^b	C ₃ H ₁₀ O	10.57	Iso-Valeraldehyde	3.98 ± 1.72	3.05 ± 1.65	0.56 ± 0.39	0.83 ± 0.56
9	141.1132	C ₆ H ₁₂ N ₄	5.67	-	2.20 ± 0.85	1.63 ± 0.76	0.51 ± 0.06	0.36 ± 0.21
9.28	139.0494	C ₆ H ₆ N ₂ O ₂	5.10	Nicotinamide N-oxide	30.14 ± 15.05	15.32 ± 9.57	3.58 ± 2.04	6.12 ± 3.66
9.6	137.0707	C ₇ H ₈ N ₂ O	5.84	N-Methylnicotinamide	83.89 ± 14.83	64.18 ± 22.85	38.00 ± 7.05	46.33 ± 17.65
10.22	132.0764	C ₄ H ₆ N ₃ O ₂	6.81	Creatine	130.89 ± 17.9	95.21 ± 40.32	101.74 ± 15.85	116.02 ± 22.66
Principle ions from TAM/Ethanol								
2.54	123.0549	C ₆ H ₆ N ₂ O	3.16	Niacinamide	83.73 ± 40.06	73.46 ± 22.97	143.85 ± 24.57	147.74 ± 39.04
2.68	133.0855	C ₆ H ₁₂ O ₃	3.16	Hydroxyisocaproic acid/5-Hydroxyhexanoic acid	4.52 ± 1.96	2.86 ± 1.85	7.35 ± 1.23	7.82 ± 1.45

Table 4.3continued

Ret. Time (min)	<i>m/z</i>	Tentative Formula	<i>m/z</i> Error (ppm)	Tentative Assignment	$\bar{x} \pm \text{SD (Peak area)}$				
					Untreated	E2	Ethanol	TAM	
2.69	177.1119 ^d	C ₈ H ₁₆ O ₄	4.52	4-Hydroxycyclohexylcarboxylic acid	2.04 ± 0.81	1.07 ± 0.69	3.77 ± 0.60	3.99 ± 0.79	
3.76	331.2052 ^c	C ₁₉ H ₃₂ O ₂	3.92	Androstenediol	0 ± 0	0.58 ± 1.01	9.96 ± 2.84	5.23 ± 5.05	
4.91	137.0452	C ₅ H ₄ N ₄ O	2.84	Hypoxanthine	694.13 ± 213.43	747.66 ± 214.98	826.09 ± 110.12	912.67 ± 117.18	
4.91	137.0452	C ₄ H ₈ O ₅	1.46	Erythronic acid/Threonic acid	694.13 ± 213.43	747.66 ± 214.98	826.09 ± 110.12	912.67 ± 117.18	
6.4	114.066	C ₄ H ₇ N ₃ O	6.13	Creatinine	5.12 ± 7.02	5.08 ± 5.37	18.61 ± 5.68	21.24 ± 4.72	
7.44	137.0450	C ₄ H ₈ O ₅	4.01	Threonic acid	32.16 ± 16.46	20.39 ± 9.41	85.26 ± 29.29	65.17 ± 10.52	
7.61	480.3438	C ₂₄ H ₃₀ NO ₆ P	3.33	LysoPC(P-16:0)	0.15 ± 0.11	0.30 ± 0.09	1.35 ± 0.73	1.06 ± 0.29	
8.08	120.0803	C ₈ H ₉ N	8.33	-	162.00 ± 65.75	124.41 ± 47.82	220.71 ± 36.44	234.7 ± 39.99	
8.08	166.0858	C ₉ H ₁₁ NO ₂	6.02	L-Phenylalanine	64.86 ± 25.32	50.01 ± 20.49	87.26 ± 13.93	83.53 ± 17.39	
8.87	104.0528 ^h	C ₂ H ₆ S	5.77	Dimethylsulfide	2.29 ± 3.57	2.56 ± 1.75	7.40 ± 1.63	7.53 ± 2.16	
8.87	150.058	C ₃ H ₁₁ NO ₂ S	5.99	Methionine	6.38 ± 4.37	4.92 ± 2.1	12.71 ± 3.03	13.25 ± 3.27	
8.87	133.0313	C ₃ H ₈ O ₂ S	7.51	-	11.43 ± 8.2	8.57 ± 3.58	23.36 ± 6.13	24.76 ± 6.87	
9.56	104.1065	C ₃ H ₁₃ NO	9.60	Choline	412.51 ± 118.73	323.33 ± 88.53	362.83 ± 15.67	427.40 ± 111.21	
9.76	116.0704	C ₃ H ₉ NO ₂	6.89	L-Proline	51.79 ± 39.02	36.99 ± 18.55	89.81 ± 22.14	94.93 ± 25.63	
9.88	247.0581 [*]	C ₄ H ₈ O ₃	1.21	4-Hydroxybutyric acid/3-Hydroxybutyric acid	0.09 ± 0.17	0.03 ± 0.05	1.30 ± 0.37	1.07 ± 0.54	
10.01	206.048	C ₇ H ₁₁ NO ₄ S	3.40	-	0.26 ± 0.47	0.09 ± 0.17	1.26 ± 0.35	1.40 ± 0.57	
10.09	477.2047	C ₂₇ H ₄₁ H ₅ O ^e	4.98	-	100.97 ± 68.23	79.98 ± 41.4	179.53 ± 34.62	194.84 ± 47.48	
10.09	239.1050	C ₁₄ H ₁₆ O ₂ ^a	2.5	10E,12E-tetradecadiene-4,6-dienoic acid	625.82 ± 173.44	551.78 ± 208.66	767.59 ± 121.32	786.49 ± 89.47	
10.17	204.0869 ^a	C ₇ H ₁₁ N ₅ O	3.91	6-methyltetrahydropterin	0.63 ± 1.25	0.09 ± 0.20	3.67 ± 0.94	4.19 ± 0.52	
10.17	608.0911	C ₁₇ H ₂₇ N ₃ O ₁₇ P ₂	2.79	Uridine diphosphate-N-acetylglactosamine	0.43 ± 0.89	0.02 ± 0.02	2.78 ± 0.76	3.29 ± 0.32	
10.26	136.062	C ₃ H ₃ N ₅	2.20	Adenine	0.28 ± 0.63	0 ± 0	2.75 ± 0.63	2.06 ± 0.77	
10.27	405.009	C ₉ H ₁₄ N ₂ O ₁₂ P ₂	2.47	Uridine 5'-diphosphate	0.36 ± 0.8	0.01 ± 0.02	5.40 ± 1.05	4.22 ± 0.65	
10.29	120.0656	C ₄ H ₉ NO ₃	4.16	Homo-serine/Allothreonine	1.13 ± 2.53	0.49 ± 1.09	4.86 ± 0.56	4.8 ± 0.87	
10.43	134.0454	C ₄ H ₇ NO ₄	4.55	Aspartate	0.67 ± 1.49	0.43 ± 0.95	3.52 ± 0.87	3.63 ± 2.09	
10.44	130.0498	C ₃ H ₇ NO ₃	4.61	N-Acryloylglycine/Pyroglutamic acid	61.17 ± 73.74	33.1 ± 26.85	130.1 ± 38.3	134.64 ± 29.43	
10.46	97.0283	C ₃ H ₄ O ₂	7.21	-	0.80 ± 1.11	0.26 ± 0.35	5.37 ± 0.66	4.23 ± 1.12	
10.68	112.0501	C ₄ H ₅ N ₃ O	3.92	Cytosine	0.85 ± 1.66	0.13 ± 0.28	3.11 ± 0.76	3.43 ± 1.2	

Table 4.3 continued

Ret. Time (min)	m/z	Tentative Formula	m/z Error (ppm)	Tentative Assignment	$\bar{x} \pm \text{SD}$ (Peak area)				
					Untreated	E2	Ethanol	TAM	
10.68	324.0596	C ₉ H ₁₄ N ₃ O ₈ P	0.31	Cytidine 2'-phosphate/Cytidine monophosphate	1.29 ± 2.68	0.33 ± 0.54	5.35 ± 1.25	4.97 ± 1.67	
10.72	152.0561	C ₅ H ₅ N ₅ O	7.23	Guanine/8-Hydroxyadenine/2-Hydroxyadenine	0.77 ± 1.71	0.07 ± 0.07	10.26 ± 2.22	7.52 ± 3.13	
10.82	613.1587	C ₂₀ H ₃₂ N ₆ O ₁₂ S ₂	1.79	Oxidized glutathione	19.23 ± 41.41	10.34 ± 19.1	58.25 ± 24.05	76.31 ± 21.33	
10.85	489.1153	C ₁₄ H ₂₆ N ₄ O ₁₁ P ₂	1.81	Citicoline	6.19 ± 12.7	1.49 ± 3.04	28.89 ± 4.34	27.82 ± 8.52	
10.89	162.1122	C ₇ H ₁₅ NO ₃	4.93	Carnitine	55.23 ± 31.08	27.53 ± 11.37	92.65 ± 13.43	90.31 ± 15.86	
11.35	229.1538	C ₁₁ H ₂₀ N ₂ O ₃	6.10	L-leucyl-L-proline/L-isoleucyl-L-proline	0.41 ± 0.86	0.07 ± 0.11	5.38 ± 1.62	4.26 ± 0.98	
11.68	146.1176	C ₇ H ₁₅ NO ₂	3.42	3-Dehydroxycarnitine	2.17 ± 3.16	1.39 ± 1.21	8.97 ± 1.89	8.73 ± 1.15	
12.8	206.0555 ⁱ	C ₅ H ₈ N ₂ O ₃	6.31	5-Hydroxymethyluracil	4.29 ± 9.59	2.04 ± 4.57	19.38 ± 4.89	21.8 ± 5.68	
Adduct - ^a Na, ^b NH ₃ adduct, ^c K adduct, ^d CH ₃ OH+H, ^e M+2Na-H, ^f 2M+Na, ^g 2M+K, ^h M+ACN+H, ⁱ M+ACN+Na									
PE-Nme - Glycerophosphoethanolamines									
PC - Glycerophosphocholines									
PE - Glycerophosphoethanolamines									

4.4 Conclusions

A ^1H NMR and HILIC-MS based metabolomics approach was used to investigate the effect of adding hormonal drugs to an ASG5 apocrine cell lines. Both analytical methods produced high quality data in which untreated and the E2 treated cells could clearly be differentiated from the TAM and ethanol treated cells when coupled with MVA techniques. Furthermore, it was observed that TAM and ethanol could not be differentiated, thus, concluded that TAM produced no additional effect to that of the ethanol-treated cells. The differences in the metabolic profile between the different hormonal treatments observed both by ^1H NMR spectroscopy and HILIC-MS were based on different sets of markers. Thus, this illustrates the complementary nature of the two analytical methodologies and demonstrates the potential value of applying both techniques to analyse biological samples.

Definitive identification of metabolites is a very challenging aspect of metabolomics for both NMR spectroscopy and LC-MS. Identification of metabolites detected by NMR was aided by the large body of information already available on human biological fluids. Thus, the information provided herein will provide a good base for the identification of apocrine sweat *in vivo*. In comparison, the available data for metabolite identification by LC-MS is less extensive and the identity of most of the metabolites contributing to the different treatments is currently unknown. However, a number of putative identifications (either metabolite ID or elemental composition) were achieved by relying on the mass accuracy of the QTOF system.

Limited conclusions could be drawn on the effect of hormonal drugs on the ASG5 cells; nevertheless, this is vastly more than is currently available in the literature. Currently, the ASG5 cells are not well characterised, thus, it is unknown whether TAM or E2 (as well as any other chemical mediators) will effect cell proliferation or have an effect on the androgen pathway. TAM would not be expected to interfere with androgen pathway directly since it inhibits the estrogen receptor, which is down stream of androgen synthesis. However, it is unsure whether the inhibition of the receptor may invoke a feedback response. Nonetheless, there is clear difference in the

cellular metabolism between the different hormone treatments which suggest that apocrine cells from males and females might behave differently due to the different levels of circulating hormones.

Chapter 5

5 Metabolomic Investigations of Human Axillary Secretions

5.1 Introduction

The human axilla region is populated with two classes of sweat glands: the eccrine glands, which produce a watery secretion in response to heat, and the apocrine glands, which produce micro-droplets of a viscous secretion in response to emotional stress. The characteristic axillary odour (commonly referred to as “body odour”) is generated when bacteria, predominately of the *Corynebacteria* and *Staphylococci* genera (Leyden *et al.*, 1981; Shehadeh and Kiligman, 1963), on the skin surface interact with apocrine secretions (Shelley *et al.*, 1953). The main contributors to axillary odour are unsaturated or hydroxylated branched fatty acids, (E)-3-methyl-2-hexenoic acid (3M2H) and 3-hydroxy-3-methyl-hexanoic acid (HMHA), with the former being the key component (Zeng *et al.*, 1991); sulfanylalkanols, particularly 3-methyl-3-sulfanylhexasan-1-ol (3M3SH) (Gautschi *et al.*, 2007; Hasegawa *et al.*, 2004; Natsch *et al.*, 2004; Troccaz *et al.*, 2004); and the odoriferous steroids, 5 α -androst-16-en-3-one and 5 α -androst-16-en-3 α -ol (Bird and Gower, 1981; Claus and Alsing, 1976). The precursor of the odorant acids have been shown to be secreted as glutamine conjugates, that are then cleaved specifically by a bacterial Zn-dependent N α -acyl-glutamine-aminoacylase (N-AGA) from *Corynebacteria* Ax20 (Natsch *et al.*, 2006; Natsch *et al.*, 2003). Sulfanylalkanols have been shown to be secreted as either a cysteine-(S) or cysteine-glycine-(S) conjugate, which are then cleaved by the sequential action of a bacterial dipeptidase and a cysteine β -lyase (Emter and Natsch, 2008; Starkenmann *et al.*, 2005). There is evidence that odoriferous steroids are formed from nonodoriferous steroid precursors, conjugated to a sulphate or glucuronic acid (Froebe *et al.*, 1990), as a result of bacterial metabolism (Decreau *et al.*, 2003; Gower *et al.*, 1997; Labows *et al.*, 1979).

These latest findings confirm the importance of bacterial activity and sweat odour precursors for the generation of body odours. It is commonly known that gender, ethnicity, emotional, physiological, and environmental factors may influence individual odours (Akutsu *et al.*, 2006; Dixon *et al.*, 2007; Penn *et al.*, 2007; Troccaz *et al.*, 2009). Furthermore, several studies have concluded that individuals have a distinct odour type, which may be used for mate selection (Wedekind and Furi, 1997; Wedekind *et al.*, 1995) as well as individual or kin recognition (Weisfeld *et al.*, 2003). Thus it is suggested that an individual's odour profile is partly determined by their major histocompatibility complex (also known as human leucocyte antigen region) (Roberts *et al.*, 2005), however, the underlying mechanism is currently unknown (Natsch *et al.*, 2010). Furthermore, MHC-dependent odour discrimination and mating preference have been presented in mice (Yamazaki *et al.*, 2000; Yamazaki *et al.*, 1976), reptiles (Olsson *et al.*, 2003), birds (Freeman-Gallant *et al.*, 2003) and fish (Reusch *et al.*, 2001), where MHC-dissimilarity may help to maximise the frequency of MHC-heterozygotes in their offspring, providing increasing resistance to disease and prevent inbreeding (Penn and Potts, 1999).

To date, the literature has limited information on the importance of skin bacteria or sweat composition in generating the characteristic axillary odour from an individual. Furthermore, most studies only consider the volatile composition or odour perception without considering their origin (i.e. left or right side) or do not specify whether samples come from one axilla or are pooled together from one individual or several donors. Side related differences have seldom been assessed in humans, and what has been reported is often contradictory. Bird and Gower found that high level of androstenone correlated with the handedness, except for one individual (Bird and Gower, 1982). Ferdenzi and co-workers reported that the left and right axillary are perceptually equivalent when sampling the general population, with only a significant difference in the left axilla in left-handed people (Ferdenzi *et al.*, 2009). However, they stated that this difference is likely to be attributed to the perception of female raters who did not use hormone-based contraception and who were likely to be in the fertile phase of their cycle (Ferdenzi *et al.*, 2009). This is consistent with the idea that there is increased awareness of stimuli between mating and fertilisation issues at the time of ovulation (Lundstrom *et al.*, 2006).

Axillary secretions and odours are of both a biological and commercial importance. Studies have shown that odours contain chemical cues that can affect an individual's mood (Jacob *et al.*, 2002; Preti *et al.*, 2003), brain activity (Jacob *et al.*, 2001; Savic *et al.*, 2001), or even alter length and timing of the human menstrual cycle (McClintock, 1978). In addition, the nature and biogenesis of these odorants that contribute to ones 'volatile metabolome', is a focus of a multibillion-pound consumer cosmetic industry, which seeks new products to counteract either odour production or perception.

In summary, the literature on apocrine sweat composition is biased towards the volatile components, thus, this chapter will use the methodologies developed in chapter two and three to provide further identification of the non-volatile components, through the use of in-house metabolite libraries and external databases. Particular emphasis will be on the odour precursors as these are considered key metabolites for odour production. Furthermore, pattern recognition techniques will be used to analyse the spectral data obtained from six volunteers, with each underarm collected separately, across five days in order to determine the inter-day or inter-individual variation.

5.2 Aims

- To identify metabolites present in human apocrine sweat, with emphasis on odour precursors, using NMR spectroscopy, HILIC-MS (QTOF) and LC-MS/MS (QTRAP) methodologies developed in chapters two and three.
- UPLC-Orbitrap-MS method initially developed by Dr Catherine Ortori will also be applied to the analysis of human apocrine sweat.
- To assess inter-subject variability in the measured profiles of odour precursors in apocrine sweat.
- To determine whether there are any intra-individual differences in the odour precursors measured in apocrine sweat from the left and right arm.

5.3 Materials and Methods

5.3.1 Chemicals

MS grade caffeine, sodium dodecyl sulfate, and sodium taurocholate were purchased from Sigma Aldrich (Poole, UK). Mass spec grade Ultramark 1621 and MRFA tetrapeptide was purchased from ABCR GmbH & Co. KG (Karlsruhe, Germany) and Research Plus Inc (Barnegat, NJ) respectively.

5.3.2 LC-MS Column

A Zorbax RRHD Eclipse Plus C₁₈ column (1.8 µm, 2.1 x 150 mm) was purchased from Agilent Technologies (Cheshire, UK). The column was equilibrated with mobile phase prior to use and washed as per manufacture recommendations.

5.3.3 Collection of Odourless Axillary Secretions

The collection of human apocrine secretions was carried out by Dr Mark Harker (Unilever, Port Sunlight) as follows: The axillae of six male volunteers who had a controlled wash in their underarms on the morning of day one with subsequent collections on morning of days two to five from both underarms, which were collected separately (right and left). After each collection their underarms were washed again. Thus, each collection point represents a 24 h time point between samples during the course of the week-long test. Both underarms were sampled using a Teflon cup and stick. The Teflon cup was placed on the skin in the underarm whilst panelists lay down with their arm raised. 1.5 ml water was applied to the buffer cup and the water was stirred with the Teflon stick for 60 s. This water was then collected using a pipette and stored on ice. This process was repeated and the two fractions were pooled. This process was then repeated for the other underarm. The two samples for each panelist were treated separately. The samples were spun at 14 000xg for 5 min to remove dead skin and bacteria. Samples were maintained at 4°C after collection until storage when they were kept at -80°C.

5.3.4 Sample Preparation

All samples were evaporated to dryness with a centrifugal evaporator (25°C, 2 h) and then re-suspended in 20 µl water. Each sample was aliquoted as follows: 5 µl aliquots into 1 mm NMR tubes with the addition of 3 µl deuterated phosphate buffer (pH* 6.0, 0.1 M) containing TSP (7.6 mM), 10 µl aliquots into MS vials with the addition of 85% acetonitrile, and the remaining 5 µl was pooled together in order to create QC samples with the addition of 85% acetonitrile for LC-MS analysis.

5.3.5 ¹H NMR Spectroscopy for the Global Profiling of Axillary Secretions

Development of the methodology for the analysis of human apocrine gland sweat secretions is discussed in chapter two (Section 2.3.3). In summary, spectra were acquired on a Bruker Avance 400 spectrometer, operating at 400.13 MHz ¹H observation frequency equipped with a 1 mm TXI micro-volume probe with an internal probe temperature of 298 K and with 256 transients being collected. All spectra were manually corrected for phase and baseline distortions using TopSpinTM 2.1 (Bruker GmbH, Germany) and chemical shifts referenced to TSP standard at 80.00 ppm.

5.3.6 2D NMR Spectroscopy

To aid spectral assignment, 2D ¹H-¹H COSY spectra were measured with solvent presaturation pulse sequence on each sample. Acquisition and processing parameters for the COSY spectra included a relaxation decay of 1.86 s, a spectra width in F1 and F2 of 5995.2 Hz, 2 k time domain points, 128 F1 increments, 64 transients per increment and qsine apodization in F1 and F2.

5.3.7 HILIC-QTOF-MS for the Global Profiling of Axillary Secretions

HILIC-QTOF-MS was used for a global profiling approach as previously described in chapter three (Section 3.2.4). In summary, data was acquired m/z 80-1000 in positive ion mode over 25 min.

5.3.8 UPLC-Orbitrap-MS for the Global Profiling of Axillary Secretions

In addition to using the HILIC-QTOF-MS developed specifically for the project, a benchtop Orbitrap mass spectrometer (Thermo Scientific Exactive), was used as another approach for global profiling. The orbitrap mass analyser has a higher resolution than that of most time-of-flight instruments ($\sim 10\,000$) and approaches that of FTICR ($\sim 100\,000$) to ensure high mass accuracy and to enable confident discrimination between co-eluting, isobaric compounds in complex samples. Such applications require mass accuracy of less than 5 ppm. Furthermore, the Exactive is capable of higher scan speeds and polarity switching without sacrificing mass accuracy. Thus, positive and negative spectra can be obtained in a single run.

All experiments were conducted on an Accela U-HPLC system equipped with quaternary pumps coupled to an Exactive orbitrap mass spectrometer (all from Thermo Scientific, Hemel Hempstead, UK), controlled by Xcalibur 2.1 software. The instrument was equipped with an ESI probe and was operated in positive-negative polarity switching mode. The spray voltage was set to 3 kV or -3 kV for positive or negative ion mode respectively. The sheath gas, auxiliary and sweep gas flows were set to 70, 40, and 2 respectively (arbitrary units) and the capillary temperature was set to 350°C. The instrument was operated in full scan mode from m/z 100-1000 and from m/z 50-200. This was in order to maintain mass accuracy at the high m/z end. It is a known limitation of the instrument where the last mass $\leq 20 \times$ first mass. The mass spectrometer was calibrated according to the manufacturer's guidelines prior to use with either caffeine, MRFA tetrapeptide (Met-Arg-Phe-Ala), and Ultramark 1621 or sodium dodecyl sulfate, sodium taurocholate, and Ultramark 1621 in an acetonitrile:methanol:water solution containing 1% acetic acid for positive and negative mode respectively.

A 5 µl aliquot of apocrine sweat mixture was injected onto a Zorbax RRHD Eclipse Plus C₁₈ column (1.8 µm particle size, 2.1 x 150 mm) operated at 40°C, with all the eluent from the LC column being directly transferred into the ion source of the MS without post column splitting. The eluent solvents were [A] water with 0.1% formic acid and [B] acetonitrile and 0.1% formic acid. The gradient duration was 16 min and was based on an in-house method developed by Dr Catharine Ortori and is summarised in Table 5.1 below.

Table 5.1 LC-MS/MS conditions for the analysis of apocrine sweat secretions. Mobile phase [A] water + 0.1% formic acid and [B] acetonitrile + 0.1% formic acid.

Time (min)	Parameter [B]	Flow rate µl/min
0	10	300
4	22	300
7	99	300
12	99	450
13	10	600
16	10	450

5.3.9 Conjugate Profiling using RP-HPLC-MS/MS

RP-HPLC-MS was used as a survey scanning method to detect amino acid conjugates without making prior assumption of identity as previously described in chapter three (Section 3.2.6). The precursor ion survey scanning method was split into two analytical replicates instead of three due to the limited sample volume. The Gln (*m/z* 147) and Cys (*m/z* 105) containing conjugates were monitored together within the same acquisition, while the Cys-Gly conjugate (*m/z* 179) were monitored separately. Thus, it must be noted that EPI spectra would only be available for the most intense ion, i.e. if Gln and a Cys conjugate co-eluted, EPI spectra will only be produced for the most concentrated metabolite.

5.3.10 Targeted Profiling using RP-HPLC-MS/MS

RP-HPLC-MS/MS was used to specifically target amino acid conjugates as previously described in chapter three (Section 3.2.6).

5.3.11 Data Analysis

Methodology for the pre-processing and subsequent data-analysis of the NMR, HILIC-MS and Q-TRAP data were carried out as discussed previously in chapter two (Section 2.3.5), chapter three (Section 3.2.8) and chapter four (Section 4.2.8). For the Exactive work, the raw data was analysed using Sieve version 1.0 (Thermo Scientific, UK); this application manager integrates peaks in the UPLC-MS data by using ChromAlign™ peak detection.

The ion intensities for each peak detected are then exported to Microsoft Excel 2007 to be normalised, within each sample, to the sum of the peak intensities of that sample. The resulting normalised peak intensities are then exported in to SIMCA P and analysed as discussed in chapter four (Section 4.2.9).

5.3.12 Compound Identification by LC-MS

Metabolite identification *via* LC-MS is based on two computational methods: matching MS/MS fragment patterns to spectral libraries or accurately measuring pseudomolecular ion to determine their *m/z* or chemical formula in order to extract potential structures from databases. In order to calculate the most likely and chemically correct formula, rules need to be followed and adhered to in order to constrain thousands of possible candidates. This work flow is discussed in chapter four (Section 4.2.10) and a recent review (Kind and Fiehn, 2007).

There are currently a range of freely and commercially accessible online databases, as summarised in Table 5.2. These databases can be searched by name, mass or structure and some have additional information, like MS fragmentation or metabolic pathways, which may provide further assistance with metabolite identification. The main databases used in this study were the biological databases such as HMDB or Lipid Maps, as these are specific to metabolites that have been reported in human biological samples. However, synthesized authentic standards are necessary for ultimate confirmation of an unknown metabolite identity. The confirmation of a metabolite's identity is not trivial and can be considered the most challenging and time consuming

process in metabolomics. Hence, the level of evidence in supporting a proposed metabolite identity is indicated by a one to three star rating for ease of interpretation in this chapter; one star, putative identification, two stars has common fragmentations to that of what would be expected, and three stars confirmed with a standard.

Table 5.2 Some commonly used metabolomic databases used for metabolite identification.

Name	Content
Compound specific databases	
PubChem	Chemical compounds and structures, links to Entrez databases, bioactivity data from high throughput screening programs
HMDB	A comprehensive database >7900 human metabolites obtained from NMR, GC-MS and MS/MS
Lipid Maps	Structure and annotations of >10,000 biological lipids in human and other mammals
KNAPSAcK	A cross-species metabolite database of >28,500 compounds mostly from plants and microorganisms
MMD	A knowledgebase of 42,687 endogenous and exogenous metabolites
Drugbank	Drug, drug targets, physicochemical, clinical, and pharmacological properties, links to other databases, 3D and chemical structure
ChemSpider	ChemSpider is an aggregated database of organic molecules containing more than 20 million compounds from many different providers. At present the database contains information from such diverse sources as a marine natural products database, ACD-Labs chemical databases, the EPAs DSSTox databases and from a series of chemical vendors
Reference databases	
NIST 08	A commercial library of >220,000 EI mass spectra from >190,000 pure chemical compounds
GMD	Mass spectra and retention indices of known plant metabolites analysed by GC-MS
METLIN	A database of LC-MS, LC-MS/MS, and LC-FTMS mass spectra of metabolites from human and microbial species. It contains >25,000 structures, including more than 8000 di and tripeptides.
MassBank	A high resolution MS/MS spectral database for standard chemical substances. More than 30,000 spectra from >1900 different compounds are available
MS2T	A MS/MS spectral tag library of phytochemical compounds
MMCD	A NMR and LC-MS spectral library of metabolite standards. It contains approximately >20,000 metabolite entries and experimental spectral data on >600 compounds
Fiehn GC-MS Database	This library contains data on 713 compounds (name, structure, CAS ID, other links) for which GC/MS data (spectra and retention indices) have been collected by the Fiehn laboratory
Pathway specific databases	
KEGG	A composite database consisting of collections of pathway maps, genes, organisms, enzymes and ligands (metabolites, drugs and other small molecules)
BioCyc	A collection of 1004 pathway/genome databases of organisms with completely or partially sequenced genomes
EcoCyc	A scientific database of Escherichia coli K-12 MG1655
MetaCyc	A database of nonredundant, experimentally elucidated metabolic pathways on >1,600 pathways from >2000 different organisms
HumanCyc	A human metabolic pathway and human genome database on 28,783 genes, their products and the metabolic reactions and pathways they catalyze
Reactome	A database of human metabolic pathways and biological processes involving small metabolites, biomolecules and their reactions/interactions. Reactome has data and pathway diagrams for >2700 proteins, 2800 reactions and 860 pathways for humans

5.4 Results and Discussion

5.4.1 Identification of Small Molecule Components of Human Apocrine Sweat

5.4.1.1 Global Analysis using ^1H NMR Spectroscopy

To my knowledge, this is the first report of applying NMR spectroscopy to the global profiling of human apocrine sweat. The results obtained in the present study confirm that NMR based metabolomics can be successfully applied to the metabolic profiling of apocrine gland sweat. A typical 400 MHz ^1H NMR spectrum of human apocrine sweat acquired using a 1 mm micro-volume probe is depicted in Figure 5.1. The increased sensitivity obtained from using a micro-volume probe has allowed 25 metabolites to be identified. Many resonances have been assigned by comparison with existing literature (Harker *et al.*, 2006; Lindon *et al.*, 2000; Nicholson *et al.*, 1995) in combination with an in-house spectral database and are tabulated (Table 5.3), together with concentrations of metabolites found in a typical sample. The major classes of metabolites identified included TCA cycle intermediates (e.g. citric acid, formic acid), ketone bodies (3-hydroxybutyrate), energy metabolites (creatinine, lactate), amino acids and nucleotide derivatives. Lactic acid was found to be the most abundant metabolite, which is consistent with observations made previously following spectroscopic analysis of human eccrine sweat (Harker *et al.*, 2006). A number of unassignable compounds or tentatively assignable compounds were also observed. In particular, the chemical shifts downfield (aromatic region) are presumed to be nucleotides or nucleotide derivatives. Furthermore, from the 2D ^1H - ^1H COSY spectra, it was shown that the doublets observed at 6.41 ppm are coupled with doublets at 7.32 ppm, indicating an AX spin system.

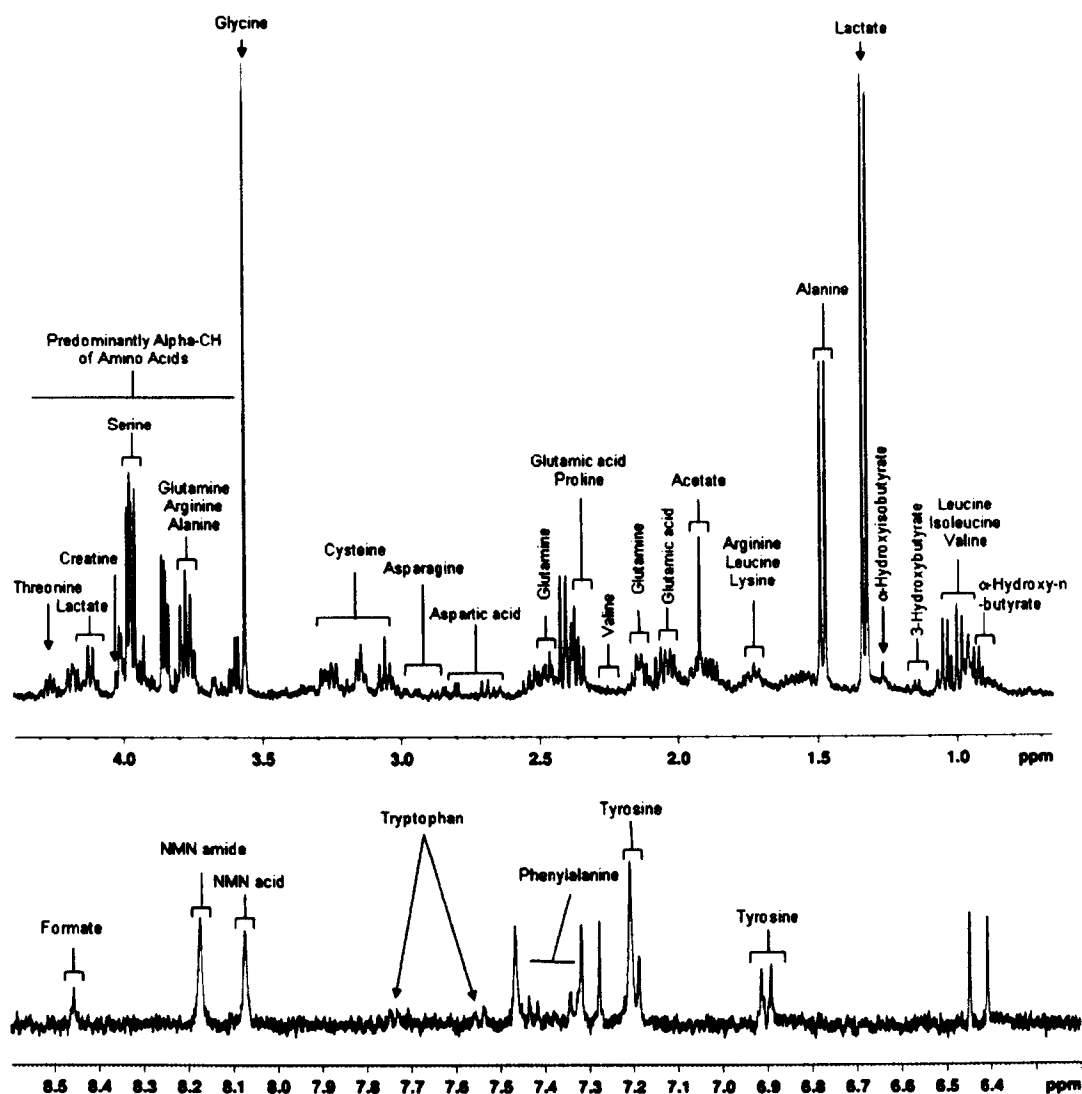


Figure 5.1 Typical 400 MHz ^1H NMR spectrum of human apocrine sweat obtained using 1 mm micro-volume probe. Some metabolites are tentatively assigned. Spectra were acquired using a standard noesy preset pulse sequence with 256 scans.

Table 5.3 Peaks assigned to metabolites in apocrine sweat and experimentally determined concentrations. No corrections for difference in T_1 relaxation have been made.

Chemical Shift	Assignment	Metabolite	Typical Concentration (mM)
0.90 (t) ^a	CH ₃	α -hydroxy-n-butyrate ^b	-
0.92 (t)	δ -CH ₃	Isoleucine	1.9 \pm 1 (0.9 - 3.8)
0.99 (d)	β -CH ₃		
0.96 (t)	δ -CH ₃	Leucine	1.2 \pm 0.6 (0.7 - 2.1)
1.72 (m)	CH ₂		
3.72 (m)	α -CH		
0.98 (d)	CH ₃	Valine	0.9 \pm 0.3 (0.5 - 1.4)
1.03 (d)	CH ₃		
2.26 (m)	β -CH		
3.59 (d)	α -CH		
1.14 (d)	CH ₃	Isobutyrate ^b	-
1.18 (d)	CH ₃	3- β -hydroxybutyrate ^b	0.2 \pm 0.1 (0.1 - 0.5)
2.28 (ABX)	CH ₂		
1.26 (s)	CH ₃	α -hydroxyisobutyrate ^b	1.8 \pm 1 (0.9 - 3.4)
1.33 (d)	CH ₃	Lactate	13.2 \pm 13.8 (2.4 - 44.8)
4.11 (q)	CH		
1.48 (d)	CH ₃	Alanine	2.4 \pm 1.1 (1.2 - 4.2)
1.48 (m)	γ -CH ₂	Lysine	-
1.73 (m)	δ -CH ₂		
1.90 (m)	β -CH ₂		
3.04 (t)	ϵ -CH ₂		
1.56 (m)	γ -CH ₂	Citrullene ^b	-
1.86 (m)	β -CH ₂		
3.13 (t)	α -CH ₂		
3.74 (t)	α -CH ₂		
1.92 (s)	CH ₃	Acetate	1.9 \pm 0.8 (0.9 - 3.1)
2.03 (m)	γ -CH ₂	Proline	-
2.36 (m) ^a	β -CH ₂		
3.35 (m)	δ -CH ₂		
3.43 (m)	δ -CH ₂		
4.15 (m) ^a	α -CH		

Table 5.3 continued

Chemical Shift	Assignment	Metabolite	Typical Concentration (mM)
2.07 (m) ^a	β-CH ₂	Glutamate	6.8 ± 3.7 (3 - 12.8)
2.35 (m)	γ-CH ₂		
2.15 (m) ^a	β-CH ₂	Glutamine	2.2 ± 1.4 (0.9 - 4.1)
2.46 (m)	γ-CH ₂		
2.51 (AB) ^a	½ CH ₂	Citrate	-
2.65 (AB) ^a	½ CH ₂		
2.68 (ABX)	β-CH ₂	Aspartate	0.2 ± 0.1 (0.1 - 0.4)
2.82 (ABX)	β-CH ₂		
3.90 (ABX)	α-CH		
3.04 (s)	CH ₃	Creatine	0.2 ± 0.1 (0.1 - 0.5)
4.02 (s)	CH ₂		
3.31 (ABX)	CH ₂	Tryptophan	0.5 ± 0.4 (0.1 - 1)
3.49 (ABX)	CH ₂		
4.06 (ABX)	CH		
7.21 (t)	C5H		
7.29 (t)	C6H		
7.33 (s)	C2H		
7.55 (d)	C7H		
7.74 (d)	C4H		
3.56 (s)	CH ₂	Glycine	3.2 ± 1.5 (1.5 - 5.9)
3.59	α-CH	Threonine	1.7 ± 0.9 (0.7 - 3.1)
4.26 (m)	β-CH		
3.85 (dd)	α-CH	Serine	3.7 ± 1.8 (1.7 - 6.4)
3.95 (dd)	β-CH ₂		
4.00 (dd)	β-CH ₂		
6.90 (d)	H3/H5	Tyrosine	0.4 ± 0.2 (0.2 - 0.7)
7.19 (d)	H2/H6		
7.33 (m)	H2/H6	Phenylalanine	0.3 ± 0.1 (0.2 - 0.5)
7.39 (m)	H4		
7.43 (m)	H/H5		
8.46 (s)	CH	Formate	0.6 ± 0.4 (0.2 - 1.4)

^aPartially obscured resonances, ^bTentatively assigned

Multiplicity is indicated as s = singlet, d = doublet, t = triplet, q = quartet, m = multiplet

5.4.1.2 Global Analysis using High Mass Accuracy LC-MS (HILIC and C₁₈)

HILIC methodology was developed to identify and characterise the aqueous fraction of apocrine sweat secretions, as discussed in chapter 3. Figure 5.2 shows a 2D LC-MS map (horizontal axis: retention time, vertical axis: m/z) for a typical QC sample acquired in positive ESI mode. A total of 580 peaks were detected with an average cumulative variation of 103% across all QC samples. This variation is considered to be large; indicating the method was not performing as expected. Only 37 metabolites had a CV of less than 25%. Altering the processing parameters, such as minimum peak intensity, to that of a higher value, e.g. 600 counts, the number of extracted peaks dropped to 190 metabolites with an average CV of 91.5%. This error also incorporates any error or inconsistencies from peak integration during the pre-processing stage. Therefore, it is considered that there was a sensitivity detection issue with the instrument which would cause this high CV error. Nonetheless, valuable information can still be obtained from this data set in regards to the presence of amino acid conjugates.

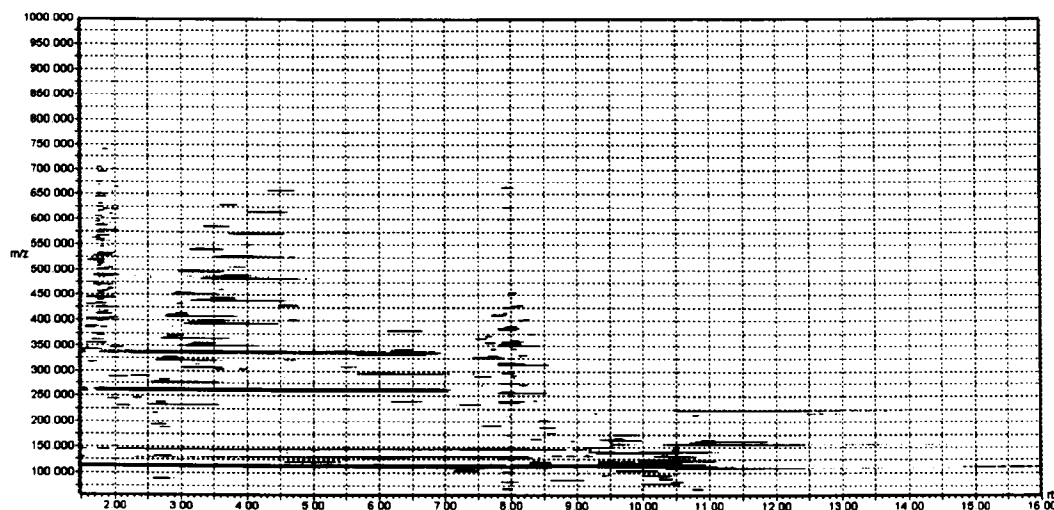


Figure 5.2 Two dimensional mass versus retention 'map' (m/z 80-1000) obtained from QTOF-HILIC-MS analysis of a human apocrine sweat sample. In this typical chromatogram, ~580 ions can be detected in 15 min.

An 'in-house' metabolomic method, previously developed in our group, using a RP-UPLC C₁₈ column coupled to an Orbitrap-MS was used for analysis of semi-polar/non-polar fraction. A typical total ion chromatogram obtained from a representative QC apocrine sweat sample is depicted in Figure 5.3 for both positive and negative ESI mode. The initial pre-processing of the UPLC-MS data using Sieve, extracted 1359 peaks with an average CV of 36% and 988 peaks with an average CV of 23%, across all QC samples in positive and negative mode respectively. Using the information gathered from the literature about the composition of human apocrine sweat (see Appendix A), putative identification of the odour precursors are summarised Table 5.4, while putative identification of known metabolites previously reported in apocrine sweat are summarised in Table 5.5.

Identification of the amino acid conjugates was based on using the accuracy of the instrument in order to extract the individual peaks from the TIC. In total, nine amino acid conjugates were shown to be detected with both the HILIC-QTOF and UPLC-Orbitrap methodologies, with 3M2H-Gln and HMHA-Gln being the most abundant conjugates detected. N- α -9-hydroxy- non-anoyl- L-glutamine, N- α -3-hydroxy-3-methyloct anoyl- L-glutamine and N- α -3-hydroxy-4-methyloct anoyl- L-glutamine (where each metabolite has a corresponding m/z 303.1927) all produce one chromatographic peak at 7.12 min, thus, no further identification is possible. 3M3SH-Cys-Gly was detected with the HILIC methodology, however, was marginally above the limit of detection. S-[1-(2-hydroxyethyl)-butyl]-L-cysteinylglycine (m/z 279.1379) produced two chromatographic peaks at 6.07 min and 8.53 min. The mass error at 6.07 min is 20.42 ppm, thus, is likely the Na⁺ adduct of 3M2H-Gln, while the peak at 8.53 min is marginally above the limit of detection in the HILIC method. Furthermore, S-[1-(2-hydroxyethyl)-butyl]-L-cysteinylglycine produced several chromatographic peaks (ranging from 1.39-12.89 min) from the UPLC C₁₈ method in negative mode only. Again, all the representative peaks were only marginally above the limit of detection, with the most intense peak eluting at 11.29 min, thus, no retention time can be reliably obtained.

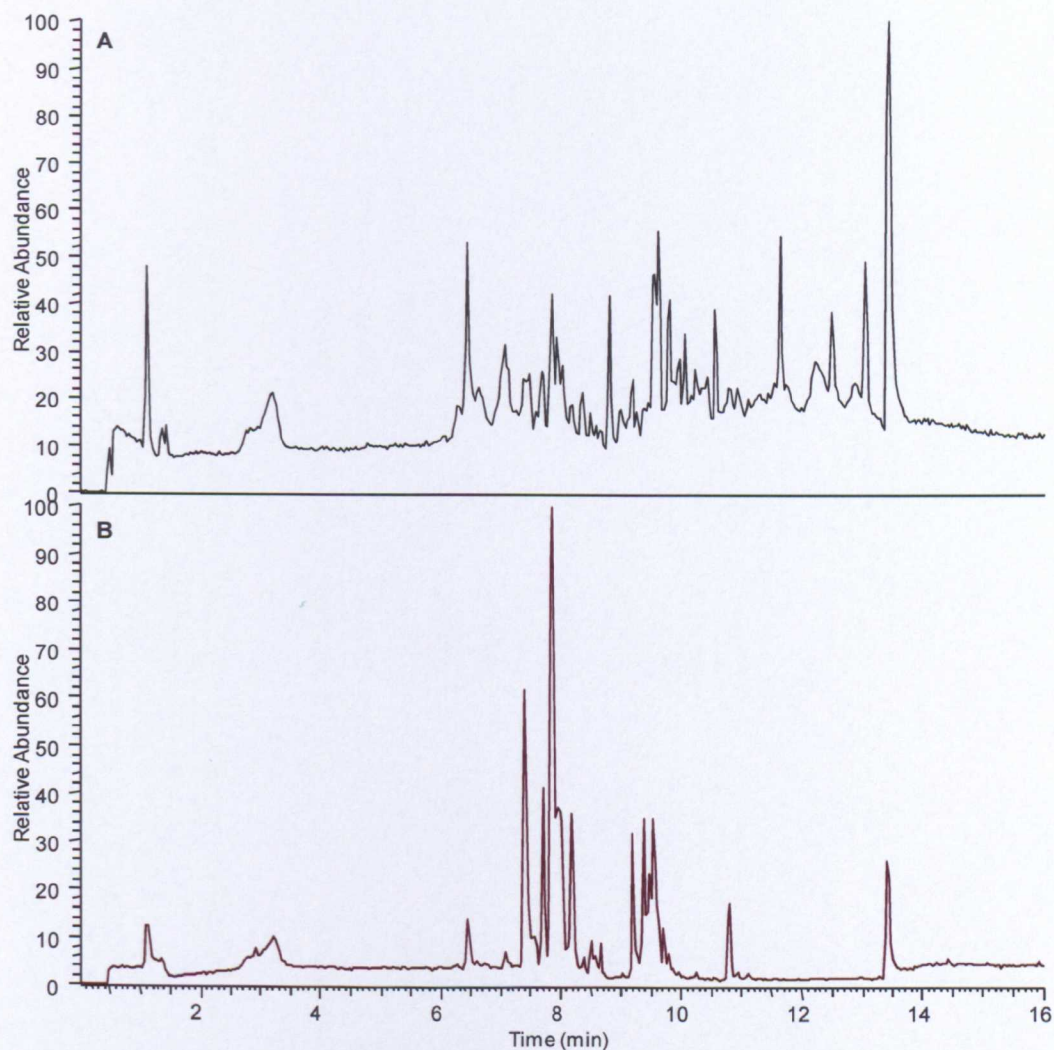


Figure 5.3 UPLC-MS total ion chromatogram acquired in **A** positive mode **B** negative mode, of a representative human apocrine sweat sample.

Table 5.4 Summary of the HILIC and UPLC retention times and HR mass spectra of the principle odour precursors in both positive and negative ion mode

Tentative ID	Formula	HILIC-QTOF-MS			UPLC-Orbitrap-MS				
		Positive mode		Retention Time (min)	Positive mode		Negative mode		
		Detected m/z	Delta (ppm)		Detected m/z	Delta (ppm)	Detected m/z	Delta (ppm)	Retention Time (min)
Gln Conjugates									
N- α -3-hydroxy-3-methylhexanoyl- L-glutamine	C ₁₂ H ₂₂ N ₂ O ₅	275.1612 ^b	1.81	8.02	297.1424 ^a	1.32	273.1452	-1.32	3.16
N- α -3-methylhex-2-enoyl-L-glutamine	C ₁₂ H ₂₀ N ₂ O ₄	279.1322 ^a	0.34	6.07	279.1319 ^a	1.32	255.1346	-1.76	6.45
N- α -4-methyl-3-oct-enoyl- L-glutamine	C ₁₄ H ₂₄ N ₂ O ₄	285.1821	2.45	4.71	307.1632 ^a	1.04	283.1661	-1.00	7.13
N- α -4-ethyl-hept-anoyl- L-glutamine	C ₁₄ H ₂₅ N ₂ O ₄	287.2002	10.79	8.08	-	-	285.1814	-2.16	7.21
N- α -3-hydroxy- 3-methylhept-anoyl- L-glutamine	C ₁₃ H ₂₄ N ₂ O ₅	289.1757 ^b	-2.07	7.58	311.1579 ^a	0.40	287.1610	-1.03	6.25
N- α -3-hydroxy-oct-anoyl- L-glutamine	C ₁₃ H ₂₄ N ₂ O ₅	289.1757 ^b	-2.07	7.58	311.1579 ^a	0.40	287.1610	-1.03	6.25
N- α -8-hydroxy-oct-anoyl- L-glutamine	C ₁₃ H ₂₄ N ₂ O ₅	289.1757 ^b	-2.07	7.58	311.1579 ^a	0.40	287.1610	-1.03	6.25
N- α -3-hydroxy-4-methylhept anoyl- L-glutamine	C ₁₃ H ₂₄ N ₂ O ₅	289.1757 ^b	-2.07	7.58	311.1579 ^a	0.40	287.1610	-1.03	6.25
N- α -4-ethyl-oct-anoyl- L-glutamine	C ₁₃ H ₂₄ N ₂ O ₄	301.2129	0.66	4.33	323.1949 ^a	2.25	299.1974	-0.91	7.49
N- α -9-hydroxy- non-anoyl- L-glutamine	C ₁₄ H ₂₆ N ₂ O ₅	303.1927	2.31	7.12	325.1736 ^a	0.68	301.1765	-1.37	6.77
N- α -3-hydroxy-3-methyloct anoyl- L-glutamine	C ₁₄ H ₂₆ N ₂ O ₅	303.2023	2.31	7.12	325.1736 ^a	0.68	301.1765	-1.37	6.77
N- α -3-hydroxy-4-methyloct anoyl- L-glutamine	C ₁₄ H ₂₆ N ₂ O ₅	303.2023	2.31	7.12	325.1736	0.68	301.1765	-1.37	6.77
Cys-Gly Conjugates									
S-[1-(2-hydroxyethyl)-butyl]-L-cysteinylglycine	C ₁₁ H ₂₂ N ₂ O ₄ S	279.1368	8.53	-3.94	-	-	-	-	-
S-[1-(2-hydroxyethyl)-1-methylbutyl]-L-cysteinylglycine	C ₁₂ H ₂₄ N ₂ O ₄ S	293.1534	8.45	-0.34	-	-	-	-	-

^aNa⁺ adduct

^bNa⁺ detected but less dominant than pseudomolecular ion

Table 5.5 Tentative identities of known compounds previously reported in apocrine sweat.

Compound Name	Formula	Positive mode			Negative mode		
		Detected <i>m/z</i>	Delta (ppm)	Actual RT	Detected <i>m/z</i>	Delta (ppm)	Actual RT
α -Pinene	C ₁₀ H ₁₆	137.1327	1.78	7.16	-	-	-
(4-Hydroxyphenyl)acetic acid	C ₈ H ₈ O ₃	153.0548	1.33	8.23	-	-	-
Geranial	C ₁₀ H ₁₆ O	153.1274	0.32	7.40	-	-	-
Geraniol	C ₁₀ H ₁₈ O	155.1433	1.93	7.16	-	-	-
Isopropylacetophenone	C ₁₁ H ₁₄ O	163.1120	1.58	7.94	-	-	-
2-Phenylethyl acetate	C ₁₀ H ₁₂ O ₂	165.0912	1.18	9.17	-	-	-
Eugenol	C ₁₀ H ₁₂ O ₂	165.0912	1.18	9.17	-	-	-
Isoeugenol	C ₁₀ H ₁₂ O ₂	165.0912	1.18	9.17	-	-	-
Jasmone	C ₁₁ H ₁₆ O	165.1276	1.13	7.35	-	-	-
(Z)-4-Methylnon-3-enoic acid	C ₁₀ H ₁₈ O ₂	171.1381	0.79	10.37	-	-	-
(E)-4-Methylnon-3-enoic acid	C ₁₀ H ₁₈ O ₂	171.1381	0.79	10.37	-	-	-
9-Decenoic acid	C ₁₀ H ₁₈ O ₂	171.1381	0.79	10.37	-	-	-
Octanedioic acid (suberic acid)	C ₈ H ₁₄ O ₄	175.0964	-0.72	9.88	-	-	-
E-Cinnamyl acetate	C ₁₁ H ₁₂ O ₂	177.0913	1.79	8.04	-	-	-
10-Undecenoic acid	C ₁₁ H ₂₀ O ₂	185.1539	1.34	7.35	-	-	-
2-Hexyl 2-pentenoate	C ₁₁ H ₂₀ O ₂	185.1539	1.34	7.35	-	-	-
1-Dodecene	C ₁₂ H ₂₄	186.2219	1.27	8.59	-	-	-
Citronellol acetate	C ₁₂ H ₂₂ O ₂	199.1695	0.97	8.82	-	-	-
Farnesene	C ₁₅ H ₂₄	205.1954	1.59	12.26	-	-	-
Pentyl salicylate	C ₁₂ H ₁₆ O ₃	209.1175	1.15	8.23	-	-	-
Methyl trans-jasmonate	C ₁₂ H ₁₈ O ₃	211.1331	0.95	6.78	-	-	-
Cyclotetradecane	C ₁₄ H ₂₈	214.2532	1.37	7.65	-	-	-
1-Tetradecene	C ₁₄ H ₂₈	214.2532	1.37	7.65	-	-	-
N,N-Dimethyl-1-dodecylamine	C ₁₄ H ₃₁ N	214.2532	1.37	7.65	-	-	-
1-Hexenyl salicylate	C ₁₃ H ₁₆ O ₃	221.1172	-0.01	9.07	-	-	-
Tetradecanal	C ₁₄ H ₂₈ O	230.2481	1.16	7.69	-	-	-
2-Tetradecanone	C ₁₄ H ₂₈ O	230.2481	1.16	7.69	-	-	-
2-Phenylundecane	C ₁₇ H ₂₈	233.2269	2.17	12.22	-	-	-
3-Phenylundecane	C ₁₇ H ₂₈	233.2269	2.17	12.22	-	-	-
4-Phenylundecane	C ₁₇ H ₂₈	233.2269	2.17	12.22	-	-	-
5-Phenylundecane	C ₁₇ H ₂₈	233.2269	2.17	12.22	-	-	-
6-Phenylundecane	C ₁₇ H ₂₈	233.2269	2.17	12.22	-	-	-
2-Pentadecanone	C ₁₅ H ₃₀ O	244.2639	1.61	7.65	225.2216	-3.30	9.99
9-Hexadecenoic acid	C ₁₆ H ₃₀ O ₂	255.2321	1.08	7.97	253.2168	-1.94	10.25
a Hexadecadienol	C ₁₆ H ₃₀ O	256.2639	1.54	7.62	-	-	-
Hexadecanal	C ₁₆ H ₃₂ O	258.2795	1.55	7.59	-	-	-
2-Hexadecanone	C ₁₆ H ₃₂ O	258.2795	1.55	7.59	-	-	-
2-Phenyl dodecane	C ₁₈ H ₃₀	264.2688	0.73	12.22	-	-	-
5-Phenyl dodecane	C ₁₈ H ₃₀	264.2688	0.73	12.22	-	-	-
6-Phenyl dodecane	C ₁₈ H ₃₀	264.2688	0.73	12.22	-	-	-
9-Heptadecenoic acid	C ₁₇ H ₃₂ O ₂	269.2480	1.67	8.13	267.2325	-1.53	10.68
7-Hexadecenoic acid methyl ester	C ₁₇ H ₃₂ O ₂	269.2480	1.67	8.13	267.2325	-1.53	10.68
9-Hexadecenoic acid methyl ester	C ₁₇ H ₃₂ O ₂	269.2480	1.67	8.13	267.2325	-1.53	10.68
Androsta-4, 16-dien-3-one	C ₁₉ H ₂₆ O	271.2060	1.18	7.85	-	-	-
Androsta-5, 16-dien-3-one	C ₁₉ H ₂₆ O	271.2060	1.18	7.85	-	-	-

Table 5.5 continued

Compound Name	Formula	Positive mode			Negative mode		
		Detected <i>m/z</i>	Delta (ppm)	Actual RT	Detected <i>m/z</i>	Delta (ppm)	Actual RT
5 α -Androst-16-en-3-one	C ₁₉ H ₂₈ O	273.2216	1.08	7.40	-	-	-
Androsta-4-, 16-dien-3 α -ol	C ₁₉ H ₂₈ O	273.2216	1.08	7.40	-	-	-
5 α -Androsta-5-, 16-dien-3 β -ol	C ₁₉ H ₂₈ O	273.2216	1.08	7.40	-	-	-
Androsta-5-, 16-dien-3 α -ol	C ₁₉ H ₂₈ O	273.2216	1.08	7.40	-	-	-
Hexadecanoic acid	C ₁₆ H ₃₂ O ₂	274.2744	1.31	7.46	255.2324	-2.14	10.94
Methyl 9-methyltetradecanoate	C ₁₆ H ₃₂ O ₂	274.2744	1.31	7.46	255.2324	-2.14	10.94
Pentadecanoic acid methyl ester	C ₁₆ H ₃₂ O ₂	274.2744	1.31	7.46	255.2324	-2.14	10.94
Ethyl tetradecanoate	C ₁₆ H ₃₂ O ₂	274.2744	1.31	7.46	255.2324	-2.14	10.94
Oleic acid	C ₁₈ H ₃₄ O ₂	283.2634	0.96	8.33	281.2482	-1.55	11.10
1-Nonadecene	C ₁₉ H ₃₈	284.3315	1.18	8.46	-	-	-
Heptadecanoic acid	C ₁₇ H ₃₄ O ₂	288.2901	1.26	7.65	269.2482	-1.50	11.29
2-Methylhexadecanoic acid	C ₁₇ H ₃₄ O ₂	288.2901	1.26	7.65	269.2482	-1.50	11.29
Hexadecanoic acid methyl ester	C ₁₇ H ₃₄ O ₂	288.2901	1.26	7.65	269.2482	-1.50	11.29
Ethyl pentadecanoate	C ₁₇ H ₃₄ O ₂	288.2901	1.26	7.65	269.2482	-1.50	11.29
5 α -Dihydrotestosterone	C ₁₉ H ₃₀ O ₂	291.2319	0.26	9.56	-	-	-
Dodecyl benzoate	C ₁₉ H ₃₀ O ₂	291.2319	0.26	9.56	-	-	-
Cyclopentanetridecanoic acid methyl ester	C ₁₉ H ₃₆ O ₂	297.2791	0.93	8.56	295.2636	-2.28	11.69
Octadecanoic acid	C ₁₈ H ₃₆ O ₂	302.3059	1.73	7.82	283.2639	-1.41	12.18
Heptadecanoic acid methylester	C ₁₈ H ₃₆ O ₂	302.3059	1.73	7.82	283.2639	-1.41	12.18
Ethyl hexadecanoate	C ₁₈ H ₃₆ O ₂	302.3059	1.73	7.82	283.2639	-1.41	12.18
Dodecyl hexanoate	C ₁₈ H ₃₆ O ₂	302.3059	1.73	7.82	283.2639	-1.41	12.18
Decyl octanoate	C ₁₈ H ₃₆ O ₂	302.3059	1.73	7.82	283.2639	-1.41	12.18
Tridecyl benzoate	C ₂₀ H ₃₂ O ₂	305.2480	1.57	7.51	-	-	-
Isooctanedioldibutyrate	C ₁₆ H ₃₀ O ₄	309.2035	-0.55	9.81	285.2068	-1.21	7.09
Hexadecanoic acid isopropyl ester	C ₁₉ H ₃₈ O ₂	316.3215	1.57	8.01	-	-	-
Ethyl heptadecanoate	C ₁₉ H ₃₈ O ₂	316.3215	1.57	8.01	-	-	-
Propanedioic acid dimethyl ester	C ₅ H ₈ O ₄	-	-	-	114.0087	1.92	8.97
Methyl N,N-diethylthiocarbamate	C ₆ H ₁₃ NOS	-	-	-	146.0642	-2.15	6.44
10-Methyltridecanoic acid	C ₁₄ H ₂₈ O ₂	-	-	-	227.2011	-2.66	10.03
Tetradecanoic acid	C ₁₄ H ₂₈ O ₂	-	-	-	227.2011	-2.66	10.03
Dodecanoic acid	C ₁₄ H ₂₈ O ₂	-	-	-	227.2011	-2.66	10.03
Tridecanoic acid methyl ester	C ₁₄ H ₂₈ O ₂	-	-	-	227.2011	-2.66	10.03
9-Pentadecenoic acid	C ₁₅ H ₂₈ O ₂	-	-	-	239.2011	-2.33	9.86
Pentadecanoic acid	C ₁₅ H ₃₀ O ₂	-	-	-	241.2168	-2.29	10.45
n-Methyltetradecanoic acid	C ₁₅ H ₃₀ O ₂	-	-	-	241.2168	-2.29	10.45
Tetradecanoic acid methyl ester	C ₁₅ H ₃₀ O ₂	-	-	-	241.2168	-2.29	10.45
Isopropyl dodecanoate	C ₁₅ H ₃₀ O ₂	-	-	-	241.2168	-2.29	10.45
2-Ethylhexyl salicylate	C ₁₅ H ₂₂ O ₃	-	-	-	249.1492	-1.80	9.35
Dodecyl octanoate	C ₂₀ H ₄₀ O ₂	-	-	-	311.2955	-0.17	9.38
17-Oxo-5-androsten-3 α -yl sulfate	C ₁₉ H ₂₈ O ₅ S	-	-	-	367.1580	-1.30	7.86
17-Oxo-5 α -androstan-3 α -yl sulfate	C ₁₉ H ₃₀ O ₅ S	-	-	-	369.1736	-1.53	7.38

The associated error with respect to the tentative identities reported in Table 5.5 are generally less than 2 ppm, however, would need to be confirmed by authenticated standards. Moreover, the metabolites that were detected in both positive and negative mode report different retention times, thus, it is likely that another unknown metabolite has the same m/z ratio. No further identification can be made from the data collected.

The high mass accuracy (<5 ppm) of the Exactive instrument was exploited in order to use the accurate masses of parent ions for databases searches (see Section 5.3.12) in order to find tentative identities to the known unknown² metabolites. The result of these searches are summarised in Appendix C, in which 473 metabolites were putatively identified. This generally works well when the composition of biological fluid is well characterised (i.e. plasma). However, when analysing biological fluids where the composition is poorly known (i.e. apocrine sweat), highly variable or limited information is only available. As a result, only ~21% of the total extracted data from Sieve produced any potential matches. Furthermore, each of the searched m/z often produced several possible metabolites hits. This can be reduced by including restriction on the elemental composition i.e. C, H, O, N, S and P, hydrogen/carbon ratios, heuristic chemical structure and bonding rules and isotopic abundances, as discussed in Tobias Kind and Oliver Fiehn (Kind and Fiehn, 2007). However, the volume of unknown unknowns³ highlight the fact that LC-MS metabolite databases are currently lagging behind NMR and GC-MS, which is a view echoed by others (Williams *et al.*, 2005b). One approach in providing identities of these unknown unknowns is to use hyphenated techniques e.g. LC-NMR-MS.

5.4.1.3 Semi-Targeted analysis using LC-MS Survey Scanning

As mentioned previously, precursor ion survey scan coupled with EPI spectra has the potential to identify common structural moieties, such as amino acid conjugates. This

² Known unknown corresponds to metabolites that are known, but have not been formally identified in a biological mixture.

³ Unknown unknown corresponds to metabolites that are truly novel and have never been identified before.

is achieved by monitoring for a specific fragment; Gln (m/z 147), Cys (m/z 105), and Cys-Gly (m/z 179). Using precursor ion survey scan coupled with full product ion spectra, a number of known and unknown amino acid conjugates were detected. In order to provide tentative assignments to the unknowns, where standards were not available, a simple set of rules were followed. Firstly, the amino acid moiety is known, thus, the FA fragment can be calculated as the remainder of the m/z ratio. Secondly, from the literature (Appendix A) it is also known that the FA fragment contains no more than four oxygen elements, with the majority of reported structures containing two or three, and generally no nitrogen elements, thereby, eliminating a number of possible empirical formula. Finally, the chromatographic retention gives additional information on the polarity of the molecule. Since RP-LC is employed, it would be expected that shorter acyl chains would elute faster than longer acyl chains due to fewer interactions with stationary phase. Moreover, the increase in unsaturation results in reduced retention due to the *cis* double bonds reducing the overall surface area that can interact with the stationary phase.

Gln conjugates

HMHA-Gln and 3M2H-Gln eluted at 5.2, and 6.5 min respectively. These amino acid conjugates were identified on the basis of retention time and EPI spectra compared to reference standards, as illustrated in Figure 5.16 and Figure 5.17. Furthermore, a number of analytes were tentatively identified as Gln conjugates. Standards were not available to confirm identification for these unknowns. However, it is known that the Gln conjugates fragments into m/z 147, which can further fragment into m/z 130. Thus, this information can provide additional confidence that the detected unknowns are actually an amino acid conjugate and not another unknown metabolite that also produces a fragment of m/z 147. Table 5.6 summarises the main finding, with the evidence to support the identities given below.

Table 5.6 Summary of the potential odour precursors identified in human apocrine sweat by LC-MS/MS using PI scanning screening approach.

<i>m/z</i>	FA Fragment (<i>m/z</i>)	Retention Time (min)	Tentative Formula	Tentative Identity	Confidence
<i>Gln Conjugates</i>					
275	129	5.2	C ₇ H ₁₃ O ₂	HMHA-Gln	***
257	111	6.5	C ₇ H ₁₁ O	3M2H-Gln	***
289	142	6.2	C ₈ H ₁₅ O ₂	N- α -3-hydroxy-4-methylhept anoyl- L-glutamine / N- α -3-hydroxy- 3-methylhept-anoyl- L-glutamine	**
289	142	6.5	C ₈ H ₁₅ O ₂	N- α -3-hydroxy-4-methylhept anoyl- L-glutamine / N- α -3-hydroxy- 3-methylhept-anoyl- L-glutamine	**
289	142	8.5	C ₈ H ₁₅ O ₂	N- α -3-hydroxy-oct-anoyl- L-glutamine / N- α -8-hydroxy-oct-anoyl- L-glutamine	**
303	156	7.1	C ₉ H ₁₇ O ₂	N- α -3-hydroxy-3-methyloct anoyl- L-glutamine / N- α -3-hydroxy-4-methyloct anoyl- L-glutamine	**
285	138	7.5	C ₉ H ₁₅ O	N- α -4-methyl-3-oct-enoyl- L-glutamine	**
301	154	8.1	C ₁₀ H ₁₉ O	N- α -4-ethyl-oct-anoyl- L-glutamine	**
271	124	6.9	C ₈ H ₁₃ O	7-Octenoic acid	*
317	170	7.7	C ₁₀ H ₁₉ O ₂	3-Hydroxydecanoic acid / azelaic acid	*
299	152	7.9	C ₁₀ H ₁₇ O / C ₁₀ H ₁₇ O ₂	(Z/E)-4-Methylnon-3-enoic acid / 9-Decenoic acid	*
313	166	8.2	C ₁₁ H ₁₉ O / C ₁₀ H ₁₅ O ₂	10-Undecenoic acid	*
315	168	8.3	C ₁₁ H ₂₀ O / C ₁₀ H ₁₆ O ₂	2-Methyldecanoic acid / 4-Ethylnonanoic acid	*
329	182	8.7	C ₁₂ H ₂₃ O / C ₁₁ H ₁₉ O ₂	8-Methylundecanoic acid / 4-Ethyldecanoic acid /	*

Table 5.6 continued

<i>m/z</i>	FA Fragment (<i>m/z</i>)	Retention Time (min)	Tentative Formula	Tentative Identity	Confidence
357	210	9.07	C ₁₄ H ₂₇ O / C ₁₃ H ₂₃ O ₂	10-Methyltridecanoic acid / Tetradecanoic acid	*
311	165	1.4	C ₁₀ H ₁₃ O ₂	Unknown	
206	59	4.1	C ₃ H ₈ O	Unknown	
<i>Cys or Cys-Gly Conjugates</i>					
208	87	3.2	C ₃ H ₁₁ O	2M3H-Cys	***
293	115	5.05	C ₇ H ₁₅ O	3-Methyl-3-sulfanylhexan-1-ol	***
265	86	1.65	C ₅ H ₁₁ O	2-Methyl-3-sulfanylbutan-1-ol / 3-Sulfanylpentan-1-ol	**
279	100	3.6	C ₆ H ₁₃ O	3-Sulfanylhexan-1-ol	**
313	134	5.13	C ₉ H ₁₁ O	Unknown thiol	
307	128	5.37	C ₈ H ₁₇ O	Unknown thiol	
309	130	6.8	C ₈ H ₁₉ O	Unknown thiol	
310	131	6.9	C ₈ H ₂₁ O	Unknown thiol	
365	186	6.6	C ₁₂ H ₁₇ O	Unknown thiol	
358	179	6.8	C ₁₂ H ₂₀ O	Unknown thiol	
375	196	7.6	C ₁₃ H ₂₅ O	Unknown thiol	
387	265	8.09	C ₁₈ H ₃₃ O	Unknown thiol	
295	116	9.5	C ₇ H ₁₇ O	Unknown thiol	

There are four potential matches where the pseudomolecular ion corresponds to an amino acid conjugate that has been reported in the literature (see Appendix A). Firstly, unknown m/z 289, which has three chromatographic peaks at retention times of 6.2, 6.5, and 8.5 min (Figure 5.18). The FA fragment is expected to have an m/z 142 which is likely to have the formula of $C_8H_{15}O_2$. There are four ions of m/z 289 that have been reported in the literature; N- α -3-hydroxy-4-methylhept anoyl- L-glutamine, N- α -3-hydroxy- 3-methylhept-anoyl- L-glutamine, N- α -3-hydroxy-oct-anoyl- L-glutamine, and N- α -8-hydroxy-oct-anoyl- L-glutamine (Natsch *et al.*, 2006). The former two conjugates would be considered the most likely candidates for the retention time of 6.2 and 6.5 min with N- α -3-hydroxy-4-methylhept anoyl- L-glutamine being slightly more retained. Where, N- α -3-hydroxy-oct-anoyl- L-glutamine would be the most likely candidate for the peak that elutes at 8.5 min.

Secondly, unknown m/z 303 has a retention time of 7.1 min (Figure 5.19). The FA fragment is expected to have an m/z 156 which is likely to have the formula of $C_9H_{17}O_2$. There are four ions of m/z 303 that have been reported in the literature; N- α -3-hydroxy-3-methyloct anoyl- L-glutamine, N- α -3-hydroxy-4-methyloct anoyl- L-glutamine, N- α -7-carboxy-hept-anoyl- L-glutamine, and N- α -9-hydroxy- non-anoyl- L-glutamine (Natsch *et al.*, 2006). Out of these reported metabolites, it would be expected the former two would be most likely candidate as the later two would be considered to be more polar. On closer inspection of the extracted precursor ion chromatogram, there are two closely eluting peaks which further suggest that N- α -3-hydroxy-3-methyloct anoyl- L-glutamine and N- α -3-hydroxy-4-methyloct anoyl- L-glutamine, with the later eluting later, as the most probable candidate.

Thirdly, unknown m/z 285 has a retention time of 7.5 min (Figure 5.20). The FA fragment is expected to have an m/z 138 which is likely to have the formula of $C_9H_{15}O$. There is only one reported match in the literature, thus, is tentatively assigned as N- α -4-methyl-3-oct-enoyl- L-glutamine, with the FA being (E)-4-Methyloct-3-enoic acid (Natsch *et al.*, 2006).

Finally, unknown m/z 301 eluted at 8.1 min (Figure 5.21). The FA fragment is expected to have an m/z 154 which is likely to have the formula of $C_{10}H_{19}O$. There is

one reported match in the literature, thus, is tentatively assigned as N- α -4-ethyl-octanoyl- L-glutamine, with the FA being 4-ethyloctanoic acid (Natsch *et al.*, 2006).

There were also a number of possible conjugates that have no potential match within the reported literature. However, the calculated FA fragments in most cases do match VFA that has been detected in apocrine sweat from the literature (see Appendix A). These are all summarised in below.

- Unknown m/z 271 has a retention time of 6.9 min (Figure 5.22). The FA fragment is expected to have an m/z 124 which is likely to have the formula of $C_8H_{13}O$.
- Unknown m/z 317 has a retention time of 7.7 min (Figure 5.23). The FA fragment is expected to have an m/z 170 which is likely to have the formula of $C_{10}H_{19}O_2$.
- Unknown m/z 299 has a retention time of 7.9 min (Figure 5.24). The FA fragment is expected to have an m/z 152 which is likely to have the formula of $C_{10}H_{17}O$ or $C_9H_{13}O_2$.
- Unknown m/z 313 has a retention time of 8.2 min (Figure 5.25). The FA fragment is expected to have an m/z 166 which is likely to have the formula of $C_{10}H_{15}O_2$ or $C_{11}H_{19}O$.
- Unknown m/z 329 has a retention time of 8.7 min (Figure 5.26). The FA fragment is expected to have an m/z 182 which is likely to have the formula of $C_{12}H_{23}O$ or $C_{11}H_{19}O_2$.
- Unknown m/z 357 has a retention time of 9.07 min (Figure 5.27). The FA fragment is expected to have an m/z 210 which is likely to have the formula of $C_{14}H_{27}O$ or $C_{13}H_{23}O_2$.

Unknown m/z 311 has a retention time of 1.40 min (Figure 5.28). The FA fragment is expected to have an m/z 165 which is likely to have the formula of $C_{10}H_{13}O_2$. However, with this size fragment you would expect the analyte to elute a lot later. Also, there is no m/z 130 peak present. Thus, it is likely that this metabolite is a false positive.

Unknown m/z 206 has a retention time of 4.1 min (Figure 5.29). The FA fragment is expected to have an m/z 59 which is likely to have the formula of C_3H_8O . Again there is no peak at m/z 130, thus, expected to be a false positive.

Cys or Cys-Gly conjugates

2M3H-Cys and 3M3SH-Cys-Gly eluted at 3.2 and 5.08 min respectively. These amino acid conjugates were identified on the basis of retention time and EPI spectra compared to reference standard, as illustrated in Figure 5.30 and Figure 5.31. Furthermore, a number of analytes were tentatively identified as Cys-Gly conjugates. Standards were not available to confirm identification for these unknowns, thus, tentative assignment was based upon characteristic product ions observed in the EPI spectra of the 3M3SH-Cys-Gly conjugate. It is known from the 3M3SH-Cys-Gly standard that the fragmentation pattern produces common product ions of m/z 179, 162, and 144 which are characteristic fragments of the Cys-Gly residue. Thus, it is reasonable to suggest that any other Cys-Gly conjugate would contain the same product ions. Table 5.6 summarises the main finding, with the evidence to support the identities given below.

There are two potential matches where an unknown pseudomolecular ion corresponds to an amino acid conjugate previously reported in the literature (see Appendix A). Firstly, an unknown m/z 265 eluted at 1.65 min (Figure 5.32). The FA fragment is expected to have an m/z 86 which is likely to have the formula of $C_5H_{11}O$. If this fragment is a thiol then it could be tentatively assigned to 3-sulfanylpentan-1-ol or 2-methyl-3-sulfanylbutan-1-ol. Secondly, an unknown m/z 279 has a retention time of 3.3 min (Figure 5.33). The FA fragment is expected to have an m/z 100 which is likely to have the formula of $C_6H_{13}O$. This thiol containing compound could be tentatively assigned to 3-sulfanylhexas-1-ol. Another addition of CH_2 group would result in 3M3SH-Cys-Gly conjugate which elutes at 5.08 min (Figure 5.31). The addition of each CH_2 group would result in a stronger retention due to the metabolite becoming less polar. This chromatographic behaviour is consistent with other metabolites that have been reported on RP systems, for example; homoserine lactones had a predictable increase in retention with increasing acyl chain length (Ortori *et al.*, 2007).

There were also a number of possible conjugates that have no potential match within the reported literature. However, the assumption would be that the non-amino acid fragment would presumably be a thiol.

- Unknown m/z 313 has a retention time of 5.13 min (Figure 5.34). The FA fragment is expected to have an m/z 134 which is likely to have the formula of $C_9H_{11}O$. The increase in retention due to increasing the carbon length is offset by the presence of double bonds, which reduce the retention time compared to their corresponding linear isomers, due to the overall surface area being reduced.
- Unknown m/z 307, 309, and 310 has a retention time of 5.37, 6.8, and 6.9 min respectively. As depicted in Figure 5.35, Figure 5.36 and Figure 5.37, these unknown metabolites have fragments higher than the pseudomolecular ion. This could be a result of being multiple charged, where that resultant fragments also fragments into common product ions being monitored. The resolution of this work is not sufficient to be able to distinguish multiple charged species by using isotope distribution of C^{12}/C^{13} . However, for a doubly charged species you would expect the isotope cluster to be half an amu apart (Hoffmann and Stroobant, 2001). The FA fragment is expected to have an m/z ~128 which is likely to have a formula of $C_8H_{16}O$.
- Unknown m/z 365 has a retention time of 6.6 min (Figure 5.38). The FA fragment is expected to have an m/z 186 which is likely to have the formula of $C_{12}H_{27}O$.
- Unknown m/z 358 has a retention time of 6.8 min (Figure 5.39). The FA fragment is expected to have an m/z 186 which is likely to have the formula of $C_{12}H_{20}O$.
- Unknown m/z 375 has a retention time of 7.6 min (Figure 5.40). The FA fragment is expected to have an m/z 196 which is likely to have the formula of $C_{13}H_{25}O$.

- Unknown m/z 295 has a retention time of 9.5 min (Figure 5.41). The FA fragment is expected to have an m/z 196 which is likely to have the formula of $C_7H_{17}O$.

5.4.1.4 RP-LC-MS/MS Multiple Reaction Monitoring for Targeted Analysis of Odour Precursors in Human Apocrine Sweat Secretions

Targeted MRM analysis requires prior knowledge of the metabolites of interest. Ideally, the CE and DP need to be optimised for each metabolite in order to obtain maximum sensitivity for the transition which is being monitored. However, due to the limited availability of standards, this could not be optimised for all the amino acid conjugates that have been reported in the literature (see Appendix A). Since all the reported odour precursors have a common structure (amino acid moiety), it is reasonable to suggest that these reported amino acid conjugates would fragment in a similar way, thereby, leaving the amino acid residue to be monitored. In comparison to precursor ion survey scanning, this approach is considered to be more sensitive, as the spectrometer is no longer scanning, since Q1 and Q3 are fixed, thus, allowing the spectrometer to monitor the precursor and fragment ions over longer times (Hoffmann and Stroobant, 2001).

As previously stated, 14 mass transitions were monitored for the analysis of odour precursors present in human apocrine sweat samples. This was based on predictions of the MRM transition, for all the reported amino acid conjugates in literature, to which standards were not available. A representative total ion chromatogram is depicted in Figure 5.4. A number of analytes were tentatively identified as amino acid conjugates as summarised in Table 5.7. As mentioned previously, standards were not available to confirm identification for these unknowns.

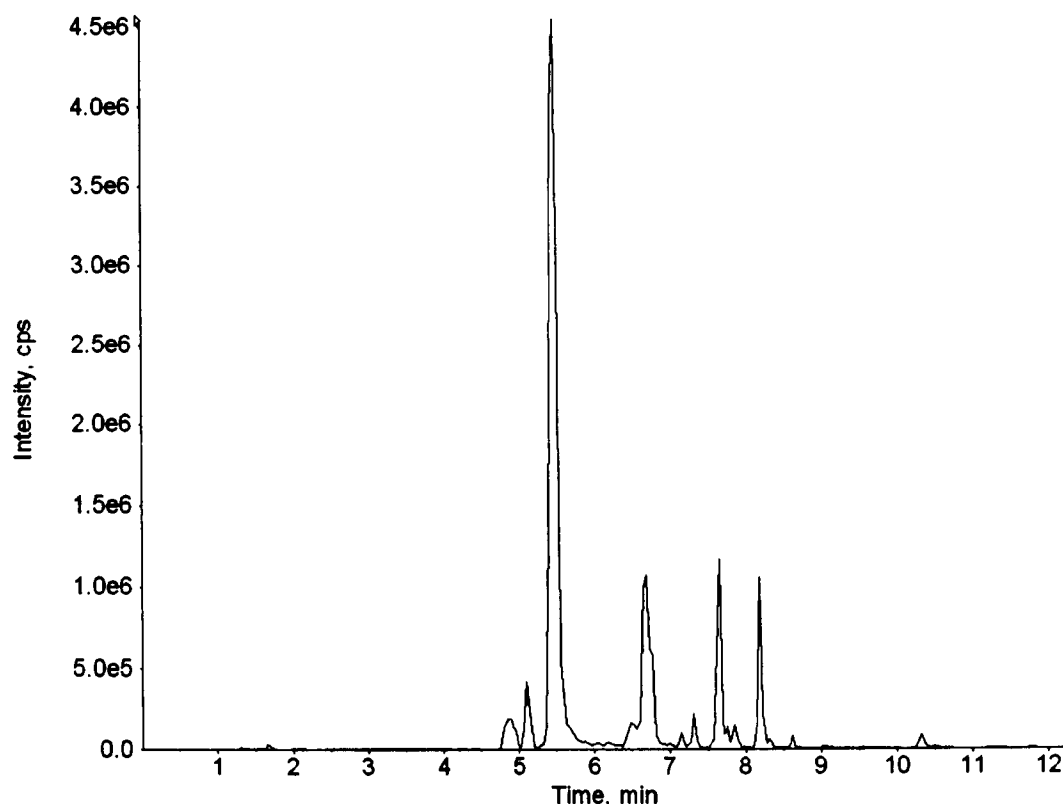


Figure 5.4 HPLC-MS/MS total ion chromatogram of a representative human apocrine sweat sample in MRM mode.

Table 5.7 Summary of the potential odour precursors identified in human apocrine sweat by LC-MS/MS using MRM.

<i>m/z</i>	% Peak Area	Retention Time (min)	Tentative Identity	Confidence
<i>Gln conjugates</i>				
257/147	11.40	6.5	N- α -3-methylhex-2-enoyl-L-glutamine	***
275/147	72.08	5.2	N- α -3-hydroxy-3-methylhexanoyl- L-glutamine	***
289/147	5.39	6.5	N- α -3-hydroxy-4-methylhept anoyl- L-glutamine	**
303/147	1.28	7.3	N- α -3-hydroxy-3-methyloct anoyl- L-glutamine	**
285/147	1.97	7.5	N- α -4-methyl-3-oct-enoyl- L-glutamine	**
301/147	0.52	8.2	N- α -4-ethyl-oct-anoyl- L-glutamine	**
287/147	0.30	7.9	N- α -4-ethyl-hept-anoyl- L-glutamine	**
259/147	0.36	6.6	N- α -3-methyl-2-oxopent-anoyl- L-glutamine	
<i>Cys or Cys-Gly conjugates</i>				
208/105	0.37	3.2	S-[1-(2-hydroxy-1-methylethyl)-ethyl]-L-cysteine	***
293/179	6.21	5.1	S-[1-(2-hydroxyethyl)-1-methylbutyl]-L-cysteinylglycine	***
279/179	0.03	4.7	S-[1-(2-hydroxyethyl)-butyl]-L-cysteinylglycine	**
236/105	0.10	5.4	S-[1-(2-hydroxyethyl)-1-methylbutyl]-L-cystein	

2M3H-Cys, 3M3SH-Cys-Gly, HMHA-Gln and 3M2H-Gln have retention times of 3.2, 5.0, 5.2, and 6.5 min respectively. These conjugates were identified on the basis of retention time and EPI spectra compared to reference standards, as noted above. While screening for the known amino acid conjugates from the literature in MRM mode, potentially, three additional conjugates were also detected that were not detected/present in the PI scanning mode. Firstly, the transition m/z 287/147 resulted in a peak that eluted at 7.9 min (Figure 5.5). This has been tentatively assigned to N- α -4-ethyl-hept-anoyl- L-glutamine which was also detected with the UPLC-Orbitrap-MS (Table 5.4). Secondly, the transition m/z 259/147 resulted in a peak that eluted at 6.6 min (Figure 5.6 A). This has been tentatively assigned to N- α -3-methyl-2-oxopent-anoyl- L-glutamine. Finally, the transition m/z 236/105 resulted in a peak that eluted at 5.4 min (Figure 5.6 B). This has been tentatively assigned to N- α -3-methyl-2-oxopent-anoyl- L-glutamine. EPI spectra were not obtained for the latter two metabolites, due to the low concentration, thus, no further evidence can suggest if these metabolite are amino acid conjugates. Evidence for the tentative identification of m/z 289, 303, 285, 301 and 279 were discussed above. Furthermore, it is also evident that the two most intense peaks are HMHA-Gln and 3M2H-Gln conjugates.

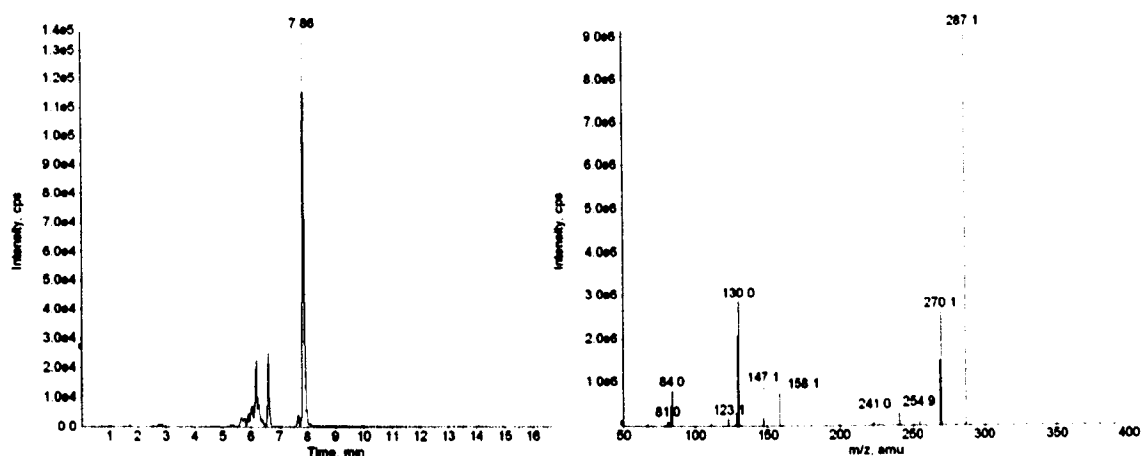


Figure 5.5 Extracted ion chromatogram from the MRM transition m/z 287/147 and EPI spectrum of the peak at 7.6 min.

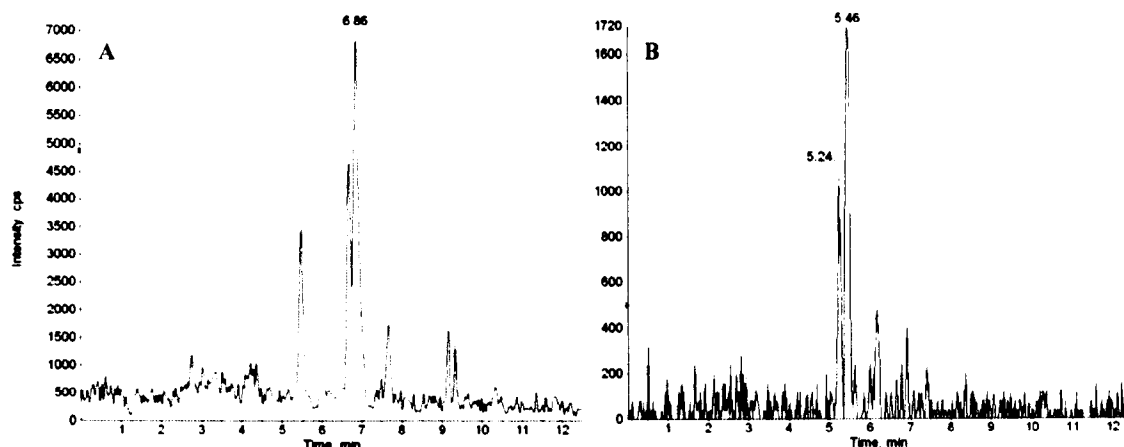


Figure 5.6 Extracted ion chromatogram from the MRM transition **A** m/z 259/147 and **B** m/z 236/105. No EPI spectra were obtained for these metabolites.

Summary of identification of small molecules compounds of human apocrine sweat.

To my knowledge, this is the first time NMR spectroscopy has been applied to human axillary secretions in which 25 metabolites were readily identified and quantified. Furthermore, identification of metabolites detected by NMR was aided by the large body of information already available on human biological fluids. While the detection of biomarkers was facile in regards to the LC-MS methodologies, the process of identification however is more demanding, due in part to the limited database available. Both global methodologies were able to detect 9 amino acid conjugates which were confirmed by a targeted MS/MS approach. The precursor ion survey scanning approach has successfully identified four amino acid conjugates present the human apocrine sweat secretions, for which standards were available and tentatively identified 26 other amino acid conjugates. Further identification of these unknown metabolites is not possible with the data presented here; all that can be hypothesized is that these are likely to be a Gln, Cys, or Cys-Gly conjugate. There is no evidence in the literature to support the presence or identity of these analytes. Moreover, this method is not selective towards the detection of amino acid conjugates alone due to prevalence of other endogenous metabolites which could produce similar fragments, thereby highlighting the limitations of this methodology.

5.4.2 Study of Temporal, Inter- and Intra-Individual Differences in Human Axillary Secretions

5.4.2.1 Inter- and Intra-Individual Differences

Visual comparison of this type of data, from both NMR spectroscopy and LC-MS data-sets could be performed, however, such analysis would be tedious, inefficient and prone to subjective error. Thus, multivariate analysis such as PCA (unsupervised) and PC-DA (supervised) were applied to all the NMR and global LC-MS (QTOF and Exactive) data-sets obtained from the apocrine sweat samples. Both mean centred and UV scaling lead to a similar degree of separation between the six classes, thus, only UV scaled models will be shown as a representative example. The PCA model (UV scaled) obtained from the NMR data resulted in R^2X (cum) of 0.354 using two PCs, where PC1 and 2 explained 21.3% and 14.1% of the total variation, respectively, as depicted in Figure 5.7. The HILIC-MS PCA model (UV scaled) resulted in R^2X (cum) of 0.275 using two PCs, where PC1 and 2 explained 17.8% and 9.6% of the total variation, respectively, as depicted in Figure 5.8. PCA model (UV scaled) obtained from the Exactive data in positive mode resulted in R^2X (cum) of 0.467 using two PCs, where PC1 and 2 explained 29.3% and 17.4% of the total variation, respectively. The negative mode PCA model (UV scaled) resulted in R^2X (cum) of 0.554 using two PCs, where PC1 and 2 explained 35.6% and 19.7% of the total variation, respectively, as depicted in Figure 5.9.

These global methodologies provided complementary information to one another as inter-person variation is clearly evident across all PCA models. As would be expected, PC-DA further improved the separation between each individual (data not shown). It is also evident that the clustering between the intra-individual variations in the PCA model obtained from the negative electrospray data are more closely defined compared to that of the NMR or MS positive mode data. This is likely to be due to the main differences between groups being metabolites that are only observed in negative mode.

The ten amino acid conjugates that were identified or tentatively identified confidently (indicated with two or more stars in Table 5.7) also provided complementary evidence to the global methodologies. Figure 5.10 illustrates the inter-volunteer variation across day one, which is a representative example across all days. The inter-person variation of the amino acid conjugates is consistent with other biological fluids, due to variation in genetic profiles as well as environmental life styles. However, it is evident that HMHA-Gln conjugate (m/z 275) is the most dominant peak, which is consistent across all volunteers, while 2M3H-Cys conjugate (m/z 208) is predominantly weak. 3M2H-Gln conjugate (m/z 257) remains relatively consistent across all samples, with slightly more produced for volunteer two. 3M3SH-Cys-Gly conjugate (m/z 293) was the most variable between each volunteer, with a higher concentration produced in volunteer two compared to the least produced in volunteer five.

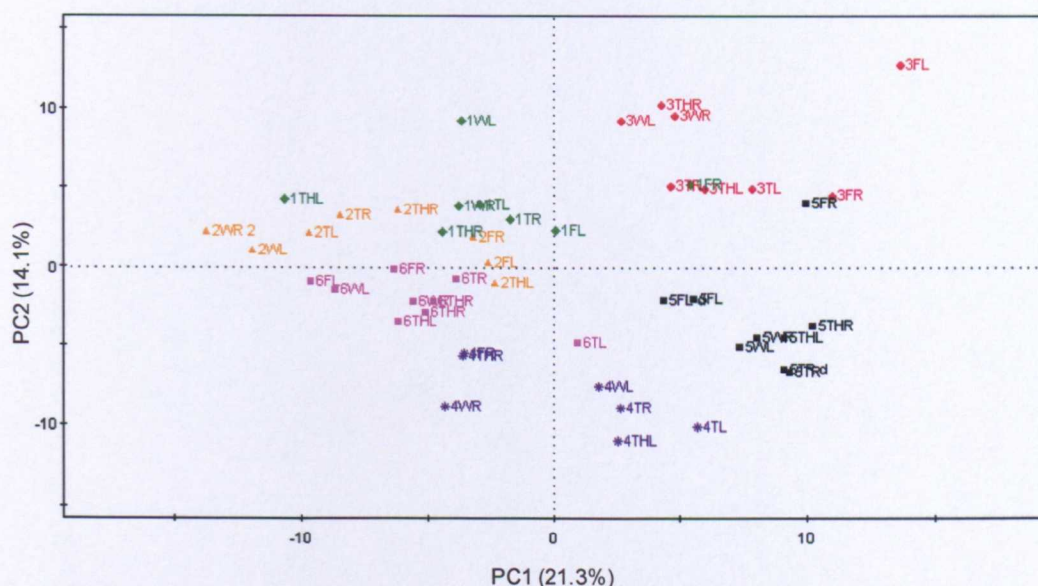


Figure 5.7 PCA score plot (UV scaled) of human apocrine sweat samples analysed by NMR spectroscopy of six healthy male volunteers (left and right axillae measured separately) across four days. Key:- Coloured by subject, T – day 1, W – day 2, TH – day 3, F – day 4 and L or R indicate the side which was sampled.

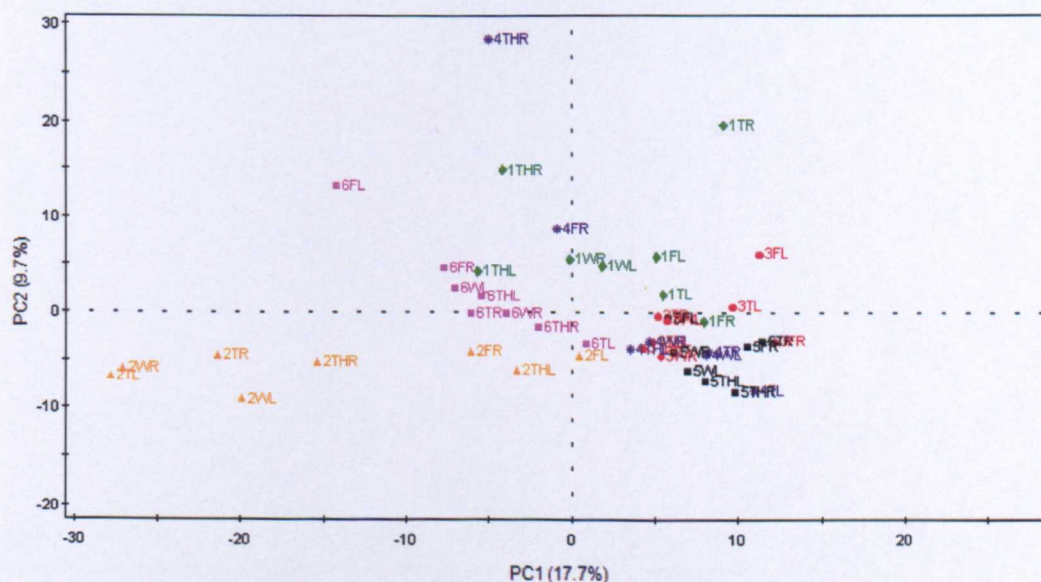
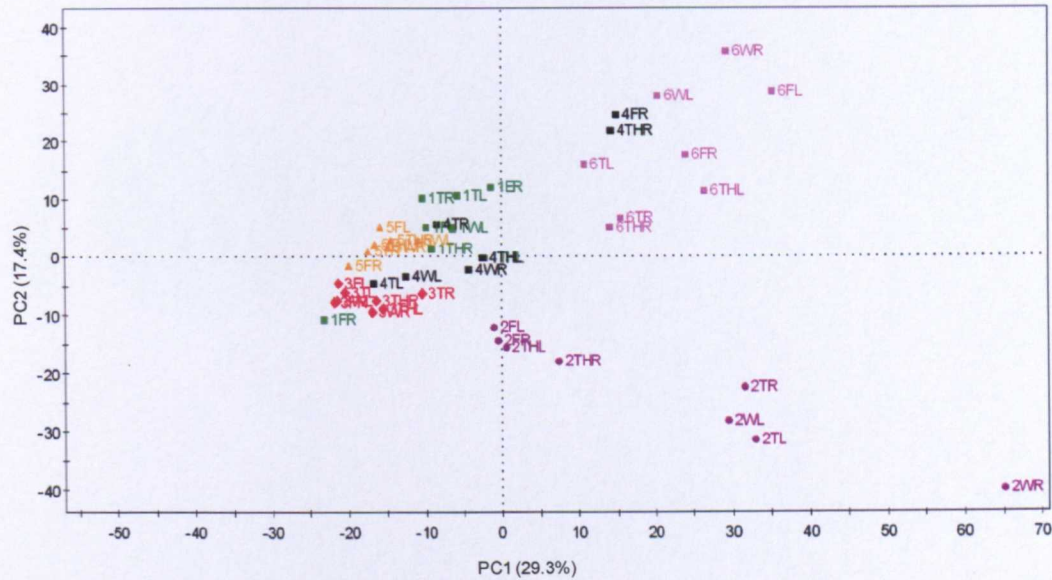


Figure 5.8 PCA score plot (UV scaled) of human apocrine sweat samples analysed by HILIC-MS of six healthy male volunteers (left and right axillae measured separately) across four days. Key:- Coloured by subject, T – day 1, W – day 2, TH – day 3, F – day 4 and L or R indicate the side which was sampled.

A



B

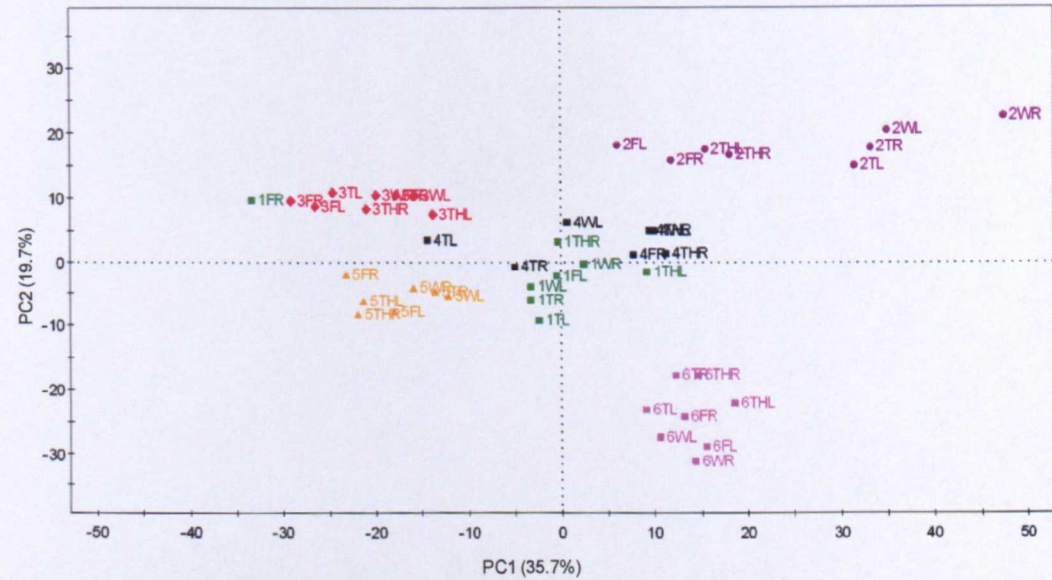


Figure 5.9 PCA score plot (UV scaled) of human apocrine sweat samples analysed by UPLC-MS of six healthy male volunteers (left and right axillae measured separately) across four days. **A** Positive mode data, **B** negative mode data. Key:- Coloured by subject, T – day 1, W – day 2, TH – day 3, F – day 4 and L or R indicate the side which was sampled.



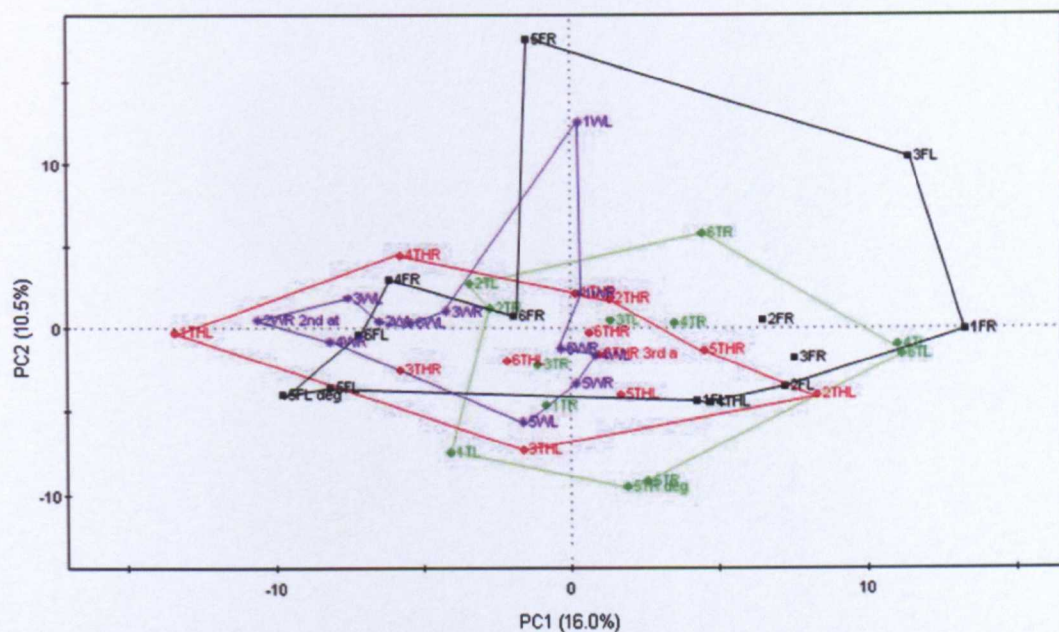
Figure 5.10 Summarises the intra-subject variation across day one using the data on amino acid conjugated obtained by targeted LC-MS/MS analysis of study samples.

5.4.2.2 Inter-Day Differences

To assess whether there is any inter-day variation from sample collection or to identify whether the sweat produced is constant across the four days; the data was mean centred per individual. This effectively minimises the dominant inter-person variation from the model, so only intra-person variation or time trends will influence the separation in the model. Both mean centring per person and UV scaling per person lead to a similar degree of separation between the four classes for all analytical methodologies, thus, only UV scaled models from NMR and LC-MS will be shown as a representative example. The PCA models from the first two PCs account for 26.6% and 44.8% of the total variation, obtained from the NMR and Exactive data respectively. PCA of the apocrine sweat profiles did not display intrinsic clustering related to sample collection as depicted in Figure 5.11.

The ten amino acid conjugates (indicated with two or more stars in Table 5.7) were selected in order to identify the degree of inter-day variation across all volunteers. As depicted in Figure 5.12, there is little difference between the 24 h time points of sample collection. This is consistent with the above finding from both the global NMR and MS data as well as the work published by Leydon and co-workers (Leyden *et al.*, 1981). However, intra-volunteer difference across each day was observed for all amino acid conjugates. A representative example is shown in Figure 5.13, highlighting a gross inter-day effect for all amino acid conjugates. This gross effect was observed for all volunteers, however, the actual inter-day levels varied between each volunteer. Thus, the observed change is attributed to a concentration effect arising from how the sample was collected or how much sweat was secreted rather than inter-day effect, as the relative proportions remain consistent across all metabolites.

A



B

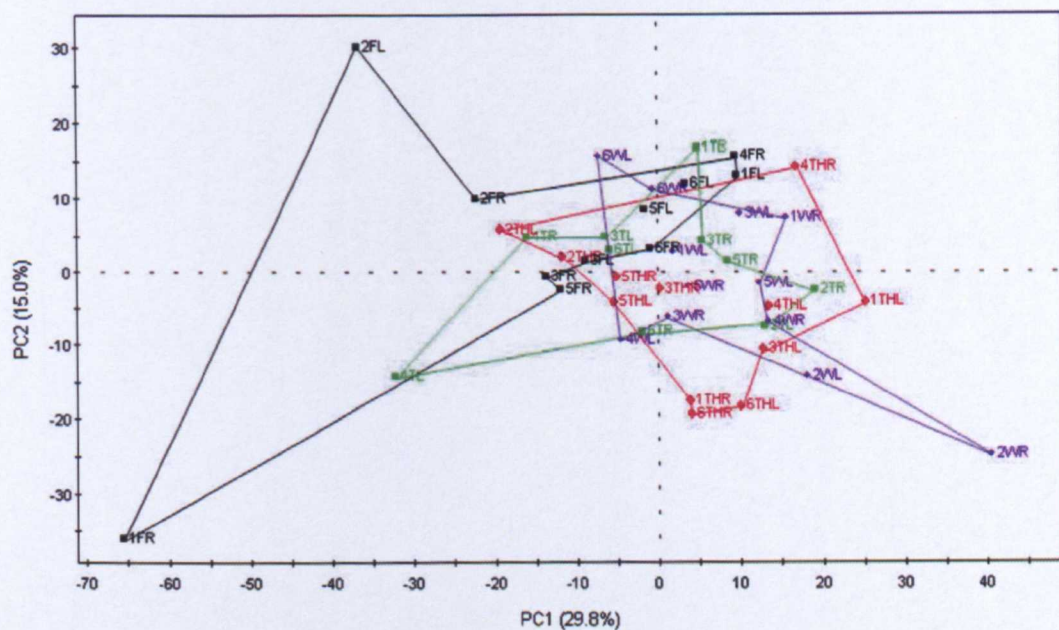


Figure 5.11 PCA scores plot (UV scaled per person) of human apocrine sweat samples analysed by **A** NMR spectroscopy **B** UPLC-MS negative mode, of six healthy male volunteers (left and right axillae measured separately) across four days. Coloured to show day to day differences, green – day 1, purple – day 2, red – day 3 and black day 4.

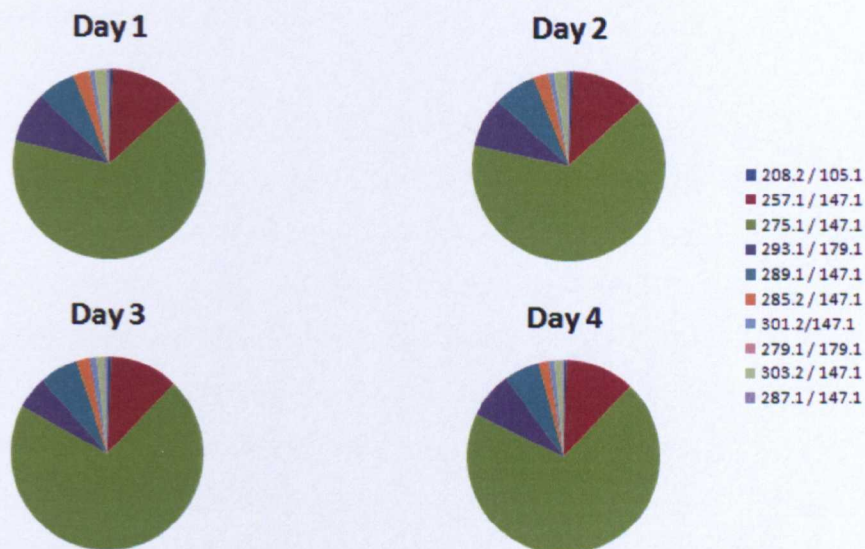


Figure 5.12 Pie charts illustrating the average inter-day variation of the targeted amino acid conjugates (LC-MS/MS), with each day representing a 24 h time point.

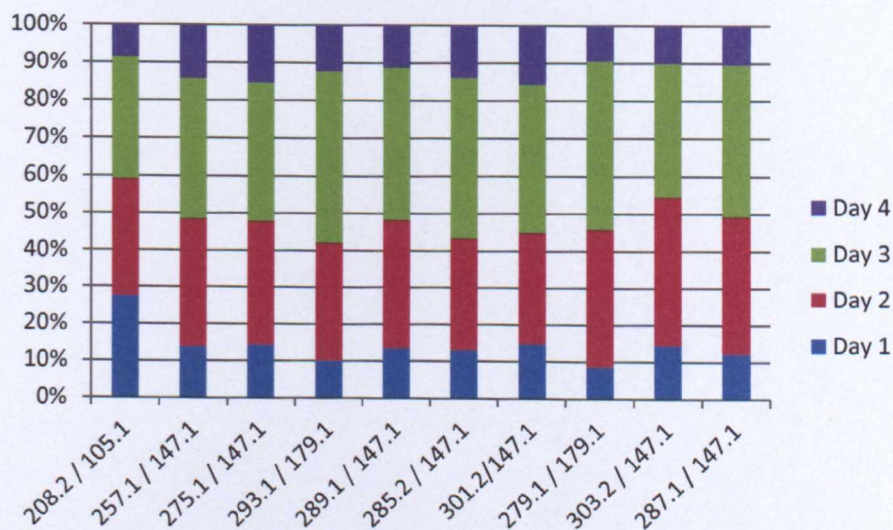
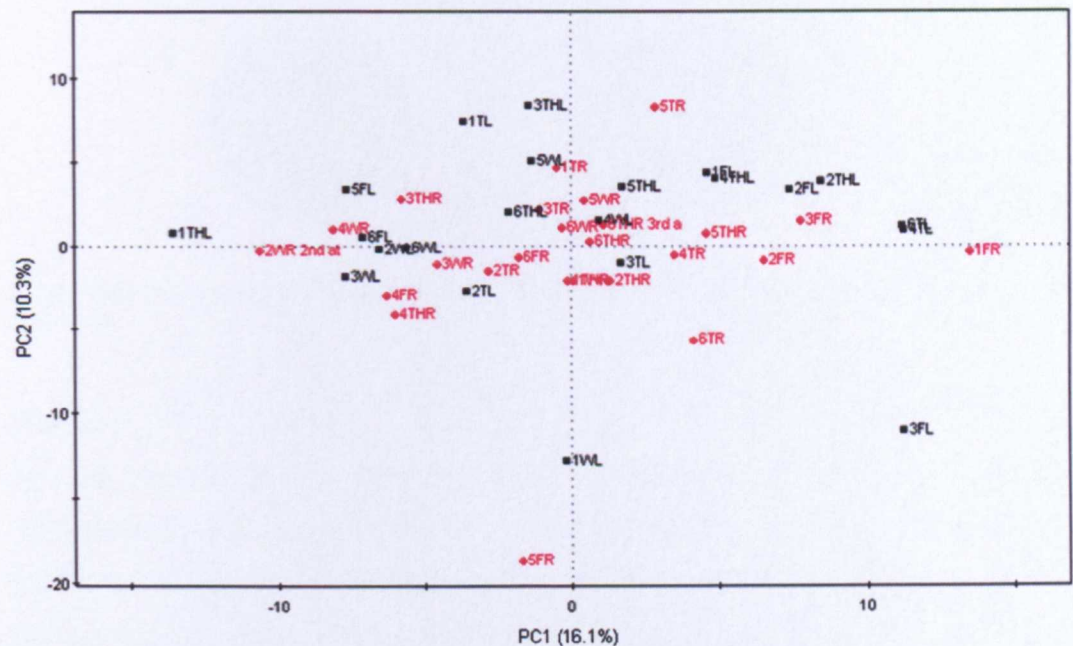


Figure 5.13 Summarises the intra-day variation of each amino acid conjugate, with each day representing a 24 h time point, obtained from volunteer one.

5.4.2.3 Left and Right Arm Differences

To assess whether there are any side related differences between the left and right axilla, the data was mean centred per person as discussed previously (Section 5.4.2.2). Both mean centring per person and UV scaled per person lead to a similar degree of separation between the two classes for all analytical methodologies, thus, only UV scaled models from NMR and LC-MS will be shown as a representative example. The PCA models from the first two PCs account for 26.6% and 44.8% of the total variation obtained from the NMR and Exactive data respectively. PCA of the apocrine sweat profiles did not display any side related differences as depicted in Figure 5.14. Furthermore, the data obtained from the targeted analysis was consistent with the above finding from both the global NMR and LC-MS data, as depicted in Figure 5.15. All identified amino acid conjugates (indicated with two or more stars in Table 5.7) were secreted in equal quantities in both the left and right arm across each day.

A



B

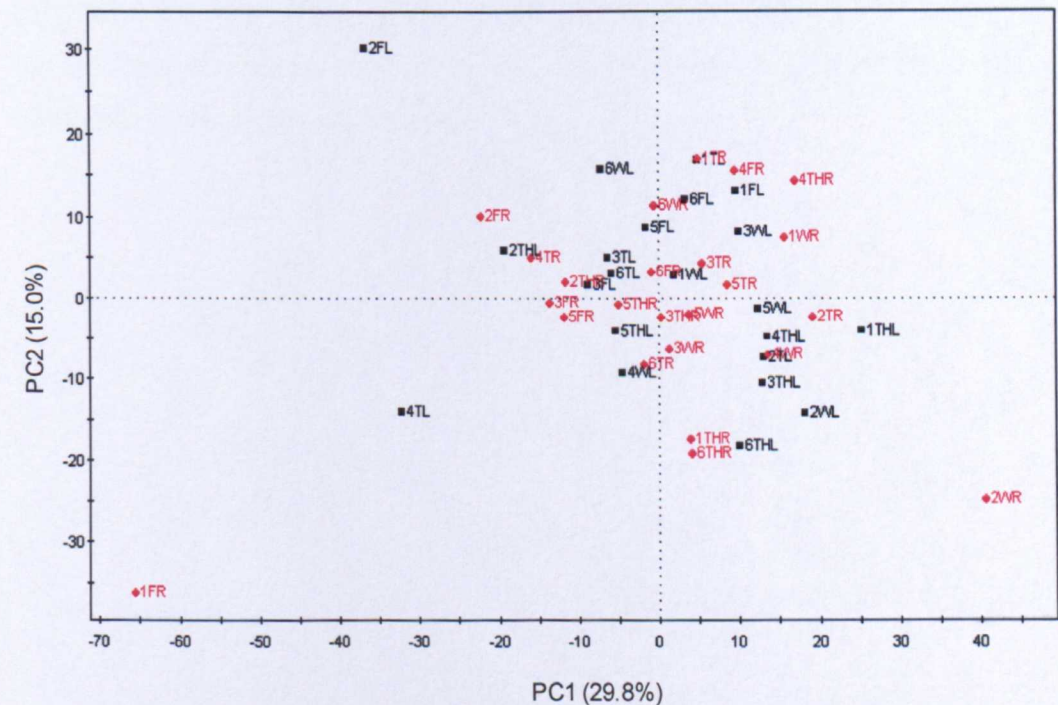


Figure 5.14 PCA scores plot (UV scaled per person) of human apocrine sweat samples analysed by **A** NMR spectroscopy **B** UPLC-MS negative mode of six healthy male volunteers (left and right axillae measured separately) across four days. Coloured to highlight the difference between left (red) and right (black) axilla.

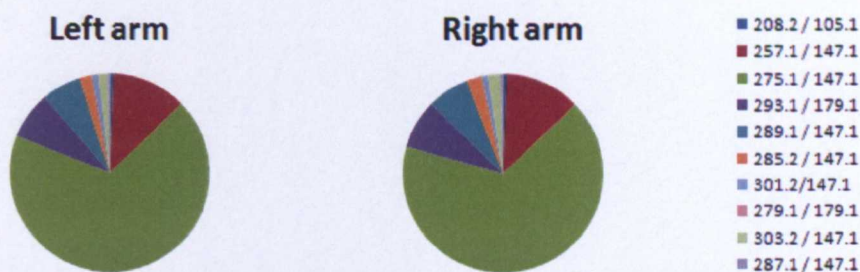


Figure 5.15 Pie chart illustrating the relative difference between the left and right arm across all volunteers.

Summary

All the analytical methodologies were capable of detecting inter-individual differences in the axillary sweat metabolic profile. Furthermore, each technique (NMR, LC-MS, and LC-MS/MS) showed that there was minimal inter-day variation and that the composition of the apocrine sweat produced from left and right axilla was consistent with one another. Thus, all techniques used herein provided complementary information, as discrimination by ^1H NMR and LC-MS was based on different sets of markers, especially in the case of the targeted approach where only ten metabolites were selected for analysis.

Gln conjugates

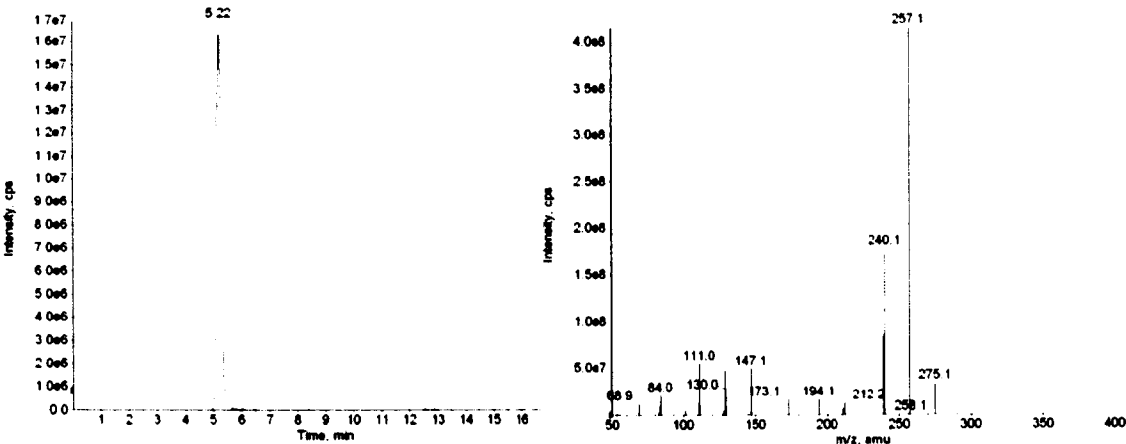


Figure 5.16 Extracted ion chromatogram of m/z 275 and EPI spectrum of the peak at 5.2 min from an EPI triggered PI scan of m/z 147.

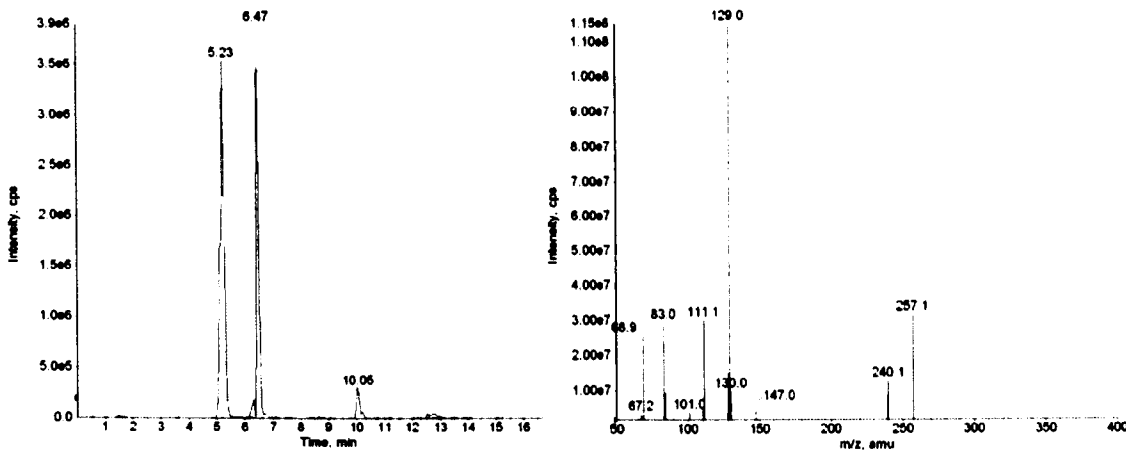


Figure 5.17 Extracted ion chromatogram of m/z 257 and EPI spectrum of the peak at 6.4 min from an EPI triggered PI scan of m/z 147.

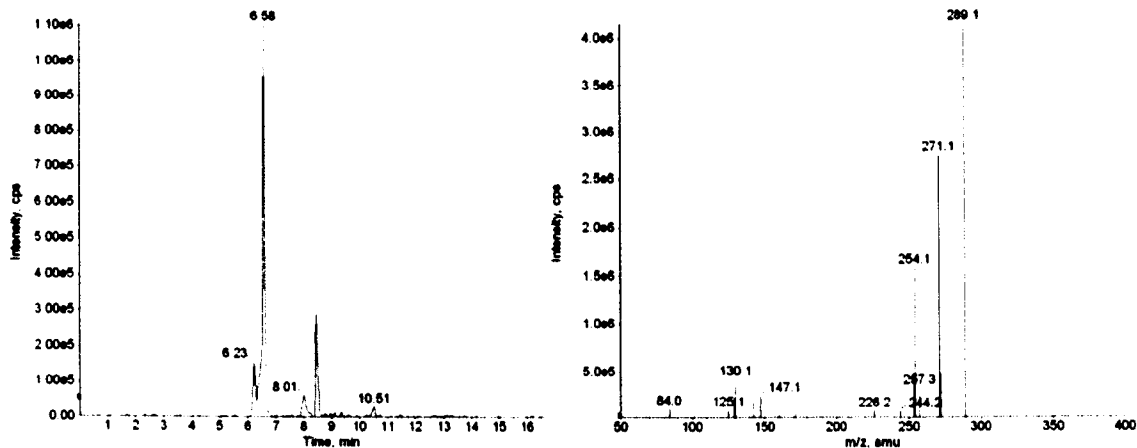


Figure 5.18 Extracted ion chromatogram of m/z 289 and EPI spectrum of the peak at 6.5 min from an EPI triggered PI scan of m/z 147.

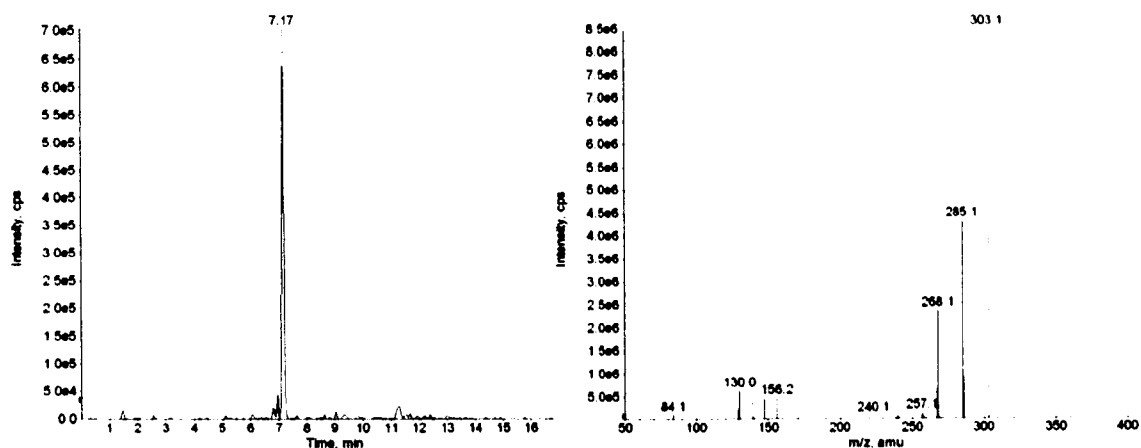


Figure 5.19 Extracted ion chromatogram of m/z 303 and EPI spectrum of the peak at 7.1 min from an EPI triggered PI scan of m/z 147.

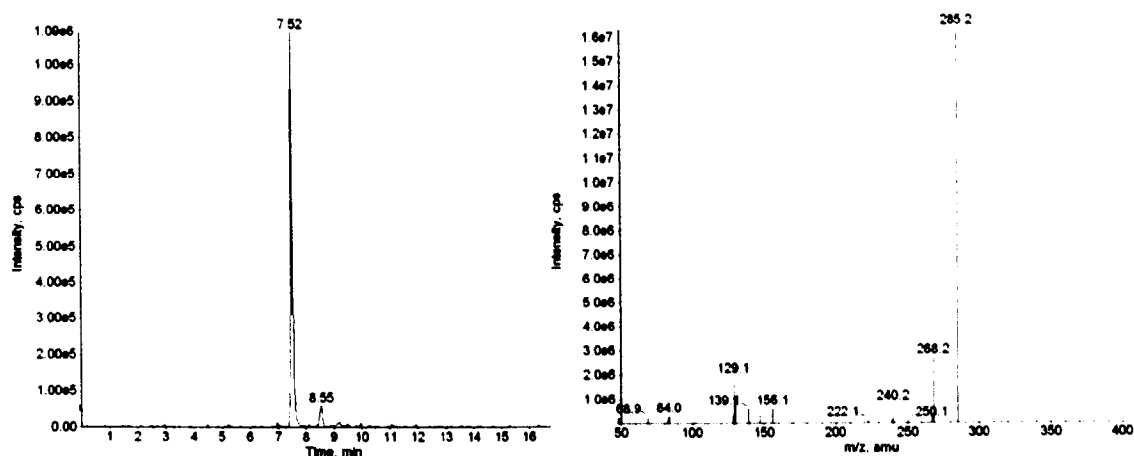


Figure 5.20 Extracted ion chromatogram of m/z 285 and EPI spectrum of the peak at 7.5 min from an EPI triggered PI scan of m/z 147.

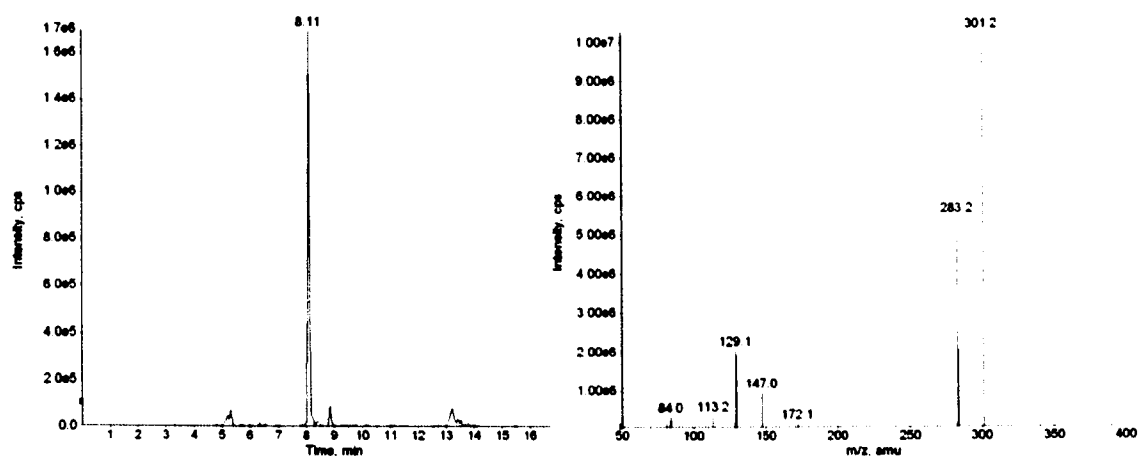


Figure 5.21 Extracted ion chromatogram of m/z 301 and EPI spectrum of the peak at 8.1 min from an EPI triggered PI scan of m/z 147.

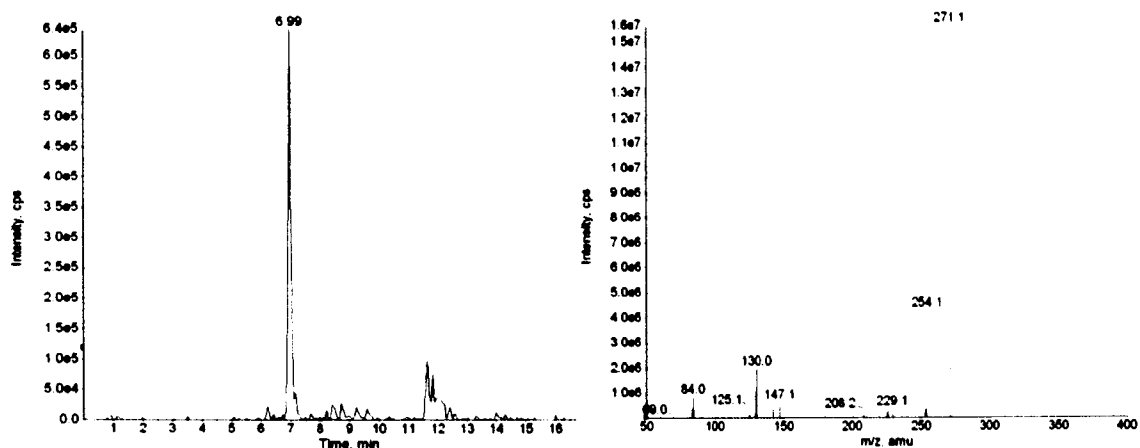


Figure 5.22 Extracted ion chromatogram of m/z 271 and EPI spectrum of the peak at 6.9 min from an EPI triggered PI scan of m/z 147.

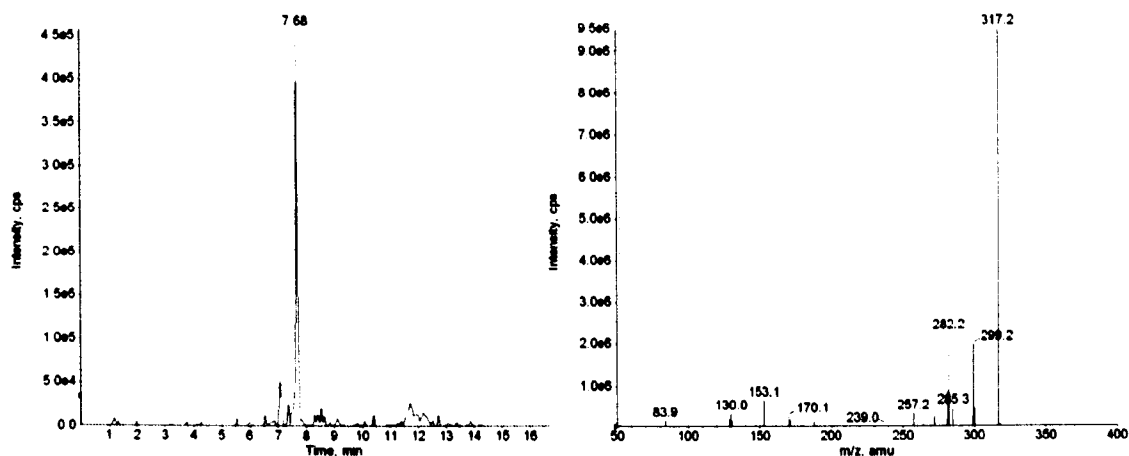


Figure 5.23 Extracted ion chromatogram of m/z 317 and EPI spectrum of the peak at 7.6 min from an EPI triggered PI scan of m/z 147.

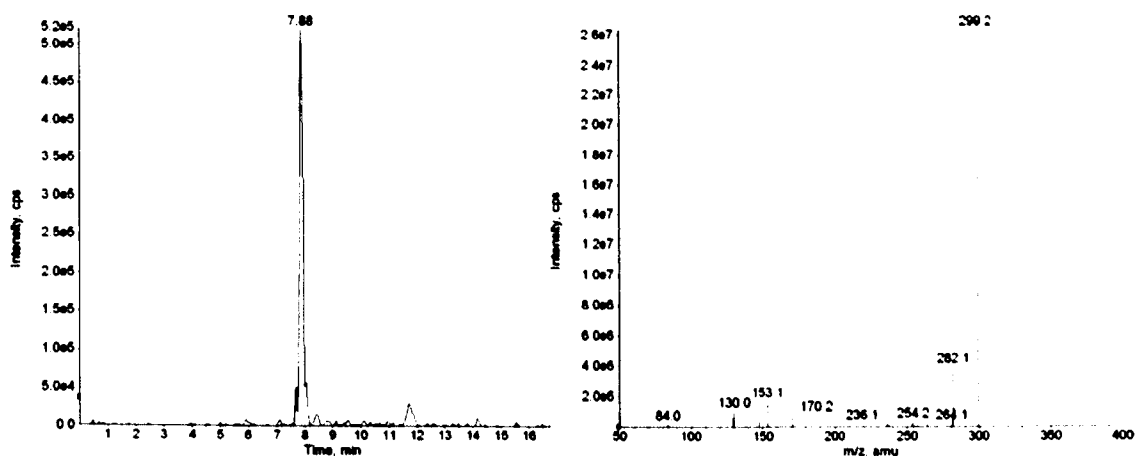


Figure 5.24 Extracted ion chromatogram of m/z 299 and EPI spectrum of the peak at 7.9 min from an EPI triggered PI scan of m/z 147.

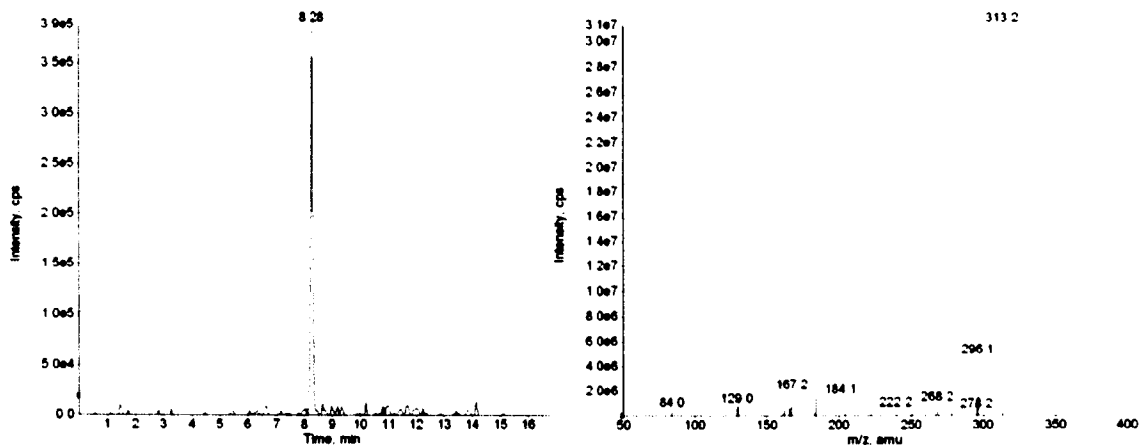


Figure 5.25 Extracted ion chromatogram of m/z 313 and EPI spectrum of the peak at 8.2 min from an EPI triggered PI scan of m/z 147.

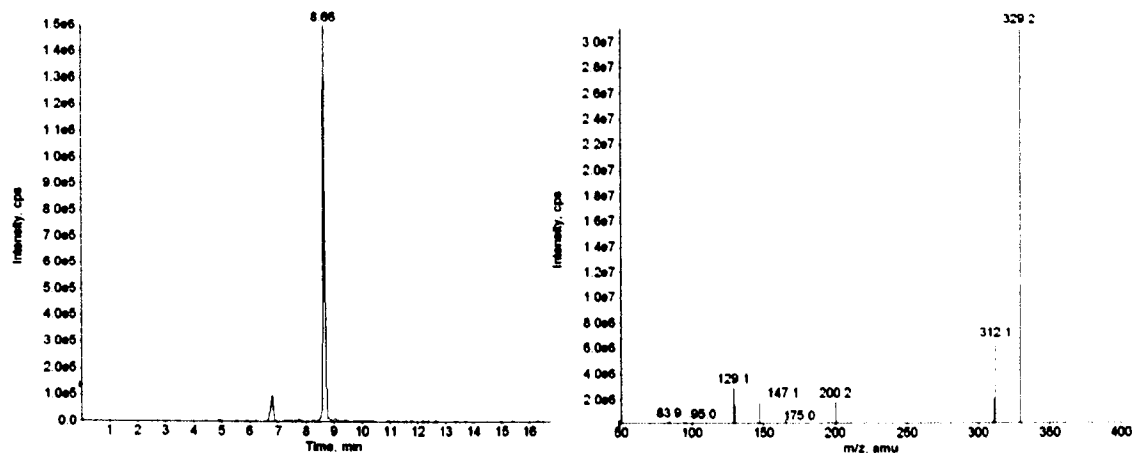


Figure 5.26 Extracted ion chromatogram of m/z 329 and EPI spectrum of the peak at 8.7 min from an EPI triggered PI scan of m/z 147.

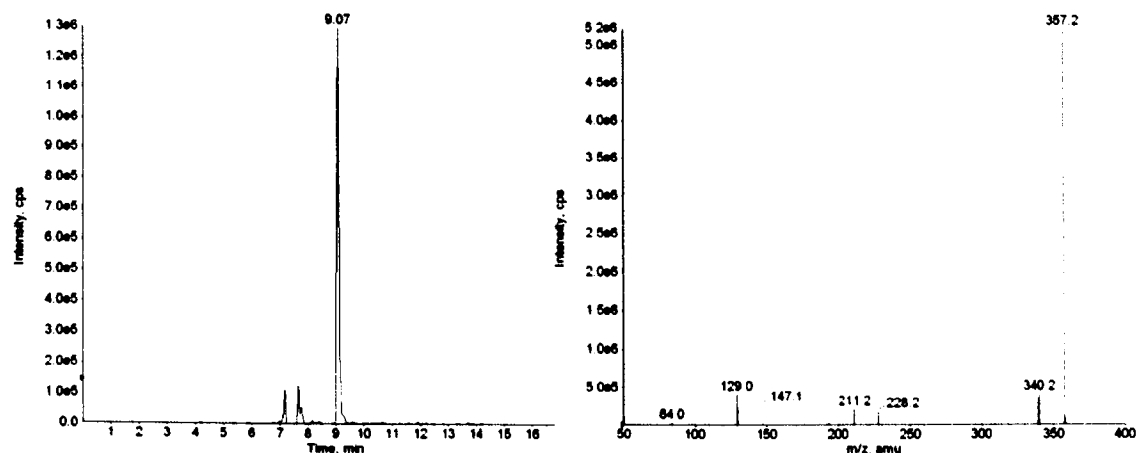


Figure 5.27 Extracted ion chromatogram of m/z 357 and EPI spectrum of the peak at 9.0 min from an EPI triggered PI scan of m/z 147.

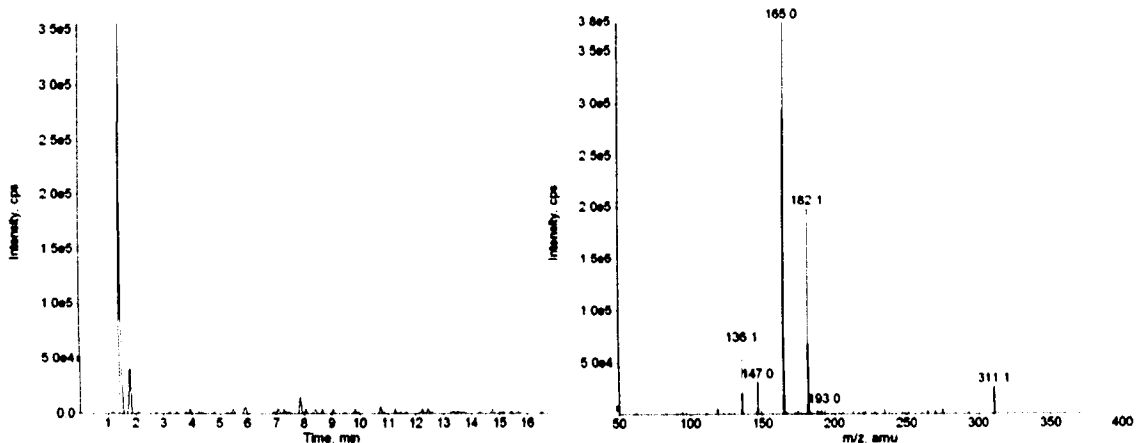


Figure 5.28 Extracted ion chromatogram of m/z 311 and EPI spectrum of the peak at 1.4 min from an EPI triggered PI scan of m/z 147.

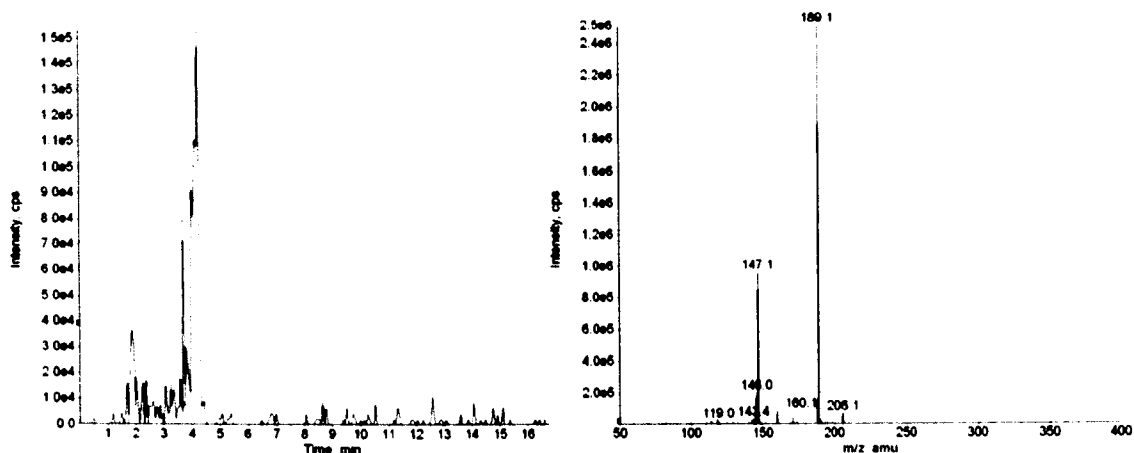


Figure 5.29 Extracted ion chromatogram of m/z 206 and EPI spectrum of the peak at 4.1 min from an EPI triggered PI scan of m/z 147.

Cys or Cys-Gly conjugates

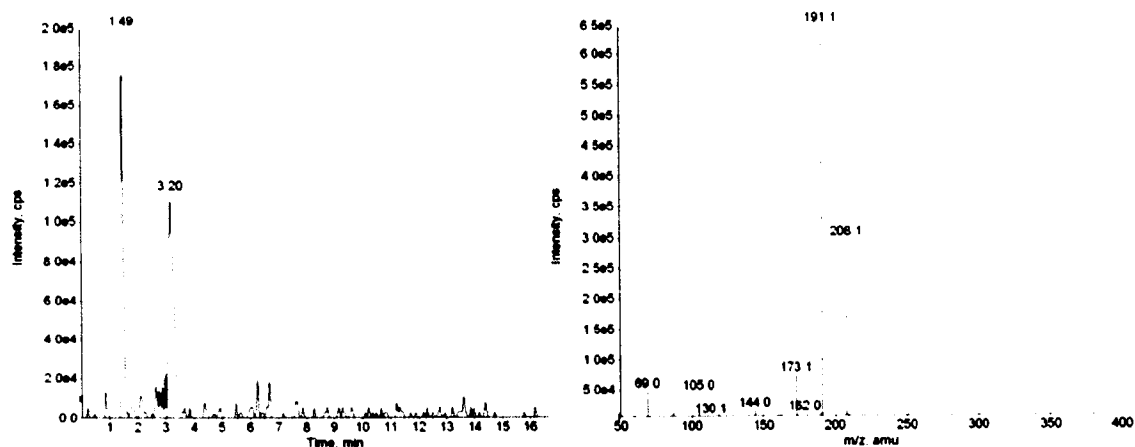


Figure 5.30 Extracted ion chromatogram of m/z 208 and EPI spectrum of the peak at 3.2 min from an EPI triggered PI scan of m/z 105.

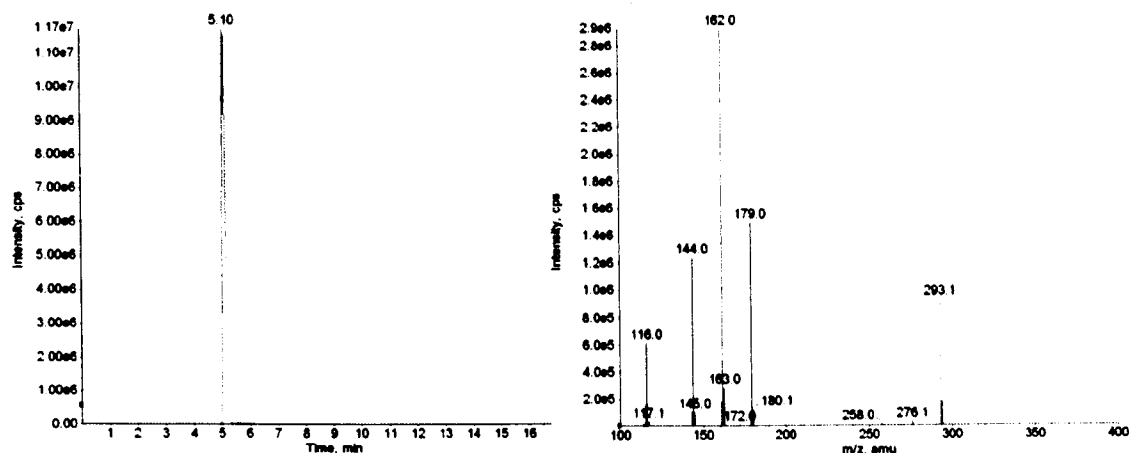


Figure 5.31 Extracted ion chromatogram of m/z 293 and EPI spectrum of the peak at 5.1 min from an EPI triggered PI scan of m/z 179.

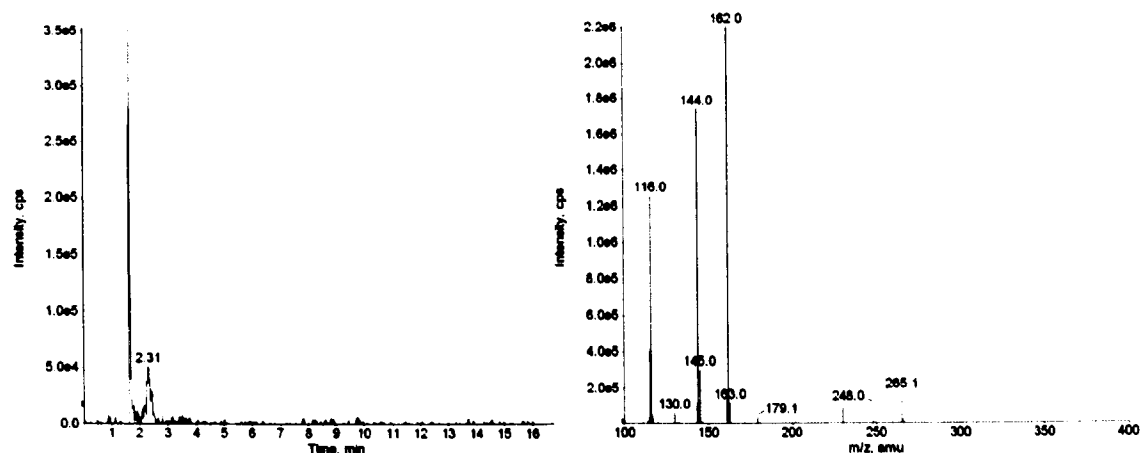


Figure 5.32 Extracted ion chromatogram of m/z 265 and EPI spectrum of the peak at 1.6 min from an EPI triggered PI scan of m/z 179.

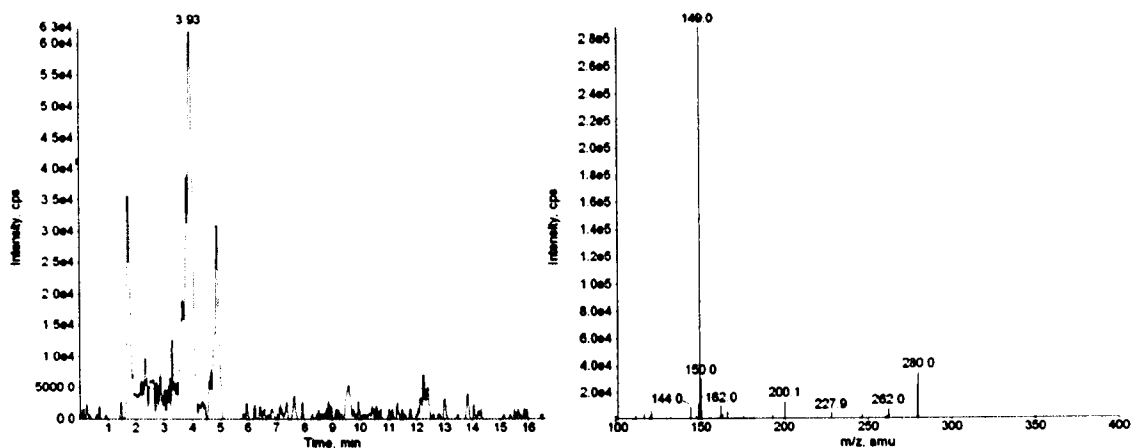


Figure 5.33 Extracted ion chromatogram of m/z 279 and EPI spectrum of the peak at 3.6 min from an EPI triggered PI scan of m/z 179.

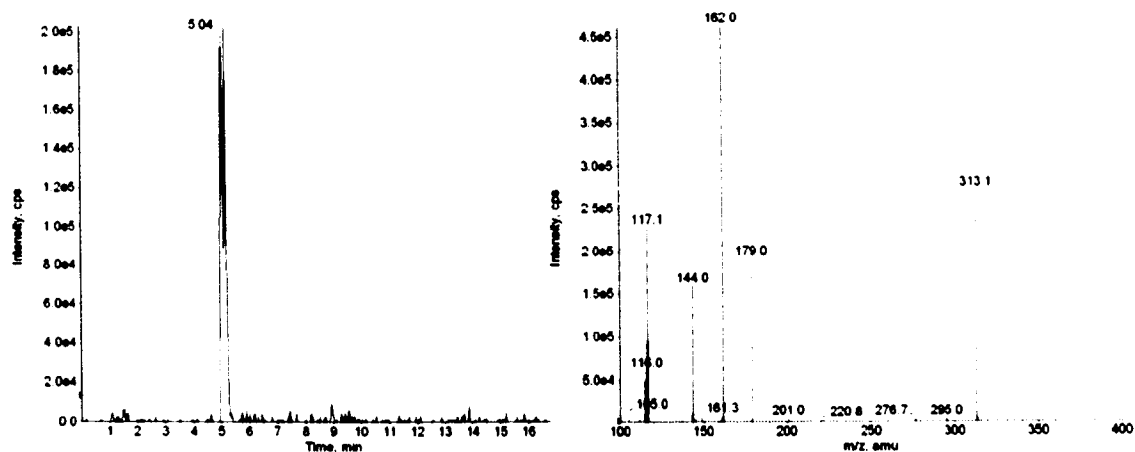


Figure 5.34 Extracted ion chromatogram of m/z 313 and EPI spectrum of the peak at 5.1 min from an EPI triggered PI scan of m/z 179.

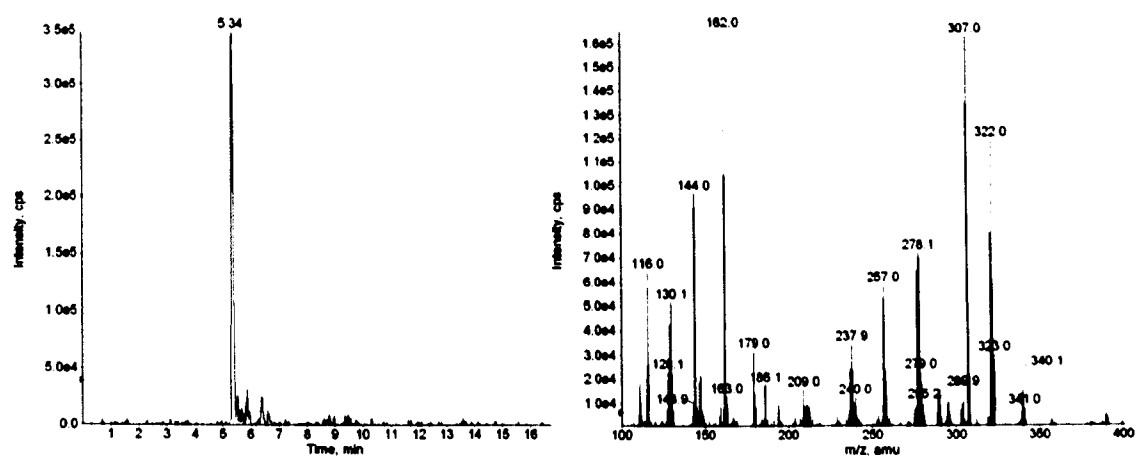


Figure 5.35 Extracted ion chromatogram of m/z 307 and EPI spectrum of the peak at 5.3 min from an EPI triggered PI scan of m/z 179.

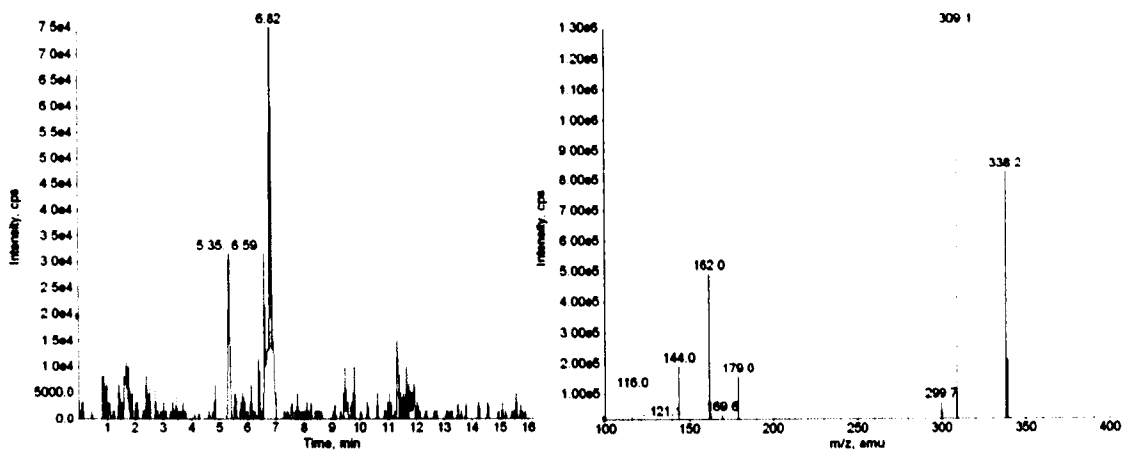


Figure 5.36 Extracted ion chromatogram of m/z 309 and EPI spectrum of the peak at 6.8 min from an EPI triggered PI scan of m/z 179.

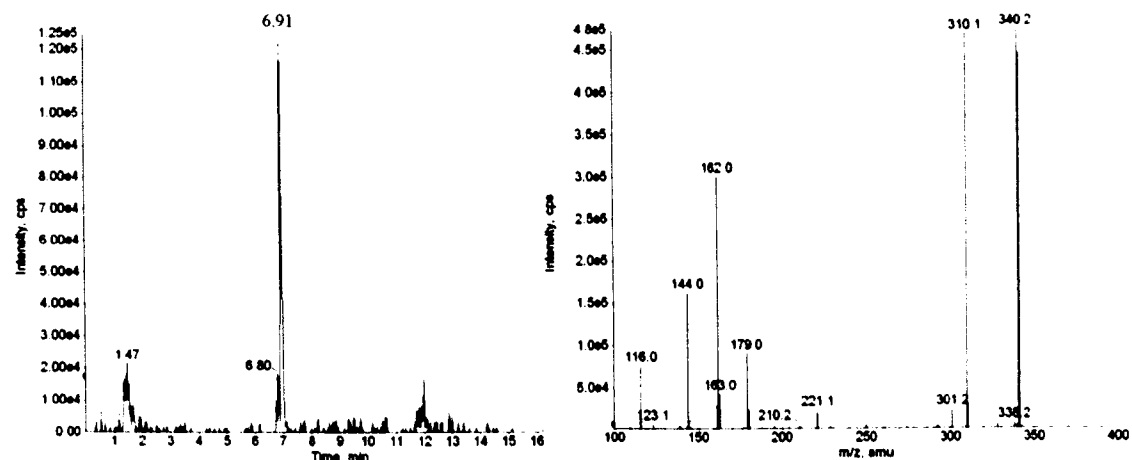


Figure 5.37 Extracted ion chromatogram of m/z 310 and EPI spectrum of the peak at 6.9 min from an EPI triggered PI scan of m/z 179.

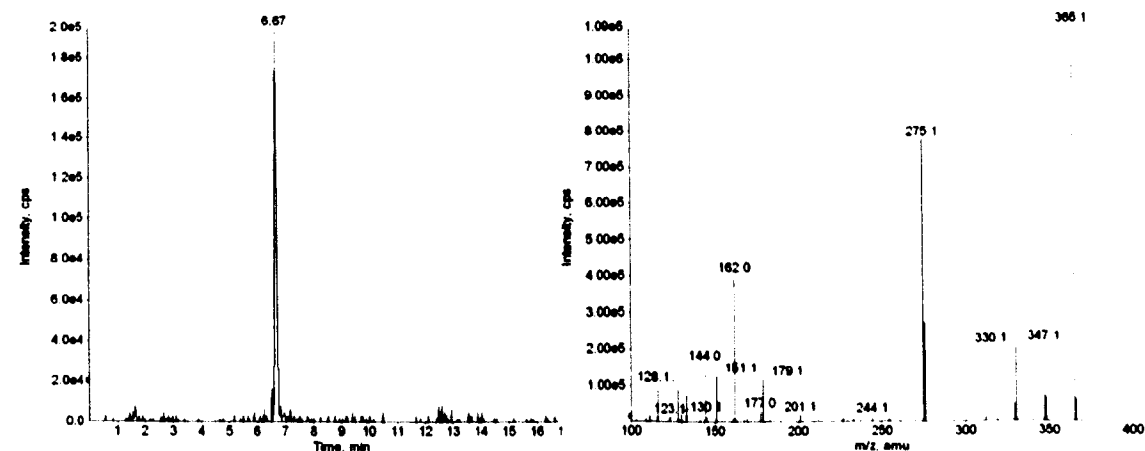


Figure 5.38 Extracted ion chromatogram of m/z 365 and EPI spectrum of the peak at 6.6 min from an EPI triggered PI scan of m/z 179.

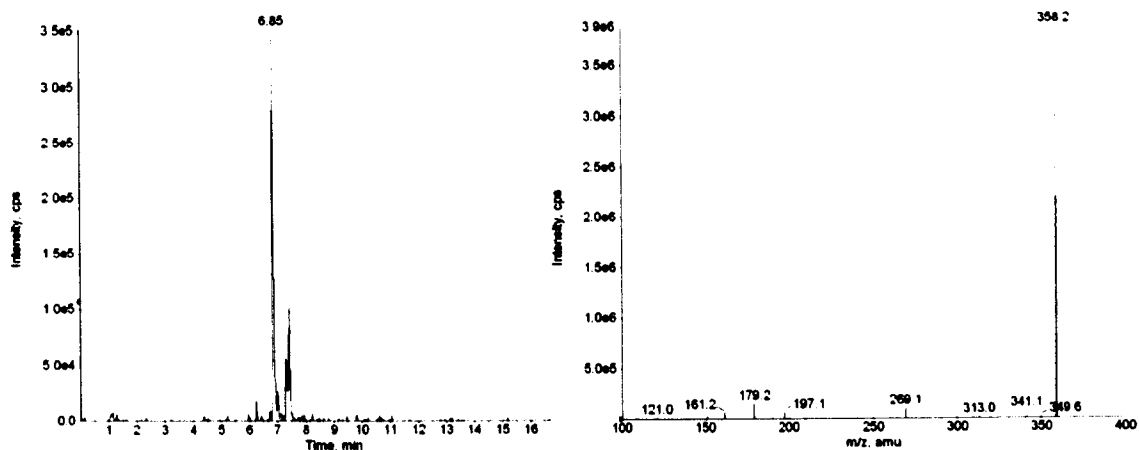


Figure 5.39 Extracted ion chromatogram of m/z 358 and EPI spectrum of the peak at 6.8 min from an EPI triggered PI scan of m/z 179.

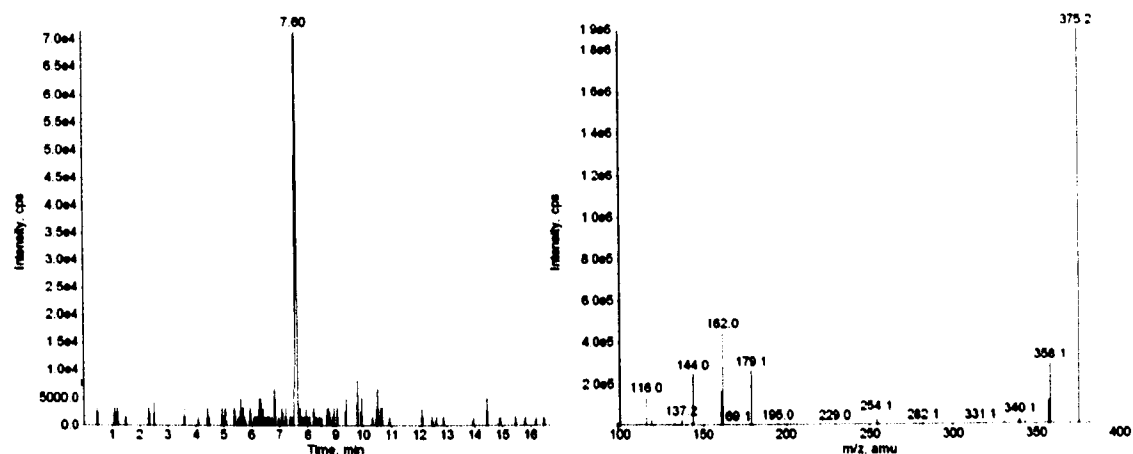


Figure 5.40 Extracted ion chromatogram of m/z 375 and EPI spectrum of the peak at 7.6 min from an EPI triggered PI scan of m/z 179.

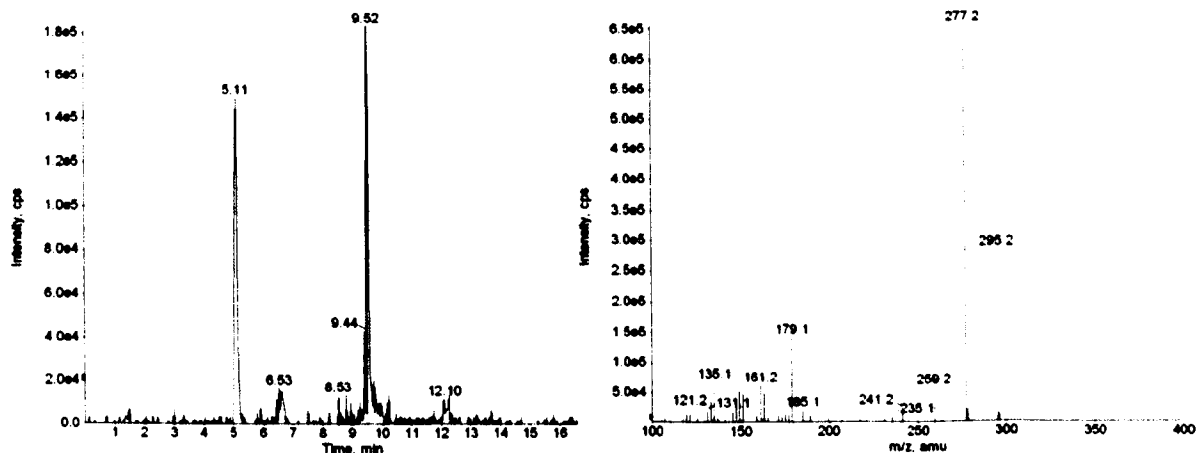


Figure 5.41 Extracted ion chromatogram of m/z 295 and EPI spectrum of the peak at 9.5 min from an EPI triggered PI scan of m/z 179.

5.4.3 Overall Discussion and Conclusions

Previous analytical studies on human apocrine sweat have predominantly focused on individual 'odour profiles' which are detectable *via* GC-MS analysis often in combination with perceived odour intensity, rated by human volunteers. The work presented herein was more focused on the chemical precursors to 'body odour'.

To my knowledge this is the first NMR study on apocrine sweat samples, in which 25 metabolites could be tentatively identified. Furthermore, inter-person variation could be identified from both the NMR and LC-MS techniques, which is consistent with the reported literature in regards to the analysis of the volatile components (Bernier *et al.*, 1999; Curran *et al.*, 2005; Natsch *et al.*, 2006; Penn *et al.*, 2007; Sommerville *et al.*, 1994).

In total, 12 odour precursors have been identified across all LC-MS techniques with a further 20 being partially identified through the use of the targeted approach, due to the increase in sensitivity over both the Exactive and QTOF systems. Definitive identification was not always possible due to the lack of synthetic standards, however, strong evidence for identity has been provided *via* LC-MS/MS fragmentation as well as accurate mass identification.

Retention times of each of the amino acid odour precursors are expected to differ when comparing against different HPLC columns, due to the differences in the composition of the stationary phase, column length and particle size dimensions. However, in the case of RP columns, the order in which these odour precursors elute are expected to be consistent with one another. In regards to the HILIC column, the elution odour is considered to be opposite to that of RP systems.

The glutamine conjugates, 3M2H-Gln and HMHA-Gln as well as the 3M3SH-Cys-Gly conjugates, have been described as the key precursors to body odour (Emter and Natsch, 2008; Natsch *et al.*, 2006; Natsch *et al.*, 2003; Starkenmann *et al.*, 2005). All three conjugates were detectable across all samples, with HMHA being the most

dominant odour precursor detected. In previous reports, the 3M3SH-Cys-Gly precursor has been shown to vary between individuals, as reported here, however, in a recent paper by Trocas and co-workers; they reported a 2:1 ratio between males and females over a three year study (Troccaz *et al.*, 2009). Furthermore, they showed that the same microflora can generate distinctively different body odours with respect to the composition of apocrine sweat.

Moreover, these reported odour precursors (Natsch *et al.*, 2006; Natsch *et al.*, 2003) have been shown to occur in different ratios between different individuals, but whether these ratios are stable over time and whether they are genetically fixed has not been reported. From the work herein, it is shown that the sweat composition of each individual is consistent from one day to the next. However, it is not certain whether the sweat composition or in particular, the odour precursors, remain constant in an individual across the course of a day.

Both NMR and LC-MS showed that there were no side related differences, nor were there any differences between each 24 h time point. This is consistent with the work by Ferdenzi and co-workers (Ferdenzi *et al.*, 2009), where they concluded that the left and right axillary can be considered as perceptually equivalent in attractiveness, intensity, or masculinity. However, if handedness is taken into account, there were reported differences between the left and right axillae in left-handed people only. It was reported that the odour, masculinity and intensity was more profound on the more active left side. This was in line with previous observations on asymmetry of axillary odour (Bird and Gower, 1982) and the rate of sweat production (Inaba and Inaba, 1992), with the view that side-related differences could be due to changes in the local environmental conditions caused by the increase in activity, favouring sweating rate or increased activity of microflora (Ferdenzi *et al.*, 2009). However, previous reports have shown the skin microflora to be quantitatively and qualitatively the same in the left and right axillae and not to be affected by handedness or sex (Leyden *et al.*, 1981). Thus, Ferdenzi's hypothesis "*that there exists an underlying activity-independent asymmetry that makes the left axilla smell stronger and that the superimposition of the activity-based asymmetry would balance both sides in right-handers but emphasize the asymmetry in left-handers*", can neither be confirmed nor dismissed from the work presented here due to the limited sample

volume and lack of available biometric data. Nonetheless, the results presented herein are in agreement with the hypothesis that individual odour differences are more likely to be influenced both by genetics and microflora (Emter and Natsch, 2008; James *et al.*, 2004; Kuhn and Natsch, 2009; Penn and Potts, 1998b; Troccaz *et al.*, 2009). There is also evidence that MHC genes can influence microflora composition (Toivanen *et al.*, 2001).

Further examining odour production in relation to the genotype can offer many practical applications. Firstly, it would be advantageous for researchers if the left or right side could be used separately as identical stimuli (doubling the amount of samples) or as a control *vs* treated. Secondly, there is increasing interest in whether human odours could be used for forensic research (Roberts *et al.*, 2005), potentially non-invasive disease diagnostics (Mantini *et al.*, 2000; Penn and Potts, 1998b; Turner and Magan, 2004; Willis *et al.*, 2004) or reducing the risk of attracting mosquitoes and other disease vectors (Penn *et al.*, 2007). Finally, understanding of how chemosensory individuality in humans is determined in part by MHC or other genes (Penn and Potts, 1998a; Penn, 2002) would provide rationale for both a direct and indirect approach to mask or eliminate these odours.

The findings of this present study illustrate the complementary nature of these analytical techniques and demonstrate the potential value of employing both NMR and LC-MS, in both a global and targeted manner, to the analysis of apocrine sweat samples. Identification of components detected by ^1H NMR spectroscopy was aided by the large body of information already available on metabolites identified in human biofluids. In comparison, the available data for metabolite identification by LC-MS is less extensive which reflects the major disadvantage of using LC-MS in metabolomics, as databases of compounds likely to be encountered in apocrine sweat have not yet been defined. However, through the use of high mass accuracy instruments, elemental compositions can be postulated. Nonetheless, further analysis would be required for structural elucidation of these metabolites *via* the application of LC-NMR-MS.

Chapter 6

6 General Discussion

The main aim of this work was to develop a series of analytical methodologies (NMR, HILIC-MS, RP-UPLC-MS and RP-LC-MS/MS) that would provide further insight into the chemical composition of human apocrine secretions, with particular reference to odour precursors, as well as identifying intra- and inter-subject variation between six individuals. Although the methods were developed for the use of apocrine gland secretions, they have the potential to be adapted for the analysis of other biological fluids such as plasma and urine. Four analytical techniques were developed in tandem, in order to provide as much information as possible on the composition of human apocrine sweat. The most significant developments in each chapter are summarised in Table 6.1.

Analytical methodologies were initially developed with an artificial sweat matrix in order to test analytical procedures and were therefore not designed to replicate apocrine secretions *per se*, due to the current uncertainties about the exact composition. Firstly, NMR procedures were developed with hypoallergenic infant formula from Neocate (www.neocate.co.uk) as the exact composition has been fully characterised and therefore allowed accurate comparison of different NMR conditions. The data evaluated in chapter two showed that a 1 mm micro-volume probe coupled to a 400 MHz spectrometer was best suited to handling small samples volumes typically obtained from human apocrine sweat. The sensitivity enhancement was ~5.3 fold over data acquired using conventional 5 mm OD NMR tubes on a 400 MHz spectrometer, and provided similar sensitivity to that of a 500 MHz spectrometer coupled with a cryo-probe. Secondly, a HILIC-MS method was developed with blood plasma as the biological matrix in order to provide a novel global approach for the separation of the more polar compounds that would ultimately complement the NMR data. This was mostly focused on the separation of amino acids

due to the range of polarities they represent. Finally, two further RP-LC-MS/MS methods were developed with available standards, providing a more selective and sensitive approach for screening against odour precursors. Furthermore, there was the opportunity to analyse the apocrine sweat samples with an orbitrap MS using RP-UPLC. However, due to time constraints, the LC conditions used were developed by Dr. Catharine Ortori (University of Nottingham). The orbitrap is more advanced than the current QTOF instrument, thereby, providing higher mass resolution; which approaches that of FTICR (~100 000) in comparison to QTOF (~10 000); greater sensitivity and mass accuracy as well as having the ability of positive and negative switching during acquisition.

Table 6.1 Summary of the main conclusions of the work carried out in each chapter

Chapter	Development
Two	Artificial sweat matrix was used to develop NMR methodologies 1 mm micro-volume probe identified as the most suitable for the analysis of apocrine sweat
Three	Developed Global HILIC-MS approach in order to characterise apocrine gland secretions Developed semi-targeted LC-MS/MS approach which is capable of screening for unknown odour precursors. Developed targeted LC-MS/MS approach for the analysis of known reported odour precursors.
Four	Reviewed analytical methodologies with sweat produced <i>in vitro</i> using an ASG5 cell line PCA and PC-DA was used to explore the metabolite differences between hormonal drug treatments Both NMR and HILIC-MS data were able to differentiate between the different treatments, thus, showing complementary information on a different subset of metabolites Putatively identified 275 metabolites ranging from amino acids, hydroxy acids, fatty acids, bile acids, nucleotides, lipids and vitamins
Five	PCA was used to explore the metabolite differences between volunteers All methodologies showed complementary information on a different subset of metabolites Left and right secretions were shown to be similar in composition Identified 12 known odour precursors and possibly identified a further 20 odour precursors Putatively identified 473 metabolites ranging from amino acids, hydroxy acids, fatty acids, bile acids, glucuronides, lipids and vitamins

To the author's knowledge, this is the first time NMR profiling of human apocrine sweat has been achieved. However, previous studies on eccrine sweat have been reported (Harker *et al.*, 2006). Moreover, to the author's knowledge, this was the first metabolomics study that has used either HILIC or RP-UPLC methodologies for the global metabolite identification of human apocrine sweat. The majority of the literature is GC based (Hasegawa *et al.*, 2004; Natsch *et al.*, 2006; Natsch *et al.*, 2004; Penn *et al.*, 2007; Starkenmann *et al.*, 2005), with some work using targeted RP-LC-MS (Emter and Natsch, 2008; Natsch *et al.*, 2006; Troccaz *et al.*, 2009) for the identification of odour precursors. However, the main novelty of the MS/MS data presented herein, comes from the PI scanning methodology to selectively scan for unknown odour precursors. Nonetheless, one of the major limitations with the MS/MS methodology currently reported is the lack of synthetic standards or isotopically labelled standards to provide absolute identification. Isotopic labelled standards would have the same chemistry and retention time as their counterpart, but would be differentiated due to the difference in molecular weight, thus, providing different MRM transitions. However, under the circumstances, typically for the MS/MS methodologies, metabolite identification proposed was based on knowledge of fragmentation profiles of other standards. If time and funds were not placing such constraints, it may have been possible to organise synthesis of more of the amino acid conjugates (odour precursors). Presence of these compounds would allow the MS/MS methodology to be validated, allowing absolute quantification of these odour precursor metabolites.

Spectral variations obtained from global methodologies (NMR, HILIC-MS, and RP-UPLC-MS) were explored using both PCA and PC-DA, in which the variation was explained by the first three PCs. It was observed that inter-variation for each volunteer was greater than intra-variation. Moreover, samples collected from the left and right arm, as well as 24 h time points, were consistent with one another. This information was also echoed by RP-LC-MS/MS data, which only monitored the odour precursors. It is also noted that a 24 h time point is considered to be a long biological time period, thus, for future studies it would be interesting to identify whether these odour precursors are secreted at a consistent rate during a 24 h period. Nonetheless, this potentially has great benefits for future projects, as not only can one

double the sample volume obtained from a single volunteer, but there is also the potential to have a test and control side per individual. Identifying the metabolites contributing to inter-person variation could not be achieved, partly due to experimental design (small sample size) and the absence of available meta data for each volunteer, thereby, identifying a major limitation. Nonetheless, it was possible to provide further insight into the metabolite composition of human apocrine washes, contributing to the research area greatly, as well as highlighting the complementary nature of the developed methodologies.

The NMR data was able to identify 25 metabolites, with lactate being the most dominant, at ~13.2 mM, which is consistent with the literature (Meyer *et al.*, 2007; Sato *et al.*, 1989) and that reported in eccrine sweat (Harker *et al.*, 2006). Furthermore, comparison of the *in vitro* produced apocrine sweat from AGS cell lines (Burry *et al.*, 2008), was shown to be of similar composition to that of an *in vivo* apocrine sweat collected from human volunteers (see Table 4.1 and Table 5.3 on page 128 and 158 respectively). Thus, it can be concluded that the *in vitro* sweat would have provided a good sample type for method development and as a result would be recommended to use for any further method development. However, when analysing the *in vitro* samples by MS/MS, odour precursors were not shown to be present. Although, 3M2H-Gln has previously been identified through GC-MS with the AGS5 cells (Burry *et al.*, 2008), it is possible that the odour precursors were removed during the extraction procedure or that these compounds were below the limit of detection with the instrumentation used.

The biggest challenge in this project was post acquisition, as in metabolomics analysis there is the requirement of converting an unidentified feature into a known chemical entity i.e. a metabolite. Currently, both NMR and LC-MS have been developed to suit high-throughput analysis. However, these have not been developed to provide automatic identification of the many hundreds of features detected. Thus, identification is still a manual or semi-automated process, which is typically biased towards metabolites of interest rather than all metabolites. Currently, many lab groups quote the number of features, often thousands from LC-MS data, as the number of metabolites detected. This is expected to be many magnitudes lower due to many metabolites producing more than one feature, for example, fragmentation products,

isotopes, multiply-charged species, or adducts (Brown *et al.*, 2009). Thus, it is not uncommon for one metabolite to produce 10 or more detectable features, adding to the complexity of the data (Dunn *et al.*, 2011b). To overcome these difficulties, a database of all reported sweat metabolites was sourced from available literature (see Appendix A), as well as using generic online databases, such as HMDB (see Table 5.2, page 155), to search for $M+H$ as well as common adducts such as Na^+ , K^+ and NH_4^+ to generate a putative identification. However, the majority of the reported literature is GC based, thus, leaving a large gap in identified metabolites *via* LC, as well as the available metabolite databases being far from a complete representation. To overcome these difficulties new MS software would need to be sourced in order to reduce the new number of detected features into a number of suitable m/z which could be used to search for hits or potential matches or to construct an accurate chemical formula based on the accurate mass. Nonetheless, 473 metabolites were putatively identified from the analysis of human apocrine sweat, with glucuronides, bile acids and sulphates being readily detected.

LC-MS/MS analyses readily identified 3M2H-Gln and HMHA-Gln, which are considered as the major odour precursor in apocrine sweat (Zeng *et al.*, 1991), as well as identifying 10 other known odour precursors, which are known to be present (Emter and Natsch, 2008; Natsch *et al.*, 2006; Natsch *et al.*, 2004; Starkenmann *et al.*, 2005; Starkenmann *et al.*, 2008). These odour precursors were also detected on both the HILIC and RP-LC-MS methodologies adding further evidence to their presence. Furthermore, the PI scanning approach was able to detect a further 20 metabolites, which have the potential to be unidentified odour precursors. In order to confirm their identities, other methodologies would need to be sourced, as the cost of sample collection, together with limited sample volumes, makes fraction collection followed by NMR analysis unfeasible in this instance. One approach would be to use an LTQ Orbitrap-Velos developed by Thermo Scientific, which would provide MS^n accurate mass fragmentation and together with the knowledge that part of the metabolite is known (i.e. contains an amino acid residue), would allow the molecular formula and structure to be calculated. Once the structure is determined, a synthetic standard would need to be synthesised for absolute clarification.

Chapter 7

7 References

- Abraham, R.J., Fisher, J. and Loftus, P. (1988) *Introduction to NMR Spectroscopy*. John Wiley & Sons, New York.
- Akutsu, T., Sekiguchi, K., Ohmori, T. and Sakurada, K. (2006) Individual comparisons of the levels of (E)-3-methyl-2-hexenoic acid, an axillary odor-related compound, in Japanese. *Chemical Senses* **31**, 557-563.
- Allen, J.A., Armstrong, J.E. and Roddie, I.C. (1973) The regional distribution of emotional sweating in man. *Journal of Physiology-London* **235**, 749-759.
- Alpert, A.J. (1990) Hydrophilic-interaction chromatography for the separation of peptides, nucleic-acids and other polar compounds. *Journal of Chromatography* **499**, 177-196.
- Alpert, A.J., Shukla, M., Shukla, A.K., Zieske, L.R., Yuen, S.W., Ferguson, M.A.J., Mehlert, A., Pauly, M. and Orlando, R. (1993). Hydrophilic-interaction chromatography of complex carbohydrates. *13th International Symposium on High-Performance Liquid Chromatography of Proteins, Peptides, and Polynucleotides*. San Francisco, Ca, pp. 191-202.
- Antonio, C., Larson, T., Gilday, A., Graham, I., Bergstrom, E. and Thomas-Oates, J. (2008) Hydrophilic interaction chromatography/electrospray mass spectrometry analysis of carbohydrate-related metabolites from *Arabidopsis thaliana* leaf tissue. *Rapid Communications in Mass Spectrometry* **22**, 1399-1407.
- Apostolou, C., Kousoulos, C., Dotsikas, Y. and Loukas, Y.L. (2008) Comparison of hydrophilic interaction and reversed-phase liquid chromatography coupled with tandem mass spectrometric detection for the determination of three pharmaceuticals in human plasma. *Biomedical Chromatography* **22**, 1393-1402.
- Aue, W.P., Karhan, J. and Ernst, R.R. (1976) Homonuclear broad-band decoupling and 2-dimensional J-Resolved NMR-spectroscopy. *Journal of Chemical Physics* **64**, 4226-4227.
- Austin, C. and Ellis, J. (2003) Microbial pathways leading to steroidal malodour in the axilla. *Journal of Steroid Biochemistry and Molecular Biology* **87**, 105-110.

Baidoo, E.E.K., Benket, P.I., Neususs, C., Pelzing, M., Kruppa, G., Leary, J.A. and Keasling, J.D. (2008) Capillary electrophoresis-fourier transform ion cyclotron resonance mass spectrometry for the identification of cationic metabolites via a pH-mediated stacking-transient isotachophoretic method. *Analytical Chemistry* **80**, 3112-3122.

Baran, R., Kochi, H., Saito, N., Suematsu, M., Soga, T., Nishioka, T., Robert, M. and Tomita, M. (2006) MathDAMP: a package for differential analysis of metabolite profiles. *Bmc Bioinformatics* **7**, 9.

Barbosa, J. and Sanznebot, V. (1994) Preferential solvation in acetonitrile-water mixtures - relationship between solvatochromic parameters and standard pH values. *Journal of the Chemical Society-Faraday Transactions* **90**, 3287-3292.

Bax, A. and Davis, D.G. (1985) Mlev-17-based two-dimensional homonuclear magnetization transfer spectroscopy. *Journal of Magnetic Resonance* **65**, 355-360.

Bedair, M. and Sumner, L.W. (2008) Current and emerging mass-spectrometry technologies for metabolomics. *Trac-Trends in Analytical Chemistry* **27**, 238-250.

Beebe, K.R., Pell, R.J. and Seasholtz, M.B. (1998) *Chemometrics: A practical guide*. Wiley, New York.

Beier, K., Ginez, I. and Schaller, H. (2005) Localization of steroid hormone receptors in the apocrine sweat glands of the human axilla. *Histochemistry and Cell Biology* **123**, 61-65.

Bernier, U.R., Booth, M.M. and Yost, R.A. (1999) Analysis of human skin emanations by gas chromatography mass spectrometry. 1. Thermal desorption of attractants for the yellow fever mosquito (*Aedes aegypti*) from handled glass beads. *Analytical Chemistry* **71**, 1-7.

Bicker, W., Wu, J.Y., Lammerhofer, M. and Lindner, W. (2008) Hydrophilic interaction chromatography in nonaqueous elution mode for separation of hydrophilic analytes on silica-based packings with noncharged polar bondings. *Journal of Separation Science* **31**, 2971-2987.

Biemann, K. and McCloskey, J.A. (1962) Mass spectra of organic molecules .2. amino acids. *Journal of the American Chemical Society* **84**, 3192-3193.

Bird, S. and Gower, D.B. (1981) The validation and use of a radioimmunoassay for 5-alpha-androst-16-en-3-one in human axillary collections. *Journal of Steroid Biochemistry and Molecular Biology* **14**, 213-219.

Bird, S. and Gower, D.B. (1982) Axillary 5-alpha-androst-16-en-3-one, cholesterol and squalene in men - preliminary evidence for 5-alpha-androst-16-en-3-one being a product of bacterial action. *Journal of Steroid Biochemistry and Molecular Biology* **17**, 517-522.

- Bloch, F., Hansen, W.W. and Packard, M. (1946) The nuclear induction experiment. *Physical Review* **70**, 474-485.
- Bloor, K. (1969) Gustatory sweating and other responses after cervico-thoracic sympathectomy. *Brain* **92**, 137-146.
- Boernsen, K.O., Gatzek, S. and Imbert, G. (2005) Controlled protein precipitation in combination with chip-based nanospray infusion mass spectrometry. An approach for metabolomics profiling of plasma. *Analytical Chemistry* **77**, 7255-7264.
- Bouchonnet, S., Denhez, J.P., Hoppilliard, Y. and Mauriac, C. (1992) Is plasma desorption mass-spectrometry useful for small-molecule analysis - fragmentations of the natural alpha-amino-acids. *Analytical Chemistry* **64**, 743-754.
- Bovell, D.L., Corbett, A.D., Holmes, S., MacDonald, A. and Harker, M. (2007) The absence of apoeccrine glands in the human axilla has disease pathogenetic implications, including axillary hyperhidrosis. *British Journal of Dermatology* **156**, 1278-1286.
- Braun, S. and Berger, S. (2004) *200 and more NMR experiments: A practical course*. Wiley-VCH Verlag GmbH.
- Braunschweiler, L. and Ernst, R.R. (1983) Coherence transfer by isotropic mixing - Application to proton correlation spectroscopy. *Journal of Magnetic Resonance* **53**, 521-528.
- Breit, G. and Rabi, II (1931) Measurement of nuclear spin. *Physical Review* **38**, 2082-2083.
- Brindle, J.T., Antti, H., Holmes, E., Tranter, G., Nicholson, J.K., Bethell, H.W.L., Clarke, S., Schofield, P.M., McKilligin, E., Mosedale, D.E. and Grainger, D.J. (2002) Rapid and noninvasive diagnosis of the presence and severity of coronary heart disease using ¹H-NMR-based metabonomics. *Nature Medicine* **8**, 1439-1444.
- Bronshvag, M.M. (1978) Spectrum of gustatory sweating, with special reference to its presence in diabetics with autonomic neuropathy. *American Journal of Clinical Nutrition* **31**, 307-309.
- Brown, M., Dunn, W.B., Dobson, P., Patel, Y., Winder, C.L., Francis-McIntyre, S., Begley, P., Carroll, K., Broadhurst, D., Tseng, A., Swainston, N., Spasic, I., Goodacre, R. and Kell, D.B. (2009) Mass spectrometry tools and metabolite-specific databases for molecular identification in metabolomics. *Analyst* **134**, 1322-1332.
- Bruning, P.F., Bonfrer, J.M.G., Hart, A.A.M., Dejongbakker, M., Linders, D., Vanloon, J. and Nooyen, W.J. (1988) Tamoxifen, serum lipoproteins and cardiovascular risk. *British Journal of Cancer* **58**, 497-499.
- Buono, M.J., Lee, N.V.L. and Miller, P.W. (2010) The relationship between exercise intensity and the sweat lactate excretion rate. *Journal of Physiological Sciences* **60**, 103-107.

Burphy, J.S., Evans, R.L., Harker, M., Kealey, G.T.E., McDonald, D.F., Burphy, J., Evans, R., Kealey, G. and McDonald, D. (2008) New apocrine cell line exhibiting long term proliferation for diagnostic, therapeutic or cosmetic preparations, and evaluating in vitro whether a material is a deodorant when topically applied to skin, Unilever Plc (Unil) Unilever Nv (Unil) Hindustan Unilever Ltd (Unil), pp. 2126053-A2:.

Cai, X.M., Zou, L.J., Dong, J., Zhao, L.L., Wang, Y.Y., Xu, Q., Xue, X.Y., Zhang, X.L. and Liang, X.M. (2009) Analysis of highly polar metabolites in human plasma by ultra-performance hydrophilic interaction liquid chromatography coupled with quadrupole-time of flight mass spectrometry. *Analytica Chimica Acta* **650**, 10-15.

Castrillo, J.I., Hayes, A., Mohammed, S., Gaskell, S.J. and Oliver, S.G. (2003) An optimized protocol for metabolome analysis in yeast using direct infusion electrospray mass spectrometry. *Phytochemistry* **62**, 929-937.

Chen, J., Wang, W.Z., Lv, S., Yin, P.Y., Zhao, X.J., Lu, X., Zhang, F.X. and Xu, G.W. (2009) Metabonomics study of liver cancer based on ultra performance liquid chromatography coupled to mass spectrometry with HILIC and RPLC separations. *Analytica Chimica Acta* **650**, 3-9.

Churms, S.C. (1996) Recent progress in carbohydrate separation by high-performance liquid chromatography based on hydrophilic interaction. *Journal of Chromatography A* **720**, 75-91.

Claridge, T.D.W. (2008) *High-Resolution NMR Techniques in Organic Chemistry*, 2nd edn. Elsevier Science, Oxford.

Claus, R. and Alsing, W. (1976) Occurrence of 5 alpha-androst-16-en-3-one, a boar pheromone, in man and its relationship to testosterone. *Journal of Endocrinology* **68**, 483-484.

Cloarec, O., Dumas, M.E., Craig, A., Barton, R.H., Trygg, J., Hudson, J., Blancher, C., Gauguier, D., Lindon, J.C., Holmes, E. and Nicholson, J. (2005) Statistical total correlation spectroscopy: An exploratory approach for latent biomarker identification from metabolic ¹H NMR data sets. *Analytical Chemistry* **77**, 1282-1289.

Coltman, C.A., Rowe, N.J. and Atwell, R.J. (1966) Amino acid content of sweat in normal adults. *American Journal of Clinical Nutrition* **18**, 373-378.

Connor, S.C., Wu, W., Sweatman, B.C., Manini, J., Haselden, J.N., Crowther, D.J. and Waterfield, C.J. (2004) Effects of feeding and body weight loss on the ¹H NMR-based urine metabolic profiles of male Wistar Han rats: implications for biomarker discovery. *Biomarkers* **9**, 156-179.

Conventz, A., Musiol, A., Brodowsky, C., Mueller-Lux, A., Dewes, P., Kraus, T. and Schettgen, T. (2007) Simultaneous determination of 3-nitrotyrosine, tyrosine, hydroxyproline and proline in exhaled breath condensate by hydrophilic interaction liquid chromatography/electrospray ionization tandem mass spectrometry. *Journal of*

Chromatography B-Analytical Technologies in the Biomedical and Life Sciences **860**, 78-85.

Coolen, S.A., Daykin, C.A., van Duynhoven, J.P.M., van Dorsten, F.A., Wulfert, F., Mathot, J., Scheltinga, M.R., Stroosma, O., Vader, H. and Wijnen, M.H. (2008) Measurement of ischaemia-reperfusion in patients with intermittent claudication using NMR-based metabonomics. *NMR in Biomedicine* **21**, 686-695.

Corcoran, O. and Spraul, M. (2003) LC-NMR-MS in drug discovery. *Drug Discovery Today* **8**, 624-631.

Cowley, J.J. and Brooksbank, B.W.L. (1991) Human exposure to putative pheromones and changes in aspects of social behaviour. *Journal of Steroid Biochemistry and Molecular Biology* **39**, 647-659.

Crnogorac, G. and Schwack, W. (2007) Determination of dithiocarbamate fungicide residues by liquid chromatography/mass spectrometry and stable isotope dilution assay. *Rapid Communications in Mass Spectrometry* **21**, 4009-4016.

Cubbon, S., Bradbury, T., Wilson, J. and Thomas-Oates, J. (2007) Hydrophilic interaction chromatography for mass spectrometric metabonomic studies of urine. *Analytical Chemistry* **79**, 8911-8918.

Curran, A.M., Rabin, S.I., Prada, P.A. and Furton, K.G. (2005) Comparison of the volatile organic compounds present in human odor using SPME-GC/MS. *Journal Of Chemical Ecology* **31**, 1607-1619.

D'Apolito, O., Paglia, G., Tricarico, F., Garofalo, D., Pilotti, A., Lamacchia, O., Cignarelli, M. and Corso, G. (2008) Development and validation of a fast quantitative method for plasma dimethylarginines analysis using liquid chromatography-tandem mass spectrometry. *Clinical Biochemistry* **41**, 1391-1395.

Daykin, C. and Wulfert, F. (2006) NMR spectroscopy based metabonomics: Current technology and applications., *Frontiers in Drug Design & Discovery*, Bentham Science Publishers. pp. 151-173.

Daykin, C.A., Foxall, P.J.D., Connor, S.C., Lindon, J.C. and Nicholson, J.K. (2002) The comparison of plasma deproteinization methods for the detection of low-molecular-weight metabolites by ¹H nuclear magnetic resonance spectroscopy. *Analytical Biochemistry* **304**, 220-230.

Daykin, C.A., Van Duynhoven, J.P.M., Groenewegen, A., Dachtler, M., Van Amelsvoort, J.M.M. and Mulder, T.P.J. (2005) Nuclear magnetic resonance spectroscopic based studies of the metabolism of black tea polyphenols in humans. *Journal of Agricultural and Food Chemistry* **53**, 1428-1434.

Decreau, R.A., Marson, C.M., Smith, K.E. and Behan, J.M. (2003) Production of malodorous steroids from androsta-5,16-dienes and androsta-4,16-dienes by *Corynebacteria* and other human axillary bacteria. *Journal of Steroid Biochemistry and Molecular Biology* **87**, 327-336.

Dekoning, W. and Vandam, K. (1992) A method for the determination of changes of glycolytic metabolites in yeast on a subsecond time scale using extraction at neutral pH. *Analytical Biochemistry* **204**, 118-123.

Dell'Aversano, C., Eaglesham, G.K. and Quilliam, M.A. (2004) Analysis of cyanobacterial toxins by hydrophilic interaction liquid chromatography-mass spectrometry. *Journal of Chromatography A* **1028**, 155-164.

Desta, Z., Ward, B.A., Soukhova, N.V. and Flockhart, D.A. (2004) Comprehensive evaluation of tamoxifen sequential biotransformation by the human cytochrome P450 system in vitro: Prominent roles for CYP3A and CYP2D6. *Journal of Pharmacology and Experimental Therapeutics* **310**, 1062-1075.

Dixon, S.J., Xu, Y., Brereton, R.G., Soini, H.A., Novotny, M.V., Oberzaucher, E., Grammer, K. and Penn, D.J. (2007) Pattern recognition of gas chromatography mass spectrometry of human volatiles in sweat to distinguish the sex of subjects and determine potential discriminatory marker peaks. *Chemometrics And Intelligent Laboratory Systems* **87**, 161-172.

Dole, M., Mack, L.L. and Hines, R.L. (1968) Molecular beams of macroions. *Journal of Chemical Physics* **49**, 2240-2249.

Dookeran, N.N., Yalcin, T. and Harrison, A.G. (1996) Fragmentation reactions of protonated alpha-amino acids. *Journal of Mass Spectrometry* **31**, 500-508.

Duda, R.O., Hart, P.E. and Stork, D.E. (2001) *Pattern classification*, 2nd edn. John Wiley, London.

Dunn, W., Brown, M., Worton, S., Davies, K., Jones, R., Kell, D. and Heazell, A. (2011a) The metabolome of human placental tissue: investigation of first trimester tissue and changes related to preeclampsia in late pregnancy. *Metabolomics*, 1-19.

Dunn, W.B., Broadhurst, D., Brown, M., Baker, P.N., Redman, C.W.G., Kenny, L.C. and Kell, D.B. (2008) Metabolic profiling of serum using ultra performance liquid chromatography and the LTQ-Orbitrap mass spectrometry system. *Journal of Chromatography B-Analytical Technologies in the Biomedical and Life Sciences* **871**, 288-298.

Dunn, W.B., Broadhurst, D.I., Atherton, H.J., Goodacre, R. and Griffin, J.L. (2011b) Systems level studies of mammalian metabolomes: the roles of mass spectrometry and nuclear magnetic resonance spectroscopy. *Chemical Society Reviews* **40**, 387-426.

Dunn, W.B. and Ellis, D.I. (2005) Metabolomics: Current analytical platforms and methodologies. *Trac-Trends in Analytical Chemistry* **24**, 285-294.

Eisenach, J.H., Atkinson, J.L.D. and Fealyey, R.D. (2005) Hyperhidrosis: Evolving therapies for a well-established phenomenon. *Mayo Clinic Proceedings* **80**, 657-666.

Eisenreich, W. and Bacher, A. (2007) Advances of high-resolution NMR techniques in the structural and metabolic analysis of plant biochemistry. *Phytochemistry* **68**, 2799-2815.

Emter, R. and Natsch, A. (2008) The sequential action of a dipeptidase and a β -lyase is required for the release of the human body odorant 3-methyl-3-sulfanylhhexan-1-ol from a secreted cys-gly-(s) conjugate by corynebacteria. *The Journal of Biological Chemistry* **283**, 20645-20652.

Eriksson, L., Johansson, E., Kettaneh, N. and Wold, S. (2001) *Multi- and megavariable data analysis: principles and applications* Umetrics Academy, Umea.

Everitt, B.S. (1993) *Cluster analysis*. Edward Arnold, London.

Faijes, M., Mars, A.E. and Smid, E.J. (2007) Comparison of quenching and extraction methodologies for metabolome analysis of *Lactobacillus plantarum*. *Microbial Cell Factories* **6**, 1-8.

FDA (2001) Guidance for industry: Bioanalytical method validation, <http://www.fda.gov/cder/guidance/index.htm>.

Ferdenzi, C., Schaal, B. and Roberts, S.C. (2009) Human axillary odor: are there side-related perceptual differences? *Chemical Senses* **34**, 565-571.

Fiehn, O. (2001) Combining genomics, metabolome analysis, and biochemical modelling to understand metabolic networks. *Comparative and Functional Genomics* **2**, 155-168.

Fiehn, O., Kopka, J., Dormann, P., Altmann, T., Trethewey, R.N. and Willmitzer, L. (2000) Metabolite profiling for plant functional genomics. *Nature Biotechnology* **18**, 1157-1161.

Forshed, J., Schuppe-Koistinen, I. and Jacobsson, S.P. (2003) Peak alignment of NMR signals by means of a genetic algorithm. *Analytica Chimica Acta* **487**, 189-199.

Foxall, P.J.D., Parkinson, J.A., Sadler, I.H., Lindon, J.C. and Nicholson, J.K. (1993) Analysis of biological fluids using 600 MHz proton NMR spectroscopy: application of homonuclear two-dimensional J-resolved spectroscopy to urine and blood plasma for spectral simplification and assignment. *Journal of Pharmaceutical and Biomedical Analysis* **11**, 21-31.

Freeman-Gallant, C.R., Meguerdichian, M., Wheelwright, N.T. and Sollecito, S.V. (2003) Social pairing and female mating fidelity predicted by restriction fragment length polymorphism similarity at the major histocompatibility complex in a songbird. *Molecular Ecology* **12**, 3077-3083.

Froebe, C., Simone, A., Charig, A. and Eigen, E. (1990) Axillary malodor production - a new mechanism. *Journal of the Society of Cosmetic Chemists* **41**, 173-185.

Fu, B.Q., Gao, X.Y., Zhang, S.P., Cai, Z.W. and Shen, J.C. (2008) Quantification of acetylcholine in microdialysate of subcutaneous tissue by hydrophilic interaction chromatography/tandem mass spectrometry. *Rapid Communications in Mass Spectrometry* **22**, 1497-1502.

Fukumoto, T., Tanaka, T., Fujioka, H., Yoshihara, S., Ochi, T. and Kuroiwa, A. (1988) Differences in composition of sweat induced by thermal exposure and by running exercise. *Clinical Cardiology* **11**, 707-709.

Gabelica, V. and De Pauw, E. (2005) Internal energy and fragmentation of ions produced in electrospray sources. *Mass Spectrometry Reviews* **24**, 566-587.

Gallagher, M., Wysocki, J., Leyden, J.J., Spielman, A.I., Sun, X. and Preti, G. (2008) Analyses of volatile organic compounds from human skin. *British Journal of Dermatology* **159**, 780-791.

Gaskell, S.J. (1997) Electrospray: Principles and practice. *Journal of Mass Spectrometry* **32**, 677-688.

Gautschi, M., Natsch, A. and Schroder, F. (2007) Biochemistry of human axilla malodor and chemistry of deodorant ingredients. *Chimia* **61**, 27-32.

Geladi, P. and Kowalski, B.R. (1986) Partial least-squares regression - A tutorial. *Analytica Chimica Acta* **185**, 1-17.

Gika, H.G., Theodoridis, G.A., Wingate, J.E. and Wilson, I.D. (2007) Within-day reproducibility of an HPLC-MS-Based method for metabonomic analysis: Application to human urine. *Journal of Proteome Research* **6**, 3291-3303.

Godejohann, M. (2007) Hydrophilic interaction chromatography coupled to nuclear magnetic resonance spectroscopy and mass spectroscopy - A new approach for the separation and identification of extremely polar analytes in bodyfluids. *Journal of Chromatography A* **1156**, 87-93.

Gonzalez, B., Francois, J. and Renaud, M. (1997) A rapid and reliable method for metabolite extraction in yeast using boiling buffered ethanol. *Yeast* **13**, 1347-1355.

Goodacre, R., Broadhurst, D., Smilde, A.K., Kristal, B.S., Baker, J.D., Beger, R., Bessant, C., Connor, S., Calmani, G., Craig, A., Ebbels, T., Kell, D.B., Manetti, C., Newton, J., Paternostro, G., Somorjai, R., Sjostrom, M., Trygg, J. and Wulfert, F. (2007) Proposed minimum reporting standards for data analysis in metabolomics. *Metabolomics* **3**, 231-241.

Goodacre, R., Heald, J.K. and Kell, D.B. (1999) Characterisation of intact microorganisms using electrospray ionisation mass spectrometry. *Fems Microbiology Letters* **176**, 17-24.

Goodacre, R., Vaidyanathan, S., Bianchi, G. and Kell, D.B. (2002) Metabolic profiling using direct infusion electrospray ionisation mass spectrometry for the characterisation of olive oils. *Analyst* **127**, 1457-1462.

Goodacre, R., Vaidyanathan, S., Dunn, W.B., Harrigan, G.G. and Kell, D.B. (2004) Metabolomics by numbers: Acquiring and understanding global metabolite data. *Trends Biotechnol* **22**, 245-52.

Goodacre, R., York, E.V., Heald, J.K. and Scott, I.M. (2003) Chemometric discrimination of unfractionated plant extracts analyzed by electrospray mass spectrometry. *Phytochemistry* **62**, 859-863.

Gordon, R.S., Thompson, R.H., Muenzer, J. and Thrasher, D. (1971) Sweat lactate in man is derived from blood glucose. *Journal Of Applied Physiology* **31**, 713-716.

Gordon, S.G., Smith, K., Rabinowit and Vagelos, P.R. (1973) Studies of trans-3-methyl-2-hexenoic acid in normal and schizophrenic humans. *Journal of Lipid Research* **14**, 495-503.

Gower, D.B., Mallet, A.I., Watkins, W.J., Wallace, L.M. and Calame, J.P. (1997) Capillary gas chromatography with chemical ionization negative ion mass spectrometry in the identification of odorous steroids formed in metabolic studies of the sulphates of androsterone, DHA and 5 alpha-androst-16-en-3 beta-ol with human axillary bacterial isolates. *Journal of Steroid Biochemistry and Molecular Biology* **63**, 81-89.

Gower, D.B., Nixon, A., Jackman, P.J.H. and Mallett, A.I. (1986) Transformation of steroids by axillary coryneform bacteria. *International Journal of Cosmetic Science* **8**, 149-158.

Green, J.M., Pritchett, R.C., Crews, T.R., McLester, J.R. and Tucker, D.C. (2004) Sweat lactate response between males with high and low aerobic fitness. *European Journal of Applied Physiology* **91**, 1-6.

Griffin, J.L. (2006) The Cinderella story of metabolic profiling: does metabolomics get to go to the functional genomics ball? *Philosophical Transactions of the Royal Society B-Biological Sciences* **361**, 147-161.

Griffin, J.L., Nicholls, A.W., Keun, H.C., Mortishire-Smith, R.J., Nicholson, J.K. and Kuehn, T. (2002) Metabolic profiling of rodent biological fluids via ^1H NMR spectroscopy using a 1 mm microlitre probe. *Analyst* **127**, 582-584.

Griffin, J.L., Williams, H.J., Sang, E. and Nicholson, J.K. (2001) Abnormal lipid profile of dystrophic cardiac tissue as demonstrated by one- and two-dimensional magic-angle spinning ^1H NMR spectroscopy. *Magnetic Resonance in Medicine* **46**, 249-255.

Griffiths, I.W. (1997) J.J. Thomson - The centenary of his discovery of the electron and of his invention of mass spectrometry. *Rapid Communications in Mass Spectrometry* **11**, 3-16.

Grimes, J.H. and O'Connell, T.M. (2011) The application of micro-coil NMR probe technology to metabolomics of urine and serum. *Journal of Biomolecular NMR* **49**, 297-305.

Grosser, B.I., Monti-Bloch, L., Jennings-White, C. and Berliner, D.L. (2000) Behavioral and electrophysiological effects of androstadienone, a human pheromone. *Psychoneuroendocrinology* **25**, 289-299.

Guillon, J., Coste, S., Guffon-Fouilhoux, N., Cohen, S., Manchond, M. and Guillaumont, M. (2009) Rapid quantification of miglustat in human plasma and cerebrospinal fluid by liquid chromatography coupled with tandem mass spectrometry. *Journal of Chromatography B-Analytical Technologies in the Biomedical and Life Sciences* **877**, 149-154.

Guo, Y. and Gaiki, S. (2005) Retention behavior of small polar compounds on polar stationary phases in hydrophilic interaction chromatography. *Journal of Chromatography A* **1074**, 71-80.

Guo, Y., Srinivasan, S. and Gaiki, S. (2007) Investigating the effect of chromatographic conditions on retention of organic acids in hydrophilic interaction chromatography using a design of experiment. *Chromatographia* **66**, 223-229.

Hager, J.W. (2002) A new linear ion trap mass spectrometer. *Rapid Communications in Mass Spectrometry* **16**, 512-526.

Hager, J.W. and Le Blanc, J.C.Y. (2003) Product ion scanning using a Q-q-Q_{linear} ion trap (Q TRAPTM) mass spectrometer. *Rapid Communications in Mass Spectrometry* **17**, 1056-1064.

Harker, M., Coulson, H., Fairweather, I., Taylor, D. and Daykin, C.A. (2006) Study of metabolite composition of eccrine sweat from healthy male and female human subjects by ¹H NMR spectroscopy. *Metabolomics* **2**, 105-112.

Harvey, C.J., LeBouf, R.F. and Stefaniak, A.B. (2010) Formulation and stability of a novel artificial human sweat under conditions of storage and use. *Toxicology in Vitro* **24**, 1790-1796.

Hasegawa, Y., Yabuki, M. and Matsukane, M. (2004) Identification of new odoriferous compounds in human axillary sweat. *Chemistry & Biodiversity* **1**, 2042-2050.

Hastie, T., Tibshirani, R. and Friedman, J. (2001) *The elements of statistical learning: Data mining, inference and prediction*. Springer-Verlag, Berlin.

Heemers, H., Vanderhoydonc, F., Roskams, T., Shechter, I., Heyns, W., Verhoeven, G. and Swinnen, J.V. (2003) Androgens stimulate coordinated lipogenic gene expression in normal target tissues in vivo. *Molecular and Cellular Endocrinology* **205**, 21-31.

Heller, D.N. and Nochetto, C.B. (2008) Simultaneous determination and confirmation of melamine and cyanuric acid in animal feed by zwitterionic hydrophilic interaction chromatography and tandem mass spectrometry. *Rapid Commun Mass Spectrom* **22**, 3624-32.

Hemstrom, P. and Irgum, K. (2006) Hydrophilic interaction chromatography. *Journal of Separation Science* **29**, 1784-1821.

Herbreteau, B., Lafosse, M., Morinallory, L. and Dreux, M. (1992) High-performance liquid-chromatography of raw sugars and polyols using bonded silica-gels. *Chromatographia* **33**, 325-330.

Herebian, D., Choi, J.H., El-Aty, A.M.A., Shim, J.H. and Spiteller, M. (2009a) Metabolite analysis in *Curcuma domestica* using various GC-MS and LC-MS separation and detection techniques. *Biomedical Chromatography* **23**, 951-965.

Herebian, D., Zuhlke, S., Lamshoft, M. and Spiteller, M. (2009b) Multi-mycotoxin analysis in complex biological matrices using LC-ESI/MS: Experimental study using triple stage quadrupole and LTQ-Orbitrap. *Journal of Separation Science* **32**, 939-948.

Hmelnickis, J., Pugovics, O., Kazoka, H., Viksna, A., Susinskis, I. and Kokums, K. (2008) Application of hydrophilic interaction chromatography for simultaneous separation of six impurities of mildronate substance. *Journal of Pharmaceutical and Biomedical Analysis* **48**, 649-656.

Hodson, M.P., Dear, G.J., Roberts, A.D., Haylock, C.L., Ball, R.J., Plumb, R.S., Stumpf, C.L., Griffin, J.L. and Haselden, J.N. (2007) A gender-specific discriminator in Sprague-Dawley rat urine: The deployment of a metabolic profiling strategy for biomarker discovery and identification. *Analytical Biochemistry* **362**, 182-192.

Hoffmann, E. and Stroobant, V. (2001) *Mass spectrometry principles and applications*, 2nd edn. Wiley-Blackwell.

Hogenboom, A.C., van Leerdam, J.A. and de Voogt, P. (2009) Accurate mass screening and identification of emerging contaminants in environmental samples by liquid chromatography-hybrid linear ion trap Orbitrap mass spectrometry. *Journal of Chromatography A* **1216**, 510-519.

Hollywood, K., Brison, D.R. and Goodacre, R. (2006) Metabolomics: Current technologies and future trends. *Proteomics* **6**, 4716-4723.

Holmes, E. and Antti, H. (2002) Chemometric contributions to the evolution of metabonomics: mathematical solutions to characterising and interpreting complex biological NMR spectra. *Analyst* **127**, 1549-1557.

Holmes, E., Nicholson, J.K., Nicholls, A.W., Lindon, J.C., Connor, S.C., Polley, S. and Connelly, J. (1997). The identification of novel biomarkers of renal toxicity using automatic data reduction techniques and PCA of proton NMR spectra of urine. *5th Scandinavian Symposium on Chemometrics (SSC5)*. Lathi, Finland, pp. 245-255.

Holmes, E., Tsang, T.M., Huang, J.T.J., Leweke, F.M., Koethe, D., Gerth, C.W., Nolden, B.M., Gross, S., Schreiber, D., Nicholson, J.K. and Bahn, S. (2006) Metabolic profiling of CSF: Evidence that early intervention may impact on disease progression and outcome in schizophrenia. *Plos Medicine* **3**, 1420-1428.

Hoogerbrugge, R., Willig, S.J. and Kistemaker, P.G. (1983) Discriminant-analysis by double stage principal component analysis. *Analytical Chemistry* **55**, 1710-1712.

Hoskins, J.M., Carey, L.A. and McLeod, H.L. (2009) CYP2D6 and tamoxifen: DNA matters in breast cancer. *Nature Reviews Cancer* **9**, 576-586.

Hozumi, Y., Kawano, M., Saito, T. and Miyata, M. (1998) Effect of tamoxifen on serum lipid metabolism. *Journal of Clinical Endocrinology & Metabolism* **83**, 1633-1635.

Hsieh, Y.S., Galviz, G., Zhou, Q. and Duncan, C. (2009) Hydrophilic interaction liquid chromatography/tandem mass spectrometry for the simultaneous determination of dasatinib, imatinib and nilotinib in mouse plasma. *Rapid Communications in Mass Spectrometry* **23**, 1364-1370.

Hu, Q.Z., Noll, R.J., Li, H.Y., Makarov, A., Hardman, M. and Cooks, R.G. (2005) The Orbitrap: A new mass spectrometer. *Journal of Mass Spectrometry* **40**, 430-443.

Huang, L.S., Marzan, F., Jayewardene, A.L., Lizak, P.S., Li, X.H. and Aweeka, F.T. (2009) Development and validation of a hydrophilic interaction liquid chromatography-tandem mass spectrometry method for determination of isoniazid in human plasma. *Journal of Chromatography B-Analytical Technologies in the Biomedical and Life Sciences* **877**, 285-290.

Idborg-Bjorkman, H., Edlund, P.O., Kvalheim, O.M., Schuppe-Koistinen, I. and Jacobsson, S.P. (2003) Screening of biomarkers in rat urine using LC/electrospray ionization-MS and two-way data analysis. *Analytical Chemistry* **75**, 4784-4792.

Idborg, H., Zamani, L., Edlund, P.O., Schuppe-Koistinen, I. and Jacobsson, S.P. (2005) Metabolic fingerprinting of rat urine by LC/MS Part 1. Analysis by hydrophilic interaction liquid chromatography-electrospray ionization mass spectrometry. *Journal of Chromatography B-Analytical Technologies in the Biomedical and Life Sciences* **828**, 9-13.

Inaba, M. and Inaba, Y. (1992) *Human body odor*. Springer-Verlag, Tokyo (Japan).

Jacob, S., Garcia, S., Hayreh, D. and McClintock, M.K. (2002) Psychological effects of musky compounds: Comparison of androstadienone with androstenol and muscone. *Hormones and Behavior* **42**, 274-283.

Jacob, S., Kinnunen, L.H., Metz, J., Cooper, M. and McClintock, M.K. (2001) Sustained human chemosignal unconsciously alters brain function. *Neuroreport* **12**, 2391-2394.

Jacoby, R.B., Brahms, J.C., Ansari, S.A. and Mattai, J. (2004) Detection and quantification of apocrine secreted odor-binding protein on intact human axillary skin. *International Journal of Cosmetic Science* **26**, 37-46.

Jahnke, W. (1996) Spatial aspects of radiofrequency inhomogeneity in high-resolution NMR and their consideration in improving isotope-editing experiments. *Journal of Magnetic Resonance Series B* **113**, 262-266.

James, A.G., Casey, J., Hyliands, D. and Mycock, G. (2004) Fatty acid metabolism by cutaneous bacteria and its role in axillary malodour. *World Journal of Microbiology & Biotechnology* **20**, 787-793.

Jander, G., Norris, S.R., Joshi, V., Fraga, M., Rugg, A., Yu, S.X., Li, L.L. and Last, R.L. (2004) Application of a high-throughput HPLC-MS/MS assay to Arabidopsis mutant screening; evidence that threonine aldolase plays a role in seed nutritional quality. *Plant Journal* **39**, 465-475.

Jauregui, O., Sierra, A.Y., Carrasco, P., Gratacos, E., Hegardt, F.G. and Casals, N. (2007) A new LC-ESI-MS/MS method to measure long-chain acylcarnitine levels in cultured cells. *Analytica Chimica Acta* **599**, 1-6.

Jeong, D.W., Kim, Y.H., Ji, H.Y., Youn, Y.S.E., Lee, K.C. and Lee, H.S. (2007) Analysis of carvedilol in human plasma using hydrophilic interaction liquid chromatography with tandem mass spectrometry. *Journal of Pharmaceutical and Biomedical Analysis* **44**, 547-552.

Ji, H.Y., Park, E.J., Lee, K.C. and Lee, H.S. (2008) Quantification of doxazosin in human plasma using hydrophilic interaction liquid chromatography with tandem mass spectrometry. *Journal of Separation Science* **31**, 1628-1633.

Jin, M.L., Dong, Q., Dong, R. and Jin, W.R. (2001) Direct electrochemical determination of pyruvate in human sweat by capillary zone electrophoresis. *Electrophoresis* **22**, 2793-2796.

Kaderbhai, N.N., Broadhurst, D.I., Ellis, D.I., Goodacre, R. and Kell, D.B. (2003) Functional genomics via metabolic footprinting: monitoring metabolite secretion by *Escherichia coli* tryptophan metabolism mutants using FT-IR and direct injection electrospray mass spectrometry. *Comparative and Functional Genomics* **4**, 376-391.

Kaiser, D., Songowil, R. and Drack, E. (1974) Hydrogen ion and electrolyte excretion of the single human sweat gland. *Pflugers Archiv-European Journal of Physiology* **349**, 63-72.

Kamleh, A., Barrett, M.P., Wildridge, D., Burchmore, R.J.S., Scheltema, R.A. and Watson, D.G. (2008) Metabolomic profiling using orbitrap fourier transform mass spectrometry with hydrophilic interaction chromatography: a method with wide applicability to analysis of biomolecules. *Rapid Communications in Mass Spectrometry* **22**, 1912-1918.

Kassidas, A., MacGregor, J.F. and Taylor, P.A. (1998) Synchronization of batch trajectories using dynamic time warping. *AIChE Journal* **44**, 864-875.

Katajamaa, M. and Oresic, M. (2005) Processing methods for differential analysis of LC/MS profile data. *BMC Bioinformatics* **6**, 12.

Kato, M., Kato, H., Eyama, S. and Takatsu, A. (2009) Application of amino acid analysis using hydrophilic interaction liquid chromatography coupled with isotope dilution mass spectrometry for peptide and protein quantification. *Journal of Chromatography B-Analytical Technologies in the Biomedical and Life Sciences* **877**, 3059-3064.

Kebarle, P. and Verkerk, U.H. (2009) Electrospray: from ions in solution to ions in the gas phase, what we know now. *Mass Spectrometry Reviews* **28**, 898-917.

Keeler, J. (2010) *Understanding NMR Spectroscopy* 2nd edn. John Wiley & Sons New York.

Kell, D.B. (2004) Metabolomics and systems biology: Making sense of the soup. *Current Opinion in Microbiology* **7**, 296-307.

Kind, T. and Fiehn, O. (2007) Seven golden rules for heuristic filtering of molecular formulas obtained by accurate mass spectrometry. *BMC Bioinformatics* **8**, 1-20.

Kind, T., Tolstikov, V., Fiehn, O. and Weiss, R.H. (2007) A comprehensive urinary metabolomic approach for identifying kidney cancer. *Analytical Biochemistry* **363**, 185-195.

King, R., Bonfiglio, R., Fernandez-Metzler, C., Miller-Stein, C. and Olah, T. (2000) Mechanistic investigation of ionization suppression in electrospray ionization. *Journal of the American Society for Mass Spectrometry* **11**, 942-950.

Kovacs, H., Moskau, D. and Spraul, M. (2005) Cryogenically cooled probes - a leap in NMR technology. *Progress in Nuclear Magnetic Resonance Spectroscopy* **46**, 131-155.

Kuhn, F. and Natsch, A. (2009) Body odour of monozygotic human twins: a common pattern of odorant carboxylic acids released by a bacterial aminoacylase from axilla secretions contributing to an inherited body odour type. *Journal of the Royal Society Interface* **6**, 377-392.

Kulik, W. and Heerma, W. (1988) A study of the positive and negative-ion fast atom bombardment mass-spectra of alpha-amino-acids. *Biomedical and Environmental Mass Spectrometry* **15**, 419-427.

Labows, J.N., Preti, G., Hoelzle, E., Leyden, J. and Kligman, A. (1979) Steroid analysis of human apocrine secretion. *Steroids* **34**, 249-258.

Labrie, F. (1991) Intracrinology. *Molecular and Cellular Endocrinology* **78**, C113-C118.

Lacey, M.E., Subramanian, R., Olson, D.L., Webb, A.G. and Sweedler, J.V. (1999) High-resolution NMR spectroscopy of sample volumes from 1 nL to 10 μ L. *Chemical Reviews* **99**, 3133-3152.

Lakso, H.A., Appelblad, P. and Schneede, J. (2008) Quantification of methylmalonic acid in human plasma with hydrophilic interaction liquid chromatography separation and mass spectrometric detection. *Clinical Chemistry* **54**, 2028-2035.

Lammerhofer, M., Richter, M., Wu, J.Y., Nogueira, R., Bicker, W. and Lindner, W. (2008) Mixed-mode ion-exchangers and their comparative chromatographic characterization in reversed-phase and hydrophilic interaction chromatography elution modes. *Journal of Separation Science* **31**, 2572-2588.

Lamont, L.S. (1987) Sweat lactate secretion during exercise in relation to womens aerobic capacity. *Journal Of Applied Physiology* **62**, 194-198.

Langrock, T., Czihal, P. and Hoffmann, R. (2006) Amino acid analysis by hydrophilic interaction chromatography coupled on-line to electrospray ionization mass spectrometry. *Amino Acids* **30**, 291-297.

Lanza, I.R., Zhang, S.C., Ward, L.E., Karakelides, H., Raftery, D. and Nair, K.S. (2010) Quantitative metabolomics by ^1H -NMR and LC-MS/MS confirms altered metabolic pathways in diabetes. *Plos One* **5**, 1-10.

Leake, C.D. (1922) The occurrence of citric acid in sweat. *American Journal of Physiology* **63**, 540-544.

Lee, G.C. and Woodruff, D.L. (2004) Beam search for peak alignment of NMR signals. *Analytica Chimica Acta* **513**, 413-416.

Lelliott, C.J., Lopez, M., Curtis, R.K., Parker, N., Laudes, M., Yeo, G., Jimenez-Linan, M., Grosse, J., Saha, A.K., Wiggins, D., Hauton, D., Brand, M.D., O'Rahilly, S., Griffin, J.L., Gibbons, G.F. and Vidal-Puig, A. (2005) Transcript and metabolite analysis of the effects of tamoxifen in rat liver reveals inhibition of fatty acid synthesis in the presence of hepatic steatosis. *Faseb Journal* **19**, 1108-1119.

Lenz, E.M., Bright, J., Knight, R., Wilson, I.D. and Major, H. (2004) A metabonomic investigation of the biochemical effects of mercuric chloride in the rat using ^1H -NMR and HPLC-TOF/MS: time dependant changes in the urinary profile of endogenous metabolites as a result of nephrotoxicity. *Analyst* **129**, 535-541.

Lenz, E.M., Bright, J., Wilson, I.D., Morgan, S.R. and Nash, A.F.P. (2003) A ^1H -NMR-based metabonomic study of urine and plasma samples obtained from healthy human subjects. *Journal of Pharmaceutical and Biomedical Analysis* **33**, 1103-1115.

Lenz, E.M., Williams, R.E., Sidaway, J., Smith, B.W., Plumb, R.S., Johnson, K.A., Rainville, P., Shockcor, J., Stumpf, C.L., Granger, J.H. and Wilson, I.D. (2007) The application of microbore UPLC/oa-TOF-MS and ^1H NMR spectroscopy to the

metabonomic analysis of rat urine following the intravenous administration of pravastatin. *Journal of Pharmaceutical and Biomedical Analysis* **44**, 845-852.

Lenz, E.M. and Wilson, I.D. (2007) Analytical strategies in metabonomics. *Journal of Proteome Research* **6**, 443-458.

Leyden, J.J., McGinley, K.J., Holze, E., Labows, J.N. and Kligman, A.M. (1981) The microbiology of the human axilla and its relationship to axillary odor. *Journal of Investigative Dermatology* **77**, 413-416.

Li, R.P. and Huang, J.X. (2004) Chromatographic behavior of epirubicin and its analogues on high-purity silica in hydrophilic interaction chromatography. *Journal of Chromatography A* **1041**, 163-169.

Liappis, N. and Hungerla, H. (1972) Quantitative study of free amino acids in human eccrine sweat during normal conditions and exercise. *American Journal of Clinical Nutrition* **25**, 661-663.

Lin, C.Y., Wu, H.F., Tjeerdema, R.S. and Viant, M.R. (2007) Evaluation of metabolite extraction strategies from tissue samples using NMR metabolomics. *Metabolomics* **3**, 55-67.

Lindegardh, N., Hanpithakpong, W., Wattanagoon, Y., Singhasivanon, P., White, N.J. and Day, N.P.J. (2007) Development and validation of a liquid chromatographic-tandem mass spectrometric method for determination of oseltamivir and its metabolite oseltamivir carboxylate in plasma, saliva and urine. *Journal of Chromatography B-Analytical Technologies in the Biomedical and Life Sciences* **859**, 74-83.

Lindon, J.C., Beckonert, O.P., Holmes, E. and Nicholson, J.K. (2009) High-resolution magic angle spinning NMR spectroscopy: Application to biomedical studies. *Progress in Nuclear Magnetic Resonance Spectroscopy* **55**, 79-100.

Lindon, J.C., Holmes, E., Bollard, M.E., Stanley, E.G. and Nicholson, J.K. (2004) Metabonomics technologies and their applications in physiological monitoring, drug safety assessment and disease diagnosis. *Biomarkers* **9**, 1-31.

Lindon, J.C., Holmes, E. and Nicholson, J.K. (2003a) So what's the deal with metabonomics? Metabonomics measures the fingerprint of biochemical perturbations caused by disease, drugs, and toxins. *Analytical Chemistry* **75**, 384A-391A.

Lindon, J.C., Holmes, E. and Nicholson, J.K. (2006) Metabonomics techniques and applications to pharmaceutical research & development. *Pharmaceutical Research* **23**, 1075-1088.

Lindon, J.C. and Nicholson, J.K. (2008) Spectroscopic and Statistical Techniques for Information Recovery in Metabonomics and Metabolomics. *Annual Review of Analytical Chemistry* **1**, 45-69.

Lindon, J.C., Nicholson, J.K., Holmes, E., Antti, H., Bollard, M.E., Keun, H., Beckonert, O., Ebbels, T.M., Reilly, M.D., Robertson, D., Stevens, G.J., Luke, P.,

Breau, A.P., Cantor, G.H., Bible, R.H., Niederhauser, U., Senn, H., Schlotterbeck, G., Sidelmann, U.G., Laursen, S.M., Tymiak, A., Car, B.D., Lehman-McKeeman, L., Colet, J.M., Loukaci, A. and Thomas, C. (2003b) Contemporary issues in toxicology - The role of metabonomics in toxicology and its evaluation by the COMET project. *Toxicology and Applied Pharmacology* **187**, 137-146.

Lindon, J.C., Nicholson, J.K., Holmes, E. and Everett, J.R. (2000) Metabonomics: Metabolic processes studied by NMR spectroscopy of biofluids. *Concepts in Magnetic Resonance* **12**, 289-320.

Lindon, J.C., Nicholson, J.K. and Wilson, I.D. (1996) Direct coupling of chromatographic separations to NMR spectroscopy. *Progress in Nuclear Magnetic Resonance Spectroscopy* **29**, 1-49.

Liu, M.L., Nicholson, J.K., Parkinson, J.A. and Lindon, J.C. (1997) Measurement of biomolecular diffusion coefficients in blood plasma using two-dimensional ^1H - ^1H diffusion-edited total-correlation NMR spectroscopy. *Analytical Chemistry* **69**, 1504-1509.

Liu, Y.H., Zhang, W.H. and Yang, Y.H. (2008a) Validated hydrophilic interaction LC-MS/MS method for simultaneous quantification of dacarbazine and 5-amino-4-imidazole-carboxamide in human plasma. *Talanta* **77**, 412-421.

Liu, Z., Mutlib, A.E., Wang, J.Y. and Talaat, R.E. (2008b) Liquid chromatography/mass spectrometry determination of endogenous plasma acetyl and palmitoyl carnitines as potential biomarkers of beta-oxidation in mice. *Rapid Communications in Mass Spectrometry* **22**, 3434-3442.

Locke, W., Talbot, N.B., Jones, H.S. and Worcester, J. (1951) Studies on the combined use of measurements of sweat electrolyte composition and rate of sweating as an index of adrenal cortical activity. *Journal of Clinical Investigation* **30**, 325-337.

Lommen, A. (2009) MetAlign: Interface-driven, versatile metabolomics tool for hyphenated full-scan mass spectrometry data preprocessing. *Analytical Chemistry* **81**, 3079-3086.

Lonsdale-Eccles, A., Leonard, N. and Lawrence, C. (2003) Axillary hyperhidrosis: Eccrine or apocrine? *Clinical and Experimental Dermatology* **28**, 2-7.

Love, R.R., Mazess, R.B., Barden, H.S., Epstein, S., Newcomb, P.A., Jordan, V.C., Carbone, P.P. and Demets, D.L. (1992) Effects of tamoxifen on bone mineral density in postmenopausal women with breast cancer. *New England Journal of Medicine* **326**, 852-856.

Lundstrom, J.N., McClintock, M.K. and Olsson, M.J. (2006) Effects of reproductive state on olfactory sensitivity suggest odor specificity. *Biological Psychology* **71**, 244-247.

- Luo, R.S., Liu, M.L. and Mao, X.A. (1999) NMR diffusion and relaxation study of drug-protein interaction. *Spectrochimica Acta Part a-Molecular and Biomolecular Spectroscopy* **55**, 1897-1901.
- Lynch, M.J., Masters, J., Pryor, J.P., Lindon, J.C., Spraul, M., Foxall, P.J.D. and Nicholson, J.K. (1994) Ultra high field NMR spectroscopic studies on human seminal fluid seminal vesicle and prostatic secretions. *Journal of Pharmaceutical and Biomedical Analysis* **12**, 5-19.
- Maharjan, R.P. and Ferenci, T. (2003) Global metabolite analysis: The influence of extraction methodology on metabolome profiles of *Escherichia coli*. *Analytical Biochemistry* **313**, 145-154.
- Makarov, A. (2000) Electrostatic axially harmonic orbital trapping: A high-performance technique of mass analysis. *Analytical Chemistry* **72**, 1156-1162.
- Makarov, A., Denisov, E., Lange, O. and Horning, S. (2006) Dynamic range of mass accuracy in LTQ Orbitrap hybrid mass spectrometer. *Journal of the American Society for Mass Spectrometry* **17**, 977-982.
- Mantini, A., Di Natale, C., Macagnano, A., Paolesse, R., Finazzi-Agro, A. and D'Amico, A. (2000) Biomedical application of an electronic nose. *Critical Reviews in Biomedical Engineering* **28**, 481-485.
- Martin, A., Saathoff, M., Kuhn, F., Max, H., Terstegen, L. and Natsch, A. (2010) A functional ABCC11 allele is essential in the biochemical formation of human axillary odor. *Journal of Investigative Dermatology* **130**, 529-540.
- Martin, G.E. and Hadden, C.E. (1999) Comparison of 1.7 mm submicro and 3 mm micro gradient NMR probes for the acquisition of ^1H - ^{13}C and ^1H - ^{15}N heteronuclear shift correlation data. *Magnetic Resonance in Chemistry* **37**, 721-729.
- Mas, S., Villas-Boas, S.G., Hansen, M.E., Akesson, M. and Nielsen, J. (2007) A comparison of direct infusion MS and GC-MS for metabolic footprinting of yeast mutants. *Biotechnology and Bioengineering* **96**, 1014-1022.
- Massart, D.L. and Kaufman, P. (1983) *The interpretation of analytical chemical data by the use of cluster analysis*. John Wiley and Sons, New York.
- Mauri, P. and Pietta, P. (2000) Electrospray characterization of selected medicinal plant extracts. *Journal of Pharmaceutical and Biomedical Analysis* **23**, 61-68.
- McCalley, D.V. (2007) Is hydrophilic interaction chromatography with silica columns a viable alternative to reversed-phase liquid chromatography for the analysis of ionisable compounds? *Journal of Chromatography A* **1171**, 46-55.
- McCalley, D.V. (2010) Study of the selectivity, retention mechanisms and performance of alternative silica-based stationary phases for separation of ionised solutes in hydrophilic interaction chromatography. *Journal of Chromatography A* **1217**, 3408-3417.

McClintock, M.K. (1978) Estrous synchrony and its mediation by airborne chemical communication (*Rattus-Norvegicus*). *Hormones and Behavior* **10**, 264-276.

McLuckey, S.A. and Wells, J.M. (2001) Mass analysis at the advent of the 21st century. *Chemical Reviews* **101**, 571-606.

McMaster, M.C. (2005) *LC/MS: A practical user's guide*. John Wiley & Sons, New Jersey.

Medek, A., Hajduk, P.J., Mack, J. and Fesik, S.W. (2000) The use of differential chemical shifts for determining the binding site location and orientation of protein-bound ligands. *Journal of the American Chemical Society* **122**, 1241-1242.

Meiboom, S. and Gill, D. (1958) Modified spin-echo method for measuring nuclear relaxation times. *Review of Scientific Instruments* **29**, 688-691.

Menon, G.K. and Kligman, A.M. (2009) Barrier functions of human skin: A holistic view. *Skin Pharmacology and Physiology* **22**, 178-189.

Meyer, F., Laitano, O., Bar-Or, O., McDougall, D. and Heingenhauser, G.J.F. (2007) Effect of age and gender on sweat lactate and ammonia concentrations during exercise in the heat. *Brazilian Journal Of Medical And Biological Research* **40**, 135-143.

Montagna, W., Chase, H.B. and Lobitz, W.C. (1953) Histology and cytochemistry of human skin. V. Axillary apocrine sweat glands. *American Journal of Anatomy* **92**, 451-470.

Mosher, H.H. (1933) Simultaneous study of constituents of urine and perspiration. *Journal of Biological Chemistry* **99**, 781-790.

Nagayama, K., Kumar, A., Wuthrich, K. and Ernst, R.R. (1980) Experimental-techniques of two-dimensional correlated spectroscopy. *Journal of Magnetic Resonance* **40**, 321-334.

Natsch, A., Derrer, S., Flachsmann, F. and Schmid, J. (2006) A broad diversity of volatile carboxylic acids, released by a bacterial aminoacylase from axilla secretions, as candidate molecules for the determination of human-body odor type. *Chemistry & Biodiversity* **3**, 1-20.

Natsch, A., Gfeller, H., Gyax, P., Schmid, J. and Acuna, G. (2003) A specific bacterial aminoacylase cleaves odorant precursors secreted in the human axilla. *Journal of Biological Chemistry* **278**, 5718-5727.

Natsch, A., Kuhn, F. and Tiercy, J.M. (2010) Lack of evidence for HLA-linked patterns of odorous carboxylic acids released from glutamine conjugates secreted in the human axilla. *Journal Of Chemical Ecology* **36**, 837-846.

- Natsch, A., Schmid, J. and Flachsmann, F. (2004) Identification of odoriferous sulfanylalkanols in human axilla secretions and their formation through cleavage of cysteine precursors by a C-S lyase isolated from axilla bacteria. *Chemistry & Biodiversity* **1**, 1058-1072.
- Nguyen, H.P. and Schug, K.A. (2008) The advantages of ESI-MS detection in conjunction with HILIC mode separations: Fundamentals and applications. *Journal of Separation Science* **31**, 1465-1480.
- Nicholson, J.K., Buckingham, M.J. and Sadler, P.J. (1983) High-resolution ^1H -NMR studies of vertebrate blood and plasma. *Biochemical Journal* **211**, 605-615.
- Nicholson, J.K., Connelly, J., Lindon, J.C. and Holmes, E. (2002) Metabonomics: A platform for studying drug toxicity and gene function. *Nature Reviews Drug Discovery* **1**, 153-161.
- Nicholson, J.K., Foxall, P.J.D., Spraul, M., Farrant, R.D. and Lindon, J.C. (1995) 750-MHz ^1H and ^1H - ^{13}C NMR spectroscopy of human blood plasma. *Analytical Chemistry* **67**, 793-811.
- Nicholson, J.K., Lindon, J.C. and Holmes, E. (1999) 'Metabonomics': Understanding the metabolic responses of living systems to pathophysiological stimuli via multivariate statistical analysis of biological NMR spectroscopic data. *Xenobiotica* **29**, 1181-1189.
- Nordstrom, A., O'Maille, G., Qin, C. and Siuzdak, G. (2006) Nonlinear data alignment for UPLC-MS and HPLC-MS based metabolomics: Quantitative analysis of endogenous and exogenous metabolites in human serum. *Analytical Chemistry* **78**, 3289-3295.
- Novakova, L., Solichova, D., Pavlovicova, S. and Solich, P. (2008) Hydrophilic interaction liquid chromatography method for the determination of ascorbic acid. *Journal of Separation Science* **31**, 1634-1644.
- Olsen, B.A. (2001) Hydrophilic interaction chromatography using amino and silica columns for the determination of polar pharmaceuticals and impurities. *Journal of Chromatography A* **913**, 113-122.
- Olson, D.L., Lacey, M.E. and Sweedler, J.V. (1998) High-resolution microcoil NMR for analysis of mass-limited, nanoliter samples. *Analytical Chemistry* **70**, 645-650.
- Olson, D.L., Norcross, J.A., O'Neil-Johnson, M., Molitor, P.F., Detlefsen, D.J., Wilson, A.G. and Peck, T.L. (2004) Microflow NMR: Concepts and capabilities. *Analytical Chemistry* **76**, 2966-2974.
- Olsson, M., Madsen, T., Nordby, J., Wapstra, E., Ujvari, B. and Wittsell, H. (2003) Major histocompatibility complex and mate choice in sand lizards. *Proceedings of the Royal Society of London Series B-Biological Sciences* **270**, S254-S256.

Ortori, C.A., Atkinson, S., Chhabra, S.R., Camara, M., Williams, P. and Barrett, D.A. (2007) Comprehensive profiling of N-acylhomoserine lactones produced by *Yersinia pseudotuberculosis* using liquid chromatography coupled to hybrid quadrupole-linear ion trap mass spectrometry. *Analytical and Bioanalytical Chemistry* **387**, 497-511.

Overy, S.A., Walker, H.J., Malone, S., Howard, T.P., Baxter, C.J., Sweetlove, L.J., Hill, S.A. and Quick, W.P. (2005) Application of metabolite profiling to the identification of traits in a population of tomato introgression lines. *Journal of Experimental Botany* **56**, 287-296.

Patterson, M.J., Galloway, S.D.R. and Nimmo, M.A. (2000) Variations in regional sweat composition in normal human males. *Experimental Physiology* **85**, 869-875.

Peck, T.L., Magin, R.L. and Lauterbur, P.C. (1995) Design and analysis of microcoils for NMR microscopy. *Journal of Magnetic Resonance Series B* **108**, 114-124.

Pellecchia, M., Meininger, D., Dong, Q., Chang, E., Jack, R. and Sem, D.S. (2002) NMR-based structural characterization of large protein-ligand interactions. *Journal of Biomolecular Nmr* **22**, 165-173.

Penn, D. and Potts, W. (1998a) How do major histocompatibility complex genes influence odor and mating preferences?, *Advances in Immunology, Vol 69*, Academic Press Inc, San Diego. pp. 411-436.

Penn, D. and Potts, W.K. (1998b) Chemical signals and parasite-mediated sexual selection. *Trends in Ecology & Evolution* **13**, 391-396.

Penn, D.J. (2002) The scent of genetic compatibility: Sexual selection and the major histocompatibility complex. *Ethology* **108**, 1-21.

Penn, D.J., Oberzaucher, E., Grammer, K., Fischer, G., Soini, H.A., Wiesler, D., Novotny, M.V., Dixon, S.J., Xu, Y. and Brereton, R.G. (2007) Individual and gender fingerprints in human body odour. *Journal Of The Royal Society Interface* **4**, 331-340.

Penn, D.J. and Potts, W.K. (1999) The evolution of mating preferences and major histocompatibility complex genes. *American Naturalist* **153**, 145-164.

Petritis, K., Chaimbault, P., Elfakir, C. and Dreux, M. (2000). Parameter optimization for the analysis of underivatized protein amino acids by liquid chromatography and ionspray tandem mass spectrometry. *6th International Symposium on Hyphenated Techniques in Chromatography and Hyphenated Chromatographic Analyzers (HTC-6)*. Brugge, Belgium, pp. 253-263.

Picariello, G., Ferranti, P., Mamone, G., Roepstorff, P. and Addeo, F. (2008) Identification of N-linked glycoproteins in human milk by hydrophilic interaction liquid chromatography and mass spectrometry. *Proteomics* **8**, 3833-3847.

Plumb, R.S., Stumpf, C.L., Gorenstein, M.V., Castro-Perez, J.M., Dear, G.J., Anthony, M., Sweatman, B.C., Connor, S.C. and Haselden, J.N. (2002) Metabonomics: the use of electrospray mass spectrometry coupled to reversed-phase

liquid chromatography shows potential for the screening of rat urine in drug development. *Rapid Communications in Mass Spectrometry* **16**, 1991-1996.

Powles, T.J., Hardy, J.R., Ashley, S.E., Farrington, G.M., Cosgrove, D., Davey, J.B., Dowsett, M., McKinna, J.A., Nash, A.G., Sinnett, H.D., Tillyer, C.R. and Treleaven, J.G. (1989) A pilot trial to evaluate the acute toxicity and feasibility of tamoxifen for prevention of breast cancer. *British Journal of Cancer* **60**, 126-131.

Preti, G., Wysocki, C.J., Barnhart, K.T., Sondheimer, S.J. and Leyden, J.J. (2003) Male axillary extracts contain pheromones that affect pulsatile secretion of luteinizing hormone and mood in women recipients. *Biology of Reproduction* **68**, 2107-2113.

Pullen, F.S., Swanson, A.G., Newman, M.J. and Richards, D.S. (1995) Online liquid-chromatography nuclear-magnetic-resonance mass-spectrometry - A powerful spectroscopic tool for the analysis of mixtures of pharmaceutical interest. *Rapid Communications in Mass Spectrometry* **9**, 1003-1006.

Qin, F., Zhao, Y.Y., Sawyer, M.B. and Li, X.F. (2008) Hydrophilic interaction liquid chromatography-tandem mass spectrometry determination of estrogen conjugates in human urine. *Analytical Chemistry* **80**, 3404-3411.

Qu, J., Chen, W., Luo, G., Wang, Y.M., Xiao, S.Y., Ling, Z. and Chen, G.Q. (2002) Rapid determination of underivatized pyroglutamic acid, glutamic acid, glutamine and other relevant amino acids in fermentation media by LC-MS-MS. *Analyst* **127**, 66-69.

Rabi, II (1937) Space quantization in a gyrating magnetic field. *Physical Review* **51**, 0652-0654.

Rashed, M.S. (2001) Clinical applications of tandem mass spectrometry: ten years of diagnosis and screening for inherited metabolic diseases. *Journal of Chromatography B-Analytical Technologies in the Biomedical and Life Sciences* **758**, 27-48.

Rashed, M.S., Bucknall, M.P., Little, D., Awad, A., Jacob, M., Alamoudi, M., Alwattar, M. and Ozand, P.T. (1997) Screening blood spots for inborn errors of metabolism by electrospray tandem mass spectrometry with a microplate batch process and a computer algorithm for automated flagging of abnormal profiles. *Clinical Chemistry* **43**, 1129-1141.

Reusch, T.B.H., Haberli, M.A., Aeschlimann, P.B. and Milinski, M. (2001) Female sticklebacks count alleles in a strategy of sexual selection explaining MHC polymorphism. *Nature* **414**, 300-302.

Rew, R. and Davis, G. (1990) Netcdf - An interface for scientific-data access. *Ieee Computer Graphics and Applications* **10**, 76-82.

Riggs, B.L. and Hartmann, L.C. (2003) Drug therapy: Selective estrogen-receptor modulators - Mechanisms of action and application to clinical practice. *New England Journal of Medicine* **348**, 618-629.

Rinaldi, P.L. (2004) Three-dimensional solution NMR spectroscopy of complex structures and mixtures. *Analyst* **129**, 687-699.

Roberts, S.C., Gosling, L.M., Spector, T.D., Miller, P., Penn, D.J. and Petrie, M. (2005) Body odor similarity in noncohabiting twins. *Chemical Senses* **30**, 651-656.

Robertson, D.G. (2005) Metabonomics in toxicology: A review. *Toxicological Sciences* **85**, 809-822.

Robinson, S. and Robinson, A.H. (1954) Chemical composition of sweat. *Physiological Reviews* **34**, 202-220.

Robosky, L.C., Reily, M.D. and Avizonis, D. (2007) Improving NMR sensitivity by use of salt-tolerant cryogenically cooled probes. *Analytical and Bioanalytical Chemistry* **387**, 529-532.

Sato, K. and Dobson, R.L. (1970) Regional and individual variations in function of human eccrine sweat gland. *Journal of Investigative Dermatology* **54**, 443-449.

Sato, K. and Dobson, R.L. (1971) Glucose metabolism of the isolated eccrine sweat gland. I. The effects of mecholyl, epinephrine and ouabain. *Journal of Investigative Dermatology* **56**, 272-&.

Sato, K., Kang, W.H., Saga, K. and Sato, K.T. (1989) Biology of sweat glands and their disorders. I. Normal sweat gland function. *Journal of the American Academy of Dermatology* **20**, 537-563.

Sato, K., Leidal, R. and Sato, F. (1987) Morphology and development of an apoeccrine sweat gland in human axillae. *American Journal of Physiology* **252**, R166-R180.

Sato, S., Soga, T., Nishioka, T. and Tomita, M. (2004) Simultaneous determination of the main metabolites in rice leaves using capillary electrophoresis mass spectrometry and capillary electrophoresis diode array detection. *Plant Journal* **40**, 151-163.

Savage, A.K., Tucker, G., Van Duynhoven, J.P.M. and Daykin, C.A. (2011) Enhanced NMR-based profiling of polyphenols in commercially available grape juices using solid phase extraction. *Magnetic Resonance in Chemistry*.

Savic, I., Berglund, H., Gulyas, B. and Roland, P. (2001) Smelling of odorous sex hormone-like compounds causes sex-differentiated hypothalamic activations in humans. *Neuron* **31**, 661-668.

Schebb, N.H., Fischer, D., Hein, E.M., Hayen, H., Krieglstein, J., Kumpp, S. and Karst, U. (2008) Fast sample preparation and liquid chromatography-tandem mass spectrometry method for assaying cell lysate acetylcholine. *Journal of Chromatography A* **1183**, 100-107.

Schlichtherle-Cerny, H., Affolter, M. and Cerny, C. (2003) Hydrophilic interaction liquid chromatography coupled to electrospray mass spectrometry of small polar compounds in food analysis. *Analytical Chemistry* **75**, 2349-2354.

Schlotterbeck, G., Ross, A., Dieterle, F. and Senn, H. (2006) Metabolic profiling technologies for biomarker discovery in biomedicine and drug development. *Pharmacogenomics* **7**, 1055-1075.

Schlotterbeck, G., Ross, A., Hochstrasser, R., Senn, H., Kuhn, T., Marek, D. and Schett, O. (2002) High-resolution capillary tube NMR. A miniaturized 5- μ L high-sensitivity TXI probe for mass-limited samples, off-line LC NMR, and HT NMR. *Analytical Chemistry* **74**, 4464-4471.

Schroeder, F.C. and Gronquist, M. (2006) Extending the scope of NMR spectroscopy with microcoil probes. *Angewandte Chemie-International Edition* **45**, 7122-7131.

Shehadeh, N. and Kiligman, A.M. (1963) The bacteria responsible for axillary odor. *Journal of Investigative Dermatology* **41**, 1-5.

Shelley, W.B., Hurley, H.J. and Nichols, A.C. (1953) Axillary odor - experimental study of the role of bacteria, apocrine sweat, and deodorants. *Ama Archives of Dermatology and Syphilology* **68**, 430-446.

Shryock, J.C., Rubio, R. and Berne, R.M. (1986) Extraction of adenine-nucleotides from cultured endothelial-cells. *Analytical Biochemistry* **159**, 73-81.

Sitter, B., Bathen, T.F., Tessem, M.B. and Gribbestad, I.S. (2009) High-resolution magic angle spinning (HR MAS) MR spectroscopy in metabolic characterization of human cancer. *Progress in Nuclear Magnetic Resonance Spectroscopy* **54**, 239-254.

Siuzdak, G. (1996) *Mass Spectrometry for Biotechnology*. Academic Press Inc. London.

Smith, K., Thompson, G.F. and Koster, H.D. (1969) Sweat in schizophrenic patients - Identification of odorous substance. *Science* **166**, 398-399.

Snyder, L.R., Glaich, G.L. and Kirkland, J.J. (1988) *Practical HPLC method development*. John Wiley and Sons, USA.

Snyder, L.R. and Poppe, H. (1980) Mechanism of solute retention in liquid solid chromatography and the role of the mobile phase in affecting separation: Competition versus "sorption". *Journal of Chromatography* **184**, 363-413.

Soga, T., Ohashi, Y., Ueno, Y., Naraoka, H., Tomita, M. and Nishioka, T. (2003) Quantitative metabolome analysis using capillary electrophoresis mass spectrometry. *Journal of Proteome Research* **2**, 488-494.

Sommerville, B.A., McCormick, J.P. and Broom, D.M. (1994) Analysis of human sweat volatiles - an example of pattern recognition in the analysis and interpretation of gas chromatograms. *Pesticide Science* **41**, 365-368.

Spielman, A.I., Sunavala, G., Harmony, J.A.K., Stuart, W.D., Leyden, J.J., Turner, G., Vowels, B.R., Lam, W.C., Yang, S.J. and Preti, G. (1998) Identification and immunohistochemical localization of protein precursors to human axillary odors in apocrine glands and secretions. *Archives of Dermatology* **134**, 813-818.

Spielman, A.I., Zeng, X.N., Leyden, J.J. and Preti, G. (1995) Proteinaceous precursors of human axillary odor - Isolation of 2 novel odor-binding proteins. *Experientia* **51**, 40-47.

Spraul, M., Freund, A.S., Nast, R.E., Withers, R.S., Maas, W.E. and Corcoran, O. (2003) Advancing NMR sensitivity for LC-NMR-MS using a cryoflow probe: Application to the analysis of acetaminophen metabolites in urine. *Analytical Chemistry* **75**, 1536-1541.

Spraul, M., Neidig, P., Klauck, U., Kessler, P., Holmes, E., Nicholson, J.K., Sweatman, B.C., Salman, S.R., Farrant, R.D., Rahr, E., Beddell, C.R. and Lindon, J.C. (1994a) Automatic reduction of NMR spectroscopic data for statistical and pattern-recognition classification of samples. *Journal of Pharmaceutical and Biomedical Analysis* **12**, 1215-1225.

Spraul, M., Nicholson, J.K., Lynch, M.J. and Lindon, J.C. (1994b) Application of the 1-dimensional TOCSY pulse sequence in 750 MHz ^1H NMR spectroscopy for assignment of endogenous metabolite resonances in biofluids. *Journal of Pharmaceutical and Biomedical Analysis* **12**, 613-618.

Starkenmann, C., Niclass, Y., Troccaz, M. and Clark, A.J. (2005) Identification of the precursor of (S)-3-methyl-3-sulfanylhexasan-1-ol, the sulfury malodour of human axilla sweat. *Chemistry & Biodiversity* **2**, 705-716.

Starkenmann, C., Troccaz, M. and Howell, K. (2008) The role of cysteine and cysteine-S conjugates as odour precursors in the flavour and fragrance industry. *Flavour and Fragrance Journal* **23**, 369-381.

Stefaniak, A.B. and Harvey, C.J. (2006) Dissolution of materials in artificial skin surface film liquids. *Toxicology in Vitro* **20**, 1265-1283.

Stjohnlyburn, E.F. (1956) A comparison of the composition of sweat induced by dry heat and by wet heat. *Journal of Physiology-London* **134**, 207-215.

Stoyanova, R., Nicholls, A.W., Nicholson, J.K., Lindon, J.C. and Brown, T.R. (2004) Automatic alignment of individual peaks in large high-resolution spectral data sets. *Journal of Magnetic Resonance* **170**, 329-335.

Strege, M.A. (1998) Hydrophilic interaction chromatography electrospray mass spectrometry analysis of polar compounds for natural product drug discovery. *Analytical Chemistry* **70**, 2439-2445.

Sweatman, B.C., Farrant, R.D., Holmes, E., Ghauri, F.Y., Nicholson, J.K. and Lindon, J.C. (1993) 600 MHz ^1H -NMR spectroscopy of human cerebrospinal-fluid -

- effects of sample manipulation and assignment of resonances. *Journal of Pharmaceutical and Biomedical Analysis* **11**, 651-664.
- tKindt, R., Storme, M., Deforce, D. and Van Bocxlaer, J. (2008) Evaluation of hydrophilic interaction chromatography versus reversed-phase chromatography in a plant metabolomics perspective. *Journal of Separation Science* **31**, 1609-1614.
- Takeda, I., Stretch, C., Barnaby, P., Bhatnager, K., Rankin, K., Fu, H., Weljie, A., Jha, N. and Slupsky, C. (2009) Understanding the human salivary metabolome. *Nmr in Biomedicine* **22**, 577-584.
- Takegawa, Y., Ito, H., Keira, T., Deguchi, K., Nakagawa, H. and Nishimura, S.I. (2008) Profiling of N- and O-glycopeptides of erythropoietin by capillary zwitterionic type of hydrophilic interaction chromatography/electrospray ionization mass spectrometry. *Journal of Separation Science* **31**, 1585-1593.
- Tayar, N.E.I., Ruey-Shiuan, T., C., P.-A. and Bernard, T. (1992) Octan-1-ol-water partition coefficients of zwitterionic alpha amino acids determination by centrifugal partition chromatography and factorization into steric hydrophobic and polar components. *Journal of the Chemical Society, Perkin Transactions 2*, 79-84.
- Thomas, M., Monet, J.D., Brami, M., Dautigny, N., Assailly, J., Ulmann, A. and Bader, C.A. (1989) Comparative effects of 17 beta-estradiol, progestin R5020, tamoxifen and RU38486 on lactate dehydrogenase activity in MCF-7 human breast cancer cells. *Journal of Steroid Biochemistry and Molecular Biology* **32**, 271-277.
- Thomson, B.A. and Iribarne, J.V. (1979) Field-induced ion evaporation from liquid surfaces at atmospheric-pressure. *Journal of Chemical Physics* **71**, 4451-4463.
- Toivanen, P., Vaahtovuori, J. and Eerola, E. (2001) Influence of major histocompatibility complex on bacterial composition of fecal flora. *Infection and Immunity* **69**, 2372-2377.
- Tolstikov, V.V. and Fiehn, O. (2002) Analysis of highly polar compounds of plant origin: Combination of hydrophilic interaction chromatography and electrospray ion trap mass spectrometry. *Analytical Biochemistry* **301**, 298-307.
- Tornkvist, A., Nilsson, S., Amirkhani, A., Nyholm, L.M. and Nyholm, L. (2004) Interference of the electrospray voltage on chromatographic separations using porous graphitic carbon columns. *Journal of Mass Spectrometry* **39**, 216-222.
- Troccaz, M., Borchard, G., Vuilleumier, C., Raviot-Derrien, S., Niclass, Y., Beccucci, S. and Starkenmann, C. (2009) Gender-specific differences between the concentrations of nonvolatile (R)/(S)-3-methyl-3-sulfanylhexasan-1-ol and (R)/(S)-3-hydroxy-3-methyl-hexanoic acid odor precursors in axillary secretions. *Chemical Senses* **34**, 203-210.
- Troccaz, M., Starkenmann, C., Niclass, Y., van de Waal, M. and Clark, A.J. (2004) 3-methyl-3-sulfanylhexasan-1-ol as a major descriptor for the human axilla-sweat odour profile. *Chemistry & Biodiversity* **1**, 1022-1035.

Trygg, J., Holmes, E. and Lundstedt, T. (2007) Chemometrics in metabonomics. *Journal of Proteome Research* **6**, 469-479.

Turner, A.P.F. and Magan, N. (2004) Electronic noses and disease diagnostics. *Nature Reviews Microbiology* **2**, 161-166.

Tweeddale, H., Notley-McRobb, L. and Ferenci, T. (1998) Effect of slow growth on metabolism of *Escherichia coli*, as revealed by global metabolite pool ("Metabolome") analysis. *Journal of Bacteriology* **180**, 5109-5116.

Vaidyanathan, S., Kell, D.B. and Goodacre, R. (2002) Flow-injection electrospray ionization mass spectrometry of crude cell extracts for high-throughput bacterial identification. *Journal of the American Society for Mass Spectrometry* **13**, 118-128.

Valette, J.C., Demesmay, C., Rocca, J.L. and Verdon, E. (2004) Separation of tetracycline antibiotics by hydrophilic interaction chromatography using an amino-propyl stationary phase. *Chromatographia* **59**, 55-60.

van den Berg, R.A., Hoefsloot, H.C.J., Westerhuis, J.A., Smilde, A.K. and van der Werf, M.J. (2006) Centering, scaling, and transformations: Improving the biological information content of metabolomics data. *Bmc Genomics* **7**, 15.

Vikingsson, S., Kronstrand, R. and Josefsson, A. (2008) Retention of opioids and their glucuronides on a combined zwitterion and hydrophilic interaction stationary phase. *Journal of Chromatography A* **1187**, 46-52.

Villas-Boas, S.G., Mas, S., Akesson, M., Smedsgaard, J. and Nielsen, J. (2005) Mass spectrometry in metabolome analysis. *Mass Spectrometry Reviews* **24**, 613-646.

Vogels, J., Tas, A.C., Vandenberg, F. and Vandergreef, J. (1993) A new method for classification of wines based on proton and carbon-13 NMR spectroscopy in combination with pattern recognition techniques. *Chemometrics And Intelligent Laboratory Systems* **21**, 249-258.

Walsh, B.W., Schiff, I., Rosner, B., Greenberg, L., Ravnkar, V. and Sacks, F.M. (1991) Effects of postmenopausal estrogen replacement on the concentrations and metabolism of plasma lipoproteins. *New England Journal of Medicine* **325**, 1196-1204.

Wang, C.L., Jiang, C.X. and Armstrong, D.W. (2008) Considerations on HILIC and polar organic solvent-based separations: Use of cyclodextrin and macrocyclic glycopeptide stationary phases. *Journal of Separation Science* **31**, 1980-1990.

Wang, X.D., Li, W.Y. and Rasmussen, H.T. (2005) Orthogonal method development using hydrophilic interaction chromatography and reversed-phase high-performance liquid chromatography for the determination of pharmaceuticals and impurities. *Journal of Chromatography A* **1083**, 58-62.

- Wedekind, C. and Furi, S. (1997) Body odour preferences in men and women: do they aim for specific MHC combinations or simply heterozygosity? *Proceedings of the Royal Society of London Series B-Biological Sciences* **264**, 1471-1479.
- Wedekind, C., Seebeck, T., Bettens, F. and Paepke, A.J. (1995) MHC-dependent mate preferences in humans. *Proceedings of the Royal Society of London Series B-Biological Sciences* **260**, 245-249.
- Weiner, J.S. and Hellmann, K. (1960) The sweat glands. *Biological Reviews of the Cambridge Philosophical Society* **35**, 141-186.
- Weiner, J.S. and Vanheyningen, R.E. (1952) Observations on lactate content of sweat. *Journal of Applied Physiology* **4**, 734-744.
- Weisfeld, G.E., Czilli, T., Phillips, K.A., Gall, J.A. and Lichtman, C.M. (2003) Possible olfaction-based mechanisms in human kin recognition and inbreeding avoidance. *Journal of Experimental Child Psychology* **85**, 279-295.
- Welthagen, W., Shellie, R.A., Spranger, J., Ristow, M., Zimmermann, R. and Fiehn, O. (2005) Comprehensive two-dimensional gas chromatography-time-of-flight mass spectrometry (GC x GC-TOF) for high resolution metabolomics: biomarker discovery on spleen tissue extracts of obese NZO compared to lean C57BL/6 mice. *Metabolomics* **1**, 65-73.
- Wilke, K., Martin, A., Terstegen, L. and Biel, S.S. (2007) A short history of sweat gland biology. *International Journal of Cosmetic Science* **29**, 169-179.
- Wilke, K., Wepf, R., Keil, F.J., Wittern, K.P., Wenck, H. and Biel, S.S. (2006) Are sweat glands an alternate penetration pathway? Understanding the morphological complexity of the axillary sweat gland apparatus. *Skin Pharmacology and Physiology* **19**, 38-49.
- Wilke, K., Wick, K., Keil, F.J., Wittern, K.P., Wepf, R. and Biel, S.S. (2008) A strategy for correlative microscopy of large skin samples: towards a holistic view of axillary skin complexity. *Experimental Dermatology* **17**, 73-80.
- Williams, R.E., Lenz, E.A., Evans, J.A., Wilson, I.D., Granger, J.H., Plumb, R.S. and Stumpf, C.L. (2005a) A combined H-1 NMR and HPLC-MS-based metabonomic study of urine from obese (fa/fa) Zucker and normal Wistar-derived rats. *Journal of Pharmaceutical and Biomedical Analysis* **38**, 465-471.
- Williams, R.E., Lenz, E.M., Lowden, J.S., Rantalainen, M. and Wilson, I.D. (2005b) The metabonomics of aging and development in the rat: an investigation into the effect of age on the profile of endogenous metabolites in the urine of male rats using ¹H NMR and HPLC-TOF MS. *Molecular Biosystems* **1**, 166-175.
- Willis, C.M., Church, S.M., Guest, C.M., Cook, W.A., McCarthy, N., Bransbury, A.J., Church, M.R.T. and Church, J.C.T. (2004) Olfactory detection of human bladder cancer by dogs: proof of principle study. *British Medical Journal* **329**, 712-714A.

Wishart, D.S. (2008) Quantitative metabolomics using NMR. *Trac-Trends in Analytical Chemistry* **27**, 228-237.

Wold, S., Sjostrom, M. and Eriksson, L. (1999). PLS-regression: A basic tool of chemometrics. *International Symposium on Partial Least Squares (PLS 99)*. Jouy En Josas, France, pp. 109-130.

Wolf, S., Schmidt, S., Muller-Hannemann, M. and Neumann, S. (2010) In silico fragmentation for computer assisted identification of metabolite mass spectra. *Bmc Bioinformatics* **11**, 148.

Wu, J.Y., Bicker, W.G. and Lindner, W.G. (2008) Separation properties of novel and commercial polar stationary phases in hydrophilic interaction and reversed-phase liquid chromatography mode. *Journal of Separation Science* **31**, 1492-1503.

Wysocki, C.J. and Preti, G. (2004) Facts, fallacies, fears, and frustrations with human pheromones. *Anatomical Record Part a-Discoveries in Molecular Cellular and Evolutionary Biology* **281A**, 1201-1211.

Xie, D., Mattusch, J. and Wennrich, R. (2008) Separation of organoarsenicals by means of zwitterionic hydrophilic interaction chromatography (ZIC (R)-HILIC) and parallel ICP-MS/ESI-MS detection. *Engineering in Life Sciences* **8**, 582-588.

Xu, J.J., Zhang, J., Dong, J.Y., Cai, S.H., Yang, J.Y. and Chen, Z. (2009) Metabonomics studies of intact hepatic and renal cortical tissues from diabetic db/db mice using high-resolution magic-angle spinning ¹H NMR spectroscopy. *Analytical and Bioanalytical Chemistry* **393**, 1657-1668.

Xuan, Y., Scheuermann, E.B., Meda, A.R., Hayen, H., von Wiren, N. and Weber, G. (2006) Separation and identification of phytosiderophores and their metal complexes in plants by zwitterionic hydrophilic interaction liquid chromatography coupled to electrospray ionization mass spectrometry. *Journal of Chromatography A* **1136**, 73-81.

Yamazaki, K., Beauchamp, G.K., Curran, M., Bard, J. and Boyse, E.A. (2000) Parent-progeny recognition as a function of MHC odortype identity. *Proceedings of the National Academy of Sciences of the United States of America* **97**, 10500-10502.

Yamazaki, K., Boyse, E.A., Mike, V., Thaler, H.T., Mathieson, B.J., Abbott, J., Boyse, J., Zayas, Z.A. and Thomas, L. (1976) Control of mating preferences in mice by genes in the major histocompatibility complex. *Journal of Experimental Medicine* **144**, 1324-1335.

Yoshida, T. (2004) Peptide separation by hydrophilic-interaction chromatography: a review. *Journal of Biochemical and Biophysical Methods* **60**, 265-280.

Yoshiura, K., Kinoshita, A., Ishida, T., Ninokata, A., Ishikawa, T., Kaname, T., Bannai, M., Tokunaga, K., Sonoda, S., Komaki, R., Ihara, M., Saenko, V.A., Alipov, G.K., Sekine, I., Komatsu, K., Takahashi, H., Nakashima, M., Sosonkina, N., Mapendano, C.K., Ghadami, M., Nomura, M., Liang, D.S., Miwa, N., Kim, D.K.,

Garidkhuu, A., Natsume, N., Ohta, T., Tomita, H., Kaneko, A., Kikuchi, M., Russomando, G., Hirayama, K., Ishibashi, M., Takahashi, A., Saitou, N., Murray, J.C., Saito, S., Nakamura, Y. and Niikawa, N. (2006) A SNP in the *ABCC11* gene is the determinant of human earwax type. *Nature Genetics* **38**, 324-330.

Zelena, E., Dunn, W.B., Broadhurst, D., Francis-McIntyre, S., Carroll, K.M., Begley, P., O'Hagan, S., Knowles, J.D., Halsall, A., Wilson, I.D., Kell, D.B. and Consortium, H. (2009) Development of a Robust and Repeatable UPLC-MS Method for the Long-Term Metabolomic Study of Human Serum. *Analytical Chemistry* **81**, 1357-1364.

Zeng, C.H., Spielman, A.I., Vowels, B.R., Leyden, J.J., Biemann, K. and Preti, G. (1996a) A human axillary odorant is carried by apolipoprotein D. *Proceedings of the National Academy of Sciences of the United States of America* **93**, 6626-6630.

Zeng, X.N., Leyden, J.J., Brand, J.G., Spielman, A.I., McGinley, K.J. and Preti, G. (1992) An investigation of human apocrine gland secretion for axillary odor precursors. *Journal of Chemical Ecology* **18**, 1039-1055.

Zeng, X.N., Leyden, J.J., Lawley, H.J., Sawano, K., Nohara, I. and Preti, G. (1991) Analysis of characteristic odors from human male axillae. *Journal of Chemical Ecology* **17**, 1469-1492.

Zeng, X.N., Leyden, J.J., Spielman, A.I. and Preti, G. (1996b) Analysis of characteristic human female axillary odors: Qualitative comparison to males. *Journal of Chemical Ecology* **22**, 237-257.

Zernecke, R., Kleemann, A.M., Haegler, K., Albrecht, J., Vollmer, B., Linn, J., Bruckmann, H. and Wiesmann, M. (2010) Chemosensory properties of human sweat. *Chemical Senses* **35**, 101-108.

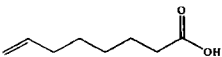
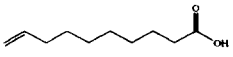
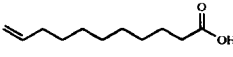
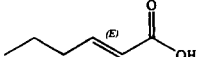

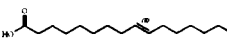
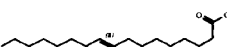
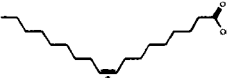
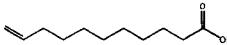
Zhang, N.R., Yu, S., Tiller, P., Yeh, S., Mahan, E. and Emary, W.B. (2009) Quantitation of small molecules using high-resolution accurate mass spectrometers - A different approach for analysis of biological samples. *Rapid Communications in Mass Spectrometry* **23**, 1085-1094.

Zhang, W., Couldwell, W.T., Song, H., Takano, T., Lin, J.H.C. and Nedergaard, M. (2000) Tamoxifen-induced enhancement of calcium signaling in glioma and MCF-7 breast cancer cells. *Cancer Research* **60**, 5395-5400.

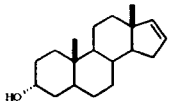
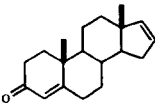
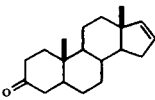
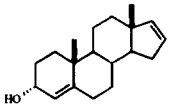
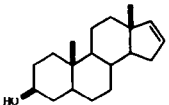
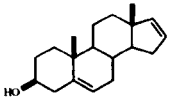
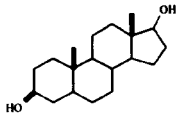
Appendix A

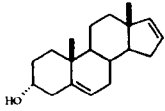
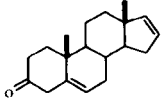
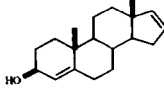
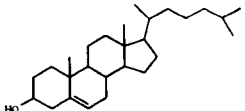
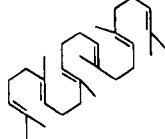
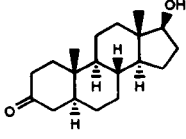
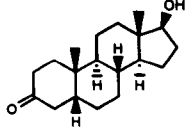
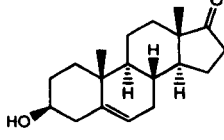
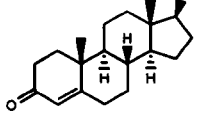
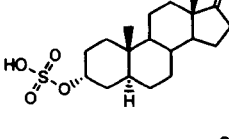
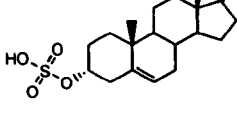
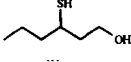
A list of reported metabolites found in human apocrine sweat secretions. For further information see Appendix A on the attached CD

Components	Structure	Molecule	Mass	M+H
3-Hydroxy acids				
3-Hydroxy-3-methylhexanoic acid		C7H14O3	146.0943	147.1021
3-Hydroxy-4-methylhexanoic acid		C7H14O3	146.0943	147.1021
3-Hydroxy-3-methylheptanoic acid		C8H16O3	160.1099	161.0628
3-Hydroxy-4-methylheptanoic acid		C8H16O3	160.1099	161.0628
3-Hydroxyoctanoic acid		C8H16O3	160.1099	161.0628
3-Hydroxy-3-methyloctanoic acid		C9H18O3	174.1256	175.1334
3-Hydroxy-4-methyloctanoic acid		C9H18O3	174.1256	175.1334
3-Hydroxy-4-methylnonanoic acid		C10H20O3	188.1412	189.1491
3-Hydroxydecanoic acid		C10H20O3	188.1412	189.1491
Unsaturated acids				
(Z)-3-Methylhex-2-enoic acid		C7H12O2	128.0837	129.0916
(E)-3-Methylhex-2-enoic acid		C7H12O2	128.0837	129.0916
4-Methyloct-4-enoic acid		C9H16O2	156.1150	157.1229
(Z)-4-Methyloct-3-enoic acid		C9H16O2	156.1150	157.1229
(E)-4-Methyloct-3-enoic acid		C9H16O2	156.1150	157.1229
(Z)-4-Methylnon-3-enoic acid		C10H18O2	170.1307	171.1385
(E)-4-Methylnon-3-enoic acid		C10H18O2	170.1307	171.1385
(E)-3-Methyl-2-octenoic acid		C9H16O2	156.1150	157.1229
(E)-3-Methyl-2-pentenoic acid		C6H10O2	114.0681	115.0759
(Z)-3-Methylhex-2-anoic acid		C7H12O2	128.0837	129.0916

7-Octenoic acid		C8H14O2	142.0994	143.1072
9-Decenoic acid		C10H18O2	170.1307	171.1385
10-Undecenoic acid		C11H20O2	184.1463	185.1542
2-Hexenoic acid		C6H10O2	114.0681	115.0759
9-Pentadecenoic acid		C15H28O2	240.2089	241.2168
9-Hexadecenoic acid		C16H30O2	254.2246	255.2324
9-Heptadecenoic acid		C17H32O2	268.2402	269.2481
Oleic acid		C18H34O2	282.2559	283.2637
Unsaturated C11 acid (10-undecenoic acid)		C11H20O2	184.1463	185.1542

Steroidal

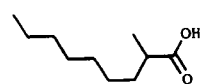
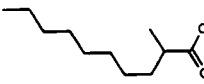
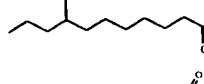
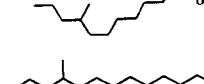
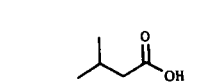
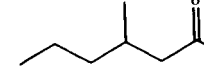
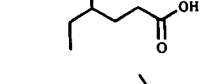
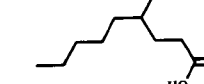
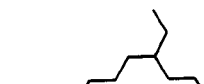

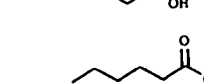
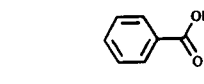
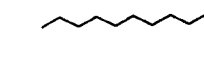
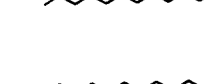
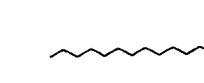
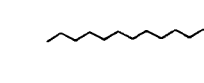
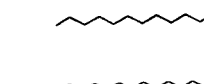


5 α -Androst-16-en-3 α -ol		C19H30O	274.2297	275.2375
Androsta-4, 16-dien-3-one		C19H26O	270.1984	271.2062
5 α -Androst-16-en-3-one		C19H28O	272.2140	273.2218
Androsta-4, 16-dien-3 α -ol		C19H28O	272.2140	273.2218
5 α -Androst-16-en-3 β -ol		C19H30O	274.2297	275.2375
5 α -Androsta-5, 16-dien-3 β -ol		C19H28O	272.2140	273.2218
Androst-5-ene-3 β -17 α/β -diols		C19H32O2	292.2402	293.2481

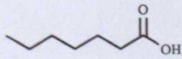
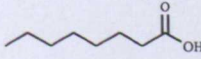

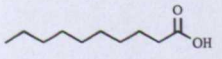
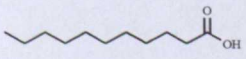
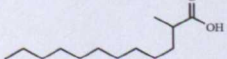
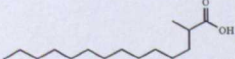
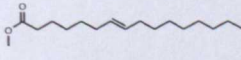
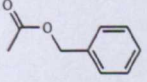
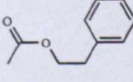
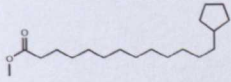
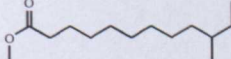
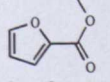
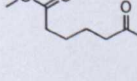
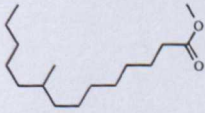
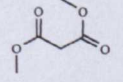
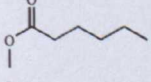
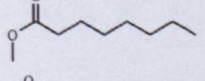
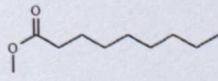
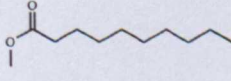
Androsta-5, 16-dien-3 α -ol		C ₁₉ H ₂₈ O	272.2140	273.2218
Androsta-5, 16-dien-3-one		C ₁₉ H ₂₆ O	270.1984	271.2062
Androsta-4, 16-dien-3 β -ol		C ₁₉ H ₂₈ O	272.2140	273.2218
Cholesterol		C ₂₇ H ₄₆ O	386.3549	387.3627
Squalene		C ₃₀ H ₅₀	410.3913	411.3991
5 α -Dihydrotestosterone		C ₁₉ H ₃₀ O ₂	290.2246	291.2324
5 β -Dihydrotestosterone		C ₁₉ H ₃₀ O ₂	290.2246	291.2324
Dehydrocpiandrosterone		C ₁₉ H ₂₈ O ₂	288.2089	
Testosterone		C ₁₉ H ₂₈ O ₂	288.2089	289.2168
17-Oxo-5 α -androstan-3 α -yl sulfate		C ₁₉ H ₃₀ O ₅ S	370.1814	371.1892
17-Oxo-5 α -androsen-3 α -yl sulfate		C ₁₉ H ₂₈ O ₅ S	368.1657	369.1736
Sulfanylalkanols				
3-Sulfanylhexasan-1-ol		C ₆ H ₁₄ OS	134.0765	135.0844

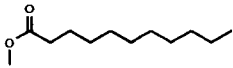
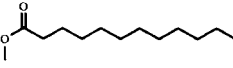
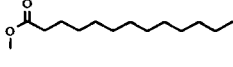
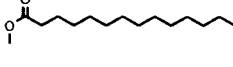
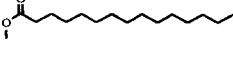
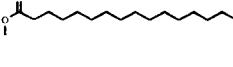
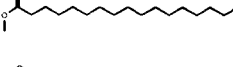
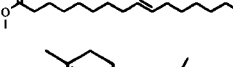
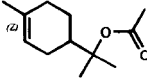
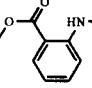
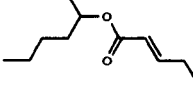
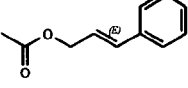
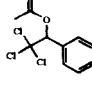
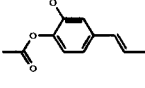
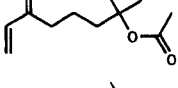
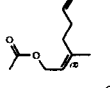
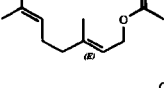
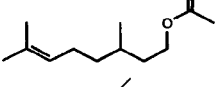
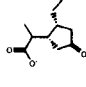
2-Methyl-3-sulfanylbutan-1-ol		C5H12OS	120.0609	121.0687
3-Sulfanylpentan-1-ol		C5H12OS	120.0609	121.0687
3-Methyl-3-sulfanylhexas-1-ol		C7H16OS	148.0922	149.1000
Dimethylsulfone		C2H6O2S	94.0089	95.0167

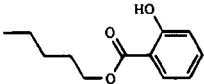
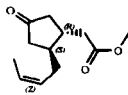
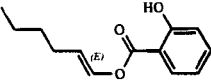
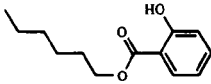
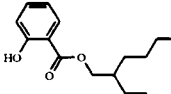
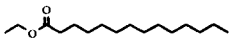
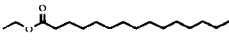
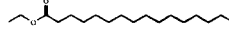
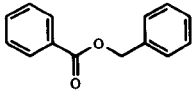
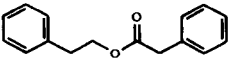
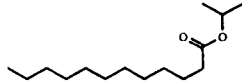
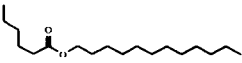
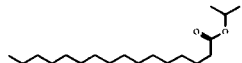
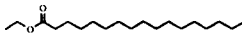
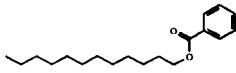
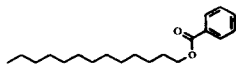
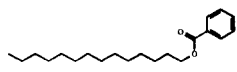
Amino acids degradation products and miscellaneous acids

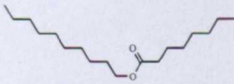
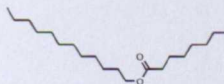

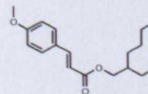
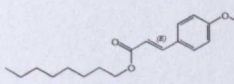
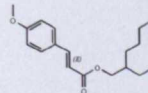
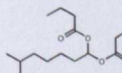
2-Hydroxypropanoic acid		C3H6O3	90.0317	91.0395
3-Methyl-2-oxopentanoic acid		C6H10O3	130.0630	131.0708
4-Methyl-2-oxopentanoic acid		C6H10O3	130.0630	131.0708
4-Ethylheptanoic acid		C9H18O2	158.1307	159.1385
Phenylacetic acid		C8H8O2	136.0524	137.0603
4-Ethyl-octanoic acid ('goat acid')		C10H20O2	172.1463	173.1542
8-Hydroxyoctanoic acid		C8H16O3	160.1099	161.1178
Octanedioic acid (suberic acid)		C8H14O4	174.0892	175.097
9-Hydroxynonanoic acid		C9H18O3	174.1256	175.1334
(4-Hydroxyphenyl)acetic acid		C8H8O3	152.0473	153.0552
Nonanedioic acid (azelaic acid)		C9H16O4	188.1049	189.1127
2-Ethylhexanoic acid		C8H16O2	144.115	145.1229
2-Piperidinone		C5H9NO	99.0684	100.0762
2-Methylhexanoic acid		C7H14O2	130.0994	131.1072
2-Methylheptanoic acid		C8H16O2	144.115	145.1229
2-Methyloctanoic acid		C9H18O2	158.1307	159.1385

2-Methylnonanoic acid		C ₁₀ H ₂₀ O ₂	172.1463	173.1542
2-Methyldecanoic acid		C ₁₁ H ₂₂ O ₂	186.162	187.1698
8-Methylundecanoic acid		C ₁₂ H ₂₄ O ₂	200.1776	201.1855
9-Methyldodecanoic acid		C ₁₃ H ₂₆ O ₂	214.1933	215.2011
10-Methyltridecanoic acid		C ₁₄ H ₂₈ O ₂	228.2089	229.2168
Isovaleric acid		C ₅ H ₁₀ O ₂	102.0681	103.0759
3-Methylhexanoic acid		C ₇ H ₁₄ O ₂	130.0994	131.1072
4-Ethylpentanoic acid		C ₇ H ₁₄ O ₂	130.0994	131.1072
4-Ethylnonanoic acid		C ₁₁ H ₂₂ O ₂	186.162	187.1698
4-Ethyldecanoic acid		C ₁₂ H ₂₄ O ₂	200.1776	201.1855
Propanoic acid		C ₃ H ₆ O ₂	74.0368	75.0446
Hexanoic acid		C ₆ H ₁₂ O ₂	116.0837	117.0916
Benzoic acid		C ₇ H ₆ O ₂	122.0368	123.0446
Dodecanoic acid		C ₁₂ H ₂₄ O ₂	200.1776	201.1855
Tetradecanoic acid		C ₁₄ H ₂₈ O ₂	228.2089	229.2168
Pentadecanoic acid		C ₁₅ H ₃₀ O ₂	242.2246	243.2324
Hexadecanoic acid		C ₁₆ H ₃₂ O ₂	256.2402	257.2481
Heptadecanoic acid		C ₁₇ H ₃₄ O ₂	270.2559	271.2637
2-Methylhexadecanoic acid		C ₁₇ H ₃₄ O ₂	270.2559	271.2637
Octadecanoic acid		C ₁₈ H ₃₆ O ₂	284.2715	285.2794

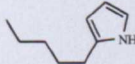
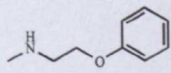
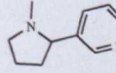
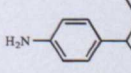

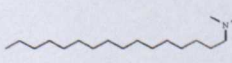
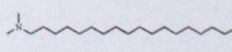
<i>n</i> -Heptanoic acid		C7H14O2	130.0994	131.1072
<i>n</i> -Octanoic acid		C8H16O2	144.115	145.1229
<i>n</i> -Nananoic acid		C9H18O2	158.1307	159.1385
<i>n</i> -Decanoic acid		C10H20O2	172.1463	173.1542
<i>n</i> -Undecanoic acid		C11H22O2	186.162	187.1698
<i>n</i> -Methyldodecanoic acid		C13H26O2	214.1933	215.2011
<i>n</i> -Methyltetradecanoic acid		C15H30O2	242.2246	243.2324
Esters				
7-Hexadecenoic acid methyl ester		C17H32O2	268.2402	269.2481
Acetic acid phenylmethyl ester		C9H10O2	150.0681	151.0759
2-Phenylethyl acetate		C10H12O2	164.0837	165.0916
Cyclopentanetridecanoic acid methyl ester		C19H36O2	296.2715	297.2794
Dodecanoic acid, 10-methyl, methyl ester		C14H28O2	228.2089	229.2168
Furancarboxylic acid methyl ester		C6H6O3	126.0317	127.0395
Hexanedioic acid dimethyl ester		C8H14O4	174.0892	175.0970
Methyl 9-methyltetradecanoate		C16H32O2	256.2402	257.2481
Propanedioic acid dimethyl ester		C5H8O4	132.0423	133.0501
Hexanoic acid methyl ester		C7H14O2	130.0994	131.1072
Octanoic acid methyl ester		C9H18O2	158.1307	159.1385
Nonanoic acid methyl ester		C10H20O2	172.1463	173.1542
Decanoic acid methyl ester		C11H22O2	186.162	187.1698

Undecanoic acid methyl ester		C ₁₂ H ₂₄ O ₂	200.1776	201.1855
Dodecanoic acid methyl ester		C ₁₃ H ₂₆ O ₂	214.1933	215.2011
Tridecanoic acid methyl ester		C ₁₄ H ₂₈ O ₂	228.2089	229.2168
Tetradecanoic acid methyl ester		C ₁₅ H ₃₀ O ₂	242.2246	243.2324
Pentadecanoic acid methyl ester		C ₁₆ H ₃₂ O ₂	256.2402	257.2481
Hexadecanoic acid methyl ester		C ₁₇ H ₃₄ O ₂	270.2559	271.2637
Heptadecanoic acid methylester		C ₁₈ H ₃₆ O ₂	284.2715	285.2794
9-Hexadecenoic acid methyl ester		C ₁₇ H ₃₂ O ₂	268.2402	269.2481
Terpinyl acetate		C ₁₂ H ₂₀ O ₂	196.1463	197.1542
Methyl- <i>N</i> -methylantranilate		C ₉ H ₁₁ NO ₂	165.079	166.0868
2-Hexyl 2-pentenoate		C ₁₁ H ₂₀ O ₂	184.1463	185.1542
<i>E</i> -Cinnamyl acetate		C ₁₁ H ₁₂ O ₂	176.0837	177.0916
α -Trichloromethyl-benzyl acetate		C ₁₀ H ₉ Cl ₃ O ₂	265.9668	266.9746
Isoeugenol acetate		C ₁₂ H ₁₄ O ₃	206.0943	207.1021
Dihydromyrcenol acetate		C ₁₂ H ₂₀ O ₂	196.1463	197.1542
Neryl acetate		C ₁₂ H ₂₀ O ₂	196.1463	197.1542
Geranyl acetate		C ₁₂ H ₂₀ O ₂	196.1463	197.1542
Citronellol acetate		C ₁₂ H ₂₂ O ₂	198.162	199.1698
Methylcis-dihydrojasmonate		C ₁₂ H ₁₉ O ₃	211.1334	212.1412

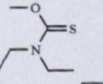
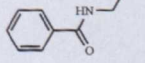
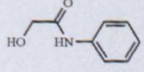
Pentyl salicylate		C ₁₂ H ₁₆ O ₃	208.1099	209.1178
Methyl trans-jasmonate		C ₁₂ H ₁₈ O ₃	210.1256	211.1334
1-Hexenyl salicylate		C ₁₃ H ₁₆ O ₃	220.1099	221.1178
1-Hexyl salicylate		C ₁₃ H ₁₈ O ₃	222.1256	223.1334
2-Ethylhexyl salicylate		C ₁₅ H ₂₂ O ₃	250.1569	251.1647
Ethyl tetradecanoate		C ₁₆ H ₃₂ O ₂	256.2402	257.2481
Ethyl pentadecanoate		C ₁₇ H ₃₄ O ₂	270.2559	271.2637
Ethyl hexadecanoate		C ₁₈ H ₃₆ O ₂	284.2715	285.2794
Benzyl benzoate		C ₁₄ H ₁₂ O ₂	212.0837	213.0916
2-phenylethyl phenylacetate		C ₁₆ H ₁₆ O ₂	240.1150	241.1229
Isopropyl dodecanoate		C ₁₅ H ₃₀ O ₂	242.2246	243.2324
Dodecyl hexanoate		C ₁₈ H ₃₆ O ₂	284.2715	285.2794
Hexadecanoic acid isopropyl ester		C ₁₉ H ₃₈ O ₂	298.2872	299.2950
Ethyl heptadecanoate		C ₁₉ H ₃₈ O ₂	298.2872	299.2950
Dodecyl benzoate		C ₁₉ H ₃₀ O ₂	290.2246	291.2324
Tridecyl benzoate		C ₂₀ H ₃₂ O ₂	304.2402	305.2481
Tetradecyl benzoate		C ₂₁ H ₃₄ O ₂	318.2559	319.2637

Decyl octanoate		C18H36O2	284.2715	285.2794
Dodecyl octanoate		C20H40O2	312.3028	313.3107
Tetradecyl octanoate		C22H44O2	340.3341	341.3420
2-Ethylhexyl 4-methoxycinnamate		C18H26O3	290.1882	291.1960
1-Octyl 4-methoxycinnamate		C18H26O3	290.1882	291.1960
2-Ethyl-hexyl 4-methoxycinnamate		C18H26O3	290.1882	291.1960
Isocetanediodibutyrate		C16H30O4	286.2144	287.2222

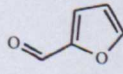
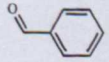
Amines









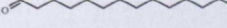




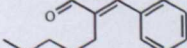
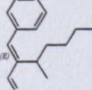
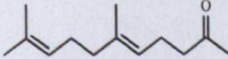

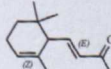
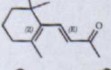
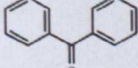
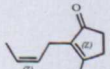
2-Pentylpyrrole		C9H15N	137.1204	138.1283
2-Phenoxyethylmethanamine		C9H13NO	151.0997	152.1075
Nicotine		C10H14N2	162.1157	163.1235
4-Sec-butylaniline		C10H15N	149.1204	150.1283
N,N-Dimethyl-1-dodecylamine		C14H31N	213.2457	214.2535
N,N-Dimethyl-1-hexadecylamine		C18H39N	269.3083	270.3161
N,N-Dimethyl-1-octadecylamine		C20H43N	297.3396	298.3474

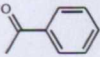
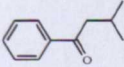
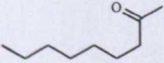
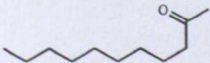
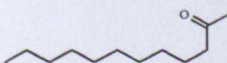
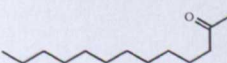
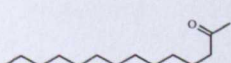
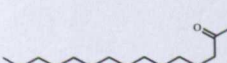
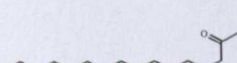





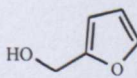
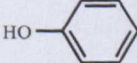
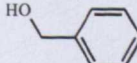
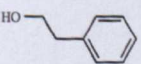
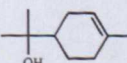
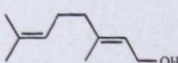
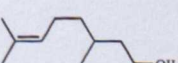
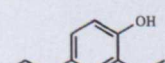
Amides

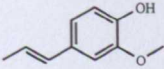
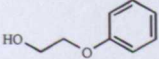
















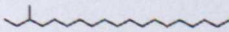


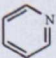
Methyl N,N-diethylthiocarbamate		C6H13NOS	147.0718	148.0796
n-Propylbenzamide		C10H13NO	163.0997	164.1075
Hydroxy acetanilide		C8H9NO2	151.0633	152.0712


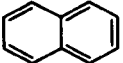

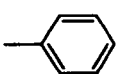
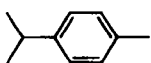
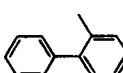
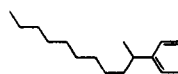
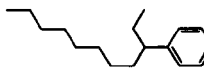
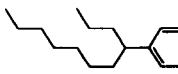
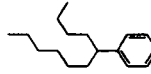
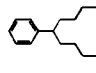
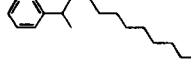
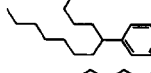
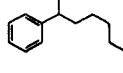
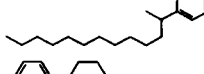
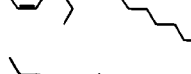
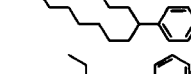
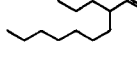




Aldehydes

2-Furancarboxaldehyde		C5H4O2	96.0211	97.029
Benzaldehyde		C7H6O	106.0419	107.0497

Hexanal		C ₆ H ₁₂ O	100.0888	101.0966
Heptanal		C ₇ H ₁₄ O	114.1045	115.1123
Octanal		C ₈ H ₁₆ O	128.1201	129.1279
Nonanal		C ₉ H ₁₈ O	142.1358	143.1436
Decanal		C ₁₀ H ₂₀ O	156.1514	157.1592
Undecanal		C ₁₁ H ₂₂ O	170.1671	171.1749
Dodecanal		C ₁₂ H ₂₄ O	184.1827	185.1905
Tridecanal		C ₁₃ H ₂₆ O	198.1984	199.2062
Tetradecanal		C ₁₄ H ₂₈ O	212.214	213.2218
Hexadecanal		C ₁₆ H ₃₂ O	240.2453	241.2531
(E)-2-Nonenal		C ₉ H ₁₆ O	140.1201	141.1279
Geranial		C ₁₀ H ₁₆ O	152.1201	153.1279
p-Anisaldehyde		C ₈ H ₈ O ₂	136.0524	137.0524
Pentylcinnamaldehyde		C ₁₄ H ₁₈ O	202.1358	203.1436
E-2-Hexylcinnamaldehyde		C ₁₅ H ₂₀ O	216.1514	217.1592
Ketones				
6,10-Dimethyl-5,9-undecadien-2-one		C ₁₃ H ₂₂ O	194.1671	195.1749
6-Methyl-5-hepten-2-one		C ₈ H ₁₄ O	126.1045	127.1123
α-Ionone		C ₁₃ H ₂₀ O	192.1514	193.1592
β-Ionone		C ₁₃ H ₂₀ O	192.1514	193.1592
Benzophenone		C ₁₃ H ₁₀ O	182.0732	183.0810
Jasmone		C ₁₁ H ₁₆ O	164.1201	165.1279

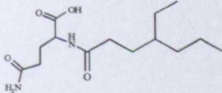
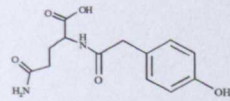
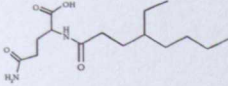
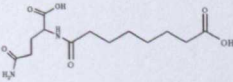
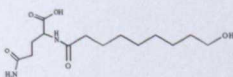
Acetophenone		C8H8O	120.0575	121.0653
Isopropylacetophenone		C11H14O	162.1045	163.1045
2-Nonanone		C9H18O	142.1358	143.1436
2-Undecanone		C11H22O	170.1671	171.1749
2-Dodecanone		C12H24O	184.1827	185.1905
2-Tridecanone		C13H26O	198.1984	199.2062
2-Tetradecanone		C14H28O	212.2140	213.2218
2-Pentadecanone		C15H30O	226.2297	227.2375
2-Hexadecanone		C16H32O	240.2453	241.2531
Alcohols				
Tridecan-1-ol		C13H28O	200.2140	201.2218
<i>n</i> -Tetradecanol		C14H30O	214.2297	215.2375
Pentadecanol		C15H32O	228.2453	229.2531
<i>n</i> -Hexadecanol		C16H34O	242.2610	243.2688
<i>a</i> Hexadecadienol		C16H30O	238.2297	239.2375
2-Furanmethanol		C5H6O2	98.0368	99.0446
Phenol		C6H6O	94.0419	95.0497
Benzyl Alcohol		C7H8O	108.0575	109.0653
2-Phenylethanol		C8H10O	122.0732	123.0810
<i>p</i> -Menth-1-en-8-ol		C10H18O	154.1358	155.1436
Geraniol		C10H18O	154.1358	155.1436
Citronellol		C10H20O	156.1514	157.1592
Eugenol		C10H12O2	164.0837	165.0916

Isoeugenol		C10H12O2	164.0837	165.0916
2-Phenoxyethanol		C8H10O2	138.0681	139.0759
Aliphatic/Aromatic				
Nonane		C9H20	128.1565	129.1643
Undecane		C11H24	156.1878	157.1956
Dodecane		C12H26	170.2035	171.2113
Tridecane		C13H28	184.2191	185.2269
Tetradecane		C14H30	198.2348	199.2426
Pentadecane		C15H32	212.2504	213.2582
Hexadecane		C16H34	226.2661	227.2739
Heptadecane		C17H36	240.2817	241.2895
Octadecane		C18H38	254.2974	255.3052
Nonadecane		C19H40	268.3130	269.3208
Eicosane		C20H42	282.3287	283.3365
Heneicosane		C21H44	296.3443	297.3521
Docosane		C22H46	310.3600	311.3678
Tricosane		C23H48	324.3756	325.3834
Tetracosane		C24H50	338.3913	339.3991
3-Methyloctadecane		C19H40	268.3130	269.3208
3-Methylnonadecane		C20H42	282.3287	283.3365
4-Methylpentadecane		C16H34	226.2661	227.2739
Nonane, 1-chloro-		C9H19Cl	162.1175	163.1254
Pyridine		C5H5N	79.0422	80.0500

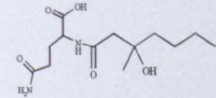
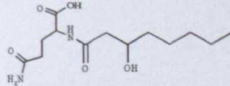
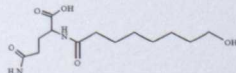
α -Pinene		C ₁₀ H ₁₆	136.1252	137.1330
Naphthalene		C ₁₀ H ₈	128.0626	129.0704
Cyclotetradecane		C ₁₄ H ₂₈	196.2191	197.2269
Toluene		C ₇ H ₈	92.0626	93.0704
p-Cymene		C ₁₀ H ₁₄	134.1096	135.1174
Methyl biphenyl		C ₁₃ H ₁₂	168.0939	169.1017
2-Phenylundecane		C ₁₇ H ₂₈	232.2191	233.2269
3-Phenylundecane		C ₁₇ H ₂₈	232.2191	233.2269
4-Phenylundecane		C ₁₇ H ₂₈	232.2191	233.2269
5-Phenylundecane		C ₁₇ H ₂₈	232.2191	233.2269
6-Phenylundecane		C ₁₇ H ₂₈	232.2191	233.2269
2-Phenyldodecane		C ₁₈ H ₃₀	246.2348	247.2426
5-Phenyldodecane		C ₁₈ H ₃₀	246.2348	247.2426
6-Phenyldodecane		C ₁₈ H ₃₀	246.2348	247.2426
2-Phenyltridecane		C ₁₉ H ₃₂	260.2504	261.2582
3-Phenyltridecane		C ₁₉ H ₃₂	260.2504	261.2582
4-Phenyltridecane		C ₁₉ H ₃₂	260.2504	261.2582
6-Phenyltridecane		C ₁₉ H ₃₂	260.2504	261.2582
1-Dodecene		C ₁₂ H ₂₄	168.1878	169.1956
1-Tetradecene		C ₁₄ H ₂₈	196.2191	197.2269
1-Nonadecene		C ₁₉ H ₃₈	266.2974	267.3052
Farnesene		C ₁₅ H ₂₄	204.1878	205.1956

Precursors

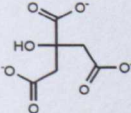
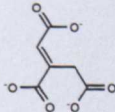
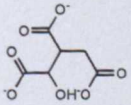
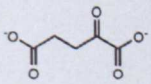
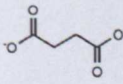
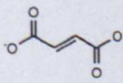
N- α -3-methylhex-2-enoyl-L-glutamine		C12H20N2O4	256.1423	257.1501
N- α -3-hydroxy-3-methylhexanoyl- L-glutamine		C12H22N2O5	274.1529	275.1607
S-[1-(2-hydroxy-1-methylethyl)-2-methylethyl]-L-cysteinyglycine		C11H22N2O4S	278.1300	279.1379
S-[1-(2-hydroxy-1-methylethyl)-1-ethyl]-L-cysteine		C8H17NO3S	207.0929	208.1007
S-[1-(2-hydroxyethyl)-1-methylbutyl]-L-cysteinyglycine		C12H24N2O4S	292.1457	293.1535
S-[1-(2-hydroxyethyl)-1-methylbutyl]-L-cystein		C10H21NO3S	235.1242	236.1320
S-[1-(2-hydroxyethyl)-butyl]-L-cysteinyglycine		C11H22N2O4S	278.1300	279.1379
N- α -3-hydroxy-4-methylhept anoyl- L-glutamine		C13H24N2O5	288.1685	289.1763
N- α -3-hydroxy-3-methyloct anoyl- L-glutamine		C14H26N2O5	302.1842	303.1920
N- α -3-hydroxy-4-methyloct anoyl- L-glutamine		C14H26N2O5	302.1842	303.1920
N- α -4-methyl-3-oct-enoyl- L-glutamine		C14H24N2O4	284.1736	285.1814
N- α -3-methyl-2-oxopent-anoyl- L-glutamine		C11H18N2O5	258.1216	259.1294
N- α -4-methyl-2-oxopent-anoyl- L-glutamine		C11H18N2O5	258.1216	259.1294

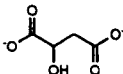
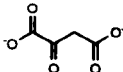
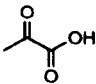
N- α -4-ethyl-hept-anoyl- L-glutamine		C14H26N2O4	286.1893	287.1971
N- α -4-hydroxyphenyl-acetyl- L-glutamine		C13H16N2O5	280.1059	281.1137
N- α -4-ethyl-oct-anoyl- L-glutamine		C15H28N2O4	300.2049	301.2127
N- α -7-carboxy-hept-anoyl- L-glutamine		C13H22N2O6	302.1478	303.1556
N- α -9-hydroxy- non-anoyl- L-glutamine		C14H26N2O5	302.1842	303.1920

Hypothetical Precursors

N- α -3-hydroxy- 3-methylhept-anoyl- L-glutamine		C13H24N2O5	288.1685	289.1763
N- α -3-hydroxy-oct-anoyl- L-glutamine		C13H24N2O5	288.1685	289.1763
N- α -8-hydroxy-oct-anoyl- L-glutamine		C13H24N2O5	288.1685	289.1763

TCA Cycle Intermediates

Citrate		C6H5O7 ³⁻	189.0035	190.0114
Aconitate		C6H3O6 ³⁻	170.9930	172.0008
Isocitrate		C6H5O7 ³⁻	189.0035	190.0114
α -Ketoglutarate		C5H4O5 ²⁻	144.0059	145.0137
Succinate		C4H4O4 ²⁻	116.0110	117.0188
Fumarate		C4H4O2 ²⁻	84.0211	85.0290

Malate		$C_4H_4O_5^{2-}$	132.0059	133.0137
Oxaloacetate		$C_4H_2O_5^{2-}$	129.9902	130.9980
Pyruvic acid		$C_3H_4O_3$	88.0160	89.0238

Appendix B

A list of putative identification of metabolites present in the *in vitro* ASG5 cell line sweat samples.

m/z	rt (s)	ppm error	MF	Adduct	Metabolites	Class
Carbohydrates						
365.105	599.05	1.78	C12H22O11	Na	1-alpha-D-Galactosyl-myo-inositol or related compounds	Carbohydrates
689.2125	682.00	0.73	C24H42O21	Na	1,1-kestotetraose or related compounds	Carbohydrates
291.0692	444.26	2.71	C9H16O9	Na	2(alpha-D-Mannosyl)-D-glycerate or related compounds	Carbohydrates
Amines						
232.1532	523.19	4.87	C11H21N04	H	3-(1-Aminoethyl)Nonanedioic Acid, Isobutyl-L-carnitine; N(alpha)-t-Butoxycarbonyl-L-leucine; O-Butanoylcarnitine	Quaternary Amines
282.2785	108.51	2.23	C18H35NO	H	Oleamide	Fatty amides
131.1175	482.98	2.97	C6H14N2O	H	epsilon-aminocaproamide or related compounds	Polyamines
137.0708	576.19	1.02	C7H8N2O	H	N-Methylnicotinamide or related compounds	Cyclic Amines
Amino Acids						
291.1288	658.24	3.81	C10H18N4O6	H	Argininosuccinic acid; N(omega)-(L-Arginino)succinate	Amino Acids
294.2411	113.38	2.58	C16H33NO2	Na	2-amino-hexadecanoic acid or related compounds	Amino fatty acids
126.0222	606.65	1.98	C2H7NO3S	H	Taurine	Amino Acids
90.0544	613.64	6.22	C3H7NO2	H	L-Alanine	Amino Acids
134.0454	625.87	4.55	C4H7NO4	H	L-Aspartate	Amino Acids
133.0608	639.57	0.23	C4H8N2O3	H	L-Asparagine	Amino Acids
132.0764	613.03	2.73	C4H9N3O2	H	Creatine	Amino Acids
120.0651	617.18	3.50	C4H9NO3	H	L-Threonine	Amino Acids
147.0759	626.82	3.54	C5H10N2O3	H	L-Glutamine	Amino Acids
150.0577	532.21	4.20	C5H11NO2S	H	L-Methionine	Amino Acids
116.0703	585.59	2.67	C5H9NO2	H	L-Proline	Amino Acids
148.0602	621.57	1.62	C5H9NO4	H	L-Glutamate	Amino Acids
130.0861	593.70	1.15	C6H11NO2	H	N4-Acetylaminobutanol or related compounds	Amino Acids
132.1017	504.56	1.51	C6H13NO2	H	L-Isoleucine; L-Leucine	Amino Acids
147.1125	597.33	2.04	C6H14N2O2	H	L-Leucyl-Hydroxylamine	Amino Acids
175.1183	637.50	3.71	C6H14N4O2	H	L-Arginine	Amino Acids
139.0495	556.97	5.11	C6H6N2O2	H	Urocanic acid or related compound	Amino Acids
146.117	700.58	3.83	C7H15NO2	H	2-amino-heptanoic acid or related compounds	Amino fatty acids
138.0551	564.84	1.01	C7H7NO2	H	2-nitrotoluene or related compounds	Amino acids derivative
152.0702	214.03	2.70	C8H9NO2	H	(E)-4-Hydroxyphenylacetaldehyde-oxime or related compound	Amino Acids
182.0805	553.37	3.68	C9H11NO3	H	L-Tyrosine	Amino Acids
220.117	523.81	0.59	C9H17NO5	H	Pantothenic acid	Amino Acids
Bile Acids						
433.248	512.78	0.30	C24H38O3	NaCl	(20S)-3beta-Hydroxychole-5-en-24-oic Acid or related compounds	Bile acids and derivatives
391.284	103.24	0.69	C24H38O4	H	(22E)-3alpha,12alpha-Dihydroxy-5beta-chole-22-en-24-oic Acid or related compounds	Bile acids and derivatives
516.3008	174.38	3.60	C26H45NO7S	H	Taurallocholic acid or related compounds	Bile acids and derivatives
549.341	118.52	2.24	C32H41NO4	NH3	3-Amino-N-(4-(2-(2,6-Dimethyl-Phenoxy)-Acetylamino)-3-Hydroxy-1-Isobutyl-5-Phenyl-Pentyl)-Benzamide or related compounds	Bile acids and derivatives
Glycerol						
482.3598	466.40	1.43	C24H52NO6P	H	1-O-Hexadecyl-lyso-sn-glycero-3-phosphocholine	Glycerophosphocholines
508.3765	464.47	0.71	C26H54NO6P	H	PC(0-18:1(11Z)/0:0) or related compounds	Glycerophosphocholines
575.3111	503.62	4.94	C27H53O8P	K	PA(12:0/12:0)	Glycerophosphates
606.3647	469.69	2.23	C29H58NO6P	NaCl	PC(0-3:1(1E)/O-18:1(9Z)) [S] or related compounds	Glycerophosphocholines
665.4133	471.96	0.83	C32H58NO10P	NH3	1-Palmitoyl-2-(5-keto-8-oxo-6-octenyl)-sn-glycero-3-phosphatidylcholine	Glycerophosphates
694.4177	481.95	1.12	C33H66NO8P	NaCl	PC(10:0/15:0)[U] or related compounds	Glycerophosphocholines
704.5168	130.30	4.61	C35H74NO6P	HCOONa	PE-NMe2(O-14:0/O-14:0)	Glycerophosphocholines
647.4851	112.18	0.93	C36H66O5	HCOONa	DG(15:0/18:2(9Z,12Z)/0:0) or related compounds	Glycerolipids
676.4928	383.12	2.42	C36H70NO8P	H	PC(10:0/18:1(9Z)) or related compounds	Glycerophosphocholines
678.5077	394.42	1.31	C36H72NO8P	H	PC(10:0/18:0) or related compounds	Glycerophosphocholines
718.5324	129.42	4.59	C36H76NO6P	HCOONa	PC(0-14:0/O-14:0)	Glycerophosphocholines
610.5413	103.58	1.34	C37H68O5	NH3	DG(14:0/20:2(1Z,14Z)/0:0) or related compounds	Glycerolipids
574.5299	382.13	4.49	C37H78NO6P	Na_HCOONa	PE(O-16:0/O-16:0)	Glycerophosphoethanolamines
663.4711	113.23	2.19	C38H68O5	NaCl	DG(15:0/20:3(5Z,8Z,11Z)/0:0) or related compounds	Glycerolipids
704.5228	380.02	3.90	C38H74NO8P	H	PC(12:0/18:1(9Z)) or related compounds	Glycerophosphocholines
706.5389	390.41	1.12	C38H76NO8P	H	PC(11:0/19:0) or related compounds	Glycerophosphocholines
706.5414	441.72	4.66	C38H76NO8P	H	PC(10:0/20:0) or related compounds	Glycerophosphocholines
692.5574	395.09	2.08	C38H78NO7P	H	PC(O-14:0/16:0)	Glycerophosphocholines
638.5733	104.49	2.38	C39H72O5	NH3	DG(14:0/22:2(13Z,16Z)/0:0) or related compounds	Glycerolipids
701.5597	448.85	0.74	C39H74NO6P	NH3	1-tetradecanyl-2-(8-[3]-ladderane-octanyl)-sn-glycerophosphoethanolamine	Glycerophosphoethanolamines
718.5387	219.08	4.18	C39H76NO8P	H	16:0-18:1-PE or related compounds	Glycerophosphoethanolamines
728.5542	420.27	3.06	C39H80NO7P	Na	PE(O-18:0/16:0)[U]	Glycerophosphoethanolamines
766.5288	190.92	1.33	C39H82NO6P	KCl	PE-NMe2(O-16:0/O-16:0)	Glycerophosphoethanolamines
782.5612	402.65	4.32	C39H82NO6P	Na_HCOONa	PE-NMe2(O-16:0/O-16:0)	Glycerophosphoethanolamines
709.4405	475.27	4.92	C40H64O5	HCOOK	DG(17:2(9Z,12Z)/20:5(5Z,8Z,11Z,14Z,17Z)/0:0)[iso2]	Glycerolipids
730.5351	399.98	0.82	C40H76NO8P	H	PC(14:0/18:2(11Z,14Z)) or related compounds	Glycerophosphocholines
780.5472	342.59	4.83	C40H84NO6P	KCl	PC(O-12:0/O-20:0)[U] or related compounds	Glycerophosphocholines
742.5404	197.93	4.77	C41H76NO8P	H	18:0-18:3-PE or related compounds	Glycerophosphates
770.5654	361.64	2.08	C41H82NO8P	Na	PC(10:0/23:0) or related compounds	Glycerophosphocholines
824.4862	252.37	2.89	C42H76NO10P	K	18:0-18:3-PS or related compounds	Glycerophosphoserines
788.5418	324.67	0.79	C42H78NO10P	H	18:0-18:2-PS or related compounds	Glycerophosphoserines
826.4996	497.21	0.16	C42H78NO10P	K	PS(18:0/18:2(9Z,12Z)) or related compounds	Glycerophosphoserines
770.5506	366.21	1.43	C42H79NO8	Na_Na	Galactosylceramide (d18:1/18:1(9Z)); Glucosylceramide (d18:1/19Z-18:1)	Glycolipids
784.5799	406.43	3.49	C42H84NO8P	Na	PC(10:0/24:0) or related compounds	Glycerophosphocholines
776.5909	398.33	0.41	C42H86NO6P	Na_Na	PC(O-16:0/O-18:1(9Z))[U] or related compounds	Glycerophosphocholines
772.5976	385.56	0.58	C42H88NO6P	K	PC(O-16:0/O-18:0)	Glycerophosphocholines
753.4658	480.16	2.44	C43H66O5	Na_HCOONa	DG(18:3(6Z,9Z,12Z)/22:6(4Z,7Z,10Z,13Z,16Z,19Z)/0:0) or related compounds	Glycerolipids
775.4798	481.19	2.17	C43H73O6P	NaCl	DG(17:0/22:4(7Z,10Z,13Z,16Z)/0:0)[iso2] or related compounds	Glycolipids
763.5828	355.45	2.66	C43H82O5	HCOOK	DG(16:1(9Z)/24:0/0:0) or related compounds	Glycerolipids
763.5885	364.87	4.81	C43H82O5	HCOOK	DG(16:0/24:1(15Z)/0:0) or related compounds	Glycerolipids
824.5581	385.15	3.52	C44H84NO8P	K	PC(14:0/22:2(13Z,16Z)) or related compounds	Glycerolipids
774.5427	179.11	2.48	C45H76NO7P	H	PE(22:6(4Z,7Z,10Z,13Z,16Z,19Z)/dm18:1(11Z)) or related compounds	Glycerophosphocholines
763.6	360.23	2.96	C45H84O5	NaCl	DG(18:1(11Z)/24:1(15Z)/0:0) or related compounds	Glycerophosphoethanolamines
806.5843	136.27	2.36	C45H86NO6P	K	1-(10-methylhexadecanyl)-2-(8-[3]-ladderane-octanyl)-sn-glycerophosphocholine	Glycerolipids
822.5794	143.75	2.53	C45H86NO7P	K	PE(22:1(13Z)/dm18:1(11Z)) or related compounds	Glycerophosphocholines
808.5851	336.63	3.04	C46H82NO8P	H	PC(16:0/22:5(4E,7E,10E,13E,16E))[U] or related compounds	Glycerophosphocholines
812.6202	340.75	2.45	C46H86NO8P	H	PC(16:0/22:3(13Z,16Z,19Z))[U] or related compounds	Glycerophosphocholines
763.6155	364.36	4.13	C46H86O5	Na_Na	DG(21:0/22:2(13Z,16Z)/0:0)[iso2]	Glycerolipids
730.5395	364.07	1.90	C47H68O5	NH3	DG(22:6(4Z,7Z,10Z,13Z,16Z,19Z)/22:6(4Z,7Z,10Z,13Z,16Z,19Z)/0:0)*	Glycerophosphocholines
834.6022	329.38	2.31	C48H84NO8P	H	PC(18:0/22:6(4E,7E,10E,13E,16E,19E))[U] or related compounds	Glycerophosphocholines
894.6423	146.39	0.86	C48H91NO8	HCOOK	Galactosylceramide (d18:1/24:1(15Z)) or related compounds	Glycolipids
792.7949	124.71	3.32	C49H90O6	NH3	TG(16:1(9Z)/4:0/16:1(9Z))[iso3]	Glycerolipids
915.6705	102.32	4.93	C53H92O6	Na_HCOONa	TG(16:1(9Z)/16:1(9Z)/18:3(9Z,12Z,15Z))[iso3] or related compounds	Triacylglycerols
929.6858	102.78	4.47	C56H92O6	HCOONa	TG(16:1(9Z)/17:2(9Z,12Z)/20:5(5Z,8Z,11Z,14Z,17Z))[iso6] or related compounds	Triacylglycerols
Fatty Acids						
184.1325	193.79	3.80	C10H14O2	NH3	1-(3,4-dimethylphenyl)ethane-1,2-diol or related compounds	Fatty Acids and Conjugates
202.1799	492.63	1.24	C11H20O2	NH3	11-Undecanolactone or related compounds	Fatty Acids and Conjugates

208.1328	436.45	1.92	C12H17NO2	H	2-sec-Butylphenyl N-methylcarbamate;3-(Dimethylamino)propyl benzoate;"3,4-Methylenedioxy-N-ethylamphetamine	Fatty Acids and Conjugates
229.1535	680.98	1.61	C12H24O	Na_Na	10-dodecen-1-ol or related compounds	Fatty alcohols
241.1542	555.30	1.95	C13H24O	Na_Na	2-tridecenal	Fatty aldehydes
239.1049	691.73	2.09	C14H16O2	Na	10E,12E-tetradecadiene-4,6-diynoic acid	Fatty Acids and Conjugates
235.206	113.43	1.57	C16H26O	H	4,6,11-hexadecatrienal	Fatty aldehydes
268.2271	110.85	0.00	C16H26O2	NH3	4,7,10-hexadecatrienoic acid or related compounds	Fatty Acids and Conjugates
254.2471	312.60	2.87	C16H28O	NH3	10,12-hexadecadienal or related compounds	Fatty aldehydes
256.263	109.00	1.87	C16H30O	NH3	6E,11Z-hexadecadien-1-ol or related compounds	Fatty alcohols
261.2201	115.22	4.71	C16H30O	Na	10-propyl-5,9-tridecadien-1-ol or related compounds	Fatty alcohols
258.2781	254.89	3.99	C16H32O	NH3	1,2-Epoxyhexadecane;11Z-hexadecen-1-ol or related compounds	Fatty alcohols
274.2733	263.19	2.73	C16H32O2	NH3	13-methyl-pentadecanoic acid or related compounds	Fatty Acids and Conjugates
288.2889	239.09	2.77	C17H34O2	NH3	(+)-14-methyl palmitic acid;10-methyl-hexadecanoic acid or related compounds	Fatty Acids and Conjugates
275.1998	112.20	2.73	C18H26O2	H	13E-octadecene-9,11-diynoic acid or related compounds	Fatty Acids and Conjugates
298.2727	115.34	4.53	C18H32O2	NH3	10E,12E-octadecadienoic acid or related compounds	Fatty Acids
284.2942	273.47	2.04	C18H34O	NH3	11-octadecenal or related compounds	Fatty alcohols
300.2906	297.59	3.00	C18H34O2	NH3	(11E)-Octadecenoic acid or related compounds	Fatty Acids and Conjugates
304.262	109.01	3.06	C18H35NO	Na	Oleamide	Fatty amides
302.3048	255.27	1.82	C18H36O2	NH3	(+)-Isostearic acid;10-methyl-heptadecanoic acid or related compounds	Fatty Acids and Conjugates
302.3048	314.89	1.82	C18H36O2	NH3	15-methyl-heptadecanoic acid or related compounds	Fatty Acids and Conjugates
316.3203	229.21	2.18	C19H38O2	NH3	(+)-16-methyl stearic acid;11-methyl-octadecanoic acid or related compounds	Fatty Acids and Conjugates
330.3358	248.00	2.54	C20H40O2	NH3	17-methyl-nonadecanoic acid or related compounds	Fatty Acids and Conjugates
340.32	241.18	2.91	C21H38O2	NH3	12Z,15Z-heneicosadienoic acid or related compounds	Fatty Acids and Conjugates
342.3362	239.30	1.29	C21H40O2	NH3	12Z-heneicosenoic acid or related compounds	Fatty Acids and Conjugates
358.3678	241.70	0.39	C22H44O2	NH3	19-methyl-heneicosanoic acid or related compounds	Fatty Acids and Conjugates
480.3083	429.95	0.31	C25H43NO2	Na_HCOONa	(-)-N-(1R-methyl-2-hydroxy-ethyl) alpha,alpha-dimethylarachidonoyl amine or related compounds	Fatty amides
677.5591	446.20	0.12	C38H76O9	H	1-(O-alpha-D-glucopyranosyl)-(1,3R,29S,31R)-dotriacontanetetraol	Fatty acyl glycosides
704.5297	441.47	2.19	C40H73NO4	Na_Na	N-ornithinyl-35-aminobacteriohopane-32,33,34-triol	Hopanoids
782.4773	493.77	4.95	C41H73NO8	KCl	bacteriohopane-32,33,34-triol-35-cyclitol;bacteriohopanetetrol cyclitol	Hopanoids
87.0443	657.38	2.76	C4H6O2	H	1,4-L-actone or related compounds	Fatty Acids
89.0595	161.09	2.36	C4H8O2	H	2-Methylpropanoate or related compounds	Fatty Acids
160.1325	718.21	4.37	C8H14O2	NH3	2-ethyl-3E-hexenoic acid or related compounds	Fatty Acids and Conjugates
156.1376	111.09	4.42	C9H14O	NH3	(3Z,6Z)-nonadienal or related compounds	Fatty aldehydes
155.106	119.97	4.19	C9H14O2	H	2,6-nonadienoic acid or related compounds	Fatty Acids
172.1325	120.17	4.07	C9H14O2	NH3	2,6-nonadienoic acid or related compounds	Fatty Acids and Conjugates
146.0594	496.09	4.38	C9H7NO	H	1(2H)-Isoquinolinone or related compounds	Fatty aldehydes
Hydroxy acids						
250.0928	166.87	0.80	C10H19NO2S2	H	S-Acetylidiolipolipamide	Lipoamides and Derivatives
223.1071	510.95	2.78	C11H11NO3	NH3	5-Methoxyindoleacetate;Indolelactate	Indoles and Indole Derivatives
239.1047	605.62	1.25	C11H20O3	K	2-hydroxy-10-undecenoic acid or related compounds	Hydroxy fatty acids
226.1438	435.97	0.13	C12H16O3	NH3	12-oxo-5E,8E,10Z-dodecatricenoic acid or related compounds	Oxo fatty acids
304.2852	148.51	1.94	C17H34O3	NH3	17-hydroxy-heptadecanoic acid or related compounds	Hydroxy fatty acids
304.2858	187.96	3.91	C17H34O3	NH3	2-hydroxy-heptadecanoic acid or related compounds	Hydroxy fatty acids
310.2375	115.40	0.52	C18H28O3	NH3	(-)-8-hydroxy-11E,17-octadecadien-9-ynoic acid or related compounds	Hydroxy fatty acids
332.3145	181.15	4.24	C19H38O3	NH3	19-hydroxy-nonadecanoic acid; 2-hydroxy-nonadecanoic acid	Hydroxy fatty acids
387.2633	112.88	0.85	C20H40O3	NaCl	20-hydroxy-eicosanoic acid;2-hydroxy-eicosanoic acid;3-hydroxy-eicosanoic acid;1,2-hydroxyphytanate	Hydroxy fatty acids
137.045	294.53	4.01	C4H8O5	H	D-threonic acid	Hydroxy fatty acids
133.0855	160.75	3.16	C6H12O3	H	(R)-3-Hydroxyhexanoic acid or related compounds	Hydroxy Acids
219.0051	638.54	1.46	C9H8O4	K	2,4-Dihydroxy-Trans Cinnamic Acid or related compounds	Hydroxy Acids
Isoprenoids						
368.4239	220.63	3.15	C25H50	NH3	4-pentacosene;6-pentacosene;9-pentacosene;C25 Monocyclic highly branched isoprenoid;C25:1 Highly branched isoprenoid	Isoprenoids
447.3383	114.34	4.25	C30H48	K	4,4'-Diapophytoene;"4,4'-Diapophytoene/ Dehydrosqualene"	Isoprenoids
489.3617	113.79	1.37	C30H54	KCl	Tetrahydrosqualene	Isoprenoids
489.35	114.72	1.74	C35H46	Na	4'-Apo-3,4-didehydrolycopene/ (4-Apo-3',4'-didehydrolycopene)	Isoprenoids
Phospholipids						
468.3079	465.94	1.17	C22H46NO7P	H	LysoPC(14:0);PC(0:0/14:0) or related compounds	Phospholipids
494.3238	464.08	0.61	C24H48NO7P	H	1-16:1-lysoPC or related compounds	Phospholipids
480.3443	456.83	1.12	C24H50NO6P	H	LysoPC(dm16:0);PC(0:16:1(11Z)/0:0) or related compounds	Phospholipids
496.3401	463.31	0.71	C24H50NO7P	H	LysoPC(16:0) or related compounds	Phospholipids
520.3404	461.86	1.25	C26H50NO7P	H	LysoPC(18:2(9Z,12Z)) or related compounds	Phospholipids
544.3384	461.39	1.95	C28H50NO7P	H	LysoPC(20:4(5Z,8Z,11Z,14Z)) or related compounds	Phospholipids
692.4062	212.33	4.87	C33H64NO8P	NaCl	PE(14:0/14:1(9Z)) or related compounds	Phospholipids
688.4941	208.14	4.27	C37H70NO8P	H	PE(14:0/18:2(9Z,12Z)) or related compounds	Phospholipids
674.5119	197.75	0.00	C37H72NO7P	H	PE(14:0/dm18:1(11Z)) or related compounds	Phospholipids
690.5069	210.44	3.62	C37H72NO8P	H	PE(14:0/18:1(11Z)) or related compounds	Phospholipids
675.5451	450.32	2.32	C37H75N2O6P	H	SM(d18:1/14:0)	Phospholipids
736.4311	223.45	0.39	C38H68NO8P	K	PE(15:0/18:4(6Z,9Z,12Z,15Z)) or related compounds	Phospholipids
738.4443	488.35	3.71	C38H70NO8P	K	PE(15:0/18:3(6Z,9Z,12Z)) or related compounds	Phospholipids
702.5098	372.47	4.26	C38H72NO8P	H	PC(14:1(9Z)/16:1(9Z)) or related compounds	Phospholipids
700.5287	193.51	1.66	C39H74NO7P	H	PE(16:1(9Z)/dm18:1(11Z)) or related compounds	Phospholipids
716.5237	204.02	1.73	C39H74NO8P	H	16:0-18:2-PE or related compounds	Phospholipids
702.5441	198.47	1.30	C39H76NO7P	H	PE(18:1(11Z)/dm16:0) or related compounds	Phospholipids
702.5408	421.81	3.40	C39H76NO7P	H	PE(16:0/dm18:1(9Z)) or related compounds	Phospholipids
702.5442	507.59	1.44	C39H76NO7P	H	1-Hexadecanoyl-2-(9Z-octadecanoyl)-sn-glycero-3-phosphoethanolamine or related compounds	Phospholipids
728.5561	520.51	0.45	C39H80NO7P	Na	PE(O-18:0/16:0)[U]	Phospholipids
728.526	348.01	4.86	C40H74NO8P	H	PC(14:0/18:3(6Z,9Z,12Z)) or related compounds	Phospholipids
716.5567	438.82	2.99	C40H78NO7P	H	PC(14:0/dm18:1(9Z)) or related compounds	Phospholipids
732.554	371.08	3.62	C40H78NO8P	H	PC(16:0/16:1(9Z)) or related compounds	Phospholipids
732.5537	408.42	3.21	C40H78NO8P	H	PC(14:0/18:1(9Z)) or related compounds	Phospholipids
732.5549	443.06	4.85	C40H78NO8P	H	PC(14:0/18:1(9E))[U] or related compounds	Phospholipids
732.5547	503.26	4.57	C40H78NO8P	H	PC(14:0/18:1(11Z)) or related compounds	Phospholipids
718.5741	378.11	0.54	C40H80NO7P	H	PC(14:0/dm18:0) or related compounds	Phospholipids
722.5098	186.64	3.78	C41H72NO7P	H	PE(18:4(6Z,9Z,12Z,15Z)/dm18:1(11Z)) or related compounds	Phospholipids
782.4689	493.25	0.51	C41H72NO8P	Na_Na	PE(14:0/22:5(4Z,7Z,10Z,13Z,16Z)) or related compounds	Phospholipids
724.5276	184.40	3.41	C41H74NO7P	H	PE(18:3(6Z,9Z,12Z)/dm18:1(11Z)) or related compounds	Phospholipids
726.5429	189.44	2.92	C41H76NO7P	H	PE(18:2(9Z,12Z)/dm18:1(11Z)) or related compounds	Phospholipids
728.5606	191.66	2.42	C41H78NO7P	H	PE(18:1(11Z)/dm18:1(11Z));PE(18:1(11Z)/dm18:1(9Z)) or related compounds	Phospholipids
744.5539	166.55	0.19	C41H78NO8P	H	PE(14:0/22:2(13Z,16Z)) or related compounds	Phospholipids
744.5557	202.25	2.61	C41H78NO8P	H	18:0-18:2-PE or related compounds	Phospholipids
744.5551	395.76	1.80	C41H78NO8P	H	PC(15:0/18:2(9Z,12Z)) or related compounds	Phospholipids
756.5543	353.49	3.90	C42H78NO8P	H	PC(14:0/20:3(5Z,8Z,11Z)) or related compound	Phospholipids
756.5505	438.70	1.12	C40H80NO8P	Na	PC(10:0/22:0) or related compounds	Phospholipids
775.5495	109.36	1.50	C42H79O10P	H	PG(18:0/18:2(9Z,12Z)) or related compounds	Phospholipids
742.5756	342.73	4.74	C42H80NO7P	H	PC(16:1(9Z)/dm18:1(11Z)) or related compounds	Phospholipids
758.5702	358.48	1.04	C42H80NO8P	H	PC(14:0/20:2(11Z,14Z)) or related compounds	Phospholipids
744.5895	352.48	0.86	C42H82NO7P	H	PC(16:0/dm18:1(11Z)) or related compounds	Phospholipids
760.585	365.23	3.10	C42H82NO8P	H	PC(14:1(9Z)/20:0) or related compounds	Phospholipids
760.583	428.20	0.47	C42H82NO8P	H	PC(14:0/20:1(11Z)) or related compounds	Phospholipids
746.6046	373.88	1.59	C42H84NO7P	H	PC(16:0/dm18:0) or related compounds	Phospholipids
780.4597	237.21	2.69	C43H68NO8P	Na	PE(18:4(6Z,9Z,12Z,15Z)/20:5(5Z,8Z,11Z,14Z,17Z)) or related compounds	Phospholipids
750.5424	184.27	1.66	C43H76NO7P	H	PE(20:4(5Z,8Z,11Z,14Z)/dm18:1(11Z)) or related compounds	Phospholipids
768.5906	335.00	3.73	C44H82NO7P	H	PC(18:2(9Z,12Z)/dm18:1(11Z)) or related compounds	Phospholipids
784.5877	347.40	3.38	C44H82NO8P	H	PC(14:1(9Z)/22:2(13Z,16Z)) or related compounds	Phospholipids
770.6083	344.05	3.26	C44H84NO7P	H	PC(18:1(11Z)/dm18:1(11Z)) or related compounds	Phospholipids

824.5595	342.49	3.54	C44H84N8O8P	K	PC(14:0/22:2(13Z,16Z)) or related compounds	Phospholipids
786.5984	381.69	2.92	C44H84N8O8P	H	PC(14:1(9Z)/22:1(13Z)) or related compounds	Phospholipids
786.6028	427.54	2.67	C44H84N8O8P	H	PC(16:0/20:2(1E,14E))[U] or related compounds	Phospholipids
786.5982	451.86	3.18	C44H84N8O8P	H	PC(18:1(10Z)/18:1(10Z)) or related compounds	Phospholipids
786.6026	505.34	2.42	C44H84N8O8P	H	PC(18:0/18:2(2E,4E)) or related compounds	Phospholipids
786.6042	594.01	4.45	C44H84N8O8P	H	PC(18:0/18:2(6Z,9Z)) or related compounds	Phospholipids
786.6028	675.87	2.67	C44H84N8O8P	H	PC(18:0/18:2(10Z,12Z)) or related compounds	Phospholipids
772.618	360.33	4.45	C44H86N8O7P	H	PC(18:0/dm18:1(11Z)) or related compounds	Phospholipids
776.5602	182.06	4.66	C45H78N8O7P	H	PE(22:5(4Z,7Z,10Z,13Z,16Z)/dm18:1(11Z)) or related compounds	Phospholipids
810.6021	333.87	4.70	C46H84N8O8P	H	20:2-18:2-PC or related compounds	Phospholipids
836.596	141.97	3.62	C46H88N8O7P	K	PC(20:1(11Z)/dm18:1(11Z)) or related compounds	Phospholipids
814.634	426.34	2.46	C46H88N8O8P	H	PC(14:1(9Z)/24:1(15Z)) or related compounds	Phospholipids
850.6111	140.03	2.92	C47H90N8O7P	K	PE(24:1(15Z)/dm18:1(11Z)) or related compounds	Phospholipids
880.6235	146.68	2.25	C48H92N8O8P	K	PC(16:1(9Z)/24:1(15Z)) or related compounds	Phospholipids
924.7379	103.23	1.34	C52H104N8O8P	Na	PC(18:0/26:0) or related compounds	Phospholipids
188.175	580.12	3.88	C9H21N3O	H	N1-Acetylspermidine or related compounds	Polymamines
188.175	623.03	3.93	C9H21N3O	H	N8-Acetylspermidine or related compounds	Polymamines
Polypeptides						
273.0825	294.95	1.25	C10H16N2O4	Na_Na	(S)-ATPA;Prolylhydroxyproline	Polypeptides
308.0904	615.60	2.21	C10H17N3O6S	H	Glutathione;Reduced glutathione	Polypeptides
229.1539	541.82	3.36	C11H20N2O3	H	L-isoleucyl-L-proline;L-leucyl-L-proline	Polypeptides
427.0954	664.31	4.40	C13H22N4O8S2	H	Cysteineglutathione disulfide	Polypeptides
613.1595	649.09	0.16	C20H32N6O12S2	H	Glutathione disulfide;Oxidized glutathione	Polypeptides
681.1999	294.13	3.21	C22H42N4O8S2	NaCl_HCOONa	D-Pantethine	Polypeptides
179.0482	614.98	1.62	C5H10N2O3S	H	Cys-Gly;Cysteine-S-Acetamide	Polypeptides
188.1751	477.34	3.40	C9H21N3O	H	N1-Acetylspermidine;N8-Acetylspermidine	Polymamines
Nucleotides and Derivatives						
275.0738	250.68	4.62	C10H12N4O4	Na	Deoxyinosine;Nebularine;Purine Riboside	Nucleoside Analogues
306.0804	507.19	1.57	C10H13N5O5	Na	8-Hydroxy-2'-Deoxyguanosine;8-Hydroxy-deoxyguanosine;Crotonoside;Guanosine;	Nucleoside Analogues
338.0497	548.33	0.12	C10H13N5O6	K	8-Hydroxyguanosine	Nucleoside Analogues
364.0643	642.29	2.69	C10H14N5O8P	H	8-Oxo-2'-Deoxy-Guanosine-5'-Monophosphate or related compounds	Nucleotides
298.0957	156.40	3.82	C11H15N5O3S	H	5'-Methylthioadenosine or related compounds	Nucleoside Analogues
565.0832	696.81	0.30	C16H26N2O16P2	H	dTDP-D-galactose or related compounds	Nucleotides
608.0896	610.25	1.23	C17H27N3O17P2	H	UDP-GlcNAc or related compounds	Nucleotides
664.1178	617.75	0.72	C21H27N7O14P2	H	Nicotinamide adenine dinucleotide or related compounds	Nucleotides
113.0341	185.11	4.07	C4H4N2O2	H	Uracil	Pyrimidines and Derivatives
129.0765	524.80	4.57	C4H5N3O	NH3	Cytosine	Pyrimidines and Derivatives
152.0561	508.74	4.93	C4H6O5	NH3	3-Dehydro-L-threonate;Malate	Purines and Purine Derivatives
152.056	642.92	4.27	C4H6O5	NH3	3-Dehydro-L-threonate;Malate	Purines and Purine Derivatives
137.0454	446.55	2.85	C5H4N4O	H	Hypoxanthine	Purines and Purine Derivatives
153.0412	314.70	3.27	C5H4N4O2	H	6,8-Dihydroxypurine;Alloxanthine;Oxypurinol	Purines and Purine Derivatives
136.0617	615.68	0.51	C5H5N5	H	Adenine	Purines and Purine Derivatives
136.0615	252.64	1.98	C5H5N5	H	Adenine	Purines and Purine Derivatives
136.0612	229.73	4.19	C5H5N5	H	Adenine	Purines and Purine Derivatives
136.0621	157.31	2.43	C5H5N5	H	Adenine	Purines and Purine Derivatives
152.0561	461.72	4.93	C5H5N5O	H	2-Hydroxyadenine;8-Hydroxyadenine;Guanine	Purines and Purine Derivatives
129.0657	629.63	1.24	C5H8N2O2	H	5,6-Dihydrothymine or related compounds	Pyrimidines and Derivatives
405.0095	616.31	4.07	C9H14N2O12P2	H	UDP	Nucleotides
Quaternary Amines						
244.1538	126.45	2.17	C12H21NO4	H	Tiglylcarnitine	Quaternary Amines
246.1694	499.59	2.36	C12H23NO4	H	2-Methylbutyrylcarnitine;Isovalerylcarnitine	Quaternary Amines
330.2638	119.83	3.03	C18H35NO4	H	4,8 dimethylnonanoyl carnitine	Quaternary Amines
398.3262	440.68	2.59	C23H43NO4	H	trans-Hexadec-2-enoyl carnitine	Quaternary Amines
400.3418	440.34	0.80	C23H45NO4	H	L-Palmitoylcarnitine	Quaternary Amines
426.357	436.45	1.81	C25H47NO4	H	Elaidic carnitine;octadecenyl carnitine;Vaccenyl carnitine;;	Quaternary Amines
162.1119	653.66	3.52	C7H15NO3	H	L-Carnitine	Quaternary Amines
204.1222	590.80	4.07	C9H17NO4	H	L-Acetylcarnitine	Quaternary Amines
Sphingoid bases						
252.2303	113.30	2.10	C14H31NO	Na	Lauryl Dimethylamine-N-Oxide;Xestaminol C;;	Sphingoid bases
310.1746	712.63	4.93	C15H23N3O4	H	Polypoline	Sphingoid bases
442.1864	609.22	4.95	C17H33N8O5P	KCl	C17 Sphinganine-1-phosphate	Sphingoid bases
318.2399	110.04	1.38	C18H33NO2	Na	(4E,8E,10E-d18:3)sphingosine;;	Sphingoid bases
320.2555	111.94	1.53	C18H35NO2	Na	(4E,8E,d18:2) sphingosine or related compounds	Sphingoid bases
648.38	200.39	3.87	C32H63NO5S	KCl	N-(tetradecanoyl)-deoxysphing-4-enine-1-sulfonate	Sphingolipids
703.575	449.57	0.26	C39H79N2O6P	H	SM(d18:1/16:0)	Sphingolipids
785.6536	446.72	0.67	C45H89N2O6P	H	SM(d18:1/22:1(13Z))	Sphingolipids
Vitamins						
417.2769	274.31	0.86	C27H38O2	Na	25-hydroxy-16,17,23,23,24,24-hexadehydrovitamin D3 / 25-hydroxy-16,17,23,23,24,24-hexadehydrocholecalciferol or related compounds	Vitamin D2 and derivatives
447.3106	115.06	1.45	C27H42O5	H	(23R)-1alpha,23,25-trihydroxy-24-oxovitamin D3 / (23R)-1alpha,23,25-trihydroxy-24-oxocholecalciferol or related compounds	Vitamin D2 and derivatives
433.3304	103.54	3.67	C27H44O4	H	(20S)-1alpha,20,25-trihydroxyvitamin D3 / (20S)-1alpha,20,25-trihydroxycholecalciferol or related compounds	Vitamin D3 and derivatives
447.3466	103.15	0.60	C28H46O4	H	(20S)-1alpha,20,25-trihydroxy-24a-homovitamin D3 / (20S)-1alpha,20,25-trihydroxy-24a-homocholecalciferol or related compounds	Vitamin D2 and derivatives
503.3072	191.93	3.93	C29H48O2	KCl	(22alpha)-hydroxy-isocholesterol or related compounds	Vitamin D2 and derivatives
461.3626	103.90	0.17	C29H48O4	H	(20S)-14alpha,20,25-trihydroxy-26,27-dimethylvitamin D3 / (20S)-1alpha,20,25-trihydroxy-26,27-dimethylcholecalciferol or related compounds	Vitamin D2 and derivatives
601.3268	506.60	4.31	C36H50O	K	11-(4-acetoxymethylphenyl)-1alpha,25-dihydroxy-9,11-didehydrovitamin D3 / 11-(4-acetoxymethylphenyl)-1alpha,25-dihydroxy-9,11-didehydrocholecalciferol or related compounds	Vitamin D2 and derivatives
725.4475	131.38	0.65	C39H64O12	H	1-Hydroxyvitamin D3 cellobioside;;	Vitamin D3 and derivatives
Miscellaneous						
224.125	193.91	3.17	C10H19NO3	Na	Capryloylglycine	Acyl Glycines
188.0704	496.37	1.12	C11H9NO2	H	Indoleacrylic acid	Indoles and Indole Derivatives
275.1412	408.38	1.53	C15H24O2	K	Capsidol;3,4-dihydroartemisininate;Famesoic acid;Helminthosporol;Hernandulcin;Latia luciferin;L.ubitin;Sirenin;;	Alcohols and Polyol
289.1792	103.80	2.14	C18H24O3	H	16,17-Epiestriol or related compounds	Steroids and Steroid Derivatives
300.3246	260.32	4.93	C19H38O	NH3	2-nonadecanone;Pristanal	Aldehydes
357.2622	113.06	3.75	C20H36O5	H	13,14-dihydro PGE1 or related compounds	Prostanoids
478.3214	198.74	4.41	C21H43N5O7	H	Gentamicin	Drug
142.0261	697.79	1.90	C21H8NO4P	H	1-Hydroxy-2-aminoethylphosphonate;Ethanolamine phosphate;;	Acyl Phosphates
604.354	189.84	2.25	C30H52O7P2	NH3	all-trans-Hexaprenyl diphosphate	Alkanes and Alkenes
790.5238	186.10	2.76	C46H73N3O4	NaCl	N-tryptophanyl-35-aminobacteriohopane-32,33,34-triol	Hopanoids
104.1064	573.42	5.67	C5H13NO	H	Choline	Aldehydes
123.0549	152.27	3.17	C6H6N2O	H	Nicotinamide	Cyclic Amines
107.0492	483.94	0.56	C7H6O	H	Benzaldehyde	Aldehydes
187.1076	646.46	0.64	C8H11NO3	NH3	5-Hydroxydopamine or related compounds	Catecholamines and Derivatives
204.0861	610.01	2.55	C8H13NO5	H	N2-acetyl-alpha-aminoadipate or related compounds	Pterins
147.0436	552.77	2.72	C9H6O2	H	Phenylpropionic acid	Alkyl Chlorides

Appendix C

A list of putitive identification of metabolites in human apocrine sweat. Bold text represents matches found in the HMDB urine database.

m/z	rt (s)	ppm error	MF	Adduct	Metabolites	Class	Ionmode
Amino Acids							
249.0615	84.30	1.73	C11H12N2O2	Na_Na	L-Tryptophan	Amino Acids	pos
369.1512	469.14	0.84	C12H24N2O8	HCOOH	Galactosylhydroxylysine	Sugar Amino Acids	neg
369.1531	504.24	4.47	C12H24N2O9	HCOOH	Galactosylhydroxylysine	Sugar Amino Acids	neg
543.1576	444.30	0.31	C18H34N2O13	NaCl	Glucosylgalactosyl hydroxylysine	Sugar Amino Acids	neg
199.9543	804.54	1.00	C2H7NO3S	KCl	Taurine	Amino Acids	pos
172.0220	67.20	4.48	C3H7NO3	HCOONa	L-Serine	Amino Acids	neg
183.9914	80.16	3.86	C3H7NO6S	H	L-Serine O-sulfate	Amino Acids	neg
164.0296	68.46	1.22	C4H9NO3	Na_Na (HCOONa)	L-Allothreonine; L-Homoserine; L-Threonine	Amino Acids	pos/neg
252.0148	66.48	0.16	C4H9NO5S	HCOONa	L-Methionine sulfone	Amino Acids	pos
191.0406	68.46	1.41	C5H10N2O3	Na_Na	L-Glutamine	Amino Acids	pos
169.0583	385.80	0.35	C5H10N2O3	Na	3-Ureidoisobutyrate	Amino Acids	pos
238.0142	63.84	4.58	C5H11NO2S	Na_HCOONa	L-Methionine	Amino Acids	neg
177.0612	64.56	1.13	C5H12N2O2	Na_Na (HCOONa)	L-Ornithine	Amino Acids	pos/neg
191.0768	64.56	0.84	C6H14N2O2	Na_Na	L-Lysine	Amino Acids	pos
185.9932	76.80	3.71	C5H7NO2	NaCl	Pyroglutamic acid	Amino Acids	neg
231.9888	66.48	1.64	C5H9NO2	NaClx2	L-Proline	Amino Acids	pos
220.0669	66.54	0.05	C6H13N3O3	Na_Na	L-Citrulline	Amino Acids	pos
200.0408	64.56	0.95	C6H9N3O2	Na_Na (HCOONa)	L-Histidine	Amino Acids	pos/neg
240.0486	81.12	2.92	C7H11NO4	HCOONa	(2 <i>S</i> ,5 <i>S</i>)-5-Carboxymethylproline or related compounds	Amino Acids	neg
144.1019	430.92	0.21	C7H13NO2	H	Proline Betaine	Amino Acids	neg
252.9794	81.12	2.10	C8H8N2O3	KCl	Nicotimurate	Cyclic Amino Acids	neg
226.0454	74.28	1.86	C9H11NO3	Na_Na	L-Tyrosine	Amino Acids	pos
307.0345	81.00	2.41	C9H16N2O5S	Na_Na	N-Acetylcyathionine	Amino Acids	neg
Di/Polypeptides							
293.1468	404.58	4.09	C10H17N3O6	NH3	Norophthalmic acid	Polypeptides	pos
319.1248	87.96	2.38	C11H20N2O3	Na_HCOONa (HCOOH)	L-Isoleucyl-L-proline; L-leucyl-L-proline	Polypeptides	pos/neg
319.1240	146.64	0.03	C11H20N2O3	Na_HCOONa (HCOOH)	L-leucyl-L-proline	Polypeptides	pos/neg
273.1454	169.86	0.73	C11H20N2O3	HCOOH	L-Isoleucyl-L-proline; L-leucyl-L-proline	Polypeptides	neg
273.1452	200.76	1.32	C11H20N2O3	HCOOH	L-leucyl-L-proline	Polypeptides	neg
273.1453	232.32	0.99	C11H20N2O3	HCOOH	L-leucyl-L-proline	Polypeptides	neg
277.1224	682.08	1.30	C11H22N2O4S	H	Pantetheine	Polypeptides	neg
363.1782	414.48	1.82	C16H22N6O4	H	Thyrotropin releasing hormone	Polypeptides	pos
533.2586	383.58	4.01	C22H40N8O5	K	Postin	Polypeptides	neg
581.2786	418.26	3.72	C22H40N8O5	HCOOK	Postin	Polypeptides	pos
177.0331	463.98	4.69	C5H10N2O3S	H	Cys-Gly; Cysteine-S-Acetamide	Polypeptides	neg
187.0716	424.98	4.17	C7H12N2O4	H	L-glycyl-L-hydroxyproline; N-Acetylglutamine	Polypeptides	neg
233.0509	191.58	3.86	C7H12N2O4	Na_Na	L-glycyl-L-hydroxyproline; N-Acetylglutamine	Polypeptides	pos
Polyamines							
239.1647	428.52	1.38	C10H26N4	K	Spermine	Polyamines	neg
301.1766	388.14	3.32	C12H28N4O	NaCl	N1-Acetylspermine	Polyamines	neg
331.2094	422.16	4.29	C14H30N4O2	Na_Na	N1,N12-Diacetylspermine	Polyamines	pos
Quaternary Amines							
338.2300	465.90	0.47	C17H33NO4	Na	Decanoylcarnitine; O-Decanoyl-L-carnitine	Quaternary Amines	pos
330.2639	444.30	3.39	C18H35NO4	H	4,8-dimethylnonanoyl carnitine	Quaternary Amines	pos
344.2793	457.86	0.58	C19H37NO4	H	Dodecanoylcarnitine	Quaternary Amines	pos
372.3106	478.02	0.64	C21H41NO4	H	Tetradecanoylcarnitine	Monocacylglycerophosphates	pos
398.3263	485.88	0.45	C23H43NO4	H	trans-Hexadec-2-enoyl carnitine	Quaternary Amines	pos
430.3164	425.28	0.33	C23H43NO6	H	Hexadecanodioic acid mono-L-carnitine ester	Quaternary Amines	pos
400.3421	501.54	0.05	C23H45NO4	H	L-Palmitoylcarnitine	Quaternary Amines	pos
414.3581	508.68	0.77	C24H47NO4	H	Heptadecanoyl carnitine	Quaternary Amines	pos
424.3422	491.70	0.16	C25H49NO4	H	Linolealidyl carnitine; Linoleyl carnitine	Quaternary Amines	pos
448.3396	508.68	0.25	C25H47NO4	Na	Elaidic carnitine or related compounds	Quaternary Amines	pos
428.3739	518.04	1.05	C25H49NO4	H	Stearoylcarnitine	Quaternary Amines	pos
584.4885	696.00	1.71	C33H65NO4	HCOOH	Hexacosanoyl carnitine	Quaternary Amines	neg
356.0420	66.54	0.42	C9H15N3O2S	HCOONa	Ergothioneine	Quaternary Amines	pos
Carbohydrates							
365.1060	70.44	4.41	C12H22O11	Na	Alpha-Lactose; D-Maltose; Melibiose; Sucrose	Carbohydrates	pos
382.1343	458.82	2.25	C14H23NO11	H	N-Acetyl-9-O-lactylneuraminic acid	Carbohydrates	pos
485.1127	587.46	3.59	C15H26N2O12	NaCl	Chitobiose	Carbohydrates	pos
201.0374	83.46	3.38	C6H12O6	Na	D-Fructose; D-Galactose; D-Glucose; D-Mannose; Myoinositol	Carbohydrates	neg
253.0140	169.44	4.58	C7H14O5S	Na_Na	4-Methylthio-Alpha-D-Mannose; O1-Methyl-4-Deoxy-4-Thio-Alpha-D-Glucose; O1-Methyl-4-Deoxy-4-Thio-Beta-D-Glucose	Amino ketones	neg
Fatty Acids and Conjugates							
173.1535	604.14	0.58	C10H20O2	H	2-methyl nonanoic acid or related compounds	Fatty Acids and Conjugates	pos
173.1536	648.06	0.23	C10H20O2	H	3-methyl-nonanoic acid or related compounds	Fatty Acids and Conjugates	pos
173.1536	703.80	0.23	C10H20O2	H	7-methyl-nonanoic acid or related compounds	Fatty Acids and Conjugates	pos
173.1536	739.08	0.29	C10H20O2	H	2-methyl nonanoic acid or related compounds	Fatty Acids and Conjugates	pos
185.1535	440.52	0.43	C11H22O2	H	11-Undecanolactone; 2-hendecenoic acid or related compounds	Fatty Acids and Conjugates	pos
213.1848	461.64	0.42	C13H24O2	H	12-tridecenoic acid; 2-methyl-2-dodecenoic acid or related compounds	Fatty Acids and Conjugates	pos
295.1885	601.20	1.05	C14H28O2	HCOONa	Myristic acid	Fatty Acids;	neg
311.1974	459.72	0.64	C16H32NO4	NH3	10E-heptadecenoic acid; 10-methyl-9-hexadecenoic acid or related compounds	Fatty Acids and Conjugates	neg
251.2005	446.22	0.20	C16H32O2	H	4,7,10-hexadecatrienoic acid or related compounds	Fatty Acids and Conjugates	pos
255.2318	476.16	0.04	C16H30O2	H	Palmitoleic acid	Fatty Acids and Conjugates	pos
253.2169	615.90	1.66	C16H30O2	H	10-hexadecenoic acid or related compounds	Fatty Acids and Conjugates	neg
297.1817	447.96	1.01	C16H30O2	Na_Na	Palmitoleic acid	Fatty Acids and Conjugates	neg
274.2739	448.20	0.55	C16H32O2	NH3 (Na_Na)	Palmitic acid	Fatty Acids and Conjugates	pos/neg
255.2325	656.88	1.92	C16H32O2	H	13-methyl-pentadecanoic acid or related compounds	Fatty Acids and Conjugates	neg
267.2326	641.82	1.27	C17H32O2	H	10E-heptadecenoic acid or related compounds	Fatty Acids and Conjugates	neg
311.1427	562.86	2.67	C18H26O2	K	13E-octadecene-9,11-diynoic acid or related compounds	Fatty Acids and Conjugates	neg
279.2318	438.66	0.25	C18H30O2	H	Alpha-Linolenic acid	Fatty Acids	pos
311.2215	466.44	0.58	C18H30O4	H	(9Z,11E,14Z)-(13 <i>S</i>)-hydroperoxyoctadeca-9,11,14-trienoate or related compounds	Fatty Acids and Conjugates	pos
341.2444	488.82	0.64	C19H38O2	Na_Na	(+)-16-methyl stearic acid or related compounds	Fatty Acids	neg
347.2200	633.30	1.04	C18H32O2	HCOONa	10E,12E-octadecadienoic acid or related compounds	Fatty Acids and Conjugates	pos
325.2115	634.44	2.03	C18H32O2	Na_Na	Linoleic acid	Fatty Acids and Conjugates	pos
295.2276	443.04	0.95	C18H32O3	H	13S-hydroxyoctadecadienoic acid	Fatty Acids;	neg
313.2371	474.30	0.67	C18H32O4	H	(9Z,11E)-(13 <i>S</i>)-13-Hydroperoxyoctadeca-9,11-dienoic acid or related compounds	Fatty Acids	pos
283.2631	499.50	0.32	C18H34O2	H	Oleic acid	Fatty Acids	pos
281.2483	509.04	1.07	C18H34O2	H	(11E)-Octadecenoic acid or related compounds	Fatty Acids	neg
283.2632	663.66	0.32	C18H34O2	H	Oleic acid	Fatty Acids	pos
327.2273	667.62	1.74	C18H34O2	Na_Na (H)	(11E)-Octadecenoic acid; (6Z)-Octadecenoic acid or related compounds	Fatty Acids	pos/neg
327.2286	479.10	1.59	C18H36O2	Na_Na	Stearic acid	Fatty Acids	neg
399.1968	477.06	2.08	C18H36O2S	HCOOK	2-mercaptop-octadecanoic acid	Fatty Acids and Conjugates	neg
325.2373	481.86	0.03	C19H32O4	H	methyl 15-hydroperoxy-9Z,12Z,16E-octadecatrienoate or related compounds	Fatty Acids and Conjugates	pos
374.2539	400.68	0.53	C19H32O6	NH3	methyl 10,12-dihydroperoxy-8E,13E,15Z-octadecatrienoate or related compounds	Fatty Acids and Conjugates	pos
327.2529	485.88	0.15	C19H34O4	H	11-methoxy-12,13-epoxy-9-octadecenoic acid or related compounds	Fatty Acids and Conjugates	pos
369.1955	443.70	1.65	C19H36O2	KCl	10E-nonadecenoic acid or related compounds	Fatty Acids and Conjugates	neg
339.2286	488.82	0.91	C19H36O2	Na_Na	10E-nonadecenoic acid; 10-methylene-octadecanoic acid or related compounds	Fatty Acids and Conjugates	neg

297.2790	513.18	0.64	C19H36O2	H	10E-nonadecenoic acid;10-methylene-octadecanoic acid;10Z-nonadecenoic acid or related compounds	Fatty Acids and Conjugates	pos
371.2116	465.72	2.51	C19H38O2	KCl	(+)-16-methyl stearic acid;"(2R,6S,10S)-pristanate";11-methyl-octadecanoic acid or related compounds	Fatty Acids and Conjugates	neg
316.3212	478.02	0.76	C19H38O2	NH3	(+)-16-methyl stearic acid;"(2R,6S,10S)-pristanate";11-methyl-octadecanoic acid or related compounds	Fatty Acids and Conjugates	pos
305.2473	448.14	0.62	C20H32O2	H	Arachidonic acid	Fatty Acids	pos
307.2640	686.28	0.94	C20H36O2	H	11,14-eicosadienoic acid or related compounds	Fatty Acids and Conjugates	neg
311.2943	528.90	0.42	C20H38O2	H	13-eicosenoic acid or related compounds	Fatty Acids and Conjugates	pos
357.2644	484.86	0.56	C20H38O5	H	11,13-dimethoxy-12-hydroxy-9-octadecenoic acid;"13,14-Dihydro PGF-1a", or related compounds	Fatty Acids and Conjugates	neg
369.2069	488.34	0.57	C22H28O2	HCOOH	4,7,10,13-Docosatetraenoic acid or related compounds	Fatty Acids and Conjugates	neg
329.2473	455.88	0.58	C22H32O2	H	Docosahexanoic acid	Fatty Acids and Conjugates	pos/neg
381.2754	531.84	0.87	C22H42O2	Na_Na	(13Z)-Docosenoic acid or related compounds	Fatty Acids and Conjugates	neg
383.2911	533.82	1.12	C22H44O2	Na_Na	19-methyl-heneicosanoic acid;3-methyl-heneicosanoic acid;Docosanoic acid;Isobhenic acid	Fatty Acids and Conjugates	neg
465.3456	801.42	1.01	C23H49N2O5P	H	Sphingosyl-phosphocholine;"2,4,6-trimethyl-2,1,5-tetracosadienoic acid";	Fatty Acids and Conjugates	pos
425.2574	592.38	4.63	C23H44O2	KCl	14E-tricosenoic acid or related compounds	Fatty Acids and Conjugates	neg
409.3039	460.80	3.44	C24H44O2	Na_Na	5,9-tetracosadienoic acid	Fatty Acids and Conjugates	pos
187.0717	75.90	1.87	C8H16O2	Na_Na	Caprylic acid	Fatty Acids and Conjugates	neg
187.0717	169.44	4.01	C8H16O2	Na_Na	Caprylic acid	Fatty Acids and Conjugates	neg
187.0710	203.52	1.98	C8H16O2	Na_Na	Caprylic acid	Fatty Acids and Conjugates	neg
187.0709	234.24	2.46	C8H16O2	Na_Na	Caprylic acid	Fatty Acids and Conjugates	neg
187.0717	388.14	4.01	C8H16O2	Na_Na	Caprylic acid	Fatty Acids and Conjugates	neg
271.0246	169.86	4.02	C9H16O2	NaClx2	2-amyl 3-butenic acid;2E-nonenic acid or related compounds	Fatty Acids and Conjugates	neg
271.0245	200.76	4.46	C9H16O2	NaClx2	2-amyl 3-butenic acid;2E-nonenic acid or related compounds	Fatty Acids and Conjugates	neg
271.0247	374.22	3.91	C9H16O2	NaClx2	2-amyl 3-butenic acid;2E-nonenic acid or related compounds	Fatty Acids and Conjugates	neg
Fatty aldehydes							
167.1430	440.52	0.30	C11H18O	H	2,5-undecadienal	Fatty aldehydes	pos
209.1898	466.44	0.81	C14H24O	H	5,8-tetradecadienal	Fatty aldehydes	pos
240.2321	462.54	0.37	C15H26O	NH3	"(1E,4S,5E,7R)-Germacl-1(10) or related compounds	Fatty aldehydes	pos
270.2794	458.88	0.96	C17H32O	NH3	14-Methyl-8E-hexadecenal or related compounds	Fatty aldehydes	pos
309.2431	561.06	1.20	C18H32O	HCOOH	9,12-octadecadienal	Fatty aldehydes	neg
367.2159	576.72	4.49	C20H38O	KCl	11Z-Eicosenal	Fatty aldehydes	neg
169.0609	169.44	0.71	C8H14O	Na_Na	2-octenal or related compounds	Fatty aldehydes	neg
Fatty alcohols							
205.1587	430.92	0.24	C14H20O	H	13-tetradecan-2,4-diy-1-ol	Fatty alcohols	pos
253.2139	562.02	0.43	C14H30O2	Na	2,2,9,9-tetramethyl-undecan-1,10-diol	Fatty alcohols	pos
297.2398	599.22	0.74	C15H32O	HCOONa	3S,7S-dimethyl-2S-tridecanol	Fatty alcohols	pos
258.2794	454.92	1.12	C16H32O	NH3	1,2-Epoxyhexadecan-11Z-hexadecen-1-ol or related compounds	Fatty alcohols	pos
311.2554	626.88	0.90	C16H34O	HCOONa	14-methyl-1-pentadecanol;1-Hexadecanol;"3S,7S-dimethyl-2S-tetradecanol"	Fatty alcohols	pos
343.1316	555.12	2.94	C17H22O2	HCOOK	"1,9Z,16-heptadecatrien-4,6-diyn-3,8-diol";"5,8,11-heptadecatriynic acid";Cicutoxin;	Fatty alcohols	pos
325.2711	587.46	0.65	C17H36O	HCOONa	14-methyl-1-hexadecanol	Fatty alcohols	pos
313.2494	480.78	1.63	C18H38O	Na_Na	3S,7S-dimethyl-2-hexadecanol;Octadecanol	Fatty alcohols	neg
371.2705	465.72	1.83	C20H42O2	NaCl	1,2-eicosanediol; 13-methyl-1,2-nonadecanediol	Fatty alcohols	neg
371.2895	465.72	3.21	C21H44O2	Na_Na	1,2-heneicosanediol;"13-methyl-1,2-eicosanediol";"15-methyl-1,2-eicosanediol";	Fatty alcohols	pos/neg
143.0452	463.98	1.47	C6H12O	Na_Na	2E-hexenol-2-Oxohexane; or Unsaturated alcohol	Fatty alcohols	neg
145.0609	424.98	1.24	C6H14O	Na_Na	3-Methylpentan-1-ol;Hexan-1-ol	Fatty alcohols	neg
Hydroxy-oxo fatty acids							
263.1618	430.92	0.04	C14H24O3	Na	(1R,2R)-3-oxo-2-pentyl-cyclopentanecarboxylic acid or related compounds	Hydroxy fatty acids	pos
285.1434	501.54	1.05	C14H24O3	Na_Na	6(R)-hydroxy-tetradeca-2E,8Z-dienoate or related compounds	Hydroxy fatty acids	pos
287.1611	374.22	2.23	C14H28O3	Na_Na	10-hydroxy-tetradecanoic acid or related compounds	Hydroxy fatty acids	neg
301.1410	558.18	0.53	C16H22O4	Na	2-Ethylhexyl phthalate;3'-carboxy-alpha-chromanol;4-prenylphlorisovalerophenone,Alpha-CEHC;Dibutyl phthalate;Diisobutyl phthalate	Hydroxy fatty acids	pos
265.1806	442.20	1.28	C16H26O3	H	(2E,6E)(10R,11S)-10,11-Epoxy-3,7,11-trimethyltrideca-2,6-dienoic acid or related compounds	Hydroxy fatty acids	neg
265.1804	549.78	1.96	C16H26O3	H	(9R,13R)-1a,1b-dinor-10,11-dihydro-12-oxo-15-phytoenoic acid or related compounds	Hydroxy fatty acids	neg
337.1985	444.30	0.68	C16H28O3	HCOONa	(1R,2R)-3-oxo-2-pentyl-cyclopentanecarboxylic acid;"(1S,2S)-3-oxo-2-pentyl-cyclopentanecarboxylic acid	Hydroxy fatty acids	pos
291.1929	446.22	0.41	C16H28O3	Na	(1S,2S)-3-oxo-2-pentyl-cyclopentanecarboxylic acid or related compounds	Hydroxy fatty acids	pos
313.1767	404.40	0.57	C16H30O3	Na_Na	(+)-12-hydroxy-9Z-hexadecenoic acid;10-keto palmitic acid or related compounds	Hydroxy fatty acids	neg
269.2119	510.30	1.19	C16H30O3	H	10-keto palmitic acid or related compounds	Hydroxy fatty acids	neg
269.2119	570.84	1.08	C16H30O3	H	10-oxo-14-methyl-pentadecanoic acid or related compounds	Hydroxy fatty acids	neg
315.1924	424.98	0.57	C16H32O3	Na_Na	11-hydroxy palmitic acid or related compounds	Hydroxy fatty acids	neg
271.2277	598.26	0.70	C16H32O3	H	14-hydroxy palmitic acid or related compounds	Hydroxy fatty acids	neg
355.2097	567.90	1.32	C16H32O4	HCOONa	10,16-Dihydroxyhexadecanoic acid or related compounds	Hydroxy fatty acids	neg
309.2043	627.54	1.39	C16H32O4	Na	3,12-dihydroxy palmitic acid or related compounds	Hydroxy fatty acids	neg
367.2106	467.94	1.20	C17H32O4	HCOONa	2-methyl-hexadecanecarboxylic acid or related compounds	Hydroxy fatty acids	neg
369.2253	443.70	1.44	C17H34O4	HCOONa	MG(0:0/14:0:0:0);MG(14:0/0:0:0:0)	Hydroxy fatty acids	neg
369.2254	487.26	1.19	C17H34O4	HCOONa	MG(0:0/14:0:0:0);MG(14:0/0:0:0:0)	Hydroxy fatty acids	neg
347.1828	430.92	3.31	C18H28O5	Na	12-oxo-14,18-dihydroxy-9Z,13E,15Z-octadecatrienoic acid	Oxo fatty acids	pos
293.2121	435.36	0.34	C18H30O3	H	(9R,13R)-10,11-dihydro-12-oxo-15-phytoenoic acid or related compounds	Hydroxy fatty acids	neg
319.2245	548.52	1.19	C18H32O3	Na (H)	(1R,2R)-3-oxo-2-pentyl-cyclopentanecarboxylic acid or related compounds	Hydroxy fatty acids	pos/neg
341.2080	450.36	1.85	C18H34O3	Na_Na	(6R,7S)-6,7-Epoxyoctadecanoic acid;(9Z)-(12S)-Hydroxyoctadecenoic acid;10-hydroxy-8-octadecenoic acid or related compounds	Hydroxy fatty acids	neg
297.2431	572.82	1.45	C18H34O3	H	10R-hydroxy-8E-octadecenoic acid or related compounds	Hydroxy fatty acids	neg
299.2588	565.02	1.30	C18H36O3	H	(R)-2-Hydroxystearate or related compounds	Hydroxy fatty acids	neg
315.2535	518.10	1.78	C18H36O4	H	(9R,10R)-Dihydroxyoctadecanoic acid or related compounds	Hydroxy fatty acids	neg
385.2562	536.70	0.39	C18H36O4	HCOONa	(9S,10S)-9,10-Dihydroxyoctadecanoate or related compounds	Hydroxy fatty acids	pos
383.2413	588.42	0.50	C18H36O4	HCOONa	10,11-dihydroxy stearic acid or related compounds	Hydroxy fatty acids	neg
337.2357	679.98	3.83	C18H36O4	Na	11,12-dihydroxy stearic acid or related compounds	Hydroxy fatty acids	neg
399.2373	571.86	2.35	C18H36O5	HCOONa	18-hydroxy-9S,10R-dihydroxy-stearic acid; 9,10,18-trihydroxystearate or related compounds	Hydroxy fatty acids	neg
371.2407	495.60	0.78	C18H36O6	Na	Sativic acid	Hydroxy fatty acids	pos
371.2320	465.72	3.85	C19H38O3	NaCl	19-hydroxy-nonadecanoic acid;2-hydroxy-nonadecanoic acid	Hydroxy fatty acids	neg
369.2751	518.10	0.16	C21H42O2	Na_Na	(+)-18-methyl-eicosanoic acid;19-methyl-eicosanoic acid;"2,6-dimethyl-nonadecanoic acid";Heneicosanoic acid;Homophytanic acid	Methyl branched fatty acids	neg
372.3476	505.38	1.13	C22H42O3	NH3	10-oxo-docosanoic acid or related compounds	Oxo fatty acids	pos
400.3789	536.70	0.92	C24H46O3	NH3	24-hydroxy-10Z-tetracosenoic acid;2-hydroxy-15Z-tetracosenoic acid;3-oxo-tetracosanoic acid;Hydroxynervonic acid	Hydroxy fatty acids	pos
133.0865	577.68	4.51	C6H12O3	H	5-Hydroxyhexanoic acid;Hydroxyisocaproic acid	Hydroxy Acids	pos
Eicosanoids							
303.2317	448.14	0.43	C20H30O2	H	(+)-Pimaric acid or related compounds	Eicosanoids	pos

319.2276	452.82	4.39	C20H32O3	H	(15S)-15-Hydroxy-5,8,11-cis-13-trans-eicosatetraenoate or related compounds	Eicosanoids	neg
321.2432	455.22	0.84	C20H34O3	H	12-HETE; 12R-HETE; 15-oxo-11Z,13E-eicosadienoic acid or related compounds	Eicosanoids	neg
356.2793	459.72	0.73	C20H34O4	NH3	10,11-dihydro-12-epi-leukotriene B4; *11,12-DHET; 11-deoxy-PGE1; 11-deoxy-PGF2a; 11-deoxy-PGF2beta; 12-keto-tetrahydro-Leukotriene B4; *14,15-DHET; *15-hydroperoxyeicosa-8Z,11Z,13E-trienone; *5,6-DHET; *5,6-dihydroxy-8,11,14-eicosatrienoic acid; *6,7-dihydro-12-epi-leukotriene B4; *8,9-DHET; *8,9-dihydroxy-5,11,14-eicosatrienoic acid; Aphidicolin; S 1033; Zoapatanol	Eicosanoids	pos
339.2530	489.78	0.12	C20H34O4	H	10,11-dihydro-12-epi-leukotriene B4; *11,12-DHET; 11-deoxy-PGE1; 11-deoxy-PGF2a; 11-deoxy-PGF2beta; 12-keto-tetrahydro-Leukotriene B4; *14,15-DHET; *15-hydroperoxyeicosa-8Z,11Z,13E-trienone; *5,6-DHET; *5,6-dihydroxy-8,11,14-eicosatrienoic acid; *6,7-dihydro-12-epi-leukotriene B4; *8,9-DHET; *8,9-dihydroxy-5,11,14-eicosatrienoic acid; Aphidicolin; S 1033; Zoapatanol	Eicosanoids	pos
583.1303	463.56	0.65	C20H36O12	NaCl*2	3'-O-N-Octanoyl-a-D-Glucopyranosyl-B-D-Fructofuranoside; N-Octanoyl-B-D-Fructofuranosyl-a-D-Glucopyranoside; Sucrose Monocaprylate	Eicosanoids	neg
369.2634	443.70	3.25	C20H36O3	HCOOH	11(R)-HEDE or related compounds	Eicosanoids	neg
369.2634	490.74	3.41	C20H36O3	HCOOH	11S-HEDE or related compounds	Eicosanoids	neg
Fatty amides							
256.2632	448.14	0.94	C16H33NO	H	Palmitic amide	Fatty amides	pos
294.2405	552.24	0.37	C16H33NO2	Na	N-(Tetradecanoyl)-ethanolamine/2-amino-hexadecanoic acid	Fatty amides/Amino fatty acid	pos
282.2790	474.30	0.60	C18H35NO	H	Elaidoylamide; Oleamide	Fatty amides	pos
348.2874	610.02	0.37	C20H39NO2	Na	N-Oleoyl ethanolamine	Fatty amides	pos
374.3031	597.24	0.45	C22H41NO2	Na	Anandamide (20:2, n-6)	Fatty amides	pos
382.3068	494.88	0.16	C22H45NO	Na_Na	Docosanamide	Fatty amides	neg
430.2857	511.26	2.00	C22H45NO2	KCl	Eicosanoyl-EA	Fatty amides	pos
504.2398	429.72	0.10	C25H43NO2	NaClx2	*(-)-N-(1R-methyl-2-hydroxy-ethyl) alpha, alpha-dimethyl arachidonoyl amine* or related compounds	Fatty amides	neg
512.3043	483.78	4.57	C25H51NO2	NaClx2	Tricosanoyl-EA	Fatty amides	neg
510.2523	469.80	5.00	C29H43NO2	KCl	(+)-N-(1-methyl-2-hydroxy-2-phenyl-ethyl) arachidonoyl amine	Fatty amides	neg
Fatty acyl glycosides							
545.3663	542.58	0.64	C26H52O7	HCOONa	1-O-alpha-D-glucopyranosyl-1,2-eicosandiol	Fatty acyl glycosides	pos
671.3632	571.62	1.16	C32H58O13	Na	25-O-(2'-beta-D-glucopyranosyl-beta-D-glucopyranosyl)-25-hydroxy-11E-eicosenoic acid	Fatty acyl glycosides	neg
691.3669	599.22	2.94	C32H62O8	NaClx2	1-(O-alpha-D-glucopyranosyl)-3-keto-(1,25R)-hexacosanediol	Fatty acyl glycosides	pos
655.4203	600.24	1.57	C34H66O9	K	1-(O-alpha-D-glucopyranosyl)-25-keto-(1,3R,27R)-octacosanetriol or related compounds	Fatty acyl glycosides	neg
Carboxylic acids							
307.1886	592.38	1.50	C16H30O4	Na	10-hydroxy-16-oxo-hexadecanoic acid; *2,3-Dihydroxycyclopentanecarboxylic acid; 9-hydroxy-16-oxo-hexadecanoic acid; Hexadecanedioic acid	Dicarboxylic acids	neg
299.2215	464.46	0.70	C17H30O4	H	8E-Heptadecanedioic acid	Dicarboxylic acids	pos
369.3013	443.70	0.87	C22H42O4	H	Di(2-ethylhexyl) adipate; Docosanedioc acid	Dicarboxylic acids	pos
393.2978	757.68	0.79	C22H42O4	Na	Di(2-ethylhexyl) adipate; Docosanedioc acid	Dicarboxylic acids	pos
402.3577	499.50	0.10	C23H44O4	NH3	Tricosanedioic acid	Dicarboxylic acids	pos
416.3737	513.18	0.65	C24H46O4	NH3	Tetracosanedioic acid	Dicarboxylic acids	pos
444.4049	554.22	0.36	C26H50O4	NH3	Hexacosanedioic acid	Dicarboxylic acids	pos
543.2937	615.90	4.58	C26H50O4	NaClx2	Hexacosanedioic acid	Dicarboxylic acids	pos
449.3599	788.94	0.56	C26H50O4	Na	Hexacosanedioic acid	Dicarboxylic acids	pos
193.0351	64.56	0.05	C6H8O7	H	Citric acid; Isocitric acid	Tricarboxylic Acids	pos
Steroids and Derivatives							
339.1573	571.44	3.45	C18H22O2	HCOONa	Estrene	Steroids and Steroid Derivatives	pos
355.1528	562.02	1.63	C18H22O3	HCOONa (HCOOK)	2-Hydroxyestrene	Steroids and Steroid Derivatives	pos/neg
357.1473	566.94	2.86	C18H24O2	HCOOK	17a-Estradiol; Estradiol	Steroids and Steroid Derivatives	pos
277.2162	434.82	0.14	C18H28O2	H	19-Norandrosterone; 19-Noretiocholanolone	Steroids and Steroid Derivatives	pos
371.1626	573.84	4.58	C19H26O2	HCOOK	Androstenedione	Steroids and Steroid Derivatives	pos
273.2213	441.54	0.11	C19H28O	H	3-Oxo-delta1-steroid; 5a-Androst-3-en-17-one	Steroids and Steroid Derivatives	pos
373.1986	442.38	0.13	C19H28O3	HCOONa	11-Ketoetiocholanolone; 16a-Hydroxydehydroisandrosterone;;	Steroids and Steroid Derivatives	pos
361.2349	485.88	0.17	C19H32O2	HCOONa	Androstanediol	Steroids and Steroid Derivatives	pos
311.2007	566.04	4.37	C21H28O2	H	16-Dehydropregesterone or related compounds	Steroids and Steroid Derivatives	neg
383.1636	429.00	4.31	C21H28O4	K	11-Dehydrocorticosterone or related compounds	Steroids and Steroid Derivatives	pos
383.1837	581.58	1.77	C21H28O5	Na	Aldosterone; Cortisone	Steroids and Steroid Derivatives	pos
385.1787	583.80	3.06	C21H30O4	K	Cortisolone	Steroids and Steroid Derivatives	pos
401.2297	455.88	0.77	C21H32O3	HCOONa	16a-Hydroxypregnenolone; 21-Hydroxypregnenolone;;	Steroids and Steroid Derivatives	pos
417.2248	438.66	0.34	C21H32O4	HCOONa	11b,21-Dihydroxy-5-pregnane-3,20-dione or related compounds	Steroids and Steroid Derivatives	pos
403.2455	463.56	0.67	C21H34O3	HCOONa	Tetrahydrodeoxycorticosterone	Steroids and Steroid Derivatives	pos
419.2403	444.30	0.17	C21H34O4	HCOONa	5a-Tetrahydrocorticosterone; *5beta-Pregnane-3alpha,17alpha,20alpha-triol-11-one*; 9-deoxy-9-methylene-PGE2; Tetrahydrocorticosterone	Steroids and Steroid Derivatives	pos
384.2743	430.92	0.39	C21H34O5	NH3	5a-Tetrahydrocortisol; Cortisone; Tetrahydrocortisol	Steroids and Steroid Derivatives	pos
367.2484	467.94	4.93	C21H36O5	H	Beta-Cortol; Cortol	Steroids and Steroid Derivatives	neg
377.1968	567.96	2.44	C21H28O6	H (HCOOH)	18-Oxocortisol	Steroids and Steroid Derivatives	pos/neg
504.2750	476.10	0.67	C26H45NO	NaClx2	25-Azacholesterol	Steroids and Steroid Derivatives	pos
455.3346	659.76	0.75	C26H46O6	H	27-norcholestancholeol	Steroids and Steroid Derivatives	pos
511.2906	447.96	1.27	C27H44O9	H	(24R)-11alpha,20,24-trihydroxycyclopentane; (25R)-11alpha,20,26-trihydroxycyclopentane; (25S)-11alpha,20,26-trihydroxycyclopentane;;	Cholesterol and derivatives	neg
417.3455	513.18	3.07	C27H48	Na_Na	5beta-cholestane	Cholesterol and derivatives	pos
454.3897	544.56	1.28	C27H48O4	NH3	3alpha,7alpha,12alpha,26-Tetrahydroxy-5beta-cholestane or related compounds	Steroids and Steroid Derivatives	pos
497.2937	527.88	4.28	C30H48O	KCl	4alpha,14alpha-dimethyl-24-methylene-cholest-7,9(11)-dien-3beta-ol	Ergosterols and C24-methyl derivatives	neg
466.3895	548.52	0.99	C28H48O4	NH3	Testosterone; Typhasterol	Ergosterols and C24-methyl derivatives	pos
459.3589	526.92	4.03	C29H50O	Na_Na	Beta-Sitosterol	Steroids and Steroid Derivatives	pos
541.3406	619.20	4.53	C29H52O	NaCl_HCOONa	23R,24R-dimethylcholestan-3b-ol or related compounds	Ergosterols and C24-methyl derivatives	neg
553.2842	549.78	4.18	C33H38N4O4	H	Integeramine	Steroids and Steroid Derivatives	neg
693.5314	712.62	4.79	C46H74O2	NaCl	episteryl palmitoleate; fecosterol palmitoleate;;	Ergosterols and C24-methyl derivatives	pos
733.5092	504.24	2.13	C46H76O2	KCl	ergosteryl olate	Ergosterols and C24-methyl derivatives	neg
Bile acids							
473.2511	518.04	3.63	C22H33NO9	NH3	(23R)-23-Hydroxy-3,7-dioxo-5beta-cholestan-24-oic acid or related compounds	Bile acids and derivatives	pos
414.3210	464.46	0.84	C23H40O5	NH3	24-Nor-5beta-cholestan-3alpha,7alpha,12alpha,22,23-pentol; PGF2alpha isopropyl ester	Bile acids and derivatives	pos
367.2293	467.94	3.89	C24H32O3	H	3-Oxochola-1,4,6-trien-24-oic Acid	Bile acids and derivatives	neg
383.2236	588.42	0.42	C24H32O4	H	(22E)-12alpha-Hydroxy-3-oxochola-1,4,22-trien-24-oic Acid or related compounds	Bile Acids	neg
399.2181	571.86	0.80	C24H32O5	H	3,7,12-Trioxo-5beta-chole-1-en-24-oic Acid or related compounds	Bile Acids	neg
355.2630	474.30	0.42	C24H34O2	H	5beta-Chola-3,8(14),11-trien-24-oic Acid	Bile acids and derivatives	pos
369.2441	443.70	1.65	C24H34O3	H	(20S,22E)-3beta-Hydroxychola-5,16,22-trien-24-oic Acid or related compounds	Bile Acids	neg
373.2735	474.30	0.56	C24H36O3	H	(20S)-3beta-Hydroxychola-5,16-dien-24-oic Acid or related compounds	Bile acids and derivatives	pos
449.2541	520.02	0.82	C24H36O5	HCOOH	(23R)-23-Hydroxy-3,7-dioxo-5beta-cholestan-24-oic Acid or related compounds	Bile Acids	neg

413.2662	752.82	0.31	C24H38O4	Na	(22E)-3alpha,12alpha-Dihydroxy-5beta-chole-22-en-24-oi Acid or related compounds	Bile acids and derivatives	pos
445.2558	453.96	2.31	C24H38O6	Na	(3r,5r)-7-((1r,2r,6r,8r,8as)-2,6-Dimethyl-8-((2r)-2-Methylbutanoyl)oxy)-1,2,6,7,8,8a-Hexahydronaphthalen-1-Yl)-3,5-Dihydroxyheptanoic Acid or related compounds	Bile acids and derivatives	pos
391.2847	512.22	1.69	C24H40O4	H	Chenodeoxycholic acid;Deoxycholic acid;Hydoxycholic acid;Isoursodeoxycholic acid;Ursodeoxycholic acid	Bile Acids	neg
431.2766	474.30	0.39	C24H40O5	Na	(22R)-3alpha,7alpha,22-Trihydroxy-5beta-chole-24-oi Acid or related compounds	Bile acids and derivatives	pos
407.2796	477.06	4.32	C24H40O5	H	1h,3a,12a-Trihydroxy-5b-choleanoic acid;Cholic acid;Hyochohic acid;Ursocolic acid	Bile Acids	neg
450.3209	457.86	1.11	C26H43NO5	H	Chenodeoxycholic acid glycine conjugate	Acyl Glycines;Bile Acids	pos
494.2848	476.10	0.99	C26H43NO5	Na_Na	3alpha,12alpha-Dihydroxy-5beta-chole-24-oylglycine or related compounds	Acyl Glycines;Bile Acids	pos/neg
516.2936	476.70	1.30	C26H43NO5	HCOONa	Chenodeoxycholic acid glycine conjugate	Acyl Glycines;Bile Acids	neg
464.3010	447.54	1.68	C26H43NO6	H	Glycocholic acid	Acyl Glycines;Bile Acids	neg
488.2986	449.16	0.63	C26H43NO6	Na	Glycocholic acid	Acyl Glycines;Bile Acids	pos
482.3475	453.96	4.73	C27H44O6	NH3	3alpha,6alpha,7alpha,12alpha-Tetrahydroxy-5beta-cholest-24-en-26-oi acid;3-Epicdysonone;Ecdysonone;Ponasterone A	Bile acids and derivatives	pos
468.3681	478.02	0.58	C27H46O5	NH3	3a,7a,12a-Trihydroxy-5b-cholestanoic acid or related compounds	Bile acids and derivatives	pos
484.3633	459.72	0.06	C27H46O6	NH3	1beta,3alpha,7alpha,12alpha-Tetrahydroxy-5beta-cholestan-26-oi acid or related compounds	Bile acids and derivatives	pos
686.3416	488.34	3.26	C52H51NO12	HCOOH	(3a,5b,7a,12a)-24-[(carboxymethyl)amino]-1,12-dihydroxy-24-oxocholan-3-yl-b-D-Glucopyranosiduronic acid	Bile Acids	neg
Vitamins and derivatives							
393.2099	86.04	1.04	C22H32O4S	H	(6R,S)-22-oxo-23,24,25,26,27-pentanorvitamin D3 6,19-sulfur dioxide adduct / (6R,S)-22-oxo-23,24,25,26,27-pentanorcholecalciferol 6,19-sulfur dioxide adduct	Vitamin D2 and derivatives	pos
415.1918	443.04	3.78	C22H34O4S	Na	(6R,S)-22-hydroxy-23,24,25,26,27-pentanorvitamin D3 6,19-sulfur dioxide adduct / (6R,S)-22-hydroxy-23,24,25,26,27-pentanorcholecalciferol 6,19-sulfur dioxide adduct	Vitamin D2 and derivatives	neg
597.3108	561.06	1.19	C37H48O3	NaCl	1alpha,25-dihydroxy-25,25-diphenyl-26,27-dinorvitamin D3 / 1alpha,25-dihydroxy-25,25-diphenyl-26,27-dinorcholecalciferol	Vitamin D2 and derivatives	neg
469.3142	620.76	1.26	C23H44O5	HCOONa	1,2-Didecanoylglycerol	Vitamin D2 and derivatives	pos
501.2882	476.70	3.49	C29H48O2	KCl	(22alpha)-hydroxy-isofucosterol;"(24R,24'R)-Fucosterol epoxide or related compounds	Vitamin D2 and derivatives	neg
453.2883	612.96	1.32	C28H44O	NaCl	(5E)-isovitamin D2 / (5E)-isoergocalciferol or related compounds	Vitamin D2 and derivatives	neg
422.3263	481.86	0.43	C25H40O4	NH3	11'-carboxy-gamma-chromanol or related compounds	Vitamin D2 and derivatives	pos
452.3368	464.46	0.49	C26H42O5	NH3	(24R)-1alpha,24,25-trihydroxy-22-oxavitamin D3 / (24R)-1alpha,24,25-trihydroxy-22-oxacholecalciferol or related compounds	Vitamin D2 and derivatives	pos
460.2728	429.00	3.17	C26H43NO	KCl	25-azavitamin D3 / 25-azacholecalciferol;	Vitamin D2 and derivatives	pos
455.2678	583.50	4.70	C27H42O2	NaCl	(22E)-1alpha-hydroxy-22,23-didehydrovitamin D3 / (22E)-1alpha-hydroxy-22,23-didehydrocholecalciferol or related compounds	Vitamin D2 and derivatives	neg
509.2575	390.90	3.28	C26H43O4P	NaCl	24-(dimethoxyphosphoryl)-25,26,27-trinorvitamin D3 / 24-(dimethoxyphosphoryl)-25,26,27-trinorcholecalciferol or related compounds	Vitamin D2 and derivatives	pos
464.3367	463.56	0.67	C27H42O5	NH3	(23R)-1alpha,23,25-trihydroxy-24-oxovitamin D3 / (23R)-1alpha,23,25-trihydroxy-24-oxocholecalciferol or related compounds	Vitamin D2 and derivatives	pos
511.2728	545.52	1.55	C27H43F	NaCl_HCOONa	3-Fluoro-9,10-secocholesta-5,7,10(19)-triene	Vitamin D3 and derivatives	neg
485.2726	734.22	1.24	C27H44O4S	Na	(6R)-25-hydroxyvitamin D3 6,19-sulfur dioxide adduct / (6R)-25-hydroxycholecalciferol 6,19-sulfur dioxide adduct or related compounds	Vitamin D2 and derivatives	neg
466.3525	470.34	0.39	C27H44O5	NH3	(23S,25R)-1alpha,23,25,26-tetrahydroxyvitamin D3 / (23S,25R)-1alpha,23,25,26-tetrahydroxycholecalciferol or related compounds	Vitamin D2 and derivatives	pos
452.3735	518.04	0.11	C27H46O4	NH3	(10R)-1alpha,19,25-trihydroxy-10,19-dihydrovitamin D3 / (10R)-1alpha,19,25-trihydroxy-10,19-dihydrocholecalciferol or related compounds	Vitamin D2 and derivatives	pos
409.3103	780.12	3.35	C28H42O2	H	calciferol D or related compounds	Vitamin D3 and derivatives	neg
553.2653	575.70	4.57	C28H45ClO3	Na_HCOONa	11alpha-(chloromethyl)-1-alpha,25-dihydroxyvitamin D3 / 11alpha-(chloromethyl)-1-alpha,25-dihydroxycholecalciferol;	Vitamin D3 and derivatives	neg
487.2770	575.70	4.10	C28H46O2	KCl	(22alpha)-hydroxy-campesi-4-en-3-one or related compounds	Vitamin D3 and derivatives	neg
499.2940	585.48	4.27	C29H46O3	NaCl	(22E)-1alpha,25-dihydroxy-26,27-dimethyl-22,23-didehydrovitamin D3 / (22E)-1alpha,25-dihydroxy-26,27-dimethyl-22,23-didehydrocholecalciferol or related compounds	Vitamin D2 and derivatives	neg
492.3680	478.02	0.73	C29H46O5	NH3	18-acetoxy-1alpha,25-dihydroxyvitamin D3 / 18-acetoxy-1alpha,25-dihydroxycholecalciferol	Vitamin D2 and derivatives	pos
497.3147	617.04	0.72	C30H48O2	NaCl	26,27-Dihomo-1alpha-hydroxy-24-epitavitamin D2;"26,27-Dihomo-1alpha-hydroxyvitamin D2";"4,4-Dimethyl-14a-formyl-5a-cholesta-8,24-dien-3b-ol";"4,4-dimethyl-14alpha-formyl-5alpha-cholesta-8,24-dien-3beta-ol"	Vitamin D2 and derivatives	neg
479.3195	662.52	0.69	C27H43FO3	HCOOH	(10E)-19-fluoro-1alpha,25-dihydroxyvitamin D3 / (10E)-19-fluoro-1alpha,25-dihydroxycholecalciferol or related compounds	Vitamin D2 and derivatives	neg
509.3297	662.52	4.59	C32H46O5	H	11-(3-acetoxy-1-propenyl)-1alpha,25-dihydroxy-9,11-didehydrovitamin D3 / 11-(3-acetoxy-1-propenyl)-1alpha,25-dihydroxy-9,11-didehydrocholecalciferol	Vitamin D2 and derivatives	neg
597.3098	398.76	1.64	C34H50O4	KCl	1alpha-hydroxy-18-[m-(1-hydroxy-1-ethylpropyl)-benzyloxy]-23,24,25,26,27-pentanorvitamin D3 / 1alpha-hydroxy-18-[m-(1-hydroxy-1-ethylpropyl)-benzyloxy]-23,24,25,26,27-pentanorcholecalciferol	Vitamin D2 and derivatives	pos
Prostaglandins							
349.1986	427.08	0.32	C18H30O5	Na	2,3-dinor-6-keto-prostaglandin F1 a or related compounds	Prostanoids	pos
365.1939	410.46	0.99	C18H30O6	Na	2,3-dinor, 6-keto-PGF1alpha;"2,3-Dinor-TXB2	Prostaglandins	pos
375.2142	446.22	4.34	C20H32O5	Na	13,14-Dihydro-15-keto-PGE2;20-Hydroxy-leukotriene B4;Prostaglandin E2;Thromboxane A2	Prostanoids	pos
373.1998	465.72	4.80	C20H32O5	Na	(13E)-11alpha-Hydroxy-9,15-dioxoprost-13-enate or related compounds	Prostanoids	neg
391.2089	429.00	0.92	C20H32O6	Na	11-Dehydro-thromboxane B2	Prostanoids	pos
393.2247	425.28	0.13	C20H34O6	Na	10,11-dihydro-20-dihydroxy-LTB4;19(R)-hydroxy-PGE1 or related compounds	Prostaglandins	pos
341.2686	503.40	0.12	C20H36O4	H	11-deoxy-PGF1a;11-deoxy-PGF1b;15S-HpEDE;PGE1 alcohol;PGF2alpha alcohol	Prostaglandins	pos
353.2385	568.92	0.76	C20H40	KCl	8-Isoprostane	Prostanoids	neg
368.2793	459.72	0.71	C21H34O4	NH3	11-deoxy-11-methylene-PGD2 or related compounds	Prostaglandins	pos
351.2529	487.80	0.31	C21H34O4	H	3alpha,11beta,17alpha-Trihydroxy-5beta-pregnan-20-one or related compounds	Prostaglandins	pos
426.2052	581.94	1.13	C23H33NO4	K	17-phenyl-trinor-PGF2alpha amide	Prostaglandins	pos
517.2413	520.02	3.48	C23H40O7	Na_HCOONa	1(3)-glyceryl-PGF2alpha,2-glyceril-PGF2alpha	Prostaglandins	neg
428.3008	429.00	0.37	C23H41NO6	H	PGF2alpha-dihydroxypropylamine	Prostaglandins	pos
554.2462	445.32	0.97	C23H41NO6	NaCl_HCOONa	PGF2alpha-dihydroxypropylamine	Prostaglandins	pos
Leukotrienes							
440.2449	438.66	1.32	C23H37NO5S	H	11-trans-LTE4;Leukotriene E4	Leukotrienes	pos
462.2284	440.52	0.19	C23H37NO5S	Na (Na)	(7E,9E,11Z,14Z)-((S,R))-6-(cystein-S-yl)-5-hydroxycosa-7,9,11,14-tetraenoate";11-trans-LTE4;Leukotriene E4;	Leukotrienes	pos/neg
442.2621	446.22	0.18	C23H39NO5S	H	Leukotriene E3	Leukotrienes	pos/neg
517.2351	429.72	2.20	C25H40N2O6S	Na	11-trans-LTD4;"14,15-LTD4";Leukotriene D4	Leukotrienes	neg

906.6986	739.08	2.01	C50H95N08	HCOONa	Galactosylceramide (d18:1/26:1(17Z));Glucoylceramide (d18:1/26:1(17Z))	Sphingolipids	pos
Glycerolipids							
381.2979	691.08	0.97	C21H42O4	Na	MG(18:0/0:0/0:0)	Glycerolipids	pos
396.3105	478.02	0.76	C23H38O4	NH3	1-Arachidonoylglycerol or related compounds	Glycerolipids	pos
401.2661	573.78	0.57	C23H38O4	Na	2-Arachidonoylglycerol or related compounds	Glycerolipids	pos
430.3891	528.90	0.00	C25H48O4	NH3	MG(0:0/22:1(13Z)/0:0);MG(22:1(13Z)/0:0/0:0)	Glycerolipids	pos
471.3659	694.98	4.50	C27H50O6	H	Tricaprin	Glycerolipids	pos
599.4249	679.32	1.52	C33H62O6	Na_Na(NaClx2)	TG(10:0/10:0/10:0)[iso]	Glycerolipids	pos/neg
613.4246	656.88	1.09	C36H64O5	K	DG(15:0/18:3(9Z,12Z)/0:0) or related compounds	Glycerolipids	neg
669.4655	790.86	3.17	C36H66O5	Na_HCOONa	DG(15:0/18:2(9Z,12Z)/0:0) or related compounds	Glycerolipids	pos
701.3729	569.76	4.65	C37H62O5	NaClx2	DG(14:0/20:5(5Z,8Z,11Z,14Z,17Z)/0:0) or related compounds	Glycerolipids	neg
697.3989	582.54	1.23	C40H64O5	KCl	DG(17:2(9Z,12Z)/20:5(5Z,8Z,11Z,14Z,17Z)/0:0)[iso]	Diacylglycerols	neg
713.4774	464.94	1.37	C40H70O5	HCOOK	DG(15:0/22:4(7Z,10Z,13Z,16Z)/0:0) or related compounds	Glycerolipids	neg
723.5552	696.72	2.28	C40H78O5	HCOOK	DG(15:0/22:0:0);DG(16:0/21:0:0/0:0)[iso];DG(17:0/20:0:0/0:0)[iso];DG(18:0/19:0:0/0:0)[iso];DG(22:0/15:0:0:0)	Glycerolipids	pos
780.5947	700.86	1.59	C42H81N07	HCOONa	DGTS(16:0/16:0)	Glycerolipids	pos
780.5947	736.14	1.59	C42H81N07	HCOONa	DGTS(16:0/16:0)	Glycerolipids	pos
780.5950	767.46	1.28	C42H81N07	HCOONa	DGTS(16:0/16:0)	Glycerolipids	pos
795.5443	550.38	4.45	C43H82O5	NaClx2	DG(16:0/24:1(15Z)/0:0) or related compounds	Glycerolipids	pos
795.5430	636.36	2.84	C43H82O5	NaClx2	DG(16:1(9Z)/24:0:0/0:0) or related compounds	Glycerolipids	pos
795.5431	775.32	2.99	C43H82O5	NaClx2	DG(18:0/22:1(13Z)/0:0) or related compounds	Glycerolipids	pos
781.5978	769.44	3.33	C46H80O5	HCOONa	DG(21:0/22:5(7Z,10Z,13Z,16Z,19Z)/0:0)[iso]	Diacylglycerols	pos
791.5926	550.38	0.19	C49H84O5	K	DG(22:5(4Z,7Z,10Z,13Z,16Z)/24:1(15Z)/0:0) or related compounds	Glycerolipids	pos
911.6267	630.54	2.72	C54H92O6	KCl	TG(16:1(9Z)/17:2(9Z,12Z)/18:3(9Z,12Z,15Z)/[iso]);TG(17:2(9Z,12Z)/17:2(9Z,12Z)/17:2(9Z,12Z))	Triacylglycerols	pos
911.6267	710.70	2.72	C54H92O6	KCl	TG(16:1(9Z)/17:2(9Z,12Z)/18:3(9Z,12Z,15Z)/[iso]);TG(17:2(9Z,12Z)/17:2(9Z,12Z)/17:2(9Z,12Z))	Triacylglycerols	pos
945.7081	775.32	0.73	C56H102O6	KCl	TG(16:0/17:0/20:3(8Z,11Z,14Z)/[iso]) or related compounds	Triacylglycerols	pos
963.7382	771.36	0.56	C62H100O6	Na	TG(17:0/20:4(5Z,8Z,11Z,14Z)/22:6(4Z,7Z,10Z,13Z,16Z,19Z)/[iso]) or related compounds	Triacylglycerols	pos
Phospholipids							
443.2405	448.14	0.02	C19H39O9P	H	PG(13:0/0:0)	glycerophosphates	pos
454.2930	751.80	0.48	C21H44N07P	H	1-16:0-lysoPE;PC(13:0/0:0);PE(16:0/0:0)	glycerophosphates	pos
531.2572	575.70	1.36	C22H43O12P	H	PI(13:0/0:0)	glycerophosphates	pos
516.2876	444.18	2.79	C24H50N06P	K	LysoPC(dm16:0);PC(O-16:1(11Z)/0:0) or related compounds	glycerophosphocholines	neg
617.2943	557.28	0.16	C25H49O12P	HCOOH	P(16:0/0:0)	glycerophosphates	pos
616.2625	189.54	0.47	C27H44N07P	Na_HCOONa	LysoPE(0:0/22:5(4Z,7Z,10Z,13Z,16Z,19Z));LysoPE(22:6(4Z,7Z,10Z,13Z,16Z,19Z)/0:0)	glycerophosphoethanolamines	neg
543.3197	586.44	1.36	C27H46N07P	NH3	LysoPE(0:0/22:5(4Z,7Z,10Z,13Z,16Z,19Z)) or related compounds	glycerophosphoethanolamines	neg
691.3055	566.94	2.10	C27H53O12P	Na_HCOONa (HCOOH)	PI(18:0/0:0)	glycerophosphates	pos/neg
557.3354	598.26	1.26	C28H48N07P	NH3	LysoPC(20:5(5Z,8Z,11Z,14Z,17Z))	glycerophosphocholines	pos
625.3041	420.18	1.28	C28H55O8P	KCl	FA(12:0/13:0)	glycerophosphates	pos
710.3937	603.12	1.77	C33H66N08P	KCl	PE(16:0/12:0);PC(16:0/15:0/15:0/15:0) or related compounds	glycerophosphoethanolamines	pos
712.3601	408.24	0.48	C34H62N010P	K	PS(14:1(9Z)/14:1(9Z))	glycerophosphoserines	neg
745.3991	571.62	1.14	C37H69O8P	KCl	16:0-18:2-PA;PA(16:0/18:2(9Z,12Z));Phosphatidyl ethanol	glycerophosphates	pos
752.4725	679.32	4.28	C37H76N07P	KCl	PE(0-16:0/16:0);PC(O-14:0/15:0) or related compounds	glycerophosphoethanolamines	pos
752.5147	542.64	3.89	C38H78N08P	Na_Na	PS(O-16:0/16:0/16:0/16:0) or related compounds	glycerophosphoserines	pos
729.3889	567.90	1.00	C39H65O8P	K	PA(18:3(9Z,12Z,15Z)/18:3(9Z,12Z,15Z)) or related compounds	glycerophosphates	neg
765.3679	463.14	3.71	C39H65O8P	KCl	18:3-18:3-PA or related compounds	glycerophosphates	neg
733.5494	587.46	0.50	C39H74N08P	NH3	PE(14:0/20:2(11Z,14Z)) or related compounds	glycerophosphoethanolamines	pos
760.5789	648.12	4.89	C39H82N06P	HCOONa	PE-NmC(16:0-16:0-16:0)	glycerophosphoethanolamines	pos
790.4674	682.08	4.78	C40H70N08P	HCOONa	PC(14:1(9Z)/18:4(6Z,9Z,12Z,15Z));PC(18:4(6Z,9Z,12Z,15Z)/14:1(9Z));PE(15:0/20:5(5Z,8Z,11Z,14Z,17Z));PE(20:5(5Z,8Z,11Z,14Z,17Z)/15:0)	glycerophosphocholines	neg
796.4550	426.06	3.06	C40H72N010P	K	16:0-18:3-PS	glycerophosphoserines	pos
842.4243	550.44	4.96	C40H74N08P	NaClx2	PC(14:0/18:3(6Z,9Z,12Z));PE(15:0/20:3(5Z,8Z,11Z)) or related compounds	glycerophosphocholines	neg
909.4085	551.34	4.39	C40H75O13P	NaClx2	PI(17:0/14:1(9Z))	glycerophosphoinositols	neg
753.4823	681.30	1.05	C40H75O8P	K	PA(18:2(9Z,12Z)/19:0:0);1-tetradecanoyl-2-(8-[3]-ladderane-octanyl)-sn-glycero-3-phospho-1'-sn-glycerol	glycerophosphates	pos
774.5945	683.22	4.92	C40H84N06P	HCOONa	PC(O-12:0-20:0/0:0/0:0);PC(O-14:0-18:0/18:0/18:0);PC(O-16:0-16:0);PC(O-20:0/0-12:0/0:0)	glycerophosphocholines	pos
738.5050	775.32	0.81	C41H72N08P	H	PE(14:0/22:5(4Z,7Z,10Z,13Z,16Z)) or related compounds	glycerophosphoethanolamines	pos
743.5705	741.00	1.02	C41H76N07P	NH3	PE(18:2(9Z,12Z)/dm18:1(11Z)) or related compounds	glycerophosphoethanolamines	pos
796.5443	542.64	0.58	C41H78N07P	HCOONa	PE(18:1(11Z)/dm18:1(11Z)) or related compounds	glycerophosphoethanolamines	pos
816.6057	701.88	3.93	C42H86N07P	HCOONa	PC(18:0-16:0) or related compounds	glycerophosphocholines	pos
838.4536	476.94	3.05	C43H76N08P	KCl	20:2-18:3-PE or related compounds	glycerophosphoethanolamines	neg
789.6122	675.42	0.73	C43H82N08P	NH3	PC(15:0/20:2(11Z,14Z)) or related compounds	glycerophosphoethanolamines	pos
839.5638	474.30	0.64	C43H83O13P	H	PI(16:0/18:0);PI(18:0/16:0)	glycerophosphoinositols	pos
820.5991	585.48	4.16	C43H88N07P	NaCl	PC(O-16:0/19:0) or related compounds	glycerophosphoethanolamines	pos
830.6205	634.44	4.78	C43H88N07P	HCOONa	PE(O-16:0/22:0) or related compounds	glycerophosphoethanolamines	pos
830.6209	737.10	4.41	C43H88N07P	HCOONa	PE(O-18:0/20:0) or related compounds	glycerophosphoethanolamines	pos
817.4409	571.86	3.56	C44H71O9P	Na_Na	1-(6-[5]-ladderane-hexanoyl)-2-(8-[3]-ladderane-octanyl)-sn-glycero-3-phospho-1'-sn-glycerol	glycerophosphoglycerols	neg
833.4513	573.18	1.82	C44H73O9P	NaCl	1-(6-[3]-ladderane-hexanoyl)-2-(8-[3]-ladderane-octanyl)-sn-glycero-3-phospho-1'-sn-glycerol	glycerophosphoglycerols	pos
834.6154	612.84	0.74	C44H90N07P	NaCl	PC(O-14:0/22:0);PC(O-16:0/20:0);PC(O-18:0/18:0);PC(O-20:0/16:0)	glycerophosphocholines	pos
844.6361	699.90	4.87	C44H90N07P	HCOONa	PC(O-14:0/22:0);PC(O-16:0/20:0);PC(O-18:0/18:0);PC(O-20:0/16:0)	glycerophosphocholines	pos
868.5003	477.06	3.15	C45H82N08P	KCl	PC(15:0/22:4(7Z,10Z,13Z,16Z)) or related compounds	glycerophosphoethanolamines	neg
846.6154	657.84	4.80	C45H90N07P	NaCl	PE(22:0/dm18:0);PE(24:0/dm16:0);	glycerophosphoethanolamines	pos
809.6154	699.90	1.57	C46H82N07P	NH3	PC(20:4(5Z,8Z,11Z,14Z)/dm18:1(11Z)) or related compounds	glycerophosphocholines	pos
809.6156	748.86	1.35	C46H82N07P	NH3	PC(20:4(5Z,8Z,11Z,14Z)/dm18:1(11Z)) or related compounds	glycerophosphocholines	pos
905.5129	492.72	1.10	C47H81O13P	Na	PI(16:0/22:5(4Z,7Z,10Z,13Z,16Z)) or related compounds	glycerophosphoinositols	neg
908.7015	739.08	4.28	C48H100N06P	Na_HCOONa	1,2-diphytanyl-sn-glycero-3-phosphocholine;PC(O-20:0/0-20:0)	glycerophosphocholines	pos
848.6309	567.00	4.61	C48H92N06P	K	1-(2E,6E-phytadienyl)-2-(2E,6E-phytadienyl)-sn-glycero-3-phosphocholine	glycerophosphocholines	pos
848.6313	644.16	2.29	C48H92N06P	K	1-(2E,6E-phytadienyl)-2-(2E,6E-phytadienyl)-sn-glycero-3-phosphocholine	glycerophosphocholines	pos
899.6350	476.10	0.23	C48H93O11P	Na	1,2-ditetradecanoyl-sn-glycero-3-phospho-(2'-lyso-3'-tetradecanoyl-1'-sn-glycerol)	glycerophosphoglycerols	pos
921.6165	476.10	0.17	C48H93O11P	Na_Na	1,2-ditetradecanoyl-sn-glycero-3-phospho-(2'-lyso-3'-tetradecanoyl-1'-sn-glycerol)	glycerophosphoglycerols	pos/neg
888.6621	659.76	4.29	C48H96N07P	NaCl	PC(22:0/dm18:0);PC(24:0/dm16:0)	glycerophosphocholines	pos
904.6939	769.38	4.70	C49H100N07P	NaCl	PC(O-19:0/22:0)	glycerophosphoethanolamines	pos
866.6684	805.50	4.63	C50H94N08P	H	PC(18:2(9Z,12Z)/24:1(15Z)) or related compounds	glycerophosphocholines	neg
980.6476	803.46	4.07	C50H98N08P	NaCl_HCOONa	PC(24:0/dm18:1(11Z)) or related compounds	glycerophosphocholines	neg
964.7150	602.16	2.02	C54H104N08P	K	PC(22:1(13Z)/24:1(15Z)) or related compounds	glycerophosphocholines	pos
Miscellaneous							
151.0478	385.80	0.13	C5H8N2O2	Na	5,6-Dihydrothymine	Pyrimidines and Derivatives	pos
167.0198	73.98	2.51	C6H8N2O	Na_Na	Methylimidazole acetaldehyde;N-Propanoylimidazole	Aldehydes Imidazoles	neg
255.9781	66.54	3.52	C7H8NO5P	K	3-Phosphonomethylpyridine-2-Carboxylic Acid	Pyradoxals and Derivatives	pos
853.5855	538.68	1.96	C54H82O4	NaCl	Ubiquinone-9	Quinones and Derivatives	pos
853.5854	636.36	2.10	C54H82O4	NaCl	Ubiquinone-9	Quinones and Derivatives	pos
853.5857	712.62	1.75	C54H82O4	NaCl	Ubiquinone-9	Quinones and Derivatives	pos
627.3831	611.94	3.63	C39H58O4	K	Coenzyme Q6;ubiquinone-6	Ubiquinones	neg
511.2729	540.72	2.01	C30H44O2	KCl	2-Phytlyl-4-naphthoquinone;demethylphyloquinone	Naphthoquinones	pos/neg
310.9307	65.58	1.80	C37H70O7P	NaCl_HCOONa	2-Phosphoglyceric acid;3-Phospho-D-glycerate;D-Glycerate 2-phosphate	Acyl Phosphates	pos
765.3972	443.04	4.49	C40H68O7P2	Na_Na	all-trans-Octaprenyl diphosphate;octaprenyl diphosphate; Prephytoene diphosphate	Acyl Phosphates	neg

308.0255	634.44	3.67	C6H12N3O8P	Na	2-(Formamido)-N1-(5-phospho-D-ribovyl)acetamidine	Sugar Phosphates	µm
687.3727	582.54	0.04	C40H60O2	NaClx2	5,6-dihydro-5,6-dihydroxy-γ,γ-Carotene or related compounds	Alcohols and Polyols	mg
611.4239	530.82	2.32	C40H60O2	K	Dihydropersiloxanthin/ 7,8,7',8'-Tetrahydroxanthin or related compounds	Alcohols and Polyols	µm
611.4236	788.94	1.82	C40H60O2	K	OH-Demethylspheridene or related compounds	Alcohols and Polyols	µm
368.9881	444.48	2.22	C14H6O8	HCOONa	Ellagic acid	Polyphenols	mg
293.1755	486.84	0.96	C16H24O2	HCOOH	2E,6Z,8Z,12E-hexadecatetraenoic acid or related compounds	Polyphenols	mg
488.2680	475.26	0.08	C18H37N9O4	Na_Na	dynorphin A (6-8)	Solanidines and alkaloid derivatives	µm
416.3524	408.48	0.24	C27H45NO2	H	22-iso-tenenine or related compounds	Solanidines and alkaloid derivatives	µm
581.4545	633.30	3.08	C36H64O4	Na	2-methylbacteriophage-32,33,34,35-tetrol	Hopanoids	mg
728.5527	646.14	2.81	C40H73N3O4	HCOONa	N-ornithinyl-35-aminobacteriophage-32,33,34-triol	Hopanoids	µm